Elucidating the mechanism of action of novel lactams on *Pseudomonas aeruginosa*

Paolo Pantalone, MSc.

Thesis submitted to the University of Nottingham for the degree of Doctor of Philosophy

March 2019

DECLARATION

Unless otherwise acknowledged, the work presented in this thesis is my own. No part has been submitted for another degree at the University of Nottingham or any other institute of learning.

Paolo Pantalone

March 2019

ABSTRACT

Biofilms are complex structures derived from the aggregation of bacteria in suspension or anchored to a surface. Due to their intrinsic biocide and antibiotic resistance, biofilm development and dispersal in healthcare, industrial and domestic environments represent a constant challenge. In bacteria such as *Pseudomonas aeruginosa*, biofilm maturation depends in part on quorum sensing (QS), a cell-to-cell communication system. This can be intercepted, thereby preventing, inhibiting or sensitizing biofilms to antimicrobials. Several natural compounds and their synthetic analogues successfully accomplish this strategy by targeting specific QS pathways. The pursuit of anti-biofilm agents as compatible as possible with the widest range of environments and applications has led to the development of new compounds for biofilm control based on the furanones produced by red algae. The aims of this project were to elucidate the mechanisms of action of a series of lactams related to the furanones and to describe how they perturb biofilm development in bacteria including *P. aeruginosa*, *Staphylococcus aureus* and *Proteus mirabilis*. For *P. aeruginosa*, reporter gene fusions, *in silico*, iso-thermal titration calorimetry, circular dichroism spectroscopy, protein crystallization and X-ray diffraction studies have revealed that the most potent compound inhibit 2-alkyl-4-quinolone (AQ) dependent quorum sensing by binding to and inhibiting the response regulator protein, PqsR. Transcriptome analysis confirmed these observations and uncovered additional potential targets involved in cell motility, RNA processing and biofilm development which were validated using reporter gene fusions and phenotypic assays. Different biofilm assays unexpectedly showed an increase of biomass in *P. aeruginosa* when the lead lactam was present at high concentrations in the growth medium.

Furthermore, studies of *P. mirabilis* and *S. aureus* unveiled the potent inhibitory properties of the lead lactam on biofilm development on the former and significant growth inhibitory effects on the latter.

In conclusion, the results of this work provide new insights into the mode of action of the lactams and suggest strategies for future development and application.

PATENTS

Part of the outcome of this work is included in the following patents:

Parry, N. J., Pantalone, P., & Williams, P. (2018). *Lactams for use in the treatment of skin lesions.* WO2018/015278Al Application PCT/EP2017/067781 Worldwide applications. EP3487495A1 European Patent Office.

Parry, N. J., Pantalone, P., & Williams, P. (2018). *Lactams for the treatment of respiratory tract infections.* WO2018015279A1 Application PCT/EP2017/067782 Worldwide applications. EP3487494A1 European Patent Office.

Parry, N. J., Pantalone, P., & Williams, P. (2018*). 4-(4-chlorophenyl)-5-methylene-pyrrol-2-one and 5-methylene-4-(p-tolyl)pyrrol-2-one for use in the treatment of gram negative bacterial infections.* WO2018015280A1 Application PCT/EP2017/067783 Worldwide applications. EP3487496A1 European Patent Office.

ACKNOWLEDGEMENTS

This work was supported by the Unilever Research and Development Laboratory, Port Sunlight, Wirral, CH62 4ZD, in particular by Dr. Neil Parry, Dr. Panos Kotsakis and Dr. Joanne O'Keeffe.

RNA-sequencing and differential gene expression analysis were performed at Centre for Genomic Research of the University of Liverpool by Lucille Rainbow, Richie Eccles, Anita Lucaci and Yongxiang Fang for Pseudomonas Aeruginosa PAO1-L Samples (Project number LIMS10522). RNA-seq on *S. aureus* samples was carried out by Charlotte Nelson, Anita Lucaci, Xuan Liu and Yongxiang Fang (Project number LIMS17399).

Transmission electron microscope figures were collected with the help of Denise McLean from the Advanced Microscopy Unit of the University of Nottingham.

In silico docking studies were carried out with the help of Dr. Fadi Soukarieh.

Circular Dichroism spectroscopy studies were performed by Rohanah Hussain, Charlotte Hughes and Giuliano Siligardi at B23 beamline, Diamond Light Source, Oxford (Project:M19141-1 and 19141-2).

Liquid Chromatography-Mass spectrometry analysis was performed by Nigel Halliday.

The construction of the PAO1-L *rhlI, lasI, pqsA* and *tac lux*-based bioreporters was carried out with the help of Dr. Matthew Fletcher.

Crystallography data were collected with the help of William Richardson and Dr. Kim Hyojung.

The work presented in this thesis would have not been possible without the support of different people in the past four years. First of all, I would like to express my gratefulness to Prof. Paul Williams for the opportunity of taking part in this interesting project and for the constant guidance, motivation and support. I would like to thank Unilever for funding my PhD and allowing me to work in close contact with their Research team. I would also like to acknowledge all my colleagues for their contribution to my scientific and personal growth.

This thesis is dedicated to Victoria, my family, my friends, far and close, and to the memory of my grandparents.

TABLE OF CONTENTS

LIST OF FIGURES

LIST OF TABLES

ABBREVIATIONS

°C	Degrees Celsius
% (v/v)	Percentage volume per volume
% (w/v)	Percentage weight per volume
3OC12HSL	*N*-(3-oxododecanoyl)-L-homoserine lactone
AA	Anthranilic acid
aa	Amino acid
AI	Autoinducer
AIP	Autoinducing peptides
Ap	Ampicillin
AQ	2-Alkyl-4-Quinoline
AUC	Area under the curve
AUM	Artificial urine medium
bp	Base pair
C4HSL	*N*-(butanoyl)-L-homoserine lactone
C9-PQS	2-nonyl-3-hydroxy-4(1*H*)-quinolone
CAUTI	Catheter-associated urinary tract infections
CBD	Co-inducer binding domain
CF	Cystic fibrosis
CFU	colony forming unit
CLSM	Confocal laser scanning microscopy
c-di-GMP	bis-(3',5') cyclic di guanylase
Cm	Chloramphenicol
COG	Clusters of Orthologous Groups
CV	Crystal Violet
DMSO	Dimethyl sulfoxide
DNA	Deoxyribonucleic acid
dNTP	Deoxynucleoside triphosphate
eDNA	Extracellular DNA
eGfp	Enhanced green fluorescence protein
EPS	Extracellular polymeric substances
Gfp	Green fluorescence protein

Gm	Gentamicin
GMP	Guanosine monophosphate
h	Hours
HCl	Hydrochloric acid
HHQ	2-heptyl-4(1*H*)-hydroxyquinoline
HQNO	4-hydroxy-2-heptylquinoline-N-oxide
HTH	Helix-turn-helix domain
IC_{50}	Inhibitory concentration 50%
IPTG	Isopropyl β-D-1-thiogalactopyranoside
ITC	Isothermal titration calorimetry
Km	Kanamycin
$K_{(D)}$	Dissociation constant
kDa	Kilo Daltons
L	Litre
LB	Lysogeny broth media
LBD	Ligand binding domain
Lttr	LysR-type transcriptional regulator
M	Molar
min	Minutes
mL	Millilitres
mM	Millimolar concentration
mm	Millimetre
MSCRAMM	Microbial surface components recognizing adhesive matrix molecule
NHQ	2-nonyl-3-hydroxy-4(1*H*)-quinolone
nM	Nanomolar concentration
OD	Optical density
O/N	Overnight culture
PA	*Pseudomonas aeruginosa*
pGpG	5'-phosphoguanylyl-(3'-5')-guanosine
PI	Propidium iodide
PIA	*Pseudomonas* isolation agar

PQS	*Pseudomonas* quinolone signal, 2-heptyl-3-hydroxy-4(1*H*)-quinolone
QS	Quorum sensing
QSSM	Quorum sensing signal molecules
QZN	Quinazolinone
rcf	Relative centrifugal force
RLU	Relative light unit
RNA	Ribonucleic acid
RPM	Revolutions per minutes
RPMI	Roswell park memorial institute media
S17	*Escherichia coli* S17
SDS	Sodium dodecyl sulphate
SDS-PAGE	Sodium dodecyl sulphate polyacrylamide gel electrophoresis
SN	Supernatant
TIIISS	Type three secretion system
T4P	Type IV pili
TCS	Two component systems
Tet	Tetracycline
UV	Ultraviolet light
µg	Microgram
µL	Microliter
µM	Micromolar concentration
µm	Micrometre

1 INTRODUCTION

1.1 *PSEUDOMONAS AERUGINOSA*

1.1.1 Characteristics and identification

Pseudomonas aeruginosa is a Gram-negative rod-shaped non-fermentative aerobe, which is capable at surviving in oxygen restricted environments. It can be identified by its distinct grape-like smell and blue-green pigmentation, is oxidase and catalase positive, and produces a single polar flagellum (Colwell, 1964; Trunk *et al.*, 2010). It normally prefers temperatures between 25 and 41 ^{O}C, but isolates have been found to grow outside of this range from 5.5 to 45 ^{o}C (Trunk *et al.*, 2010).

1.1.2 General phylogeny

A vast number of species belong to the genus *Pseudomonas* and it continues to expand as more are identified (Gomila *et al.*, 2015). The *P. aeruginosa* phylogenetic tree shows a clear division into 3 groups. Group 1 contains the reference strain PAO1, group 2 the wound isolate PA14 and group 3, PA7 (Freschi *et al.*, 2018). Sequencing of the *P. aeruginosa* genome revealed a 6.3 mega bases (Mb) chromosome with 5,570 predicted open reading frames. Of this, 17.5% on average represents the core genome. Frequent gene rearrangement and acquisition indicates a high degree of flexibility, supporting successful adaption to numerous different environments (Boyle *et al.*, 2018; Kung *et al.*, 2010; Stover *et al.*, 2000).

1.1.3 Clinical and industrial significance

1.1.3.1 *P. aeruginosa* in industry: uses and issues

P. aeruginosa possess several qualities which can benefit certain industrial practices, however its versatility can also be problematic for other sectors. Firstly, *P. aeruginosa* can metabolise a wide variety of organic molecules including hydrocarbons, aromatic molecules and recalcitrant insecticides

(Ebadi *et al.*, 2017; Kotresha & Vidyasagar, 2008; Kulkarni & Kaliwal, 2014; Mukherjee & Bordoloi, 2012; Safdari *et al.*, 2017; Sakthipriya *et al.*, 2016). It can also take in and use heavy metals such as copper, iron, magnesium, zinc and chromium (Awasthi *et al.*, 2015; Kang *et al.*, 2015; Silva *et al.*, 2009). These properties make it a suitable organism for bioremediation, and it has been effectively utilised to remove environmental contaminants such as xenobiotics.

P. aeruginosa can also be employed in the production of desirable molecules. These include polyhydroxyalkanoates (PHAs), used in biodegradable plastics and in the pharmaceutical industry for drug delivery (Fernández *et al.*, 2005; Singh & Mallick, 2009). Another class of products are the biosurfactant molecules, rhamnolipids, useful as a more environmentally friendly alternative to other synthetic biosurfactants and detergents (Maier & Soberon-Chavez, 2000; Nitschke & Costa, 2007; Soberón-Chávez *et al.*, 2005). *P. aeruginosa* also produces useful enzymes when grown in the presence of certain nutrients. It can therefore be used in fermenters to generate lipases and proteases (Mahanta *et al.*, 2008; Sharon *et al.*, 1998).

The principle behaviour which makes *P. aeruginosa* a nuisance and even a hazard in industry is its ability to form biofilms. This will be discussed in greater detail in section 1.4, but essentially means that the bacterium forms thick, sticky masses which are difficult to eliminate and rapidly spread (Meliani & Bensoltane, 2015). This results in contamination in the food industry, the water supply (Geldreich *et al.*, 1972; Moritz *et al.*, 2010; Raposo *et al.*, 2017) and in home appliances such as dishwashers and washing machines (Brands & Bockmühl, 2015; Raghupathi *et al.*, 2018; Sánchez-Carrillo *et al.*, 2009)

1.1.3.2 *P. aeruginosa* as a pathogen

P. aeruginosa is recognised as an important human pathogen. Its high prevalence in natural and industrial environments means that the average person will frequently encounter multiple strains in their life-time. However, *P. aeruginosa* normally only becomes a problem for people with impaired immune defences. It can take advantage of a breach in the body's natural barriers, or overcome a suppressed or abnormally functioning immune response (Goldberg, 2010).

P. aeruginosa has been isolated from a number of different body sites (Berghmans *et al.*, 2003; Monsó *et al.*, 1995; Nicotra *et al.*, 1995; Oliver *et al.*, 2000; Papi *et al.*, 2006; Smith *et al.*, 1996). One group of high risk patients are those who are intubated with a respiratory ventilation device. Ventilator associated pneumonia (VAP) is a serious condition, which affects the critically ill. Unfortunately, there is a high incidence of antibiotic resistance/tolerance which is mainly attributed to biofilm growth (Ramirez-Estrada *et al.*, 2016). This begins with the lumen of the tracheal tube in the upper respiratory tract and progresses down into the lower airways, instigating acute leucocytosis and fever (Fricks-Lima *et al.*, 2011). Less aggressive than VAP, but still a significant health concern, are catheter-associated urinary tract infections (CAUTI). These also show a high degree of biofilm mediated antibiotic tolerance (Ramirez-Estrada *et al.*, 2016). Like VAP, biofilm centred infections begin in the catheter lumen and can migrate into the bladder and eventually via the ureter to colonise and damage the kidneys (Cortese *et al.*, 2018).

To underline the frequency of CAUTI, up to 25% of hospitalised patients rely on catheters during their stay and residents of nursing homes may need this intervention for months (Warren, 2001; Warren *et al.*, 1989). Of these, an estimated annual mortality of 7, 500 is associated with infection of the urinary tract (Stamm, 1991). After *E. coli* and *Enterococci, P. aeruginosa* is the most common bacterium associated with CAUTI (Kunin, 1994). As yet, *P. aeruginosa* CAUTI biofilms are dealt with by removing the infected catheter and replacing it with a new one. This is however limited in success, as infection of the new catheter can quickly occur (Costerton *et*

al., 1995; Stewart & Costerton, 2001). Alternative strategies are thus needed to treat CAUTI biofilms more effectively.

P. aeruginosa can also cause soft tissue infections. Two examples of this are burn wound infections and diabetic wounds infections involving ulcerated lower limb lesions. Burn wound infections tend to be more aggressive, with *P. aeruginosa* inducing upregulation of acute phase virulence factors (Turner *et al.*, 2014). In chronic wounds, *P. aeruginosa* biofilms have been isolated in combination with other opportunistic pathogens. Interestingly, *P. aeruginosa* has been isolated, deeper within the lungs than its co-infecting neighbours, suggesting that it is better able to cope with a lack of oxygen than other opportunists such as *S. aureus* (Kirketerp-Møller *et al.*, 2011).

P. aeruginosa constitutes a problem for cystic fibrosis (CF) patients. Risk of infection increases with age and the majority of patients are colonised by the time they reach their 18 years of age ("Cystic Fibrosis Patient Registry ", 2015; Filkins & O'Toole, 2015). Once infected, aggressive antibiotic therapy is commenced in order to eliminate the invading strain from the patient's respiratory tract. This is effective up to a point, but inevitably there comes a day when the bacterium is not cleared using this strategy and antibiotics play more of a role suppressing numbers than removing the infection entirely. *P. aeruginosa* is far from the only CF respiratory pathogen, but it tends to dominate the microbiota in late stage CF lung disease (Acosta *et al.*, 2018; O'Toole, 2018), representing a source of evidence linking it to disease progression. *P. aeruginosa* is hugely successful at adapting to the CF lung environment, typically forming heavily mucoid biofilms containing alginate, resistant to neutrophil attack and antimicrobial penetration. It migrates deep within the viscous mucus layer covering the airway epithelia, an environment which becomes increasingly hypoxic (Worlitzsch *et al.*, 2002).

The wide variety of infection sites colonised by *P. aeruginosa* demonstrates its flexibility both metabolically and in the coordination of a tailored virulence strategy. The quorum sensing, a global regulatory system involved in this adaptability will be discussed in detail in section 1.2.

1.1.4 Virulence

P. aeruginosa produces a multitude of virulence factors including pyocyanin, rhamnolipids, elastase, pyoverdine and pyochelin (Lau *et al.*, 2004; Pearson *et al.*, 1997; Zulianello *et al.*, 2006), toxins like exoenzyme S, phospholipase C, exotoxin A that are all regulated by quorum sensing (Khalifa *et al.*, 2011). Table 1.1 summarises the common virulence factors produced by *P. aeruginosa* and identifies regulation by the QS system where applicable. The wide variety of infection sites colonised by *P. aeruginosa* demonstrates its flexibility both metabolically and in the coordination of a tailored virulence strategy. The regulation of the sessile/biofilm phenotype and the alternative virulent/motile behaviour is controlled by a complex series of interconnected processes (Balasubramanian *et al.*, 2012; Moradali *et al.*, 2017) summarised in Figure 1.1.

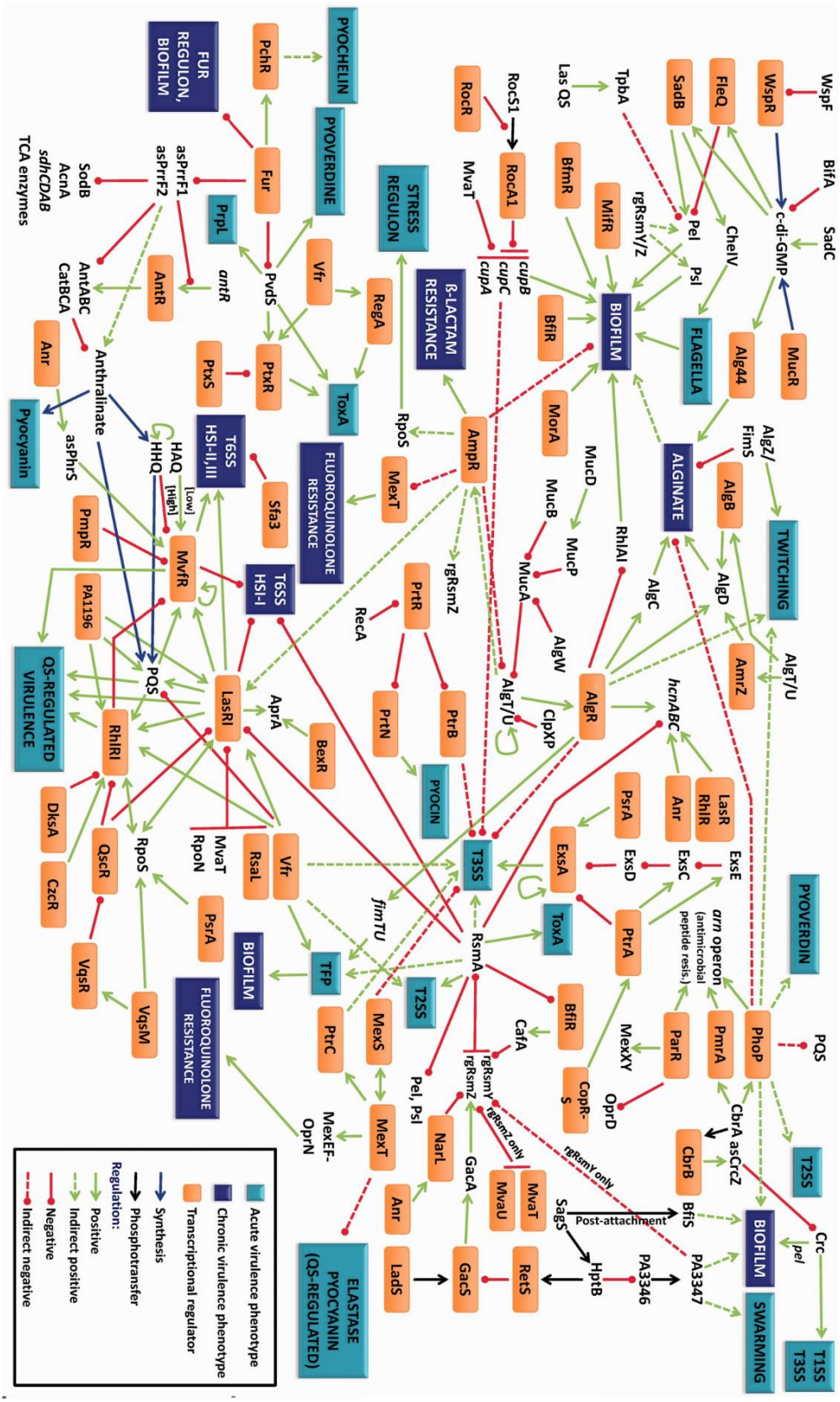

Figure 1.1 The *P. aeruginosa* phenotype regulatory network. From (Balasubramanian *et al.*, 2012).

Table 1.1 Virulence factors produced by *P. aeruginosa*

Virulence Factor	Description	Reference
Exoproteases	Including alkaline protease, protease IV and small protease. Disruptive effect on several components of the immune system	(Suter, 1994) (Marquart *et al.*, 2005) (Engel *et al.*, 1998)
Elastase	Attacks cellular tight junctions Includes elastase A (LasA) and elastase B (LasB)	(Wretlind & Pavlovskis, 1983)
Exoenzymes	Includes exoenzyme S, U and Y Cytotoxic	(Iglewski *et al.*, 1978; Sato *et al.*, 2003)
Exotoxin A	Disrupts protein synthesis and induces apoptosis	(Michalska & Wolf, 2015)
Phospholipase C	Phosphate scavenging Hydrolysis of phosphatidylcholine	(Meyers *et al.*, 1992)
Lipopolysaccharide (LPS)	Resistance to phagocytosis	(Darveau & Hancock, 1983; Rocchetta *et al.*, 1999)
Pyocyanin	Cellular toxin Role in redox balancing	(Dietrich *et al.*, 2008; Lau *et al.*, 2004)
Pyochelin	Siderophore, iron chelation	(Lamont *et al.*, 2009)
Pyoverdin	Ion chelator for iron and assorted other (mainly divalent) biologically relevant ions	(Lamont *et al.*, 2009)
Rhamnolipids	Surfactant involved in surface motility (swarming), biofilm development and immune defence modulation	(Itoh *et al.*, 1971; Pearson *et al.*, 1997)
Flagella	Motility (swarming and swimming) Biofilm formation and dispersal	(Feldman *et al.*, 1998; O'Toole & Kolter, 1998a)
Type IV pili	Twitching motility Role in biofilm structure	(Costerton *et al.*, 1999)
Type III Secretion System	Toxin transport Effector proteins production and release	(Hauser, 2009)
Cyanide	Toxin	(Williams *et al.*, 2006)

1.2 QUORUM SENSING IN BACTERIA

Quorum Sensing (QS) is a bacterial cell-to-cell communication system that coordinates gene expression as a function of cell population density. QS cells produce and secrete particular signal molecules (QSSMs) also herein referred as autoinducers (AIs). Once a threshold concentration of AI has been detected, bacteria synchronize the expression of specific QS dependent genes in order to benefit the whole population.

At low cell densities (LCDs) the AIs do not reach the necessary threshold concentration, and thus the cells express genes for individual behaviours. In contrast, high cell densities (HCDs) result in high AI concentrations which accumulate in the environment and lead to expression of those genes required for cooperative behaviours. A wide number of physiological processes are under QS control including virulence factor and antibiotic production, bioluminescence, sporulation, motility, conjugation, competence, and biofilm development (Miller & Bassler, 2001; Williams *et al.*, 2007). Careful coordination of these processes gives bacteria an increased survival advantage and facilitates beneficial interactions in natural habits.

Gram-negative and Gram-positive species employ different QS communication circuits (Figure 1.2). Gram-positive strains usually produce autoinducing peptides (AIPs) as signalling molecules whereas Gram-negative bacteria typically use heterocyclic molecules such as acylated homoserine lactones (AHLs) and 2-alkyl-4-quinolones (AQs) (Figure 1.3) (Higgins *et al.*, 2007; Ji *et al.*, 1995; Wei *et al.*, 2011; Williams & Cámara, 2009).

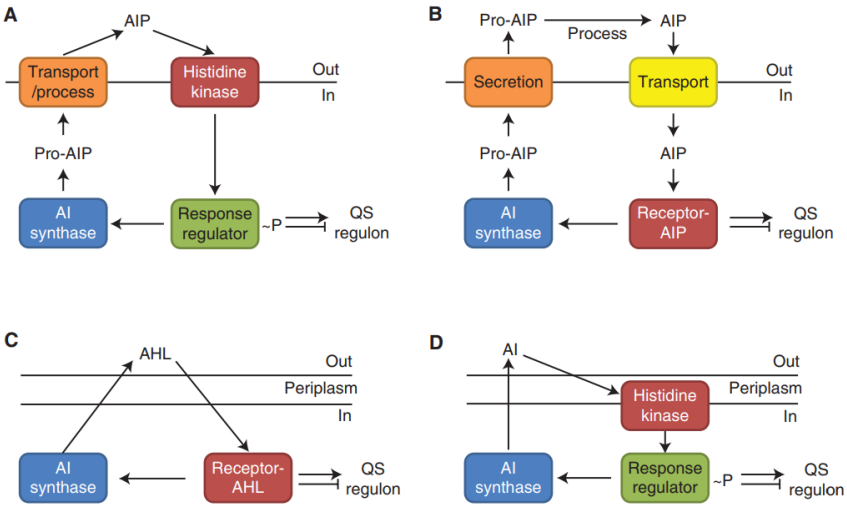

Figure 1.2 Schematic representation of QS circuits. Gram-positive circuits: (A) two-component signalling, (B) an AIP-binding transcription factor. Gram-negative circuits (C) a LuxI/LuxR-type system, (D) two-component signalling. From Rutherford and Bassler (2012)

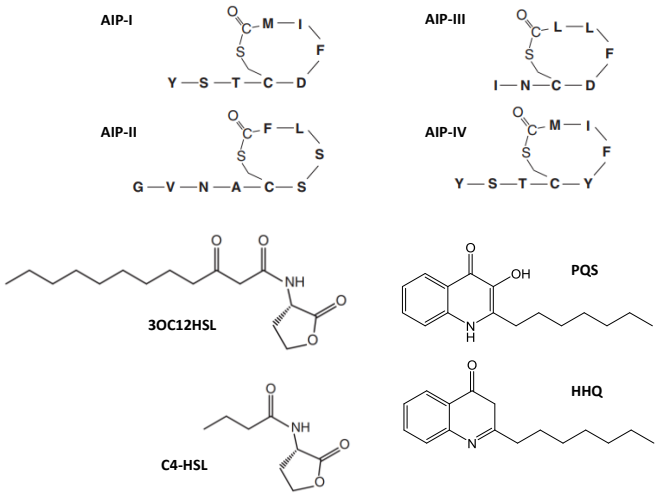

Figure 1.3 *S. aureus* AIPs (I-IV) and *P. aeruginosa* QSSMs AHLs (3OC12HSL and C4-HSL) and AQs (PQS and HHQ).

1.2.1 Quorum Sensing in Gram-positive bacteria

In HCD conditions, Gram-positive bacterial AIPs bind and activate two-component signal transduction pathways (Havarstein *et al.*, 1995). The binding of an AIP induces the autophosphorylation of the membrane bound sensor kinase that passes a phosphoryl group to a cytoplasmic response regulator protein (Hoch *et al.*, 1995; Inouye & Dutta, 2002; Simon *et al.*, 2007). The phosphorylated response regulator acts as a transcriptional regulator and activates the expression of QS target genes, usually grouped in an operon which includes the histidine kinase receptor, response regulator, pro-AIP peptide and transporter (Novick & Geisinger, 2008). These last two elements are characteristic of Gram-positive QS systems: AIPs are secreted and synthesized from precursor peptides (pro-AIP) by membrane transporters in *S. aureus* (Havarstein *et al.*, 1995; Magnuson *et al.*, 1994; Mayville *et al.*, 1999; Otto, 2004). The phosphorylation of the receptor triggers the transcription of the QS target genes, which results in a positive self-induction cycle that leads bacteria to collectively switch from a LCD to a HCD expression program.

1.2.1.1 AIP signalling in *Staphylococcus aureus*

The *agr* QS circuit in *Staphylococcus aureus* is the paradigmatic example of a Gram-positive QS system (Figure 1.4). Firstly, the pre-AIP encoded by the *agrD* gene and the AgrB transporter generate the peptide thiolactone by truncation and cyclization to form the mature AIP that will be secreted extracellularly (Ji *et al.*, 1995; Saenz *et al.*, 2000; Thoendel & Horswill, 2009, 2010). In HCD conditions the AIP is detected by AgrC located at the membrane, stimulating autophosphorylation of the cytoplasm domain and transferring a phosphate group to the response regulator AgrA. The phosphorylated AgrA activates the espression of the *agrBDCA* operon called RNAII (Lina *et al.*, 1998; Novick *et al.*, 1995), and the P3 promoter of *hld*, related to the δ-hemolysin and RNAIII (Janzon & Arvidson, 1990; Novick *et al.*, 1993). This regulatory RNA is an important element for *S. aureus* pathogenicity since it activates the production of α-toxin and represses the expression of *rot*, leading to more virulence factor production, and down-regulation of surface proteins such as the

fibronectin-binding proteins FnbA and FnbB and immunoglobulin-binding protein A (Dunman *et al.*, 2001; Geisinger *et al.*, 2009; Morfeldt *et al.*, 1995; Said-Salim *et al.*, 2003).

Therefore, activation of the *agr* system promotes virulence while discouraging the expression of colonization factors (Boles & Horswill, 2008; Vuong *et al.*, 2000). This regulatory cascade inhibits biofilm formation in the HCD state, while in the LCD state biofilm development is promoted. Consequently, in LCD conditions, *S. aureus* has time to establish a biofilm community, while in HCD it can secrete virulence factors and allow their diffusion in the host by inactivating surface colonization factor proteins (Yarwood *et al.*, 2004).

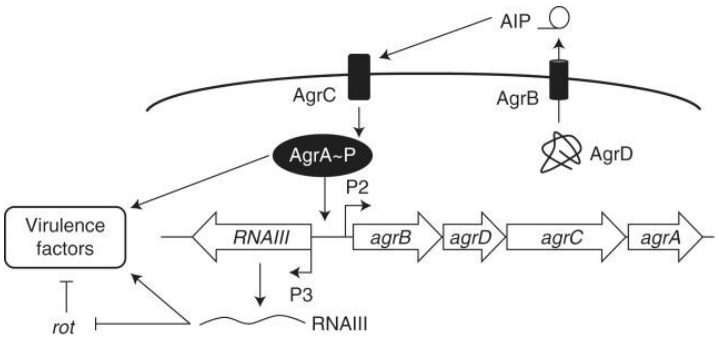

Figure 1.4 A canonical Gram-positive two-component-type QS system. From Rutherford and Bassler (2012).

One unique feature of the *S. aureus agr* quorum sensing system is the strain-to-strain hypervariability in *agrD*, *agrB* and *agrC* genes. This phenomenon implies that the different AIPs can only activate QS by binding with their cognate AgrC sensor kinase (Dufour *et al.*, 2002). If a receptor detects a non-cognate AIP, the interaction may result in QS inhibition (Jarraud *et al.*, 2011). This feature allows *S. aureus* to establish a "priority order" during infection: the first invading strain can activate its own QS cascade while "competitors" are inhibited. *S. aureus* can also be categorized in 4 specific groups (I-IV) based on the variability of AIP structure (Figure 1.4)(Ji *et al.*, 1997; MDowell *et al.*, 2001).

1.2.1.2 The extracellular processing of AIPs in *B. cereus*

In other Gram-positive bacteria, the processing of pro-peptides is mediated by extracellular proteases rather than membrane proteins such as AgrB from *S. aureus*. Pro-AIPs are secreted and imported back in the cytosol as mature AIPs to bind to transcription factors. In *Bacillus cereus* (Figure 1.5), for instance, a secretory system is able to export the precursor peptide PapR, which is processed into the mature signal heptapeptide by the extracellular protease NprB (Pomerantsev *et al.*, 2009). The AIP is taken up into the bacterium via the Opp permease (Gominet *et al.*, 2001), it will modify the conformation of the DNA-binding protein PlcR, enabling the transcription of *plcR* and *papR* genes and the divergent gene *nprB* (Declerck *et al.*, 2007; Okstad *et al.*, 1999). In addition to creating a feedback circuit for QS gene expression, the PlcR-AIP complex activates and regulates a plethora of extracellular proteins such as phospholipases, proteases, enterotoxins and haemolysins (Agaisse *et al.*, 1999; Gohar *et al.*, 2008; Lereclus *et al.*, 1996). Finally, the specificity of PapR and AIP binding sites allows the classification of *B. cereus* in four groups (Slamti & Lereclus, 2005) and the low-compatibility of ligands suggests the presence of an inter-species competition mechanism, as in *S. aureus*.

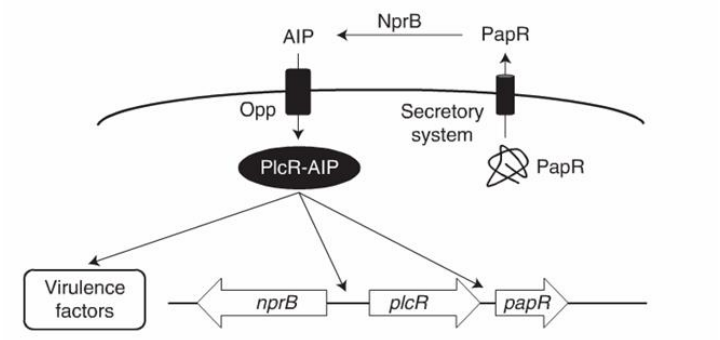

Figure 1.5 *B. cereus* QS circuit. From Rutherford and Bassler (2012).

1.2.2 Quorum Sensing in Gram-negative bacteria

1.2.2.1 LuxIR-like QS systems: from *V. fischeri* to *P. aeruginosa*

This basic regulatory circuit is the most studied QS system since the finding that the bioluminescence of the marine symbiotic species *Vibrio fischeri* is directly linked to bacterial population density within the light organ of the squid *Euprymna solopes* (Kempner & Hanson, 1968). The emission of light in response to population density is dependent on the autoinducer *N*-acyl homoserine lactone concentration, and hence QS (Ruby, 1996). The synthesis of AHLs is determined by LuxI which catalyses acylation and lactonization between the precursor S-adenosylmethionine (SAM) and an acyl carrier protein (ACP). The related *luxI* gene is part of the *luxICDABE* operon and its transcription is mediated by the cytosolic transcriptional regulator LuxR (Engebrecht *et al.*, 1983; Engebrecht & Silverman, 1984). When AHLs achieve a critical threshold concentration, they bind to LuxR and its activation forms an autoinduction positive feedback loop culminating in an amplification of signal molecule production and luminescence. AHL molecules, unlike Gram-positive AIPs, are able to passively cross the membrane of bacteria.

A large number of Gram-negative bacterial species possess LuxI/LuxR homologs (Case *et al.*, 2008) and each strain produces different kinds of AHLs, which have different side chain lengths and substituents (Fuqua *et al.*, 2001). Moreover, the LuxR proteins have different binding pockets to accommodate a specific AHL, resulting in a highly specific intraspecies cell-cell communication system (Vannini *et al.*, 2002; Watson *et al.*, 2002).

1.2.3 *P. aeruginosa* and QS

QS exerts a crucial role in the lifestyle of *P. aeruginosa* due to its control over a wide number of genes. This pathogen uses three main QS systems, which are mutually and hierarchically connected. Two of these employ acylated homoserine lactones (AHLs) as QSSMs, while a third, the PQS system, employs 2-alkyl-4-quinolones (AQs).

1.2.3.1 The AHL-signalling systems

Both LasI and RhlI are autoinducer synthases and LasI produces *N*-(3-oxododecanoyl)-L-homoserine lactone (3OC12HSL) while RhlI produces *N*-(butanoyl)-L-homoserine lactone(C4HSL) (Latifi *et al.*, 1996). The LasR protein (LuxR homologue) binds to 3OC12HSL when the molecule reaches a critical threshold level, depending on the relative rates of production and turnover of the AHL, as well as RhlR and C4HSL. The LasR/3OC12HSL complex activates the transcription of several secreted virulence factors including elastase LasB, protease LasA, exotoxin A and an alkaline protease AprA (Laarman *et al.*, 2012; Park *et al.*, 2000; Pearson *et al.*, 2000; Wolz *et al.*, 1994). LasR activates the *lasI* gene generating a feed-forward loop in which the level of 3OC12HSL is constantly maintained by the transcriptional repressor RsaL. This counteracts the loss of AHLs by diffusion or by pH-dependent lactonolysis (Yates et al. 2002).

Further targets of the LasR/3OC12HSL complex are *rhlI* and *rhlR*, the second *luxI/luxR* homologues in *P. aeruginosa* (Latifi *et al.*, 1996). RhlR binds the second AI, C4HSL, produced by RhlI. This is activated via the RhlR-C4HSL complex itself, which leads to the autoinduction. The RhlR-C4HSL complex also promotes the expression of *aprA* and *lasB*, already controlled by LasR-3OC12HSL, and new target genes encoding for other pathogenicity determinants. These include rhamnolipids, cyototoxic lectins LecA and LecB, exoproteases, elastases, siderophores, cyanide and pyocyanin (Gallagher *et al.*, 2002; Khalifa *et al.*, 2011; Lau *et al.*, 2004; Pearson *et al.*, 1997; Winzer *et al.*, 2000; Zulianello *et al.*, 2006).

Therefore the LasI/LasR circuit activates *rhlI/rhlR* expression, triggering the second circuit. However, as previously mentioned, the large number of regulatory genes involved in QS adds further levels of control.

1.2.3.2 The AQ-signalling system

Apart from the LuxI/LuxR systems, *P. aeruginosa* also uses an autoinducing system dependent on 2-alkyl-4-quinolones (AQs). The Pseudomonas Quinolone Signal (PQS) (2-heptyl-3-hydroxy-4(1*H*)-quinolone) and its precursor HHQ (2-heptyl-4(1*H*)-hydroxyquinoline) are

the major AQs responsible for activating this specific QS pathway and are characterized by a C7 alkyl chain (Figure 1.14). Albeit different C9- chained AQs like NHQ (2-nonyl-3-hydroxy-4*H*-quinolone) and C9-PQS (2-nonyl-3-hydroxy-4*H*-quinolone) are as active as the C7 congeners (Diggle *et al.*, 2007; McGrath *et al.*, 2004; Wade *et al.*, 2005; Xiao *et al.*, 2006b). The biosynthesis of AQs depends on the *pqsABCDE* operon, regulated by the LysR-type transcriptional regulator PqsR (MvfR) (Figure 1.6) (Gallagher *et al.*, 2002; Xiao *et al.*, 2006b). PqsA encodes for an anthranilate coenzyme A ligase that activates anthranilate (Coleman *et al.*, 2008), while PqsB and PqsC are acyl carrier proteins that elongate the acyl side chain of AQ precursors (Dulcey *et al.*, 2013). PqsE, a putative metallo-β-lactamase (Yu *et al.*, 2009) acts as a thioesterase hydrolyzing 2-aminobenzoyl-acetylcoenzyme A to form 2-aminobenzoylacetate, the HHQ precursor, however the thioesterase TesB may act as a substitute when PqsE is inactived; its deletion reduces production of virulence factors such as pyocyanin and rhamnolipids (Deziel *et al.*, 2005; Diggle *et al.*, 2003; Farrow *et al.*, 2008; Rampioni *et al.*, 2010). Recent transcriptome studies revealed its PQS-independent control over expression of pyocyanin and the MexGHI-OpmD efflux pump, however the way by which PqsE controls virulence factor expression in an AQ independent manner has yet to be elucidated (Diggle *et al.*, 2003; Rampioni *et al.*, 2016).

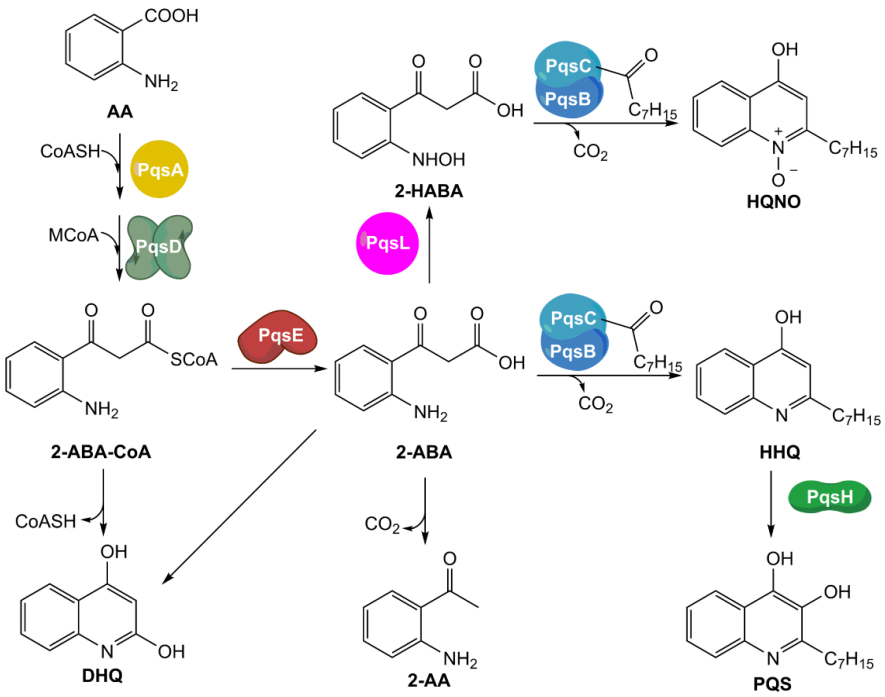

Figure 1.6 Alkylquinolones biosynthesis AA, anthranilic acid; CoASH, Coenzyme A; MCoA, malonyl-CoA; 2-ABA-CoA, 2-aminobenzoylacetyl-CoA; 2-ABA, 2-aminobenzoylacetate; DHQ, dihydroxyquinoline; 2-AA, 2-aminoacetophenone; 2-HABA, 2-hydroxylaminobenzoylacetate; HHQ, 4-hydroxy-2-heptylquinoline; HQNO, 4-hydroxy-2-heptylquinoline-N-oxide; PQS, Pseudomonas Quinolone Signal, 2-heptyl-3,4-dihydroxyquinoline. From Allegretta *et al.* (2017).

PqsR also activates transcription of anthranilate synthase genes *phnAB* placed adjacent to the *pqsABCDE* operon and before *pqsR*. The *pqsH* and *pqsL* genes are also involved in AQ biosynthesis, but their location is far from the other AQ system genes. The monoxygenase PqsH introduces a hydroxyl group at position 3 of HHQ quinolone ring, converting it to PQS which has additional functionalities compared with HHQ. For example, PQS is responsible for microvesicle formation, interacting with the Lipid A side of LPS (Mashburn-Warren *et al.*, 2008) and iron chelation, inducing expression of the pyoverdine and pyochelin (Diggle *et al.*, 2007). PqsR possesses a ligand-binding domain, described in Ilangovan *et al.* (2013). This study described the crystal structure of the PqsR co-inducer/ligand binding domain ($PqsR^{CBD}$) and a complex of PqsR with its agonist NHQ (Figure 1.7). NHQ and the other AQs localize within the co-ligand binding domain assuming the same pose: the bicyclic ring is buried within a region called pocket B whilst the alkyl chain extends into the A pocket, the extension of which may determines activity. Also, structure-activity relationship studies led to the generation of new AQ analogues such as 7Cl-

PQS, which is the most potent PqsR agonist so far described (EC_{50}=0.01 μM).

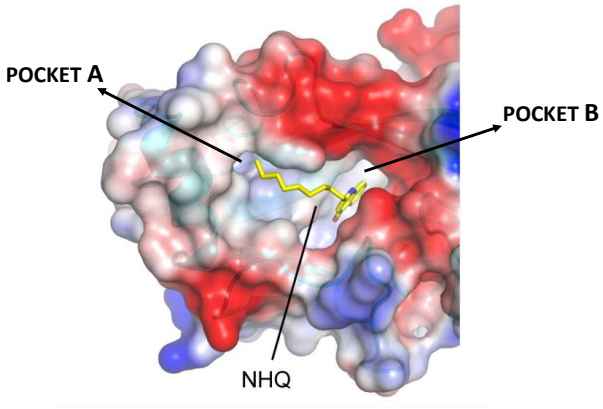

Figure 1.7 Charge surface representation of the PqsR^{CBD} pockets A and B with NHQ. The colours discriminate residues by pH, acidic (red) and basic (blue). Modified from Ilangovan *et al.* (2013).

The AQ dependent system is regulated by Las and Rhl circuits, thus it is an additional link in these two *P. aeruginosa* QS systems. For instance, RhlR/C4HSL negatively regulates *pqsR* and *pqsA,* whereas the transcription of *pqsR* is positively regulated by LasR/3OC12HSL (Diggle *et al.*, 2007; Xiao *et al.*, 2006a). In addition, the PqsR/AQ complex triggers the Rhl circuit by enabling the synthesis of C4-HSL, only after activation of the Las cascade (Figure 1.8). This particular feed-forward loop between the circuits produces accelerated pulse-like responses (Alon, 2007).

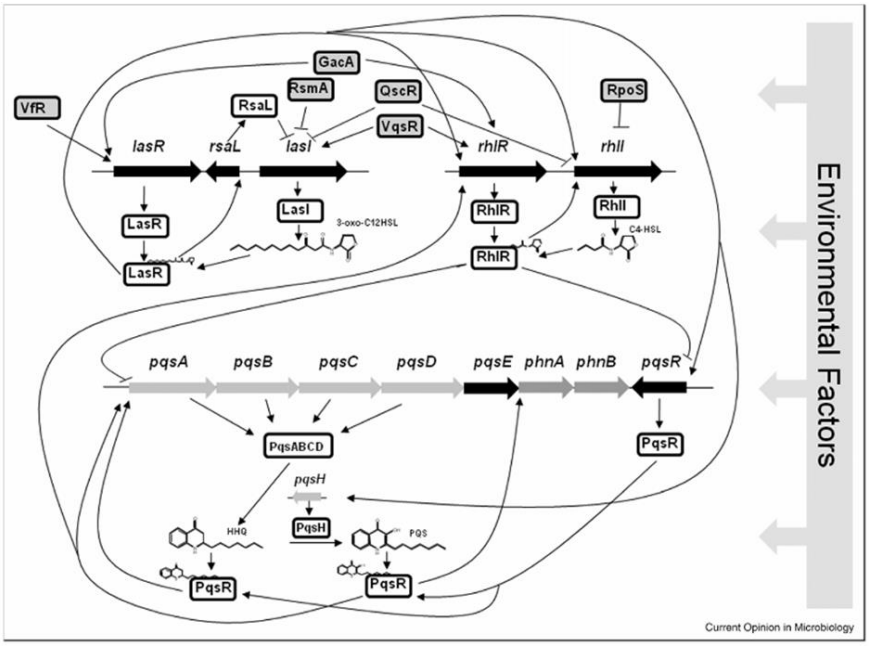

Figure 1.8 Representation of the AHL-dependent and AQ-dependent QS network in *P. aeruginosa*. From Williams and Cámara (2009).

1.3 INHIBITING QUORUM SENSING: STRATEGIES AND TARGETS

Interception of QS cell-cell communication systems is a promising strategy for preventing biofilm development and bacterial virulence. Common antibiotics exert their action on vital biochemical pathways which lead to the insurgence of antimicrobial resistance by selective pressure (Davies & Davies, 2010). For this reason, QS is considered a promising target for the attenuation of bacterial activity with a limited risk of resistance outbreak (Williams, 2017).

QS inhibition can be achieved by blocking cell-cell communication, a phenomenon known as "quorum quenching" (QQ). There have been a variety of approaches to QQ, which can be broadly divided into the following categories: inactivation of AIs by sequestration or direct degradation, disruption of signal molecule biosynthesis, and inhibition of AI-receptor binding (Figure 1.9) (Rampioni *et al.*, 2014).

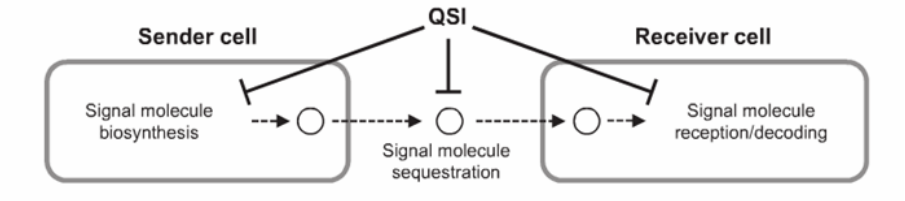

Figure 1.9: Potential targets within a generalized QS system. From Rampioni *et al.* (2014)

1.3.1 Inactivation of AI signals

AIs can be disrupted before reaching the threshold required for QS activation. The main strategy is to degrade the AHLs by enzymatic hydrolysis. Lactonases hydrolyze the HSL ring of AHLs, while acylases are able to break the amide bond of AHLs in an acyl chain length-Dependent Manner (Yates *et al.*, 2002). Therefore the action of acylases is more specific than lactonases which can disrupt a wider range of AHLs (Hong *et al.*, 2012). Enzymatic or alkaline lactonolysis are identical and both can be reversed by acidification (Yates *et al.*, 2002).

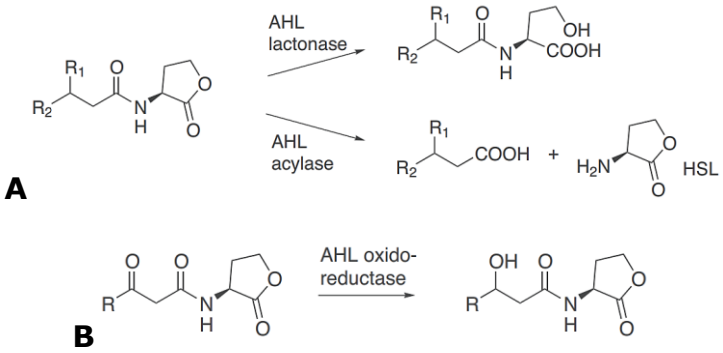

Figure 1.10 Examples of mechanisms of AHL-degrading enzymes. A. AHL lactonase and acylase reactions. B. AHL oxido-reductase reaction. From Fetzner (2015).

Another strategy consists of modifying or changing the activity rather than hydrolyzing the AHL by the use of oxidases and reductases (Chan *et al.*, 2011). Lastly, antibodies (Kaufmann *et al.*, 2006) and molecularly-imprinted polymers (Piletska *et al.*, 2011) have been developed to specifically sequester AHLs. In *S. aureus*, signal sequestration has revealed itself to be an efficient strategy since AIPs proved to be unexpectedly resistant to proteases. Indeed, monoclonal antibodies for AIP-IV for *S. aureus* reduced virulence in a mouse skin infection model (Park *et al.*, 2007).

1.3.2 Inhibition of AI biosynthesis

Compared to the other strategies, relatively few biosynthesis inhibitors have been developed. However, this is thought to be a promising approach as several studies present evidence that the deletion of genes involved in AI synthesis negatively affects biofilm formation. In *P. aeruginosa* for example, mutation of *lasI* abolishes synthesis of 3OC12HSL and results in the formation of thinner biofilms where cells are more closely packed compared to the wild type (Shih & Huang, 2002). One method used to disrupt AHL biosynthesis is through inhibition of *S*-adenosyl-methionine (SAM) and/or fatty acid biosynthesis. To produce AHLs, LuxI type proteins transfer an acyl group from an acylated acyl carrier protein to the methionyl amino group of *S*-adenosyl-methionine (SAM). *S*-adenyl-homocysteine (SAH), sinefungin, 5-methylthioadesine (MTA), SAM analogues and cycloleucine (a SAM biosynthesis inhibitor) have been used to inhibit AHL production in this manner (Hanzelka & Greenberg, 1996).

In *P. aeruginosa,* the antibiotic azithromycin reduces bacterial adhesion and interferes with AHL production (Favre-Bonte *et al.*, 2003; Tateda *et al.*, 2001). Furthermore, PqsA, the first enzyme in the PQS biosynthetic pathway (Amara *et al.*, 2009), is a promising target for virulence attenuation. It is required for AQ production and its deletion negatively impacts biofilm formation (Allesen-Holm *et al.*, 2006; Kim *et al.*, 2015; Rampioni *et al.*, 2010). PqsA is a CoA-ligase which converts anthranilic acid into anthraniloyl-CoA (Figure 1.6) (Amara *et al.*, 2016; Amara *et al.*, 2009). The first approach at inhibiting this enzyme was to expose it to substrate analogues, for example halogenated anthranilate derivatives. For an effect to be detected, a high concentration (millimolar) of the inhibitor was required and thus these anthranilate analogues are not sufficiently active to be therapeutically useful (Coleman *et al.*, 2008; Lesic *et al.*, 2007).

Another approach executed by Ji *et al.* (2016) designed and created anthraniloyl-AMP analogs by replacing the phosphate bridge present in the native molecule with a sulphonamide based linker. When presented to *P. aeruginosa* in an in vitro enzymatic assay, the inhibitors only reduced AQ biosynthesis and associated pyocyanin production to a small extent, suggesting that PqsA was only being weakly inhibited, that there was a compensating mechanism, or (most likely) the molecules were unable to permeate the cell envelope efficiently (Chang *et al.*, 2014; Ganin *et al.*, 2013; Ji *et al.*, 2016).

The future looks more promising for the design of more powerful PqsA inhibitors which are able to penetrate the cell envelope. Witzgall *et al.* (2017), has now resolved the crystal structure of the PqsA ligand binding domain. This will facilitate greater opportunities for *in silico*-based design and development of inhibitors.

1.3.3 Targeting the QSSM receptors: deception of the signal transduction cascade

Several inhibitors have been generated by modifying the structure of native QS agonists in order to obtain an antagonist that binds to but does not activate the QSSM receptor. Focusing on *P. aeruginosa*, many AHL analogues have been discovered that are able to competitively inhibit LuxR proteins (Figure 1.11). The compounds S7 and mBTL are excellent antagonists of AHLs. The first is solely able to antagonize LasR, while mBTL is effective against both LasR and RhlR.

An alternative approach is to recognize accessible sites in the binding pocket that could be susceptible to covalent modification. For example, compound 1 has been developed by following this concept and it is able to modify an accessible cysteine residue in the LasR binding site (Figure 1.11) (Amara *et al.*, 2009).

Many natural products that quench QS have been described. Some organisms have developed molecular deception methods in response of the widespread use of QSSMs by bacteria. Many of these compounds have shown to have inhibitory effects on AHL-dependent QS. For example allicin and ajoene were extracted from garlic and some *Penicillum* species were identified to negatively affect QS (Rasmussen *et al.*, 2005). Similarly, bergamottin and dihydroxybergamottin isolated from grapefruit and pomelos have exhibited inhibitory effects on the AHL-dependent system, reducing biofilm formation in *P. aeruginosa* (Adonizio *et al.*, 2008; Girennavar *et al.*, 2008).

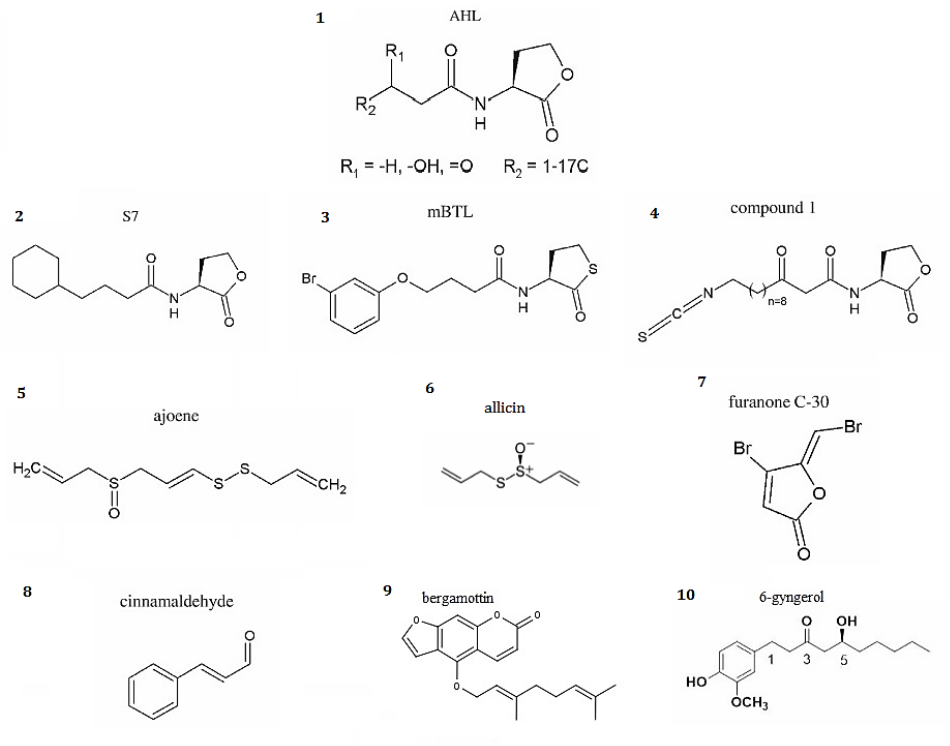

Figure 1.11 Structures of AHL (1) and AHL-dependent QS system inhibitors (2-10)

1.3.3.1 The furanone molecules as inhibitors of QS in *P. aeruginosa*

Moreover, some of the earliest natural molecules discovered to inhibit AHL QS are the furanones from the marine macroalga *Delisea pulchra* (Hentzer *et al.*, 2002). The particular biological properties of this alga were reported by Pettus Jr *et al.* (1977) which described this organism as "remarkably free of normal fouling organisms (micro and macro) which colonize other algae in the immediate area". A number of halogenated furanones of the compounds produced by *Delisea pulchra* have been termed fimbrolides (König *et al.*, 1995). A specific class of fimbrolides (Figure 1.12-1), the brominated furanones, have been described to inhibit the AHL-mediated QS (Givskov *et al.*, 1996). In particular, they were shown to act as antagonists of the *Vibrio fischerii* LuxR receptor (Manefield *et al.*, 1999). These compounds also inhibited QS-dependent phenotypes in other species like *V. harveyi, Erwinia carotovora*, *Serratia liquefaciens* and *Chromobacterium violaceum* (Givskov *et al.*, 1996; Manefield *et al.*, 2000; Manefield *et al.*, 2001; Martinelli *et al.*, 2004). Nevertheless, the natural brominated furanones exhibited a weak inhibition in LasR-dependent AHL

biosensor tests (Hentzer *et al.*, 2002). C30, a synthetic analogue of these halogenated furanones shown to be a QS antagonist using the same biosensor and to significantly inhibit *P. aeruginosa* QS in a murine lung infection model (Hentzer *et al.*, 2003).

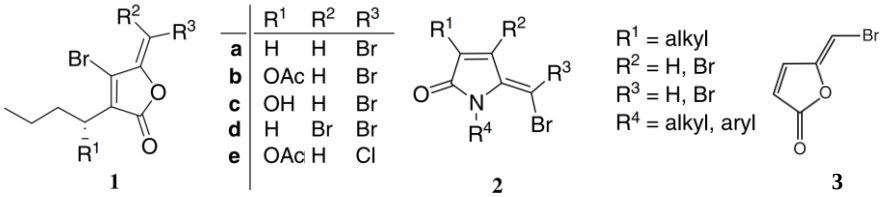

Figure 1.12 Natural fimbrolides from *Delisea pulchra* (1), their synthetic analogues, the dihydropyrrol-2-ones (2) and C-30 furanone (3). Modified From Goh *et al.* (2007)

This has encouraged the synthesis of new compounds for this purpose, such as the 1,5-dihydropyrrol-2-ones (lactams), derived from the modification of the furanone ring of the fimbrolides (Figure 1.12). This modification improves its stability in physiological conditions by reducing the susceptibility of the lactone to ring-opening reactions. Numerous methods for the production of pyrrol-2-ones have been discussed in the literature, (Egorova *et al.*, 2001; Ghelfi *et al.*, 2003; Mase *et al.*, 1999) but many lack the preservation of the halogenated substitutions on the ring that are important for biological activity (Rittschof, 2001). However, an efficient lactone-lactam conversion reaction was developed by Goh *et al.* (2007) that overcomes such limitations. Although some compounds generated with this technique target AHL-mediated QS system, through an *in silico* antagonistic binding with LasR (Goh *et al.*, 2015), other lactams negatively interact with mannitol dehydrogenase (MDH) and extracellular DNA, as described by *in silico* and activity studies in Ye *et al.* (2015).

1.3.3.2 Inhibition of the *P. aeruginosa* PQS System

The LysR-type transcriptional regulator PqsR has been considered as a target for QS inhibition in *P. aeruginosa*. Lu *et al.* (2012) modified the molecule HHQ by modifying the aliphatic chain and the benzene moiety of the quinolone ring thereby identifying a PqsR antagonist (1a and 1b in Figure 1.13). Using an *E.coli* reporter system, a promising inhibitory activity was observed. However, when the inhibitors were tested for their

effect on pyocyanin production by *P. aeruginosa* a disappointingly small effect was seen and accordingly little change to elastase, rhamnolipid and AQ generation occurred (Lu *et al.*, 2012) (Lu *et al.*, 2017). The discrepancy between the two findings was explained by a PqsH mediated oxidation of the quinolone ring, which converted them into potent agonists. At the light of this, a new more potent compound was designed (1c in Figure 1.13)

Another group of PqsR inhibitors has been described by Klein *et al.* (2012). These were modified from N-hydroxybenzamides, with changes to the para-position and triazole scaffold. These also were only weakly inhibitory with one compound (2 in Figure 1.13) showing an IC_{50} of 26 μM (Boles *et al.*, 2005) and another compound (3 in Figure 1.13). showing an IC_{50} of 23.6 μM (Welsh *et al.*, 2015) in *P. aeruginosa*. The production of pyocyanin was slightly affected at these concentrations of inhibitor.

Through a structure-activity design, Ilangovan *et al.* (2013) synthesized a set of natural ligand-derivatives and novel quinazolinone analogues, subsequently analysing their effect on biofilm development and virulence factor production. One of the competitive antagonists developed, 3-NH2-7-Cl-C9-QZN (QZN) (Figure 1.14a), was shown to strongly inhibit PqsR activity, being the first to possess an IC_{50} in low micromolar range. Crystal soaking experiments demonstrated that this compound binds within the $PqsR^{CBD}$ ligand binding pocket similar to the natural agonists, but forms more H-bonds to the side chain of Thr265 and the main chain of Leu207, on its carbonyl group. This tighter binding prevents PqsR from assuming the active conformation for transcriptional regulation (Figure 1.14-B). Indeed, QZN addition reduced the production of pyocyanin, AQs and biofilm in *P. aeruginosa* (Ilangovan *et al.*, 2013). In addition, Starkey *et al.* (2014) and Spero Therapeutics developed a PqsR antagonist which showed efficacy at submicromolar concentrations, additionally having a remarkable impact on virulence determinants although only at concentrations higher than 1 μM (4 in Figure 1.13) (Maura & Rahme, 2017; Zahler, 2016). Further development of these inhibitors has not yet been disclosed. Finally, Soukarieh *et al.* (2018) developed several PqsR inhibitors (5 in Figure 1.13) working in the low micromolar range which were able to inhibit AQs

synthesis, pyocyanin, and inhibit biofilm development in synergy with tobramycin.

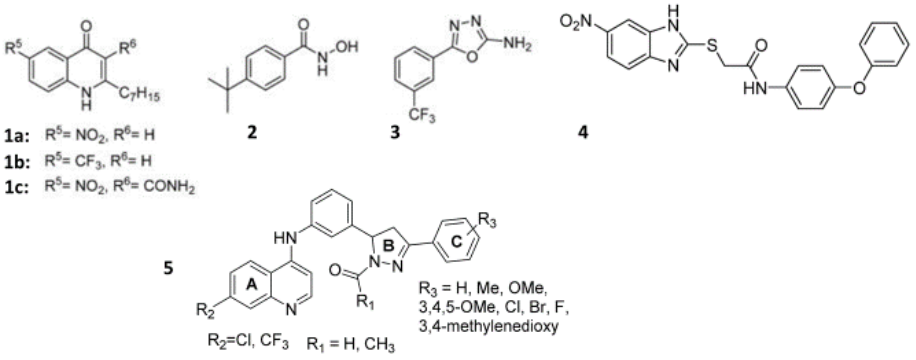

Figure 1.13 Structures of PqsR inhibitors.

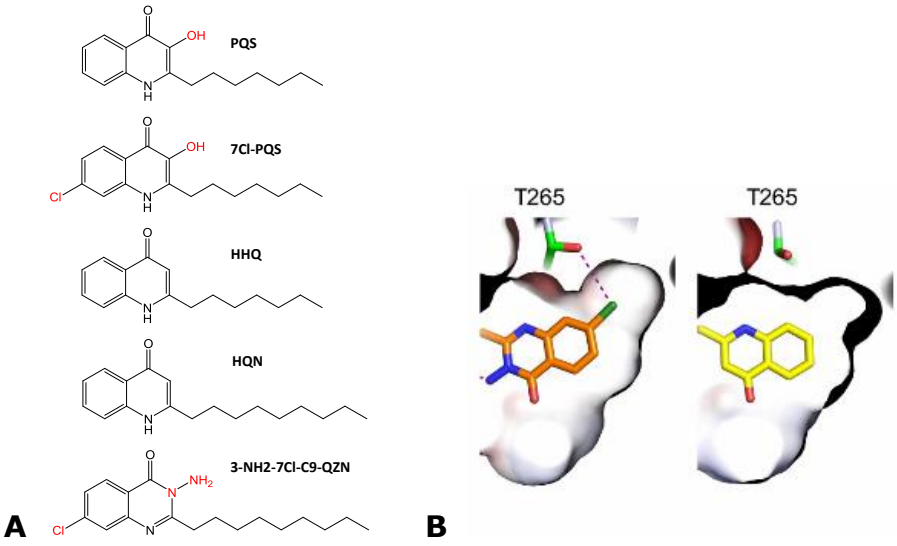

Figure 1.14 A) Structures of the PqsR agonists PQS, 7Cl-PQS, HHQ, NHQ and the PqsR antagonist 3-NH2-7Cl-C9-QZN. B) Orientation of the bicyclic rings of 3-NH2-7Cl-C9-QZN (left) and HQN (right) within the pocket B of PqsR^{CBD}. The dotted line represents the hydrogen bond between Thr265 and Cl which causes a small conformational change. From Ilangovan *et al.* (2013).

1.4 BIOFILM FORMATION

1.4.1 General

When microbes aggregate together to form a structured group of cells which are embedded in a self-produced gel-like substance composed principally of exopolysaccharides and DNA, the community as a whole is termed a biofilm (Donlan & Costerton, 2002). Biofilms are ubiquitous in nature and originate from a multitude of microbial organisms. They can be single or multispecies, and are frequently found in natural environments (Aruni *et al.*, 2015; Tyson *et al.*, 2004).

Bacterial cells in biofilms are more tolerant to host defences and standard antimicrobial treatments, making biofilm development an effective strategy for growth in hostile environments (Stewart & Costerton, 2001). This community-based resistance is thought to have both a structural and biological basis. Penetration of antibacterials is impeded due to their interactions with the outer layers of the biofilm and extracellular polymeric substances (EPS) layer. The cells in the biofilm also show an altered metabolic rate, with cells deeper from the biofilm surface exhibiting reduced metabolic activity (Fux *et al.*, 2005; Stewart & Costerton, 2001). This is illustrated in Figure 1.15 by Stewart and Costerton (2001).

Moreover cells can disengage from the biofilm surface and reverting to a motile state. This allows dispersal into other environments to colonize new surfaces and/or infect new sites (Lindsay & von Holy, 2006; O'Toole & Kolter, 1998b). Thus, biofilms can act as a depot for the generation of repeated colonisation, withstanding the environmental insults which remove their planktonic counterparts (Rasamiravaka *et al.*, 2015).

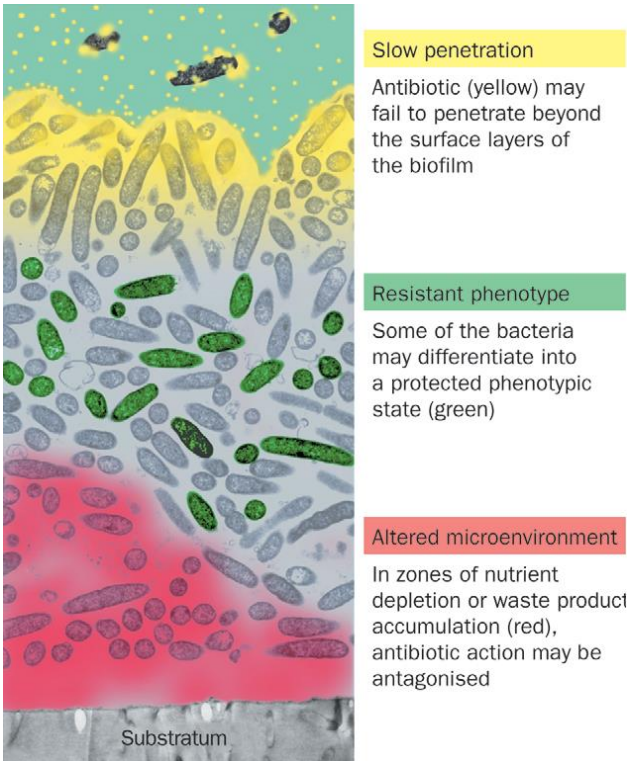

Figure 1.15 How biofilms confer antibiotic resistance. From Stewart and Costerton (2001).

1.4.2 *P. aeruginosa* biofilms

P. aeruginosa biofilms have been found in numerous settings including both industrial and clinical environments (Costerton *et al.*, 1987; Khoury *et al.*, 1992; Watters *et al.*, 2013; Worlitzsch *et al.*, 2002). Although varying depending on the specific environment, they are typically composed of the substances described below and follow the same cyclic growth pattern (O'Toole *et al.*, 2000; Rasamiravaka *et al.*, 2015; Stoodley *et al.*, 2002).

1.4.2.1 The EPS matrix

EPS represents an average of 85% of the total biofilm mass and forms a biological scaffold to structure the encased cells (Rasamiravaka *et al.*, 2015). It is a highly hydrated mixture comprised of exopolysaccharides, extracellular DNA (eDNA), polypeptides and assorted biomolecules such as membrane vesicles (MV) (Flemming *et al.*, 2007; Rasamiravaka *et al.*, 2015; Schooling & Beveridge, 2006). The particular make-up of a biofilm's EPS varies depending on the environment. A classic example of this is the

overproduction of the polysaccharide alginate by mucoid *P. aeruginosa* strains isolated from cystic fibrosis patients (Ciofu *et al.*, 2008). The main components are summarised below.

Three main polysaccharides have been identified in *P. aeruginosa* biofilms: Pel, Psl and Alginate. The polymer Pel is composed of 1-4 linked galactosamine and glucosamine which are partially acetylated. It is positively charged and this probably facilitates interaction with the negatively charged eDNA also present in the matrix. The charge depends on the pH (7 and slightly lower) which represents that of typical microcolony environment (Jennings *et al.*, 2015; Wilton *et al.*, 2016). Psl is a polymer composed of L-rhamnose, D-mannose and D-glucose (Byrd *et al.*, 2009). Showing no charge (unlike Pel) at the aforementioned pH values, crosslinking with eDNA does not occur and thus Psl supports the biofilm in a different manner to that of the other exopolysaccharides (Byrd *et al.*, 2009). Overrepresentation of alginate in biofilm EPS is a feature mainly associated with chronic cystic fibrosis lung infections and arises through a mutation in the *mucA* gene. Alginate is made up of the monomers D-mannuronic acid and L-gluluronic acid and plays a role in fluid and nutrient retention (Ertesvåg & Valla, 1998).

Whitchurch *et al.* (2002) demonstrated the importance of eDNA for the structural integrity of *P. aeruginosa* biofilms by showing their vulnerability to dispersal by detergents, following DNAse I treatment. eDNA facilitates cellular interconnections and together with Type IV pili, helps to align cells within the biofilm (Gloag *et al.*, 2013). eDNA can also be used by the cells as a nutrient, particularly when resources are scarce (Finkel & Kolter, 2001). There is evidence linking the release of eDNA with the PQS system and thus the impaired biofilm production seen in *P. aeruginosa pqs* mutants could be due to a reduced secretion of eDNA (Allesen-Holm *et al.*, 2006; D'Argenio *et al.*, 2002; Thomann *et al.*, 2016; Yang *et al.*, 2007). The PQS system is not the only player involved in eDNA release however and the global regulatory mechanism remains to be discovered (Turnbull *et al.*, 2016). The distribution of eDNA throughout the biofilm is also a process which has yet to be understood completely. Although its release has been shown to be evenly divided throughout the matrix and its structural shape

is dependent on the Psl network (Mann & Wozniak, 2012), other evidence has shown the distribution of eDNA to be located in distinct areas of the biofilm (Parsek & Tolker-Nielsen, 2008; Yang *et al.*, 2007).

Aside from the polysaccharide and eDNA components of a biofilm, this closely associated group of cells is also rich with secreted proteins, membrane vesicles and cyclic β glucans (Wei & Ma, 2013). These have been reported to improve the structural integrity of the biofilm as well as perform functions such as iron sequestration, metabolism under hypoxia, and virulence (Toyofuku *et al.*, 2012).

1.4.2.2 Cellular life

Analogous with multicellular organisms, cells within a biofilm differentiate to perform separate functions which in combination make the biofilm very resilient to external forces and hostile environments (Klausen *et al.*, 2003). Cells furthest from the microcolony surface have an altered, slower metabolism, with a component of these differentiating into persister cells. These deep-lying cells are highly resistant to antibiotics and allow the biofilm to regenerate after such an attack (Ciofu *et al.*, 2017; Wood *et al.*, 2013). Cells at the surface tend to be more metabolically active and show greater motility. A subset of these surface-dwellers are dispersed for the colonisation of new niches (Hall-Stoodley *et al.*, 2004; Mann & Wozniak, 2012). The arrangement of the cells within the biofilm depends largely on the environment; the carbon source, for example, influences whether a mushroom or flat architecture is achieved.

1.4.2.3 Life cycle of the *P. aeruginosa* biofilm

Biofilm growth is a cyclical process requiring a high level of coordination. This process includes reversible attachment, irreversible attachment, structural maturation and dispersal (O'Toole *et al.*, 2000; Stewart, 2003; Stoodley *et al.*, 2002).

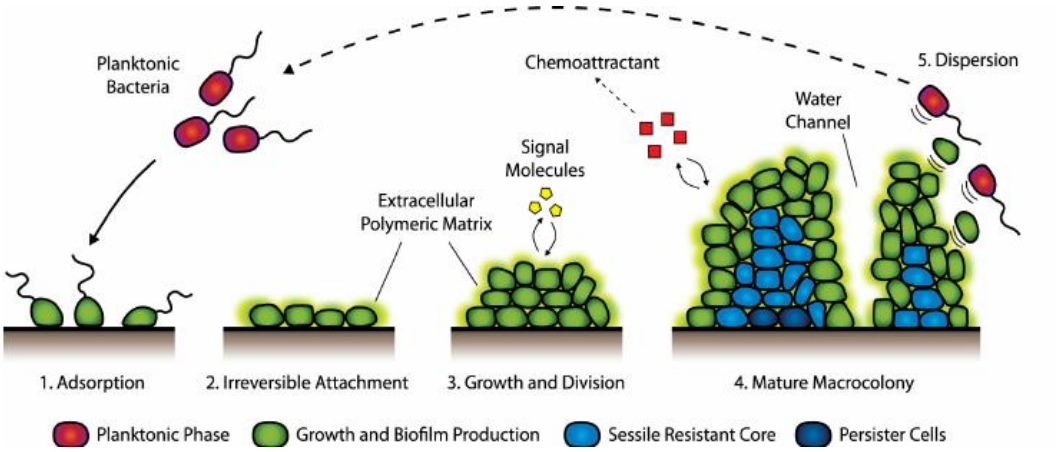

Figure 1.16 Life cycle of a *P. aeruginosa* biofilm. (1) Reversible attachment, (2) irreversible attachment, (3) expansion of microcolonies, (4) maturation, differentiation and dispersal. From Gilmore (2011), adapted from Harrison *et al.* (2005).

1.4.2.3.1 Reversible attachment

Planktonic bacteria encounter a surface or group of cells and form an attachment to it. This process can be facilitated by eDNA, rhamnolipids, flagella, Type I and Type IV pili, but the role these factors play can vary upon the environment (Costerton *et al.*, 1999; Mattick, 2002a; O'Toole *et al.*, 2000; Pamp & Tolker-Nielsen, 2007; Vallet *et al.*, 2004). QS and lectins help coordinate this process (De Kievit *et al.*, 2001; Diggle *et al.*, 2006b; Tielker *et al.*, 2005).

1.4.2.3.2 Irreversible attachment

The attached cells begin the transformation to a sessile, biofilm phenotype. Signals are released and gene expression altered in response to these. Microcolonies begin to form and secretion of the EPS is initiated. Type IV pili and eDNA work in combination to align and combine cells (Allesen-Holm *et al.*, 2006; Gloag *et al.*, 2013; Klausen *et al.*, 2003; Stoodley *et al.*, 2002; Wei & Ma, 2013).

1.4.2.3.3 Maturation

A structured, differentiated community of cells with a developed EPS is formed. The presence of water channels can also be observed at this stage, which are thought to facilitate nutrient acquisition and waste removal (Donlan & Costerton, 2002).

1.4.2.3.4 Dispersal

Some cells near the surface of the biofilm differentiate from a sessile to planktonic state. These cells are then released to find new sites to attach

to and to begin the formation of new biofilm (Chua *et al.*, 2015). The exact nature of this process is still under investigation and involves a combination of molecular signalling and environmental stimuli (Kim & Lee, 2016).

1.4.2.3.5 Global coordination of biofilm development by c-di-GMP

The intracellular concentration of the global secondary signalling molecule bis-(3'-5')-cyclic dimeric guanosine monophosphate (c-di-GMP) stimulates either a planktonic or sessile growth strategy (Liberati *et al.*, 2006). A high concentration of c-di-GMP promotes a biofilm lifestyle through stimulation of surface adhesion, cell aggregation and production of EPS (Hengge, 2009; Römling *et al.*, 2005). The amount of c-di-GMP is the result of a balancing reaction between diguanylate cyclase (DGC) and phosphodiesterase (PDE)(Merritt *et al.*, 2010) mediated enzyme activity. DGCs catalyse the formation of c-di-GMP from 2 molecules of GTP; PDE's then catalyse the conversion of c-di-GMP to 5'-phosphoguanylyl-(3'-5')-guanosine (pGpG) and/or GMP(Figure 1.17).

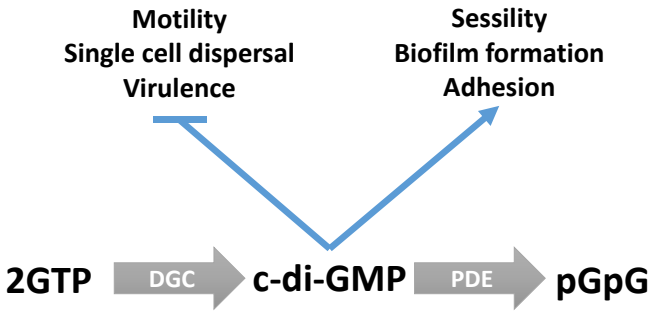

Figure 1.17 Schematic of synthesis and hydrolysis of c-di-GMP

These enzymes respond to environmental and intracellular inputs including oxygen, light, starvation and the presence of antibiotics (Jenal & Malone, 2006; Klebensberger *et al.*, 2007; Ryan *et al.*, 2006). Mutants of oligoribonucleases involved in c-di-GMP catabolism system, such as Orn, lead to high accumulation of c-di-GMP levels, with consequent improved biofilm development (Cohen *et al.*, 2015; Orr *et al.*, 2015).

1.4.2.4 Motility and its role in biofilm growth

P. aeruginosa has two appendages which facilitate different types of movement (Tremblay & Deziel, 2010; Yoon *et al.*, 2011). The first is a flagellum, which allows *P. aeruginosa* to swim towards (chemotaxis) desired substances (chemo-attractants) through liquid media or away from

toxic substances (chemo-repellents). It also facilitates coordinated migration through semi-solid media, called swarming, when combined with rhamnolipids, which fulfil the roles of biosurfactants that reduce surface tension and are depend on the *rhl* and *pqs* systems for expression. Type IV pili, the second motility appendage, may also be required for swarming but this is still debated (Anyan *et al.*, 2014; Overhage *et al.*, 2005). Flagella are composed of over 20 different proteins (Dasgupta *et al.*, 2004) and are encoded on 3 separate gene clusters in non-contiguous regions. The regulators involved in managing flagella motion and target purpose (in swimming or attachment for example), include RpoN, FliA, FliQ, FliR, FliN, FliSR and FleQ but are not limited to these factors (Dasgupta *et al.*, 2004). FleQ has generated particular interest because of its interaction with c-di-GMP and indeed studies have demonstrated the importance of flagella for biofilm formation. The appendage appears particularly important for the initial attachment and dispersal stages in biofilm development and this importance is dependent on the environmental conditions (Costerton *et al.*, 1999; Klausen *et al.*, 2003; O'Toole *et al.*, 2000).

Type IV pili facilitate a type of movement called twitching, which happens along a surface. The fine protrusions extend and retract to pull the bacterium along. Over 40 genes are involved in making and regulating Type IV pili. These reside in the *pil* operon and are under the control of various regulators including RpoN, Vfr, AlgR and PilSR (Beatson *et al.*, 2002; Mattick, 2002a). Type IV pili are also implicated in biofilm development. Their role is principally thought to join the small clusters of initially attached cells together because loss of function mutants typically form large separated microcolonies which expand only through clonal growth conditions (Costerton *et al.*, 1999; Klausen *et al.*, 2003; O'Toole *et al.*, 2000). Moreover, attachment of Type IV pili to a surface has been shown to stimulate c-di-GMP and cAMP/Vfr activity and as such helps promote biofilm growth when appropriate to the cell (Luo *et al.*, 2015).

1.4.3 Mixed species biofilms

The previous sections describe the processes undergone by a single species, *P. aeruginosa*, when forming biofilms. In nature, however, it is

more common to find multispecies biofilms (Aruni *et al.*, 2015; Tyson *et al.*, 2004). These frequently develop in clinical settings such as in the urinary tracts of long-term catheterised patients (CAUTI). Such polymicrobial infections can complicate treatment and reduce favourable outcomes (Azevedo *et al.*, 2017; Cole *et al.*, 2014; Li *et al.*, 2016).

Dual species biofilms are subject to cooperation and competition between the species. Microbes can help each other metabolically; while there can also be fierce competition for space and nutrients (Burmølle *et al.*, 2006; Cowan *et al.*, 2000; Hibbing *et al.*, 2010). The environment can exacerbate competition, with infection sites quickly becoming depleted of essential nutrients such as iron, carbon and nitrogen sources. Strategies to combat nutrient limitation can involve antibiosis (normally antimicrobial attack from one species to another) and scavenging, which by their nature are usually antisocial (Arias *et al.*, 2015; Hibbing *et al.*, 2010; Tanabe *et al.*, 2012; West & Buckling, 2003). Interestingly, the type of relationship existing between the cohabiting microbes is often reflected in its structure. A cooperative relationship is indicated by a compartmentalised biofilm where the different bacteria reside in different, metabolically diverse, niches. Competitive style biofilms on the other hand, typically exhibit a domination of the space by one of the species. The combination of more than one species in a biofilm can influence the structure and even susceptibility to antibiotics (Burmølle *et al.*, 2006; Cowan *et al.*, 2000; Hibbing *et al.*, 2010).

1.4.3.1 Coexistence of *P. aeruginosa* and *P. mirabilis*

An example of dual species biofilms are those produced by *P. aeruginosa* and *Proteus mirabilis* (Li *et al.*, 2016). *P. mirabilis* is connected with a biomineralisation process which arises in urinary tract infections through alkalinisation mediated via bacterial urease (Griffith *et al.*, 1976). The mineral crystals formed are made of struvite (magnesium ammonium phosphate) or apatite (hydroxyl calcium phosphate)and can cause encrustation and blockages of the catheter (Jacobsen & Shirtliff, 2011; Stickler *et al.*, 1993; Wilks *et al.*, 2015) which leads to a multitude of complications for the patient (Jones *et al.*, 2007). A study by Li *et al.* (2016) compared *P. mirabilis-P. aeruginosa* biofilms grown in conditions

favouring biomineralisation with those that inhibited it. Under both conditions, *P. aeruginosa* was initially more abundant, however after 18 hours there was a divergence in phenotypes. In biomineralisation favourable conditions, mineral formation became more apparent and the biomass of *P. mirabilis* increased. Furthermore, there was vertical stratification of the two species, with *P. mirabilis* occupying the surface of the biofilm with *P. aeruginosa* residing in the lower, deeper locations. The co-location of the mineral deposits and *P. mirabilis* was positively correlated. The non-mineralised biofilm showed an overall dominance of *P. aeruginosa* with no stratification. Similarly, *P. aeruginosa* out-competed *P. mirabilis* in planktonic conditions. This study illustrates the importance of considering environmental factors when studying interspecies biofilms and using model systems.

1.4.3.2 Coexistence of *P. aeruginosa* and *S. aureus*

P. aeruginosa and *S. aureus* can also form biofilms together and these can be more resistant to immune and antimicrobial action than the biofilms formed from the single species (Dalton *et al.*, 2011; Folkesson *et al.*, 2012; Maliniak *et al.*, 2016; Sibley *et al.*, 2008). Why this is, is still being investigated and as the study of multispecies biofilm studies is relatively extensive, there remains much to be discovered (Baldan *et al.*, 2014; DeLeon *et al.*, 2014a; Kumar & Ting, 2015b; Michelsen *et al.*, 2014). *P. aeruginosa-S. aureus* biofilms have been isolated from a number of infection sites including: diabetic foot and leg ulcers, sinusitis, burn wounds and cystic fibrosis (CF) respiratory tracts (Serra *et al.*, 2015; Zhang *et al.*, 2015), indicating that this is not a phenomenon linked with a particular infection type or host location. However, these infections have in common a chronic nature and this likely to be the key to allowing coexistence of the two pathogens. Illustrating this argument is the difference in behaviour observed between laboratories, or early CF isolated *P. aeruginosa* strains, and later stage CF isolated *P. aeruginosa* strains. The early isolated, more acute strains are more aggressive towards *S. aureus* and outcompete it, whereas the more chronic isolates are able to coexist with *S. aureus* (Baldan *et al.*, 2014).

The CF respiratory tract is an excellent example of *P. aeruginosa* and *S. aureus* coinfections. On the face of it, there is a negative correlation between *P. aeruginosa* colonisation and the presence of *S. aureus* in the lungs of CF patients, with *P. aeruginosa* 'replacing' *S. aureus* as the patient ages ("Cystic Fibrosis Patient Registry ", 2015; Harrison, 2007; Hauser *et al.*, 2011; Sagel *et al.*, 2009). However, this is now thought not to be the whole story. *S. aureus* and *P. aeruginosa* together appear to induce greater lung damage and confer enhanced antibiotic resistance than either species alone (Hauser *et al.*, 2011; Hubert *et al.*, 2013; Sagel *et al.*, 2009). This effect of poorer disease prognosis is not limited to CF respiratory infections. Coinfection of the two bacteria in wounds has been shown to delay wound healing and stimulate an increased inflammatory response, as well as increased tolerance to antibiotics (Dalton *et al.*, 2011; Pastar *et al.*, 2013; Seth *et al.*, 2012). The studies suggest that *P. aeruginosa* as the dominant (most aggressive and present in the highest numbers) pathogen, is responsible for 'choosing' whether to eliminate or coexist with *S. aureus* and this is largely mediated via QS (Hotterbeekx *et al.*, 2017).

Competitive and cooperative mechanisms of interaction between *P. aeruginosa* and *S. aureus* have begun to be identified. A study by (Lightbown & Jackson, 1954), showed that 2-heptyl-4-quinolone-N-oxide (HQNO) production by *P. aeruginosa*, effectively inhibited cytochrome b mediated electron transport in *S. aureus,* which promoted small colony variant (SCV) formation (Hoffman *et al.*, 2006; Lightbown & Jackson, 1954). Furthermore, Hoffman *et al.* (2006) found that *P. aeruginosa* secreted LasA (elastase A, staphylolysin) which lysed *S. aureus* (Fugere *et al.*, 2014; Mashburn *et al.*, 2005). Not to be forgotten is the cytotoxic, redox active secondary metabolite pyocyanin, which appears to act antagonistically on *S. aureus* and other gram-positives, giving *P. aeruginosa* a competitive edge (Hotterbeekx *et al.*, 2017).On the cooperative side, *P. aeruginosa* was shown protecting *S. aureus* from phagocytic attack by the slime mould *Dictyostelium discoideum*, when the species were co-cultured in a biofilm (Yang *et al.*, 2011). Additionally, interactions between CF adapted *P. aeruginosa* isolates and CF respiratory

commensals are supported by multiple studies (Antonic *et al.*, 2013; Baldan *et al.*, 2014; Michelsen *et al.*, 2014).

P. aeruginosa secreted biofilm components, such as EPS, can support multispecies biofilms. The three main polysaccharides found in *P. aeruginosa* (Pel, Psl and Alginate (section 1.4.2.1)) are present in different proportions depending on external conditions, affecting the structure. Some biofilm structural types have been associated with the promotion of multispecies biofilms. Psl dominant *P. aeruginosa*, show the production of a looser biofilm, where there is a lesser amount of cross-linking within the extracellular matrix. This is thought to allow other micro-organisms such as *S. aureus* to infiltrate the biofilm. Psl dominant *P. aeruginosa* on the other hand, produce a more elastic matrix due to strong cross-linking between Psl and other EPS components (Chew *et al.*, 2014). The location of *S. aureus* in a Psl dominant biofilm seems to be less clear than in Pel dominant biofilms, with some studies (Chew *et al.*, 2014) showing the formation of species specific separate microcolonies with other (Billings *et al.*, 2013) showing *S. aureus* residing at the air-liquid interface. As well as affecting the architecture of the biofilm, the type of dominating polysaccharide can affect the level of resistance to specific antibiotics. For example, Psl resists penetration by colistin and polymyxin B, while Pel is a more effective shield against aminoglycosides (Billings *et al.*, 2013; Colvin *et al.*, 2012). Regardless of whether the relative proportions of Pel or Psl, existing in a biofilm with *P. aeruginosa* can protect *S. aureus* from external antibiotics, the Gram positive bacterium has to withstand the antimicrobial metabolites produced by *P. aeruginosa* itself (Hotterbeekx *et al.*, 2017). In contrast to Pel and Psl, alginate has not been associated with the enhancement of *S. aureus* biofilm formation. As afore mentioned, heavily alginated *P. aeruginosa* biofilms are usually a product of chronic CF infections, facilitating the resistance of macrophages and macrophage secreted chemicals (Ryder *et al.*, 2007). More information is needed to determine whether this type of biofilm is amenable to *S. aureus* co-residence.

Finally, it has been shown that Type IV pili help *P. aeruginosa* to form mixed species microcolonies with *S. aureus*, likely by interacting with

eDNA. This was demonstrated by Yang *et al.* (2011) who showed DNAse I addition to *mixed P. aeruginosa* and *S. aureus* biofilms retarded the growth of microcolonies. Nevertheless, protein A (SpA) is an adhesive protein produced by *S. aureus* that it is thought to work alongside the Type IV pili of *P. aeruginosa*. It binds to either Type IV pili or Psl, helping or hindering interactions between *S. aureus* and *P. aeruginosa*. (Armbruster *et al.*, 2016).

1.5 HYPOTHESIS AND AIMS OF THE PROJECT

The lactam technology developed by Unilever consists of a series of compounds that were reported to inhibit biofilm formation or development by bacterial species including *P. aeruginosa, P. mirabilis* and *S. aureus*. Certain lactams were also noted to inhibit *N*-acylhomoserine lactone dependent quorum sensing in *Chromobacterium violaceum*. Among the lactams, preliminary Unilever structure activity analysis identified the five most potent compounds (Figure 2.1). These required a concentration of at least 100 μM to prevent biofilm formation (Unilever, unpublished data). However further improvement of lactam efficacy requires a detailed understanding of their mechanism of action and biological activities.

The primary objective of this study is to gain further insights into the mechanism(s) of action of the lactams as quorum sensing and biofilm inhibitors in *P. aeruginosa*. Literature on the synthetic furanones and pyrrolones frequently reports that *N*-acylhomoserine lactone-based QS is the main target for the anti-biofilm action (section 1.3.3.1). Hence if QS inhibition is detected, the mechanism of action will be studied in detail using an array of assays. Biofilm formation in static and fluidic conditions will be tested to verify the impact of the compounds and their potential applications. The biofilm, growth inhibitory and mode of action of the lactams on other species including *P. mirabilis* and *S. aureus* will also be investigated.

2 MATERIALS AND METHODS

2.1 MATERIALS

2.1.1 General chemicals

Unless otherwise stated, all reagents were purchased from Sigma-Aldrich. AQs and QZN were synthesized by Alex Truman (University of Nottingham) as described in Diggle *et al.* (2006a), dissolved in methanol for 10 mM stocks and stored at -20° C.

2.1.2 Bacterial strains

Table 2.1 Strains used in this study

Strain	Genotype	Source or reference
E. coli		
S17-1 λpir	*recA, thi, pro*, *hsdR*-M+RP4: 2-Tc:Mu:Km Tn7 *λpir*, Tp^R Sm^R	(Simon *et al.*, 1983)
DH5	F^- Φ80*lac*ZΔM15 Δ(*lac*ZYA-*arg*F) U169 *rec*A1 *end*A1 *hsd*R17 (rK^-, mK^+) *pho*A *sup*E44 λ- *thi*-1*gyr*A96 *rel*A1	(Grant *et al.*, 1990)
BL21(DE3)	*fhuA2 [lon] ompT gal (λ DE3) [dcm] ΔhsdS* *λ DE3 = λ sBamHIo ΔEcoRI-B int::(lacI::PlacUV5::T7 gene1) i21 Δnin5*	EMD4Biosciences
P. aeruginosa		
PAO1-L	Lausanne subline, wild-type	Holloway collection
PAO1-N	Nottingham subline, wild-type	Holloway collection
PAO1-UW	University of Washington subline, wild-type	(Stover *et al.*, 2000)
PAO1-UW mTurquoise	mTurquoise-tagged Tc^R, UW subline	Laboratory collection (unpublished)
PAO1-UW mCherry	mCherry-tagged Tc^R, UW subline	Laboratory collection (unpublished)
PAO1-L Δ*pqsA*	*pqsA* chromosomal deletion mutant	(Aendekerk *et al.*, 2005)
PAO1-L Δ*pqsR*	*pqsR* chromosomal deletion mutant	Laboratory collection (unpublished)
PAO1-L Δ*lasR*	*lasR* chromosomal deletion mutant	(Heurlier *et al.*, 2005)
PAO1-L Δ*pqsAH*	*pqsAH* chromosomal double deletion mutant	(Diggle *et al.*, 2007)

PAO1-N Δ*pqsAHR*	*pqsAHR* chromosomal triple deletion mutant	(Ilangovan *et al.*, 2013)
PA ATCC 15442	Environmental (animal room water bottle) isolate	Unilever, accession no. AYUC00000000 on DDBJ/EMBL/GenBank
PAO1-Unilever	LJMU, environmental (washing machine) isolate	Unilever R&D Collection
PA14	wild type	(Mathee, 2018)
PA14 AL191	CF clinical isolate from München, ID 1350, ≥95 % PA14 homology	Université Laval collection
PAK 6085	CF clinical isolate from Québec, ID 1331, ≥95 % PAK homology	Université Laval collection
PA7 48	CF clinical isolate from Montréal, ID 197S020911BSL_PA3, ≥95 % PA7 homology	Université Laval collection
Proteus mirabilis		
P. mirabilis	Hauser 1885, wild type	(Wenner & Rettger, 1919)
P. mirabilis DsRed	DsRed-tagged Gm^R, Hauser 1885	Laboratory collection
Staphylococcus aureus		
SH1000	Derivative of NCTC 8325	(Horsburgh *et al.*, 2002)
SH1000 eGFP	eGFP-tagged Cm^R, SH1000	Laboratory collection
USA300	Clinical isolate. Mec^R, Ery^R, Cli^R, TetR	(McDougal *et al.*, 2003)
ATCC 6538	Subsp. *aureus* Rosenbach 1884	Unilever R&D Collection

2.1.3 Plasmids

Table 2.2 Plasmids used in this study

Plasmid	Characteristics	Source or reference
CTX-*lux*	*P.aeruginosa* integration promoterless vector with *luxCDABE* operon	(Becher & Schweizer 2000)
CTX::P*pqsA-lux*	*pqsA* promoter region fused to *luxCDABE* and inserted in EcoRI/PstI sites of pminiCTX-*lux* Tc^R	(Diggle *et al.*, 2007)
CTX::P*lasI-lux*	*lasI* promoter region fused to *luxCDABE* and inserted in BamHI/HindIII sites of pminiCTX-*lux* Tc^R	(Rampioni *et al.*, 2006)
CTX::P*rhlI-lux*	*rhlI* promoter region fused to *luxCDABE* and inserted in BamHI/HindIII sites of pminiCTX-*lux* Tc^R	This study

CTX::P*tacΔlacI^{Q}-lux*	*tacΔlacI^{Q}* gene fused to *luxCDABE* and inserted in XhoI/EcoRI sites of pminiCTX-*lux* Tc^{R}	This study
CTX::P*phzA1-lux*	*phzA1* promoter region fused to *luxCDABE* and inserted in EcoRI/XhoI sites of pminiCTX-*lux* Tc^{R}	(Higgins *et al.*, 2018)
CTX::P*lecA-lux*	*lecA* gene promoter region to *luxCDABE* and inserted in SalI/EcoRI sites of pminiCTX-*lux* Tc^{R}	(Fletcher *et al.*, 2007)
CTX::P*orn-lux*	*orn* gene promoter region to *luxCDABE* and inserted in EcoRI/BamHI sites of pminiCTX-*lux* Tc^{R}	This study
BBRMCS-*5-pqsABCD*	*pqsABCD* operon inserted in pBBRMCS-5	(Niewerth *et al.*, 2011)
ET28a::*pqsR$^{C94-309}$*	*pqsR$^{94-309}$*construct inserted in pET28a Km^{R} Cm^{R}	(Ilangovan *et al.*, 2013)

2.1.4 Primers

Oligonucleotide primers were synthesised by Sigma-Aldrich (UK). Primer sequences used in this work are listed in Table 2.3.

Table 2.3 Primers used in this study

Primer	Sequence 5' to 3'	Function
*rhlI*_FW	CATCTCAAGCTTCGAGCGCGAGGAAAT	*rhlI* amplification with HinDIII recognition site
*rhlI*_RV	TTCCAGGGATCCAGAGAGCAATTCGAT	*rhlI* amplification with BamHI Recognition site
*tac*_FW	AAACTCCTCGAGCATCAAATGAAACTG	*tac* amplification with XhoI recognition site
*tac*_Rv	GAGCTCGAATCCTGTTTCCTGTGTGAA	*tac* amplification with EcoRI recognition site
*pqsA*_FW	CTGTGAGAATTCGGAGGCGATTTGCCG	*pqsA* amplification with EcoRI recognition site
*pqsA*_RV	TGGCCACTGCAGACATGACAGAACGTT	*pqsA* amplification with PstI recognition site
*lasI*_FW	TCCAGAAAGCTTCCTGGCTTTCCCGTC	*las* amplification with HinDIII recognition site
*lasI*_RV	ACTTGTGGATCCCGCCCAGCAGTTTTT	*las* amplification with BamHI recognition site
*orn*_FW	TATAAGCTTCGACCTCTACCTGAA	*orn* amplification with EcoRI recognition site
*orn*_ RV	TATGGATCCGATCCAGATAAGGTT	*orn* amplification with BamHI recognition site
*pqsR^{94}*_FW	TGCTAGCAATCTCCGGGTGCTGCT	*pqsR* amplification with NheI recognition site

pqsR^{309}_RV	CGATAAGCTTTCAGCTCGGTTGCCAGGC	*pqsR* amplification with HindIII recognition site

2.1.5 Unilever Lactams

The lactams provided by Unilever (Port Sunlight, UK) are listed in Table 2.4 and shown in Figure 2.1 and Figure 2.2. Dimethyl sulfoxide (DMSO), according to the datasheets provided by Unilever, is the ideal solvent for lactams; however, due to its toxicity towards *P. aeruginosa* (Ansel, H. C. *et al* 1969), the compounds were also solubilized in methanol (MeOH) to reduce solvent impact on bacterial growth if required. MeOH proved to be an acceptable solvent for compound stock concentrations of up to 50 mM, allowing the testing of high final concentrations necessary for dose-response assays.

Table 2.4 Unilever lactams

Trivial ID	Name	Molecular Formula	Molecular Weight
131	5-hydroxy-5-methyl-4-phenyl-1,5-dihydro-2*H*-pyrrol-2-one	$C_{11}H_{11}NO_2$	189.21
258	4-(4'-fluorophenyl)-5-hydroxy-5-methyl-1,5-dihydro-2*H*-pyrrol-2-one	$C_{11}H_{10}FNO_2$	207.20
316	4-(4'-bromophenyl)-5-hydroxy-5-methyl-1,5-dihydro-2*H*-pyrrol-2-one	$C_{11}H_{10}BrNO_2$	268.11
488	4-(4'-chlorophenyl)-5-methylene-1,5-dihydro-2*H*-pyrrol-2-one	$C_{11}H_8ClNO$	205.64
491	5-methylene-4-(p-tolyl)-1,5-dihydro-2*H*-pyrrol-2-one	$C_{12}H_{11}NO$	185.23
295	4-(4'-bromophenyl)-5-methylene-1,5-dihydro-2*H*-pyrrol-2-one	$C_{11}H_8BrNO$	250.1
2022339	3-(4'-chlorophenyl)-5-methylen-1-methyl-2h-pyrrol-2-one	$C_{12}H_{10}ClNO$	219.668
483	-	-	193.63
310	4-(2'-fluorophenyl)-5-methylene-1,5-dihydro-2*H*-pyrrol-2-one	$C_{11}H_8FNO$	189.19
490	4-(5'-chlorophenyl)-5-methylene-1,5-dihydro-2*H*-pyrrol-2-one	$C_{11}H_8ClNO$	205.641
495	4-(2'-chlorophenyl)-5-methylene-1,5-dihydro-2*H*-pyrrol-2-one	$C_{11}H_8ClNO$	205.64
Cationic lactam	-	-	185.22
476	4-(4'-chlorophenyl)-5-hydroxy-5-methyl-1,5-dihydro-2methyl-pyrrol-2-one	$C_{11}H_{10}ClNO_2$	223.66

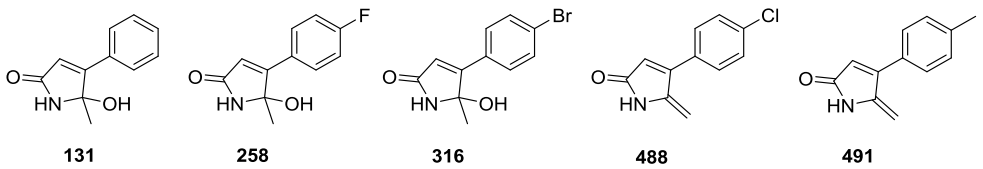

Figure 2.1 Structures of the first set of lactams provided by Unilever

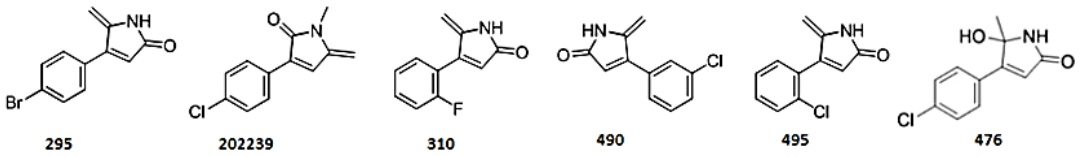

Figure 2.2 Structures of the second set of lactams provided by Unilever.

2.1.6 Bacterial Growth Media

All media were autoclaved at 121°C for 20 minutes after preparation if not stated otherwise. Fresh media were always used where possible. Antibiotic(s) were added for selection and maintenance when required: for *P. aeruginosa* tetracycline (125 µg ml^{-1}), for *E. coli* tetracycline (10 µg ml^{-1}), chloramphenicol (30 µg ml^{-1}) and kanamycin (50 µg ml^{-1}), for *P. mirabilis* gentamycin (25 µg ml^{-1}) and for *S. aureus* chloramphenicol (25 µg ml^{-1}).

2.1.6.1 Lysogeny Broth Media

All strains were grown in LB broth (Hussain *et al.*, 2012b), unless otherwise stated. LB broth was prepared by adding 10 g tryptone, 10 g NaCl and 5 g yeast per litre of distilled water. LB agar was prepared by adding 0.8% (w/v) Technical Agar No. 3 (Oxoid).

2.1.6.2 Pseudomonas Isolation Agar

PIA was purchased from Sigma-Aldrich and contains 20 g enzymatic digest of gelatin (peptone), 1.4 g $MgCl_2$, 10 g K_2O_4S dipotassium sulfate, 0.025 g 5-chloro-2-(2,4-dichlorophenoxy) phenol (Irgasan™*)* and 13.6 g Technical Agar No. 3 (Oxoid) and made up to 1L with distilled water. This medium was used primarily for bacterial conjugation processes to inhibit the growth of *E. coli*.

2.1.6.3 Artificial Urine Medium

Artificial Urine Medium was prepared following Brooks and Keevil (1997). One gram of peptone L37, 0.005 g yeast extract, 0.1 g lactic acid, 0.4 g citric Acid, 2.1 g $NaHCO_3$, 10 g urea, 0.07 g uric acid, 0.8 g creatinine, 0.37 g $CaCl_2 \cdot 2H_20$, 5.2 g NaCl, 0.0012 g $FeSO_4 \cdot 7H_2O$, 3.2 g $Na_2O_4S \cdot 10\ H_2O$, 0.95 g KH_2PO_4, 1.2 g HK_2O_4P, 1.3 g NH_4Cl were made up to 1 L with distilled water. HCl (molarity e.g. 2.5 M) was used to adjust the pH to 6.5. Finally, the medium was filter-sterilized via a 0.22 µm membrane-filter (Millipore).

2.1.6.4 Tryptone Soya Broth

Tryptone soya broth (TSB) was prepared by adding 30 g of dehydrated TSB culture medium (Oxoid - containing 17g pancreatic digest of casein, 3g enzymatic digest of soya bean, 5 g NaCl, 2.5 g K_2HPO_4 and 2.5 g glucose) and making up to 1 L with distilled water. TSB agar was prepared by adding 1.5% (w/v) Bactoagar (Oxoid).

2.1.6.5 Brain Heart Infusion Broth

Brain Heart Infusion Broth (BHI) was purchased from Sigma-Aldrich and contains beef heart (infusion from 250g), 5 g L^{-1}, calf brains (infusion from 200g), 12.5 g L^{-1}, disodium hydrogen phosphate (2.5 g L^{-1}), D(+)-glucose (2 g L^{-1}), peptone (10 g L^{-1}), sodium chloride (5 g L^{-1}).

2.1.6.6 Soft top agar

LB soft top agar was prepared by adding 10 g tryptone, 5 g NaCl, 6.5 g Technical Agar No. 3 (Oxoid) and making up to 1 L with distilled water.

2.1.6.7 M9 minimal medium

M9 medium contains 240.7 mgL^{-1} $MgSO_4$, 11.098 mgL^{-1} $CaCl_2$ and D-glucose at 0.4 %. A 5x stock solution of M9 salts was prepared for a final concentration of: 1 gL^{-1} NH_4Cl, 6.78 gL^{-1} Na_2HPO_4, 3 gL^{-1} KH_2PO_4 and 0.5 gL^{-1} NaCl.

2.1.6.8 RPMI 1640 medium

Roswell Park Memorial Institute (RPMI) 1640 medium was purchased from Lonza (UK) without L-Glutamine or phenol red.

2.1.6.9 Fastidous Anaerobic Broth

Fastidous Anaerobic Broth (FAB) medium was supplemented with glucose 10 mM. One litre of modified FAB medium contained the following components: 2g of $(NH_4)_2SO_4$, 6g $Na_2HPO_4 \cdot 2H_2O$, 3g KH_2PO_4, 3g NaCl, 93g $MgCl_2$, 11mg $CaCl_2$ and 1ml of trace metals solution. The trace metals solution contained $CaSO_4 \cdot 2H_2O$ (200 mg L^{-1}), $FeSO_4 \cdot 7H_2O$ (200 mg L^{-1}), $MnSO_4 \cdot H_2O$ (20 mg L^{-1}), $CuSO_4 \cdot 5H_2O$ (20 mg L^{-1}), $ZnSO_4 \cdot 7H_2O$ (20 mg L^{-1}), $CoSO_4 \cdot 7H_2O$ (10 mg L^{-1}), $NaMoO_4 \cdot H_2O$ (10 mg L^{-1}), H_3BO_3 (5 mg L^{-1}).

2.1.6.10 Christensen's Urea Agar

Christensen's Urea Agar was purchased from Sigma Aldrich and contains peptic digest of animal tissue 1 g, dextrose 1 g, Sodium chloride 5g, Disodium phosphate 1.2g, Monopotassium phosphate 0.8 g, Phenol red 0.012 g and agar 15 g.

2.2 METHODS

2.2.1 Bacterial growth conditions and storage

All bacterial strains were grown at 37°C in 5 ml LB medium in 50 ml Falcon tubes overnight with shaking at 200 rpm, unless otherwise stated. Recombinant *P. aeruginosa* and *E.coli* S17-1 strains were grown in LB medium containing gentamicin 25 µg/ml unless otherwise stated. All the strains were stored at -80°C in screw topped 2 mL Eppendorf tubes in glycerol at a concentration of 25% v/v in water; 750 µl of washed overnight culture was added to 750 µl of sterilized glycerol 50% v/v in water. Before conducting an experiment, the frozen strain was plated and the following day an overnight culture was made from a single colony. Freshly plated strains were always used to avoid differences in strain behaviour due to random mutations. The strains used in this work are summarised in Table 2.1. When required, a spectrophotometer (Thermo Scientific) was used to measure the optical density of a culture at a wavelength of 600 nm (OD_{600} nm). For the measurement, the culture was diluted 1:10 in its liquid medium into a 1 cm depth cuvette (Fischer Scientific) and the readings

were compared to a blank medium sample. In all experiments involving lactams, the solvent used was present in an equal amount for all the samples tested, never exceeding 6% and 0.6% v/v for MeOH and DMSO respectively.

2.2.2 Nucleic acid techniques

2.2.2.1 Chromosomal DNA isolation

Chromosomal DNA (gDNA) was extracted using of the Promega genomic DNA kit according to the manufacturer's instructions. A starting culture volume of 1 ml was used and a yield of 50 µl gDNA solution eluted.

2.2.2.2 Polymerase Chain Reaction

Primer design was achieved with the help of Primer-Blast, a NCBI online tool where the likelihood of non-specific binding was checked and a screening for potential secondary structures was performed ("Primer-BLAST website," 2019). For the development of biosensors and protein expression vectors, Q5® High-Fidelity DNA Polymerase was used according to the manufacturer's (New England Biolabs) recommended conditions. To check for DNA contamination after RNA extraction, OneTaq® DNA polymerase (Promega) was used as high fidelity was not required in this case. For cloning, primers were modified to include restriction sites specific to the vector of choice (Table 2.2). In general, the following thermocycling steps were used: a 30 secs initial denaturation of 98 ^{o}C, then 30 cycles of 30 s denaturation (98 ^{o}C), 30 s annealing (45 ^{o}C) and 45 s extension (72 ^{o}C). A final 2 min extension of 72 ^{o}C preceded a holding step at 4^{o}C. Table 2.3 lists the primers used in this study.

2.2.2.3 DNA gel electrophoresis and DNA gel extraction

Gels were prepared as described by Sambrook (2012) using 1% w/v agarose in 65 mL 1x TAE buffer with ≈2 µl Syber Safe. The DNA samples, in DNA loading buffer (NEB) (1:5), were loaded into the wells. One µg of 1 kb marker was loaded into the first well to verify the size of DNA. Electrophoresis was performed at 100 V for 1 h. Agarose gel electrophoresis was used to analyse digestion products and to identify the appropriate sized bands for excision and purification using a Monarch gel

extraction kit (New England Biolabs) according to the manufacturer's instructions. The DNA extracted was eluted in 10 µl of molecular biology grade water.

2.2.2.4 DNA restriction and ligation

Following PCR, ~1µg DNA was digested for 1-2 h at 37 °C using 0.5µl of each of the appropriate restriction enzyme (New England Biolabs) and 1x Cutsmart Buffer into a final volume of 50 µL. The fragments were ligated together with T4 DNA ligase (Promega). Ligations were performed using a 1:5 vector to insert ratio at 16°C for 2 h and at 4°C overnight.

2.2.2.5 Plasmid extraction from *E.coli*

The *E.coli* strain carrying the selected plasmid was cultured overnight in 5 mL. 1 mL of culture was used for plasmid extraction. DNA isolation was carried out using the Qiagen Miniprep Kit according to the manufacturer's protocol. The final elution from the cell lysate was performed using 50 µl of distilled water.

2.2.2.6 DNA quantification

The Nanodrop Spectrophotometer 1000 (Thermo Scientific) was used to establish the quantity and purity of DNA. The measurement was based on 1 µl of material, blanked with 1 µl of molecular biology grade water.

2.2.2.7 Preparation of electrocompetent *E. coli*

Electrocompetent *E.coli* cells were prepared by inoculating 1 % (v/v) overnight *E. coli* culture into 100 ml LB in a 1 L conical flask and grown at 37 °C, 200 rpm to an OD_{600} of 0.4-0.8 for 6 hours. The culture was centrifuged at 5500 g for 10 min at 4 °C and washed twice in sterile, ice cold 10 % (v/v) glycerol containing 1 mM 4-Morpholinepropanesulfonic acid (MOPS) before being resuspended in 1 ml of the same buffer.

2.2.2.8 Transformation of *E. coli*

For cloning and protein expression purposes, constructs were transformed into either *E. coli* DH5α or BL21 (DE3). After each cloning step, DNA constructs were screened by PCR and sequenced. Prior to electroporation, salts were removed from the DNA solution using filter dialysis on 0.025 µm Millipore filters for a minimum of 30 min. Electroporation was performed in

0.2 cm electrode gap Gene Pulser cuvettes containing 50 µl of competent cells and 2-3 µl dialysed DNA. Immediately after the electroporation pulse (electroporation time ~5 ms), 1 ml of LB broth was added to the cells which were then incubated at 30 °C for 1 h. 1/10 of the culture was subsequently plated onto LB agar plates containing appropriate antibiotics to select for the desired transformants and grown overnight at 37 °C. In case of the miniCTX-*lux* plasmid, the transformation was verified by viewing the plates under a light camera (Hamamatsu, Wasabi software), which facilitated the selection of bioluminescent colonies. For negative controls, electrocompetent cells with no plasmid were treated likewise, in parallel with the samples.

2.2.2.9 Conjugation

E. coli S17-1 was used as the donor strain to transfer plasmid DNA into a *P. aeruginosa* recipient strain. Both strains were incubated overnight but under different temperature conditions: donor cells (*E. coli*) were grown at 37°C, while recipient cells (*P. aeruginosa*) were grown at 42°C in order to inactivate restriction/modification enzymes that degrade donor DNA. The cells were washed twice in LB broth by centrifugation at 5500 rpm for 5 min. The final pellets were resuspended in 100 µl of LB broth. Donor and recipient cells in a ratio of 1:1 were mixed in an Eppendorf and spotted onto an LB agar plate. The spots were air-dried and the plates incubated at 30°C for 4-8 h. The cells were resuspended in 1 ml LB broth in an Eppendorf, centrifuged at 10000 rpm for 5 min and then re-suspended again in 100 µl of LB broth. Fifty microliters of each final product was plated on a PIA agar plate containing an antibiotic to select for the correct transconjugant and incubated overnight at 37 °C. After conjugation and transformation with the miniCTX plasmid, the plates were viewed under the light camera (Hamamatsu, Japan; Wasabi software) in order to select bioluminescent colonies.

2.2.2.10 RNA extraction, quantification and quality control

RNA was extracted from biological triplicates of *P. aeruginosa* PAO1-L in presence and absence of lactam 488 at 50 and 100 µM at two time points, 8 and 12 h. Briefly, the initial cultures were standardized at OD_{600}=0.01 in

10 mL of LB and incubated at 37°C and 200 rpm and total RNA extracted after 8 h and 12 h. Since 488 inhibits the growth of *Staphylococcus aureus* ATCC 6538, the lactam was added to the culture grown to mid-log phase (4.5h) in TSB at concentrations of 15 or 25 µM and incubated for 1 h. In both cases, cells were collected and adjusted to an OD_{600} of 1.5 and 4.7 for *P. aeruginosa* and *S. aureus* respectively. RNA extraction was carried out using RNAprotect and the RNeasy Mini Kit (QIAGEN) following the manufacturer's protocols for prokaryotic organisms. After incubation with 488, 1500 µL RNAprotect reagent (Qiagen) was added to 500 µL of each culture, incubated for 5 min at room temperature and centrifuged for 10 min at 4000 rpm. Supernatant was removed and the pellets stored at -80 °C. After thawing and resuspension in 200 µL TE buffer (30 mM Tris-HCl, 1 mM EDTA, pH 8.0) containing 15 mg/mL lysozyme and 20 µL of 15 mg/mL proteinase K solution for *Pseudomonas* or lystostaphin 50 µg/mL for *Staphylococcus*, samples were incubated for 10 and 15 min respectively. After mixing with 700 µL of buffer RLT Plus (QIAGEN, UK) containing 10 µl β-mercaptoethanol, the homogenate was mixed with 500 µL of 100 % EtOH and transferred to RNeasy Mini spin column for purification until final collection with 50 µl of water. Before storage at -80°C, the elution was treated with Ambion® Turbo DNase according to the manufacturer guidelines, the efficacy of which was tested through PCR and gel electrophoresis. A Nanodrop Spectrophotometer 1000 (Thermo Scientific) was employed to quantify the RNA concentration and to check for contaminants from the extraction process. Finally, RNA integrity was confirmed using an Agilent 2100 BioAnalyzer.

2.2.2.11 RNA sequencing

Samples were sent to the Centre for Genomic Research at the University of Liverpool for sequencing and data generation. For each sample, 1 µg of total RNA was depleted with the Illumina Ribo-Zero rRNA Removal (Kit for mixed bacteria) from Illumina, Inc. (UK). The extent of depletion was checked visually on a Bioanalyzer RNA pico-chip. RNA-Seq libraries were prepared from the enriched material using the NEB Ultra Directional RNA Library Preparation Kit. All of the enriched material was used as input material and following 15 cycles of PCR amplification, the libraries were

purified using AMPure XP beads (Beckman Coulter, USA). Each library was quantified using Qubit (ThermoFisher) and the size distribution assessed using the Agilent 2100 Bioanalyzer. The final libraries were pooled in equimolar amounts using the Qubit and Bioanalyzer data. The quantity and quality of each pool was assessed by Bioanalyzer and subsequently by qPCR using the Illumina Library Quantification Kit from Kapa (KK4854) on a Roche Light Cycler LC480II according to manufacturer's instructions. The template DNA was denatured according to the protocol described in the Illumina User guide and loaded at 300 pM. Sequencing was carried out on one lane of an Illumina HiSeq4000 at 2x150 bp paired-end.

2.2.2.12 Transcriptomic analysis

The expression of each gene was calculated from read alignment files using Htseq-count (Anders *et al.*, 2015). The count numbers were also converted into FPKM (Fragments per Kilobase per Million reads) values. The count numbers per gene were used during the subsequent differential expression analysis. The main analytical processes employed included data variation assessment, data modelling, model fitting, testing and DE (Differentially Expressed) gene detection. All the DE expression analyses were performed in an R (version 3.2.2) environment using the edgeR (Robinson *et al.*, 2010) package. Differential expression analysis was applied to gene count values. Variations of the count data were modelled by a negative binomial distribution and modelled using a generalized linear model (GLM)(Nelder & Wedderburn, 1972). A GLM containing 6 parameters, representing the mean expression of corresponding sample groups, was used. Finally, the $\log_2$ Fold Change (logFC) values for the required comparisons of sample groups were computed based on the model fitting results. Therefore, the contrasts obtained describe the change in expression among the treated/untreated samples and the two time points. The functional groups analysis relies on the mapping of clusters of orthologous groups of proteins (COG) for *P. aeruginosa* PAO1 based on the 2014 update available at NCBI’s COG database ("NCBI’s COG database" 2014).

2.2.3 Lux-based reporter gene fusion assays

The TECAN Infinite® 200 microplate reader was used to monitor bioluminescence as Relative Light Units (RLU) and cell density (OD_{600}) of bacteria in Greiner 96 well flat black microtiter plates. Before conducting readings, cultures were normalized to an OD_{600} 0.1 in a final volume of 200 µl of LB per well. Readings were automatically performed every 30 min at 37°C for 24 h. Negative and positive controls were employed: a strain defective of the gene for the related *lux* promoter fusion provided the negative control, whilst the positive controls were achieved by using a constitutive P*tac::lux* promoter fusion biosensor and by adding the same concentration of solvent as the samples with highest concentration of lactam. For the dose-response curves, a range of linear dilutions of lactams were made. Each sample was monitored in triplicate and its luciferase activity (bioluminescence) calculated dividing the RLU value by OD_{600}. Only the maximum value over time (peak RLU/OD_{600}) was taken into account for the analysis. The raw data were analysed using Microsoft Excel 2010 software. EC_{50} and IC_{50} values were extrapolated from sigmoidal dose-response curves generated by Graphpad Prism software 6 and 7 (San Diego, USA).

2.2.4 Phenotypic assays

2.2.4.1 Growth curves

Growth curves were generated by growing biological triplicates of bacterial cultures with a gradient of increasing concentrations of lactam in 96-well plates and measuring the OD_{600} with a TECAN Infinite® 200 microplate reader. Where possible, cells were grown in 100 mL flasks and aliquots were taken every 1 or 2 h over the growth curve to obtain the OD_{600} until stationary phase together with a final OD_{600} after 24 h.

2.2.4.2 Pyocyanin production

Pyocyanin levels were measured using an assay based on the method of Essar *et al.* (1990). Overnight bacterial cultures were adjusted to OD_{600} 1.0 before being diluted 1 in 100 in 10 ml LB and grown in 100 ml flasks at 37 °C with shaking at 200 rpm for 16 h. The culture was then centrifuged and

7.5 ml of the resulting supernatant was filter-sterilized with a 0.22 µm membrane-filter. A 4.5 ml volume of chloroform was added to the filtered supernatant and mixed. The resulting blue coloured chloroform layer was transferred to a fresh tube and mixed with 1.5 ml of 0.2 M HCl. After vortexing, the sample was centrifuged and the top pink layer, containing 0.2 M HCl, was removed and the absorption read at 520 nm using a spectrophotometer (Novaspec II; Pharmacia).The pyocyanin concentration (µg/ml) was calculated by multiplying the value obtained by 17.072, its mass extinction coefficient value, and then again by 1.5 to compensate for the loss during the chloroform step. The concentrations were divided by the OD_{600} of the cultures. Assays were repeated in triplicate.

2.2.4.3 Elastase activity assay

The elastin-Congo Red assay was used to quantify elastase production in *P. aeruginosa* strains, as described in Caballero *et al.* (2001). Cultures set up in biological triplicate were standardized at OD_{600} 0.01 and incubated for 16 h at 37°C 200 rpm. For each sample, the cell amount was standardized and the supernatant obtained by filter-sterilization of the centrifuged culture. One hundred microliters of the supernatant was transferred to a 2 ml Eppendorf containing 900 µl of the ECR buffer (12.1 g/L Tris base, 194.7 mg/L $CaCl_2$, pH 7.5) and 20 mg/mL of elastin-Congo red (insoluble). To allow the elastase to optimally break its substrate, the samples were incubated at 37 °C, shaking at 200 rpm for 4 hours. Finally, the samples were centrifuged and 800 µl of supernatant was collected and transferred into a plastic cuvette to measure the absorbance at 495 nm with a spectrophotometer. The measurements were blanked with an un-inoculated LB medium control which was treated likewise by adding 900 µl of ECR and elastin-Congo Red.

2.2.4.4 Motility media

The medium used for swarming and swimming motility assays was 0.8 g/L Nutrient Broth No.2 (Oxoid) with 0.5% and 0.3% (w/v) Bacto agar (Difco) respectively. After autoclaving, all motility media were cooled to 50 °C in a water bath for 1 h prior to use. The medium used for the twitching assays consisted of 1 % tryptone, 0.5 % yeast extract, 1 % NaCl and 1% agar

2.2.4.5 Swarming assay

Swarming assays were performed on plates with 20 mL of agar medium supplemented with D-glucose 0.5% (v/v), as described in Ha *et al.* (2014a). After pouring, the medium was allowed to solidify at room temperature for 10 min and dried for 30 min under laminar flow. For the inoculum, an overnight culture was standardized to OD_{600}=1 and washed once with the equivalent volume of LB. Three microliters of these cells were spotted onto the surface of the plates which were incubated at 37 °C for 16 h.

2.2.4.6 Swimming assay

Plates were left to solidify and dry on the bench prior to use for 15 min. Condensation from the lids was removed by drying to minimize the moisture within the plate. One microlitre of standardized OD_{600}=1 overnight culture was inoculated into the semi-solid agar. Plates were incubated at 37 ºC for approximately 16 h. This assay was performed according to Ha *et al.* (2014b).

2.2.4.7 Twitching assay

Plates contained 15 ml of medium which after pouring was dried for 15 min under laminar flow. Overnight colonies from a freshly streaked plate were stabbed to the bottom of each plate using sterile toothpicks as described by Turnbull and Whitchurch (2014) and incubated at 37 ºC for 48 h inside a semi-sealed bag containing damp paper towel to retain high humidity. Finally, the agar layer was carefully removed and the twitching cells were stained with 1 % crystal violet.

2.2.4.8 Urease activity test.

P. mirabilis cells were inoculated into plates of Christensen's Urea Agar by stabbing the surface with a sterile toothpick, used to pick a single colony from a freshly streaked plate. Urease action was assessed by the presence of the pH indicator Phenol Red which turns red in response to ammonia release. Plates were visualised after 24 h of incubation at 37 °C.

2.2.5 Statistical analysis

Statistical analyses were performed using Graphpad Prism software 6 and 7 (San Diego, USA). Comparisons between each treated and untreated were analysed with unpaired t-test with Welch's correction and asterisks were used for reference as follows (*) if *p* value ≤0.05, (**) if *p* value ≤0.01, (***) if *p* value ≤0.001 and (****) if *p* value ≤0.0001.

2.2.6 Biofilms

2.2.6.1 *P. aeruginosa* biofilms

2.2.6.1.1 Static biofilms

Overnight cultures of *P. aeruginosa* were standardized to OD_{600}=0.05 in 500 µl of the appropriate growth medium in polystyrene 24-well plates (Greiner). After a seeding step of 2 h static growth at 37 °C, the plate was moved to an incubator shaking at 200 rpm and at 37 °C. Visualization or quantification was assessed using either live/dead. For the former, the BacLight Bacterial Viability Kit L7007 (Thermo Fisher) was employed which consists of two stock solutions: "A" containing SYTO 9 dye, 1.67 mM and Propidium iodide (PI), 1.67 mM and "B" containing SYTO 9 dye, 1.67 mM and PI, 18.3 mM. The final staining solution was prepared with 1.5 µl of each solution (A and B) diluted into 1 mL of Tris-buffered Saline (TBS) (150 mM NaCl, 50 mM Tris-HCl, pH 7.6). After removing the planktonic cells, the biofilm was covered in foil and incubated at room temperature with 300 µl of the staining solution. It was then washed with water to allow visualization/quantification.

Alternatively, biofilms were grown in LB 10% in 96 well plates (Greiner) and stained with 0.1 % w/v crystal violet in water with 5 % v/v EtOH for 15 min after one wash with PBS pH7.4. Excess CV was washed three times with PBS pH7.4, and, once dry, the absorption measured at 595 nm in a TECAN plate reader.

2.2.6.1.2 Microfluidic biofilm

The microfluidic Bioflux™ system (Conant *et al.*, 2009) was employed to emulate biofilm growth under shear flow conditions. The specifically-designed 48-well plates were used along with the Bioflux™ 200 system. Firstly, each channel was primed by adding 100 µL of sterile LB 10 % in the outlet well and allowing it to flow at 2 dyn/cm^2 for 3 min until a drop appeared in the connected inlet. Subsequently, 50 µL of standardized (OD_{600} =0.05) *P. aeruginosa* culture was added to the outlet and pushed through the channel at 2 dyn/cm^2 for 5 sand a further 200 ul of sterile LB 10% v/v was added to the inlet. The inclusion of the growth media in the inlet was carried out to help balance the system and counteract gravity. The bacterial culture in the outlet was pushed through the channel at 2 dyn/cm2 for 5 s. After the injection of bacterial cells, the seeding step was continued by incubating the plate for 1 h at 37 °C without flow. Finally, the inlet wells were filled with 1000 µl of LB 10 % v/v supplemented with 1 µL of the A+B (50%+50%) mixture of BacLight Bacterial Viability Kit L7007 and the Bioflux was set to run in the direction of inlet>outlet with a flow rate of 0.25 dyn/cm^2 for 16 h. To ensure a consistent temperature was maintained throughout the experiment, the plate was placed on a heated block (37 °C). Upon completion of the run, the biofilms were observed under CLSM.

2.2.6.1.3 Rotating immersion biofilm

The rotating immersion biofilm is an innovative technique where a *P. aeruginosa* biofilm is formed under shear conditions by cyclic immersions of circled glass cover slips (Fisherbrand) into a bacterial suspension (unpublished) (Figure 2.3). Firstly, the coverslips were attached to a wheel and autoclaved along with a glass tank supporting a volume of 900 ml medium (10 mM glucose enriched FAB). Following sterilisation, an overnight of *P. aeruginosa* was used for the inoculum (OD_{600}=0.05) which was poured into the tank. After attaching the wheel to the motor engine, the whole system was transferred into an incubator at 30 °C for 24 h. Two containers of water were also placed inside the incubator to maintain humidity and reduce evaporation. Two to four coverslips were recovered, washed in PBS and water, before staining with 70 µL of staining solution

(1 ml TBS with 3 µl of A+B mixture from BacLight Bacterial Viability Kit L7007, Thermo Fisher). Samples were observed with CLSM. The remaining coverslips were placed inside 4 petri dishes containing clean FAB medium with 10 mM glucose supplemented with DMSO 0.4% v/v only, ciprofloxacin 180 µM (60 µg/ml), 488 200 µM and ciprofloxacin 60 µg/ml with 488, 200 µM respectively. The dishes were incubated for a further 24 h at 30 °C and stained as described for CLSM visualization (section 2.2.7.1). This further incubation was performed to test the antibiotic susceptibility on preformed biofilms exposed to 488.

Figure 2.3 Rotating immersion biofilm assay.

2.2.6.2 *P. mirabilis* biofilms

P. mirabilis biofilms were set up in polystyrene 24-well plates (Greiner) using artificial urine (AU) supplemented with calcein (2 µM). After adjusting the OD_{600} to 0.05, a culture of DsRed-tagged *P. mirabilis* Hauser 1885 was incubated statically at 37 °C for 2h and then incubated under gentle shaking (70 rpm) for 72h. Bacterial attachment and biomineralisation were imaged and quantified using CLSM.

2.2.6.3 *S. aureus* biofilms

A eGFP-labelled *S. aureus* SH1000 overnight culture in TSB was washed once and restarted in a clean 5 ml volume of BHI. Once OD_{600}=0.3 was reached, the cells were diluted to OD_{600} 0.05 and 1 mL of the standardized culture was transferred into the relative well of the polystyrene 24-well plates (Greiner). The biofilms were left growing at 37 °C for 2 h in static conditions and shaking (70 rpm) for 16 h.

2.2.6.4 Multi-species biofilms

A multi-strain biofilm experiment was carried out with DsRed-labelled *P. mirabilis* Hauser 1885, mTurquoise-labelled *P. aeruginosa* PAO1-UW and *e*GFP-labelled *S. aureus* SH1000. The OD_{600} for each strain was adjusted for the inoculum at 0.05 with AU medium in polystyrene 24-well plates (Greiner), left seeding for 2 h statically at 37 °C and incubated for a further 22 h at 70 rpm for a total of 72 h. *P. mirabilis* was grown first, followed by *P. aeruginosa* and finally *S. aureus* for a total of 72 h. Before addition of the new inoculum, the medium was carefully removed and the new bacterial suspension gently added.

2.2.6.5 Biofilm quantification and analysis

Single-species *P. aeruginosa* biofilms grown in 24 well plates and treated with live/dead staining were analysed and quantified using a TECAN infinite® F200 PRO plate reader for crystal violet staining and a TECAN Spark® Multimode Microplate Reader for live/dead staining. To enable analysis of Z-stack images generated with Confocal Laser Scanning Microscopy (section 2.2.7.1), 3D pictures were processed using the Maximum intensity Projection function in Zen 2.3 SP1 (black) software (Carl Zeiss, Jena, Germany). This tool generates a bi-dimensional (2D) image per channel, constituted by pixels containing the maximum value over all images in the Z-stack at the single pixel location. Each new picture was exported in tiff format (64bit) with no compression into Zen 2.3 (Blue edition). Analysis and quantification were performed on the entire image using the Measure function in ImageJ 1.52i software (Rueden *et al.*, 2017) implemented with Fiji plugin bundle (Schindelin *et al.*, 2012). The data generated per single picture are the man grey value defined as sum of the grey values of all the pixels, divided by the number of pixels and the related standard deviation. Final data represent the mean values of the samples grown under a specific condition as the average of the mean grey values generated among the collected images per well.

2.2.7 Microscopy

2.2.7.1 Confocal Laser Scanning Microscopy

Confocal Laser Scanning Microscopy (CLSM) was used to visualize and generate Z-stack representations for the bioflux, rotative immersion, *P. mirabilis*, *S. aureus* and mixed species biofilms. Visualisation was performed with a Zeiss LSM 700 confocal laser scanning microscope (Carl Zeiss, Ltd, Welwyn, UK) controlled by the ZEN 2009 software platform (Carl Zeiss, Ltd, Welwyn, UK), using a 5x or 10x objective. The acquisition settings depended on the fluorescence: pinhole 1.0, laser intensity 5%-15% and gain between 450 and 700 for bio-fluorescent strains. Laser intensity 15%, gain 460 and pinhole 1.0 were the settings used for samples treated with live-dead staining. Nevertheless, once adjusted to optimize the visualization, settings were never modified within an experiment to facilitate an unbiased comparison. The Z-stack height was set for each acquisition in a new well by starting from the first point where no emission was detected (just prior to the start of the biofilm), through the biofilm itself, until a point of no emission was again reached, which was set as the last slice. Spacing, once set, was kept constant within the experiment. Spacing and height was kept constant among all the rotating immersion biofilm experiments.

2.2.7.2 Transmission electron microscopy

The fixation solution was prepared by mixing 600 µL 25% glutaraldehyde in 2.5 mL of 0.2 M cacodylate buffer (pH 7.4), diluted with 1.9 mL distilled water. For fixation, 50 µL of each overnight culture of *P. aeruginosa* PAO1-L standardized to OD_{600} = 0.5 was diluted into the fixation solution and incubated for 1 h. Cells were then centrifuged at 4000 rpm for 5 minutes and the supernatant was removed. Samples were washed 3 times interspaced with a 10 minute incubation step using 1 mL of 0.1 mM of cacodylate buffer before each centrifugation. The final pellet was resuspended in 100 µL of molecular grade water and fixed cells were placed on 200 mesh copper grids with carbon support. The single cells were visualised with a Tecnai T12 Biotwin transmission electron microscope at

an accelerating voltage of 110 kV and photographed using a Mega View SIS camera.

2.2.8 Chemistry analysis

2.2.8.1 2-alkyl-4-quinolones extraction

The extraction of AQs was based on the protocol described by Ortori *et al.* (2014). Triplicate cultures of *P. aeruginosa* strains were standardised to OD_{600} 0.05 in 10 ml LB and incubated for 16 h at 37°C and 200 rpm. After centrifugation at 10000 g for 5 min, the supernatants were collected and filtered (0.22 µm) of which 100 µL were then diluted with 400 µL of distilled water. An internal standard, deuterated PQS (d4-PQS), was added to a final concentration of 20 nM. Five hundred microlitres of acidified ethyl acetate (0.1% acetic acid) were added and mixed by vortexing for 2 min. After centrifugation, the top organic layer was transferred into a 2 ml Eppendorf. The extraction step was repeated twice more, combining the extracts of each sample into one ~1.5 ml extract before drying by evaporation using a rotary Speedvac evaporator (R-114, Buchi). Dried samples were stored at -20°C.

2.2.8.2 Thin Layer Chromatography and overlay with bioluminescent reporter

The assay was performed as described in Fletcher *et al.* (2014). A phase silica 60_{F254} (Merck) TLC plate was soaked for 30 min in 5 % (w/v) KH_2PO_4 and activated by baking at 100 °C for 1 h. 5 µl of AQs extracted as previously described were spotted in line 3 cm from the bottom of the plate. For the control, a lane was reserved for 2 µl of 10 mM synthetic PQS and HHQ. Once dried and placed in a closed chamber, the extracts were separated using a dichloromethane (DCM): MeOH (95:5) mobile phase until it reached the top of the plate. The plate was visualised using a UV transilluminator (UVP, USA). The TLC plates used to detect AQs were overlaid with 0.3 % (w/v) LB soft top agar seeded with 0.5 % (v/v) of overnight culture of the *P. aeruginosa* Δ*pqsA* pCTX::P*pqsA-lux* bioreporter. This mutant is unable to produce endogenous AQs but responds to exogenous AQs on the TLC surface. After incubation at 37 °C for 16 h, bioluminescence was imaged using a CCD camera (model C5405-51), an

amplifier (C2741-3OH) and an intensifying unit (M4314, Hamamatsu Photonics K.K., Hamamatsu, Japan). Pyocyanin was visualized and photographed under visible light.

2.2.8.3 Liquid Chromatography Tandem Mass Spectrometry (LC-MS/MS)

AQ extracts (2.2.4.4) were resuspended in 100 µL of MeOH. For each sample, 2 µL was injected onto into the appropriate liquid chromatography column (Phenomenex Gemini C18, 3.0 µm, 100 x 3.0 mm) at a flow rate of 450 µL/min, 40°C with mobile phases composed of: A) 0.1% (v/v) formic acid (CH_2O_2) in water containing 2 mM 2-picolinic acid; B) 0.1% (v/v) CH_2O_2 in MeOH. AQs were separated with a linear gradient consisting of 30% to 99% mobile phase B over 5 min, 99% B for an additional 3 min before going down to 30% B for 1 minu. A further 4 min were required to allow for column equilibration. An Applied Biosystems Qtrap 4000 hybrid triple-quadrupole linear iron trap mass spectrometer (Foster City, CA, USA) was employed as the MS platform with an electrospray ionisation interface. The system was controlled with Analyst software (Foster City, CA, USA). The LC eluents were screened using positive electrospray (+ES) with multiple reaction monitoring (MRM). Finally, AQs were quantified by calculating peak area and dividing the analyte peak area by the internal standard (d4-PQS) peak area.

2.2.9 PqsR^{CBD} purification and ligand binding studies

PqsR co-inducer binding domain (CBD) protein-related cloning, expression, purification and crystallization conditions were based on Ilangovan *et al.* (2013). Thus, the construct PqsR-C$^{94\text{-}332}$ was expressed in *E.coli* BL21 DE3 pET28a::*pqsR*$^{C94\text{-}309}$.

2.2.9.1 *In silico* molecular modelling of PqsR/lactam interactions

Molecular modelling was carried out as described below. To investigate the molecular dynamics of the interaction between the lactams and PqsR, the crystal structure of the PqsR^{CBD}, binding modes and docking scores were generated using Maestro software (Schrödinger, LLC) a molecular modelling and visualization program. Firstly, the crystal structure of the PqsR^{CBD}/3NH$_2$-7Cl-C9QZN antagonist complex (PDB-ID: 4JVD) from the RCSB Protein Databank was loaded into the software. The final structure of the protein for the docking was subsequently obtained by removing the quinazolinone (QZN) ligand molecule. The lactam structures were drawn using ChemBioDraw Ultra software (PerkinElmer Inc.) and loaded into the Maestro graphic environment to calculate all the probable conformations within a binding pocket grid, generated from the residues Ala102, Pro129, Ile149, Thr166, Ala 168, Val 170, Ile186, Ile189, Gln194, Ser196, Leu196, Leu197, Leu207, Leu208, Pro210, Val211, Trp234, Gly235, Pro238 and Ser255. The inner and outer grid boxes were set to 10 Å and 20 Å respectively. Finally, the docking scores of the lactams were calculated as an evaluation of the strength of the interactions of the docked molecules.

2.2.9.2 Expression of the PqsR^{CBD}

A colony of *E.coli* BL21 (DE3) (Novagen) pET28a::*pqsR*$^{C94\text{-}309}$ from a kanamycin (50µg/mL) and chloramphenicol (35 µg/mL) resistant plate was transferred to 2.5 mL of LB and left to grow overnight at 37°C and 200 rpm. This starter culture was used to inoculate 0.5 L of LB media containing LB agar plate was transferred to 2.5 mL of LB and left to grow overnight at 37°C and 200 rpm. This starter culture was used to inoculate 0.5 L of

LB medium containing kanamycin (50 μgmL^{-1}), which was incubated at 37° to an OD_{600} of 0.8, whereupon 0.5 mL of 1M IPTG was added to give a final concentration of 1 mM. The culture was incubated for a further 24 h at 16°C and 200 rpm. Bacterial cells were harvested by centrifugation at 4°C at 5,000 *g* for 30 min in two 500 ml bottles and the cell-free supernatant removed. Each pellet was resuspended in 35 ml of 20 mM Tris-HCl, 150 mM NaCl, pH 7.4. The resuspended cells were frozen at -80°C until use and to facilitate cell lysis.

2.2.9.3 Purification of PqsR^{CBD} by Ni2+ affinity chromatography

The expression vector pET28a::*pqsR*$^{C94\text{-}309}$ contains a histidine (His) tag at the 5'end of a multiple cloning site allowing purification by nickel affinity chromatography. The frozen bacteria were thawed and then lysed by sonication (Thermo Fisher). The culture was sonicated on ice for 20 cycles consisting of a 15 s pulse at an amplitude of 15 microns with 15 s pauses. The cell lysate was centrifuged at 13,000 *g* for 30 min to remove insoluble cell debris and the supernatant decanted and passed through a 0.45 μm filter (Millipore, UK). The lysate was loaded using with a peristaltic pump at a flowrate of 1 ml/min onto a 5 mL HisTrap™ HP column (GE Healthcare), precharged with $NiCl_2$. A liquid chromatography handling system (AKTAprime, GE Healthcare) was used to run a gradient elution of 0 - 500 mM imidazole at a flowrate of 2 mL/min, collecting 5 mL eluent fractions which were analysed via SDS-PAGE.

2.2.9.4 Sodium dodecyl sulphate polyacrylamide gel electrophoresis (SDS PAGE) and Coomassie blue staining

SDS-PAGE analysis was carried on polyacrylamide gels prepared using the Mini PROTEAN® System (BioRad) using the components listed in Table 2.5. After the addition of N,N,N',N'-tetramethylethylenediamine (TEMED) and ammonium persulphate (APS), the resolving gel was poured between the glass plates and topped with 1 mL layer of isopropanol. Once polymerization was complete, the isopropanol was removed and the stacking gel was poured on top of the resolving gel. A plastic comb (BioRad) was inserted in the stacking gel to create the wells required for sample loading. The comb was removed gently after the gel had solidified.

Table 2.5 Resolving and stacking SDS gels components

	16% - Resolving gel	*6% - Stacking gel*
Acrylamide (30 % stock)	4.27 mL	1 mL
1 M Tris-HCl (pH 6.8)	-	1.25 mL
1.5 M Tris-HCl (pH 8.8)	2 mL	-
Distilled water	1.6 mL	2.6 mL
10% SDS	80 µL	50
10% APS	80 µL	50 µL
TEMED	8 µL	5 µL

Before loading, samples were mixed with 6 x loading buffer (Promega) and boiled for 10 min at 95°C in a heat block (Grant QBA2, Scientific Laboratory Supplies). The gel was simultaneously placed in an electrophoresis tank (Biorad) and immersed in SDS running buffer. As molecular weight markers, the standard broad range pre-stained protein ladder (NEB) was loaded. Electrophoresis was performed at 200 V for 45 min or until samples reached the bottom of the glass plate. Gels were stained with 25 v/v % ethanol, 10 % v/v acetic acid and 0.25 % w/v Coomassie Blue R for 1 h and destained with a solution of 10 % v/v ethanol containing 12 % v/v acetic acid.

2.2.9.5 Dialysis

The fractions eluted from the gradient were dialysed overnight at 22°C using a sealed dialysis membrane (molecular weight cut off 6-8 kDa) (Spectra/Por1, Spectrum Labs) suspended in 500 ml of buffer containing 20 mM Tris-HCl, 0.5 mM DTT and 1mM EDTA, pH 7.4 . The dialysis ensured the cleaning of the samples from an excess of imidazole and salts whilst the reducing agents prevented precipitation of the protein. The dialysis ensured removal of excess imidazole and salts whilst the reducing agents prevented precipitation of the protein.

2.2.9.6 Determination of protein concentration

Protein content and concentration was determined using a Nanodrop Spectrophotometer 1000 (Thermo Scientific). The measurement was based on 3 µl of material, blanked with 3 µl of corresponding buffer. Protein concentration was determined through the Beer-Lambert law equation

using the extinction coefficient value for PqsR^{CBD} calculated with the online program ProtParam (ExPASy). The calculation is described by the following equation:

$$[Protein] = \frac{absorbance\ at\ 280\ nm}{Extinction\ coefficient}$$

2.2.9.7 Purification of PqsR ^{CBD} by gel filtration

Size exclusion chromatography (SEC) was used increase the purity of the PqsR^{CBD} protein after Ni^{2+} affinity chromatography for crystallization, isothermal titration calorimetry (ITC) or synchrotron radiation dichroism (SRCD). A HiLoadTM 26/600 Superdex^{TM} 75 gel filtration column (Amersham Biosciences) was initially washed and equilibrated with a running buffer (SEC buffer) consisting in 20 mM Tris-HCl, pH 7.4, and 150 mM NaCl. The 10 mL sample loop was washed with 10 mL of running buffer prior to loading the protein sample. The gel filtration proceeded using a flowrate of 2 ml min^{-1}. The eluted protein fractions were analysed by SDS-PAGE before snap-freezing and storage at -80°C, unless they were concentrated for crystallization.

2.2.9.8 Iso-thermal titration calorimetry (ITC)

ITC was performed using the MicroCal PEAQ-ITC from Malvern Panalytical (UK). Before each set of experiments, the sample-cell was deep-cleaned by soaking with MeOH for 1 h. Additionally, the sample-cell and syringe were washed and rinsed between each experiment. PqsR^{CBD} protein and lactam 488 were diluted in SEC buffer supplemented with 4% v/v DMSO for 400 µM and 20 µM final concentrations respectively. The temperature was set at 25 °C and differential power at 5 with high feedback. The titration curve was constructed starting with the first injection of 2 µL ligand into the cell containing PqsR^{CBD} for 150 s, followed by 18 injections every 90 s. The analysis was conducted with the Malvern analysis software (Malvern Panalytical, UK).

2.2.9.9 Synchrotron radiation circular dichroism (SRCD)

xperiments were performed using a nitrogen-flushed Module A for temperature studies and Module B for far UV ligand titration studies using the HT-CD multi-cell system end-station spectrophotometer at B23

Synchotron Radiation CD Beamline at the Diamond Light Source (Didcot, UK) (Hussain *et al.*, 2016; Hussain *et al.*, 2012a, 2012b; Hussain & Siligardi, 2016; Javorfi *et al.*, 2010; Siligardi & Hussain, 2015; Zinna *et al.*, 2017) as well as ChirascanPlus CD spectro-polarimeter (Applied Photophysics Ltd, Leatherhead, UK) for near-UV measurements. Five achiral ligands were used: C7-PQS, NH_2-PQS, 488, 3-NH_2-7-Cl-C9-QZN, and HHQ. The ligands were dissolved to 100 µM 0.5% v/v DMSO solution for far-UV measurements and 200 µM in neat DMSO for near-UV CD measurements. $PsqR^{CBD}$ was supplied as a frozen aliquot of 500 µl per tube in 20 mM Tris-HCl, pH 7.4 containing 150 mM NaCl. Scans were acquired using an integration time of 1 s, a path-length of 0.02 cm for the far-UV measurements 1.2 nm bandwidth, 2 nm for the near-UV measurements at 20 °C. Results obtained were processed using CDApps (Provencher & Glockner, 1981) and OriginLab™. Spectra were normalized using an average amino acid molecular weight of 113. Secondary structure estimation from CD spectra was carried out using CDApps using Continll algorithm (Provencher & Glockner, 1981).

2.2.9.10 Crystallization of PqsR ^{CBD} and soaking with lactam 488

Crystallization experiments were carried out with protein purified on the same day to avoid precipitation and using the highest quality sample available. Therefore, the protein was concentrated with Vivaspin 2 MWCO 10,000 spin column (GE Healthcare) to 7, 10 and 15 mg/ml and spotted into 24 well hanging-drop plates. Reservoirs contained 0.1 M trisodium citrate and 0.2 M ammonium acetate with a range of pHs (from 5 to 6 - top to bottom wells) and 2-Methyl-2,4-pentanediol (MPD) % v/v (1 to 6 – left to right wells). Crystals appeared after 24 h at 19°C although the incubation was continued for one further week to allow the crystals to grow in size, thus providing better diffraction. Before the biggest crystals were left soaking overnight at 19° C with lactam 488 dissolved in ethylene glycol.

2.2.9.11 Diffractometry

The 488-soaked crystals were harvested from the precipitant solution (0.1 M tri-sodium citrate pH-6.0, 0.2 M ammonium acetate and 5% MPD (v/v)) and transferred to a cryoprotectant solution with 30% ethylene glycol for

several minutes before being flash-frozen in liquid nitrogen. The 488-soaked PqsR^{CBD}crystals were sent for Synchrotron experiments to the I24 beamline at Diamond Light Source (Didcot, UK) (Figure 2.4). Using a wavelength of 0.97 Å, the crystals were exposed to X-ray beams with 50 µm apertures for 0.25 s per 0.5° oscillation (total of 180°, 90s) and the detector distance was set to 510.75 mm. The protein structure was solved with Phaser from the CCP4 software suite (McCoy *et al.*, 2007) using the structure of PqsR^{CBD} from RCSB (PDB-ID: 4JVD) and the model refined with Refmac5 (Vagin *et al.*, 2004) The 488 ligand was apparent in the later stages of refinement and were added into the model.

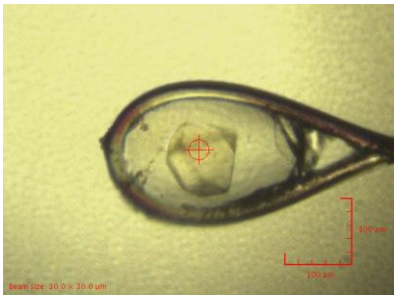

Figure 2.4 A PqsR^{CBD} crystal soaked in 488 held in a fibre cryoloop.

3 UNILEVER LACTAMS AS QUORUM SENSING INHIBITORS IN *P. AERUGINOSA*

INTRODUCTION

The dihydropyrrol-2-ones (lactams) provided by Unilever are synthetic analogues, of fimbrolides (halogenated furanones) isolated from the marine red alga *Delisea pulchra* (Goh *et al.*, 2007). These molecules were found to possess quorum sensing (QS)-inhibitory properties, specifically against *N*-acyl-L-homoserine lactone (AHL)-mediated QS systems thus affecting QS-regulated related phenotypes (Hentzer *et al.*, 2002; Manefield *et al.*, 1999; Shetye *et al.*, 2013). Through LuxR-based *E. coli* reporter activity studies, additional fimbrolide analogues have recently shown similar inhibitory activities. *In silico* docking studies with the *P. aeruginosa* LuxR orthologue LasR suggested that the lactams could also bind to the LasR ligand binding site. However, no biological assays were carried out to confirm the *in silico* analysis (Goh *et al.*, 2015). Internal Unilever studies have also reported inhibitory effects of the lactams on biofilm formation on different species. Against this background, the impact of each lactam on QS in *P. aeruginosa* was first explored, as the mechanism of action had not been established.

3.1 IMPACT OF THE LACTAMS ON QUORUM SENSING IN *P. AERUGINOSA*

P. aeruginosa was chosen as the first bacterial species to investigate the QS inhibitory activity of the first set of Unilever lactam analogues provided (Figure 2.1). The expression of *rhl, pqs* and *las* genes was evaluated using *lux*-based *rhlI*, *pqsA* and *lasI* promoter fusions. These genes were selected as they represent the primary targets of the transcriptional regulators LasR, PqsR and RhlR. The *lux*-based promoter fusion constructs were

constructed using the miniCTX-*luxCDABE* plasmid system (Becher & Schweizer, 2000) which facilitates integration of surrogate promoter fusions into the CTX phage site in the *P. aeruginosa* chromosome. Thus the resulting bioluminescence is related to the expression of the *lux*-fused promoter and can be quantified independent of the original gene.

P. aeruginosa PAO1-N P*tac*::*lux* was used as a positive control as it constitutively expresses *luxCDABE* and hence light. Any reduction in light output in this strain in the presence of a lactam will indicate whether or not a compound has an adverse effect on light output. The lack of reduction light output from P*tac::lux* shows that there is no interference between the compounds and either the luciferase or fatty acid reductase (Figure 3.1). As shown in Figure 3.2 and Figure 3.5, the compounds 491 and 488, in particular, are more potent than the others especially on P*pqsA*::*lux* gene expression (Figure 3.2). Moreover, 488 caused a ~40% reduction in the expression of *lasI* (Figure 3.3). The five lactams had little effect on *rhlI* expression with 488 and 491 reducing expression by <10% (Figure 3.4).

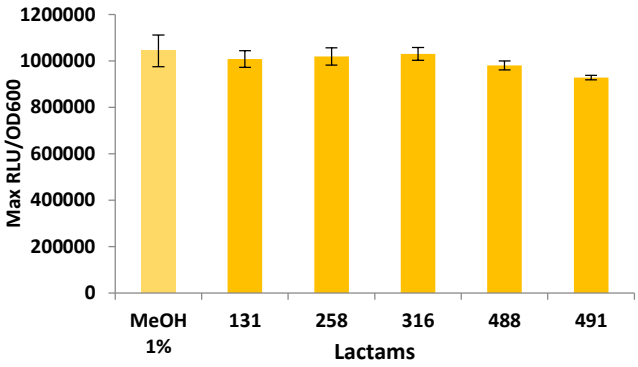

Figure 3.1 Effect of lactams (100 µM) on *tac* promoter expression using the PAO1-L pCTX::P*tacΔlacI*^{Q}*-lux* biosensor. This bioreporter was constructed and employed to test the eventual impact on the lux operon or on bioluminescence metabolism. Positive control (solvent only) is shown on the left column. Error bars represent standard deviation of biological triplicates.

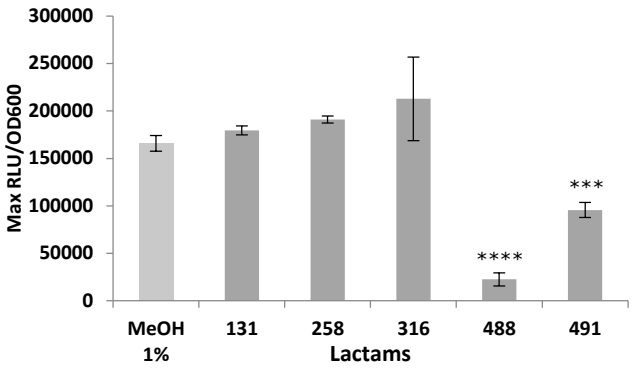

Figure 3.2 Effect of lactams (100 µM) on *pqsA* promoter expression using the PAO1-L pCTX::P*pqsA-lux* biosensor. Positive control (solvent only) is shown on the left column. Error bars represent standard deviation of biological triplicates. Statistical significance was calculated with Welch's t test, (***) represents *p* value <0.001, (****) <0.0001.

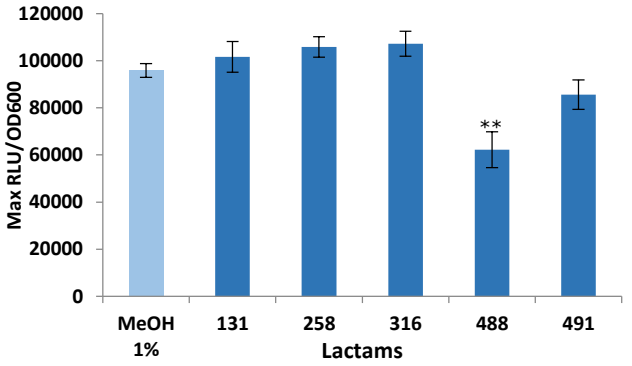

Figure 3.3 Effect of lactams (100 µM) on *lasI* promoter expression using the PAO1-L pCTX::P*lasI-lux* biosensor. Positive control (solvent only) is shown on the left column. Error bars represent standard deviation of biological triplicates. Statistical significance was calculated with Welch's t test, (**) represents *p* value <0.01.

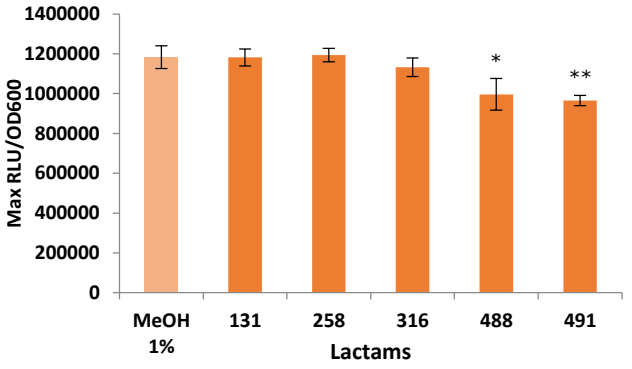

Figure 3.4 Effect of lactams (100 µM) on *RhlI* promoter expression using the PAO1-L pCTX::P*rhlI-lux* biosensor. Positive control (solvent only) is shown on the left column. Error bars represent standard deviation of biological triplicates. Statistical significance was calculated with Welch's t test, (*) represents *p* value <0.05, (**) *p* value <0.01.

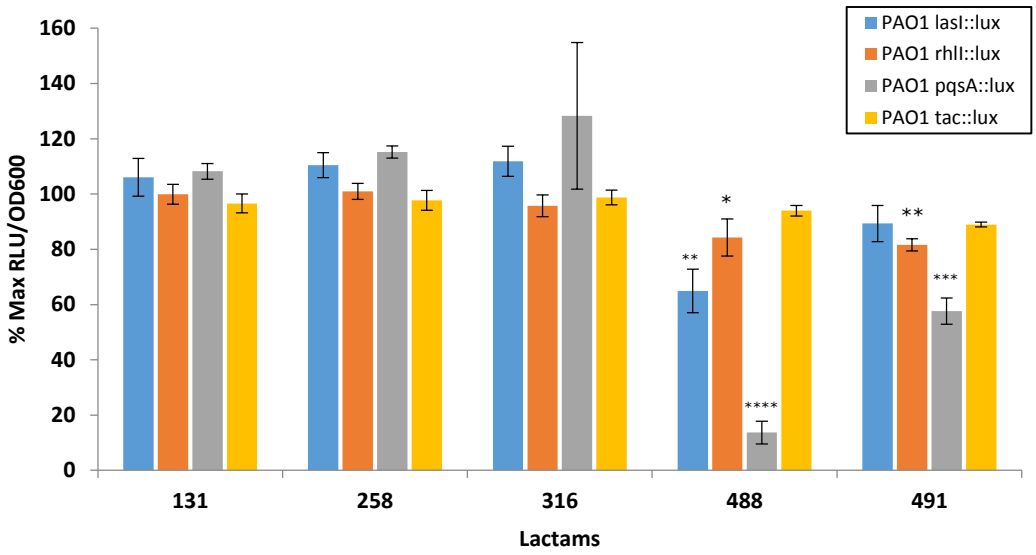

Figure 3.5 Overview of the effect of lactams at 100 µM on QS reporter genes expression in *P. aeruginosa* PAO1-L. For each biosensor, the expression was normalized by the value of the respective solvent only control. Error bars represent the standard deviation between biological triplicates. A series of t-tests were performed on the original data to determine statistical significance in each group, (**) represents *p* value <0.01, (***) *p* value <0.001 (****) *p* value <0.0001.

3.2 EVALUATION OF THE INHIBITORY EFFECTS OF LACTAM 488 AND 491 ON PQS SYSTEM EXPRESSION

3.2.1 Antagonism assays

The preliminary data shown in Figure 3.5 reveals that lactams 488 and 491 at 100 µM are primarily inhibitors of the *pqs* QS system in *P. aeruginosa*. Hence, to quantify the degree of inhibition was assayed by employing the PAO1-L P*pqsA::lux* biosensor was subjected to linearly increasing concentrations of lactams in order to construct a dose-response curve for each lactam from which IC_{50} values can be derived. Lactam 488 exhibited a lower IC_{50} value than 491, and was therefore the more active of the compounds tested (Figure 3.6 and Figure 3.7). IC_{50} values of 21.72 ± 0.71 µM for 488 and 43.91 ±1.87 µM for 491 were calculated, confirming the previously reported preliminary observations (Figure 3.2 and Figure 3.5). Furthermore, 491 did not reduce *pqsA* expression to zero at maximal activity since significant residual light output remained (Figure 3.7). Lactam 488 reduced *pqsA* expression to close to zero at a concentration of 200 µM and so was considerably more potent (Figure 3.6).

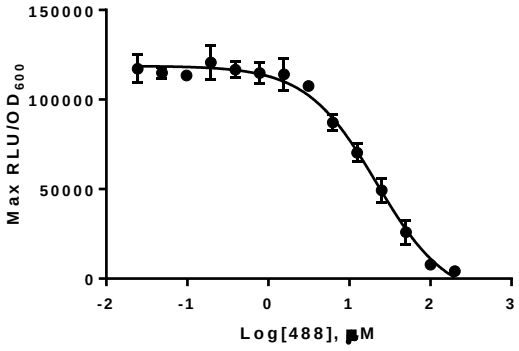

Figure 3.6 Effect of lactam 488 on expression of P*pqsA::lux* in PAO1-L (IC_{50} =21.72 ± 0.71). Error bars represent standard deviation of technical triplicates.

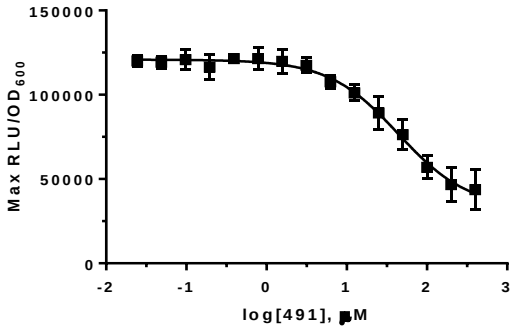

Figure 3.7 Effect of lactam 491 on expression of P*pqsA::lux* in PAO1-L (IC_{50} 43.91 ±1.87). Error bars represent standard deviation of technical triplicates.

The impact of the lactams on *pqsA* expression in *P. aeruginosa* strains PA14 and ATCC 15442 was also evaluated following the introduction of a chromosomal P*pqsA::lux* fusion. Figure 3.8 shows that 488 has comparable inhibitory effects on strain PA14 to those previously described for strain PAO1. For PA14, the IC_{50} extrapolated from the inhibition curve was calculated as 19.84±3.2µM.

Figure 3.9 shows that 488 does not inhibit P*pqsA::lux* expression in strain ATCC 15442. However the very low light output and hence *pqsA* expression in this strain, along with the lack of pyocyanin, suggests the PQS system is inactive, conferring similar phenotypic characteristics as that observed for e.g *pqsA* mutants (Aendekerk *et al.*, 2005; Gallagher *et al.*, 2002). Indeed, after a BLASTP analysis of the PQS genes from the ATCC 15442 genome, using sequences from the PAO1-L WT genome as query, a missense mutation was detected in PqsR in position 176 (Histidine>Proline). Being very close to the binding site, this mutation could affect the protein structure and its substrate binding affinity.

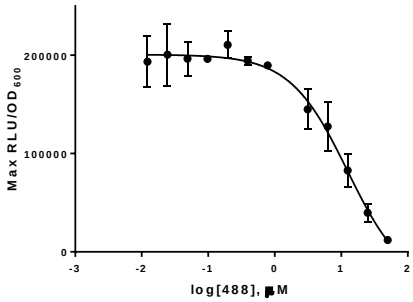

Figure 3.8 Effect of lactam 488 on expression of P*pqsA::lux* in PA14 (IC_{50} =19.84±3.2). Error bars represent standard deviation of technical triplicates.

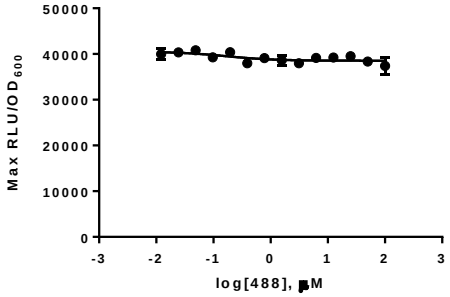

Figure 3.9 Effect of lactam 488 on expression of P*pqsA::lux* in PA ATCC 1544. Error bars represent standard deviation of technical triplicates.

3.2.2 Competition assays

The major quorum sensing signal molecules in the *P. aeruginosa pqs* system are the alkylquinolones, PQS and its precursor HHQ (Williams & Camara 2009). HHQ biosynthesis depends on the PqsABCDE enzymes and is converted to PQS by the activity of the mono-oxygenase PqsH. Both HHQ and PQS can drive autoinduction of their own biosynthesis through activation of the transcriptional regulator PqsR. The inhibitory action of lactam 488 may therefore involve inhibition of AQ biosynthesis or it may behave like an antagonist and block ligand-dependent activation of the PQS receptor, PqsR. Consequently, experiments were designed to determine the nature and degree of this inhibitory action, starting from the analysis of potential PqsR inactivation.

To determine whether the antagonism between PQS and 488 was competitive or non-competitive, four dose response curves were constructed using PAO1-L Δ*pqsA*, P*pqsA::lux.* Due to deletion of *pqsA* this strain in unable to produce any AQs and hence produce light but nevertheless it responses proportionally to the provision of exogenous PQS or HHQ. The curves were thus generated activating the bioreporter with increasing amounts of AQ in presence of fixed concentrations of lactam. The experiment was initially carried out employing PQS molecule as the exogenous AQ necessary for bioluminescence. The results obtained (Figure 3.10) show that as 488 concentrations are increased, maximal light output is substantially reduced, suggesting 488 functioning as a non-competitive antagonist.

However, due to the poor water solubility of PQS (Lépine *et al.*, 2003), the dose response curves did not reach a plateau at high concentrations such that a definite competitive dose response curve could not be obtained. The assay was repeated using the PQS analogue 7Cl-PQS (Figure 3.11). 7Cl-PQS is ~200 times more active (EC_{50} 0.014 μM) as a PqsR agonist than PQS (EC_{50} ~2-3 μM) and is the most powerful PqsR agonist so far described thanks to its 7Cl substituent that can form a hydrogen bond with the side chain of Thr625 within the $PqsR^{CBD}$ ligand binding pocket. 7Cl-PQS induces

higher levels of *pqsA* expression at lower concentrations (Ilangovan *et al.*, 2013). This characteristic allowed a full dose response curve to be generated, overcoming the limits previously described for PQS (Ilangovan *et al.*, 2013).

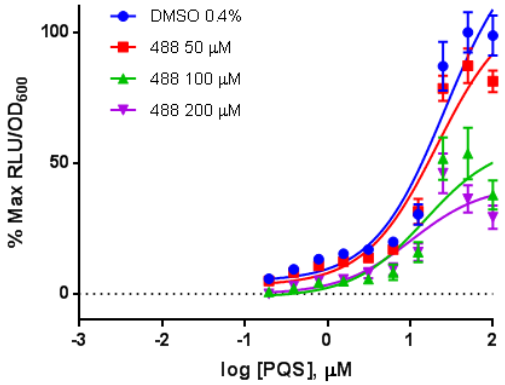

Figure 3.10 Effect of 488 at 0, 50, 100, 200 µM on the exogenous PQS-dependent expression of P*pqsA::lux* in *P. aeruginosa* PAO1-L Δ*pqsA*. (Standardized response). Error bars represent standard deviation of technical replicates.

Figure 3.11 compares the 7Cl-PQS dose response curves obtained in the absence or presence of 488 at different concentrations. With increasing concentrations of the antagonist, the respective curve plateau decreases, indicating the inability of the agonist to reach a full response. Therefore, the shape of the curves and the lack of significant changes of EC_{50} values suggest that 488 behaves as a non-competitive inhibitor.

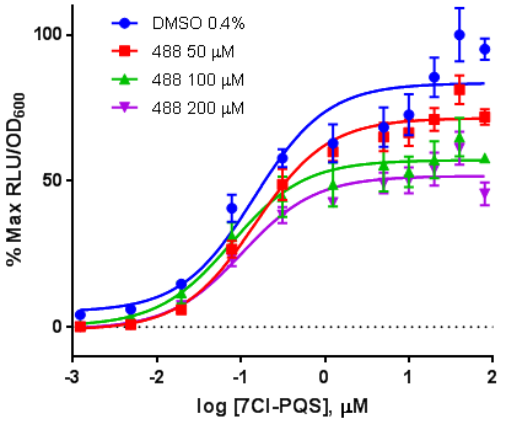

Figure 3.11 Effect of 488 at 0, 50, 100, 200 µM on the exogenous 7Cl-PQS-dependent expression of P*pqsA::lux* in *P. aeruginosa* PAO1-L Δ*pqsA*. (Standardized response). Error bars represent standard deviation of technical triplicates.

3.2.3 Evaluation of the inhibitory effects of lactam 488 on the PQS-dependent, PqsR-independent activation of pqsA

PQS is capable of weakly activating *pqsA* in the absence of PqsR via a mechanism that is not entirely understood but appears to be partially depending on the iron-chelating properties of PQS (Rampioni *et al.*, 2016). The aim of this experiment was to clarify whether lactam 488 is also inhibitory for *pqsA* expression via the PqsR independent response. The P*pqsA::lux* biosensor based on the triple mutant PAO1-N Δ*pqsAHR* is defective for the production of AQs because the genes coding for the key biosynthetic enzymes (PqsA and PqsH) and regulation (PqsR) have been deleted but still responds to exogenous PQS. This response is, however, much weaker that the PqsR-dependent response. Figure 3.12 shows the impact of 488 on the PqsR-independent expression of *pqsA* in the presence or absence of 40 μM PQS. 488 has a small inhibitory effect on the PqsR-independent pathway at high concentrations.

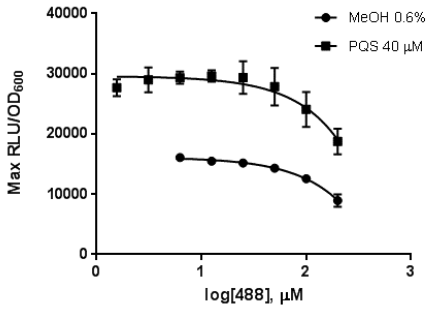

Figure 3.12 PqsR-independent activity of 488 on the expression of P*pqsA::lux* in PAO1-N Δ*pqsAHR* with and without PQS 40 μM. Error bars represent standard deviation of technical replicates.

3.2.4 Evaluation of partial agonist effects of lactam 488 on *P. aeruginosa*

A PAO1-L Δ*pqsA* P*pqsA::lux* biosensor-based assay was performed to determine whether lactam 488 exhibits any partial agonist activity at higher concentrations. A partial agonist is a molecule that can bind to and activate a receptor resulting in a non-complete response compared with a full agonist. Graphically, an antagonist that is also a partial agonist exhibits agonist activity at high concentrations. Figure 3.13 shows that 488 has no partial agonist activity as it was unable to activate *pqsA* expression at concentrations up to 800 µM. This observation disagrees with its activity as an antagonist in the presence of 10 or 40 µM PQS.

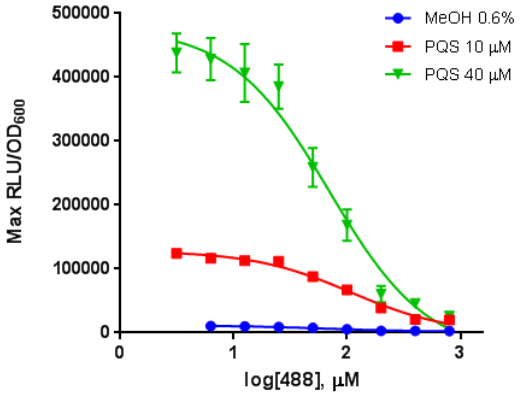

Figure 3.13 Effect of lactam 488 on the expression of P*pqsA::lux* in PAO1Δ*pqsA* in the presence of PQS at 0 µM, 10 µM or 40 µM. Error bars indicate standard deviation of technical triplicates.

3.3 EFFECT OF 488 ON ALKYL-QUINOLONE PRODUCTION

3.3.1 Qualitative AQ biosynthesis analysis

To determine whether 488 is capable of inhibiting the enzymes (PqsABCD) involved in AQ biosynthesis, the *P. aeruginosa* PAO1-N Δ*pqsAHR* was exploited. This mutant cannot produce AQs because the genes coding for the key biosynthetic enzymes (PqsA and PqsH) and regulation (PqsR) have been deleted. To restore HHQ production in a PqsR-independent manner in PAO1-N Δ*pqsA,* the *pqsABCD* genes were introduced into a plasmid (pBBR::*pqsABCD)*. *P. aeruginosa* PAO1-N Δ*pqsAHR* and *P. aeruginosa* PAO1-N Δ*pqsAHR pqsABCD* were both incubated overnight in LB in the presence or absence of 488 (200 μM). The cultures were extracted with acidified ethyl acetate, the organic phase removed, dried and resuspended in methanol subjected to thin layer chromatography (TLC). After chromatography using a dichloromethane-methanol mobile phase, the TLC plates were overlaid with a thin agar layer containing the AQ biosensor strain PAO1-L Δ*pqsA* P*pqsA::lux* (Fletcher *et al.*, 2007) incubated and examined for reporter output. Figure 3.14.panel A shows the TLC plate under UV illumination after chromatography. The biosensor strain produces light (Figure 3.14 panel C) and pyocyanin (Figure 3.14 panel B) in response to AQs present on the TLC plate which bind to PqsR and activate the *pqsA* promoter. Qualitatively, no HHQ production change was observed according to the pyocyanin production and luminescence production while, as expected, PQS molecule was not detected from PAO1-N Δ*pqsAHR* and PAO1-N Δ*pqsAHR pqsABCD* extractions.

The combined employment of TLC and AQ biosensor overlay provide a sufficient sensitivity to discriminate between the two AQs without the use of sophisticated techniques. On the other hand, only methods like Liquid chromatography-mass spectrometry (LCMS) or RP-HPLC are able to reach the sensitivity required for a definitive quantitative chemical analysis of the culture extracts (Diggle *et al.*, 2006a; Lépine *et al.*, 2004).

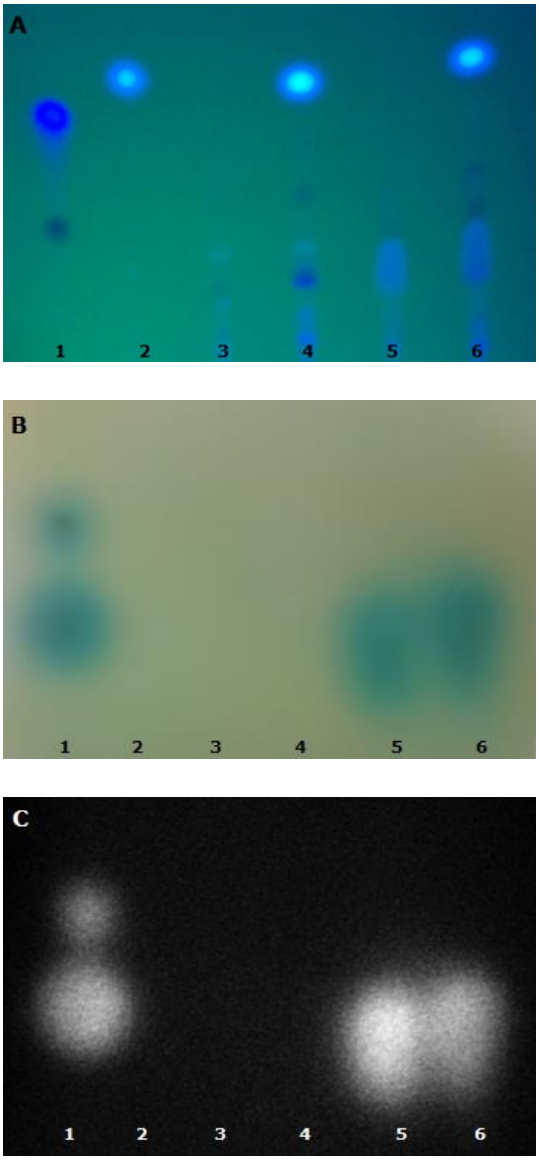

Figure 3.14 TLC analysis of HHQ production. (Panel **A**) TLC plate under UV light at 312 nm, showing PQS (lane **1** upper spot) and HHQ (lane **1** lower spot) standards together, 488 standard (lane **2**), organic solvent supernatant extracts of PAO1-N Δ*pqsAHR* grown without (lane **3**) and with (lane 4) the compound 488 and organic solvent supernatant extracts of PAO1-N Δ*pqsAHR pqsABCD* grown without (lane **5**) and with 488 (lane **6**). Pyocyanin production (Panel **B**) and light output (Panel **C**) occurs via PAO1-L Δ*pqsA* P*pqsA::lux* present in the agar overlay. Both pyocyanin and light output are dependent on the presence of AQs. Bioluminescence was captured using a luminograph photon camera. The uppermost bright spot on the UV illuminated plate (Panel **A**, lanes **2**,**4** and **6**) is 488

	LEGEND Figure 3.14
1	PQS, 10 mM + HHQ, 10 mM, 2 µL
2	488 10 mM, 5 µL
3	PAO1-N Δ*pqsAHR* organic extract, 10 µl
4	PAO1-N Δ*pqsAHR* + 488 200 µM organic extract, 10 µL
5	PAO1-N Δ*pqsAHR pqsABCD* organic extract, 10 µL
6	PAO1-N Δ*pqsAHR pqsABCD* + 488 200 µM organic extract, 10 µL

3.3.2 Liquid chromatography-mass spectrometry (LC-MS) analysis of AQs production

In order to obtain more quantifiable data compared to the TLC overlay, and to study the effect of the lactam 488 on AQ production, Liquid Chromatography Tandem Mass Spectrometry (LCMS/MS) was used. The AQs were extracted and LC-MS performed as described in the Materials and Methods (section 2.2.8.3). The uniformly deuterated PQS-analogue d4-PQS was spiked at a 20 nM final concentration into each sample immediately before the extraction process and used to permit quantification of the data. The results of all strains tested are summarised in Figure 3.15. Several PQS system mutants including PAO1-L Δ*pqsA,* PAO1-L Δ*pqsR* and PAO1-N Δ*pqsAHR* were employed as negative controls to check for the presence of contamination during the analytical process and to verify that no AQs were retained on the columns during the elution steps. None of the negative-control strains produced AQs (Figure 3.15). The *P. aeruginosa* strain ATCC 15442 was also analysed and the absence of AQ production confirmed that this strain has an inactivated PQS system. The other strains analysed were PAO1-L, PA14, PAO1-N Δ*pqsAHR pqsABCD*, PAO1 Unilever and the cystic fibrosis (CF) clinical isolates PA14 AL191, PA7 48, PAK 6085. The strains PA14 AL191 and PA7 48 both have several mismatches compared to the PAO1 *pqsA* reference gene sequence. However, only one of the mismatches translates into a unique substitution in the PqsA protein, G285S for PA14 AL191 and A345T for PA7. Furthermore, PA14 AL191 has a missense mutation in PqsR which changes A288V. Nevertheless, no significant phenotypic differences were observed due to the described changes on the analysed strains, although PA14 AL191 showed a low pyocyanin production (Figure 3.18) (Oton, 2018). It is worth mentioning that, apart from the *pqsA* and *pqsR* genes, no other alignment analysis were performed on these strains.

Whereas 488 had little effect on AQ production in PAK 6085 (Figure 3.16 F) (Figure 3.15), at high concentrations, it reduced AQ production by PA14 AL191 and PA7 48 (Figure 3.16 C and D). Indeed, the highest impact was

observed on PA7 48 and PAO1 Unilever, which was the most 488-sensitive strain (Figure 3.16 G). As also observed from the TLC overlay, PAO1-N Δ*pqsAHR pqsABCD* does not produce PQS due to the lack of PqsH and synthesizes HHQ and HQNO regardless of the presence of 488 (Figure 3.16 E). Wild type strains PAO1-L and PA14 also are not or slightly affected (Figure 3.16 A and B).

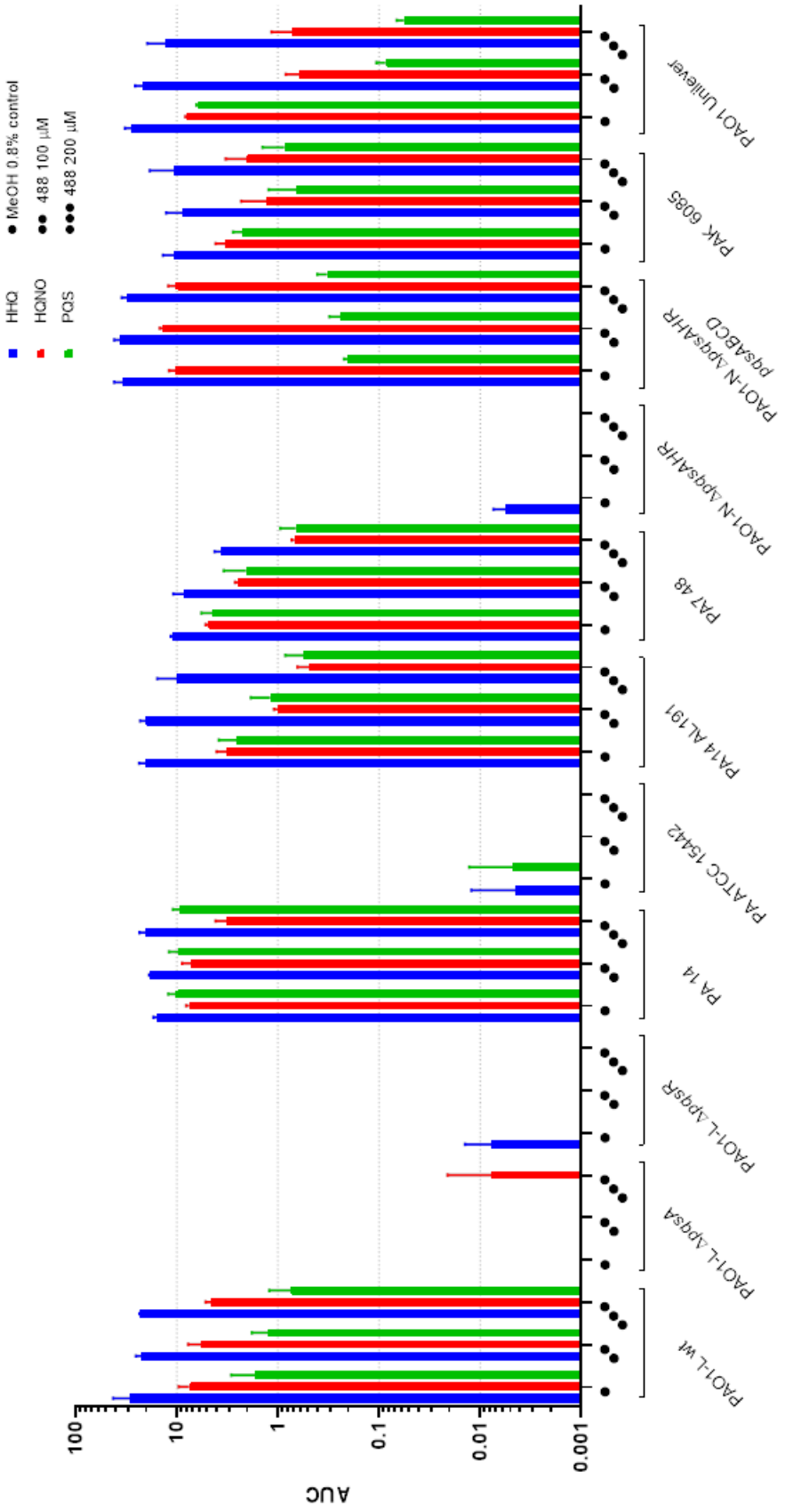

Figure 3.15 Overview of absolute quantification of AQs produced by different *P. aeruginosa* strains with 488 at 100 and 200 µM using LC-MS. Error bars represent the standard deviation of the technical triplicates.

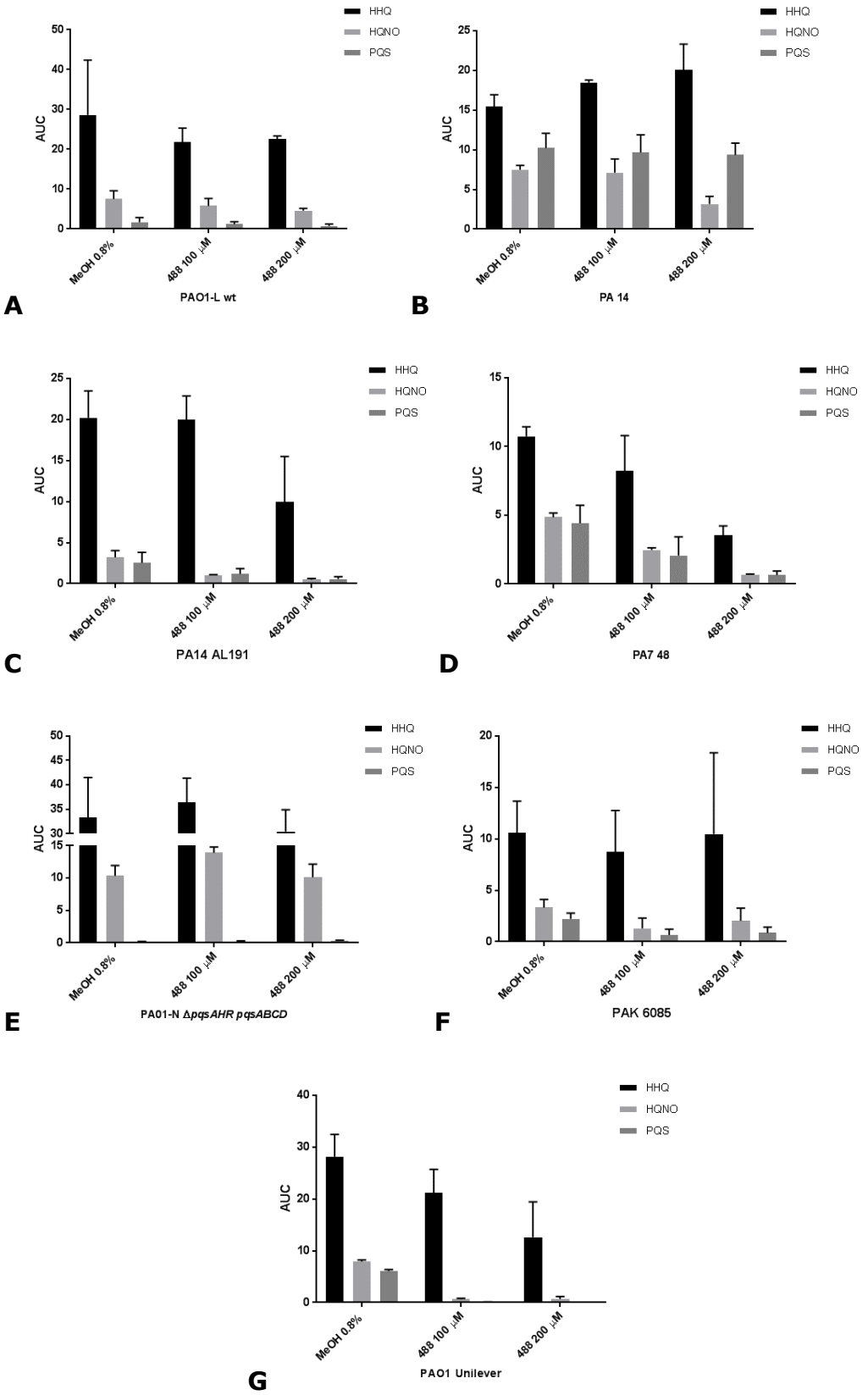

Figure 3.16 Quantification of AQs (HHQ, HQNO, PQS) produced by different *P. aeruginosa* strains with 488 at 100 and 200 µM using LC-MS. Panel **A** PAO1-L, panel **B** PA14, panel **C** PA14 AL191, panel **D** PA7 48, panel **E** PAO1-N Δ*pqsAHR pqsABCD* ,panel **F** PAK 6085, panel **G** PAO1 Unilever. Deuterated internal standard d4-PQS was used at 20 nM. Error bars represent one standard deviation of technical triplicates.

3.4 IMPACT OF 488 ON PQS DEPENDENT PHENOTYPES

3.4.1 Pyocyanin

Pyocyanin is a secondary metabolite produced by *P. aeruginosa* that plays a fundamental role during infections by increasing bacterial virulence (Lau *et al.*, 2004). Since the PQS system controls pyocyanin expression (Cao *et al.*, 2001), its downregulation constitutes an potential target for reducing *P. aeruginosa* virulence. Pyocyanin was extracted and quantified following the method described in section 2.2.4.2 (Essar *et al.*, 1990). For a more robust comparison, the supernatants employed for the LCMS/MS analysis were assayed for pyocyanin. As shown in Figure 3.17, all the pyocyanin-producing strains are strongly affected by the presence of 488: pyocyanin levels decreased with 100 µM 488 (except for PAO1-L) and drastically with 200 µM in PA 14. PAO1-N Δ*pqsAHR*, PAO1-N Δ*pqsAHR pqsABCD*, PAO1-L Δ*pqsA*, PAO1-L Δ*pqsR*, ATCC 1544 were used as negative controls. The strain PA14 AL191 showed only a modest reduction in of pyocyanin The differences between AQ levels and pyocyanin could be explained by the direct effect of 488 on *pqsE* expression, which is able to act in both PqsR-dependent and independent ways and up-regulates the phenazine (*phz*) biosynthesis genes (Farrow *et al.*, 2008; Rampioni *et al.*, 2016; Rampioni *et al.*, 2010).

.

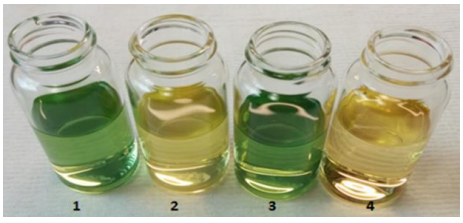

Figure 3.17 Pyocyanin production by PAO1-N grown in the presence of lactam 488 in 0 (1), 100 (2) and 10 µM (3). (4) is a LB only control.

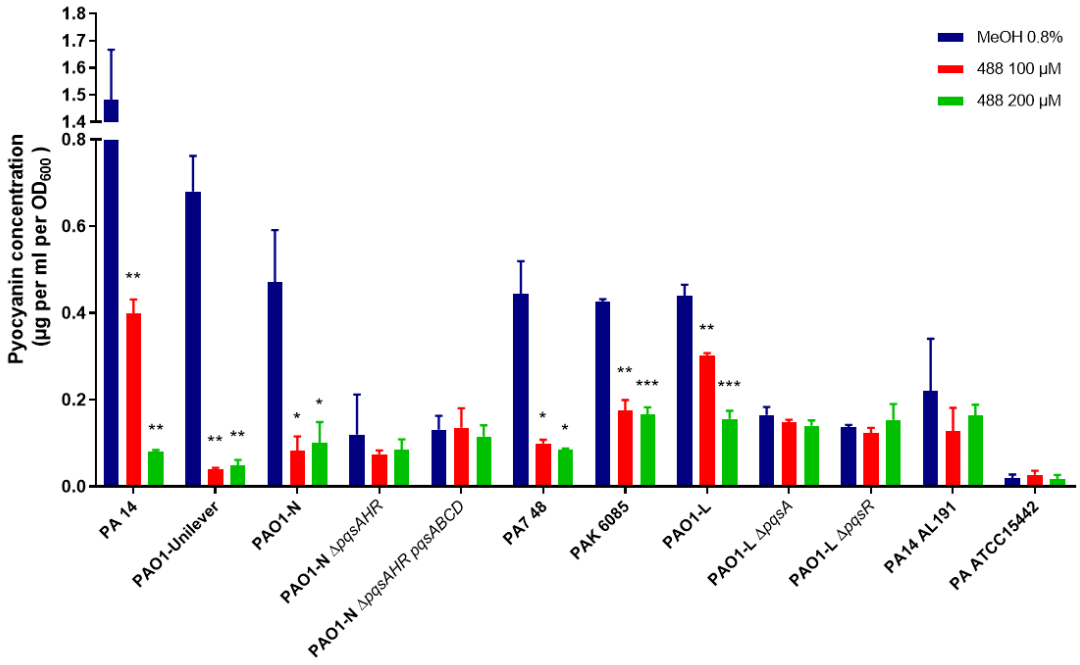

Figure 3.18 Quantification of pyocyanin production of *P. aeruginosa* strains treated with 488 at 100 and 200 µM. Methanol only was used as the solvent control. Error bars indicate the standard deviation of biological triplicates. Multiple t-tests were performed to determine statistical significance in each group (*) represents p value < 0.05, (**) *p* value < 0.01 and (***) *p* value < 0.001.

To be effectively synthesized, pyocyanin requires the expression of the either or both *phzA1B1C1D1E1F1G1* and *phzA2B2C2D2E2F2G2* operons which are directly responsible for the production of phenazine-1-carboxylic acid (PCA), the pyocyanin precursor (Mavrodi *et al.*, 2001). As the first gene in the operon, the expression of *phzA1* was studied using the transcriptional reporter PAO1-L pCTX::P*phzA1-lux*. Albeit the expression of the homologues gene *phzA2* must be also analysed, *phzA1* downregulation confirms the inhibitory activity of 488 on pyocyanin production (Figure 3.19). Further assays will be required to confirm any possible direct interactions between 488 and *pqsE.*

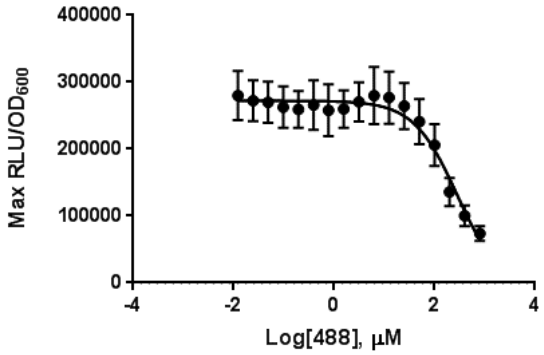

Figure 3.19 Effect of lactam 488 on expression of P*phzA1::lux* in PAO1-L (IC_{50} 282.7±18.06).

3.4.2 Elastase production

Elastase is a metallo-protease and a virulence factor involved in tissue destruction; its expression depends on the QS regulation, mainly on the *las* and *rhl* systems (Calfee *et al.*, 2001; Diggle *et al.*, 2007). For this reason, the *lasR*-mutant strain (PAO1-N Δ*lasR*) was used as a negative control along with PAO1-N Δ*pqsA* which, as shown in this experiment, showed a slight difference from the wild type. Furthermore, 488 shows no effects on elastase production by PAO1-N and negligible effects in the *pqsA* mutant (Figure 3.20). The lack of significant 488-dependent inhibition in PAO1-N is surprising since 488 reduced *lasI* expression by ~40% in PAO-1-L (Figure 3.3)

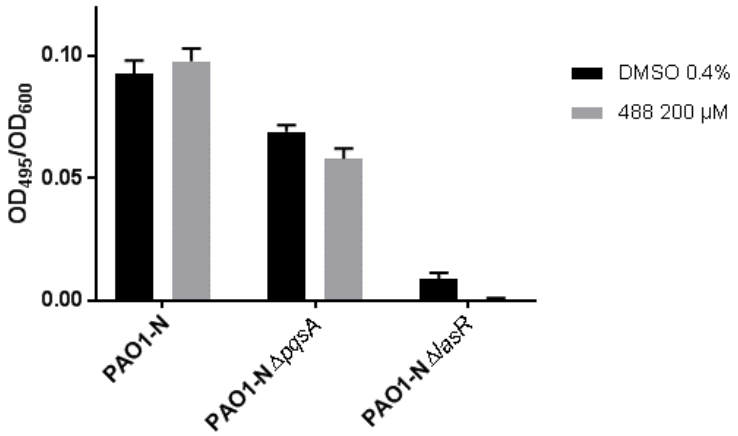

Figure 3.20 Elastase activity assay in *P. aeruginosa.* Quantification was performed by reading the absorbance (OD_{495}) after incubating the filtered supernatant for 4 hours with Elastin-Congo red. Error bars represent standard deviation from biological replicates.

3.4.3 Lectin expression

The galactose specific lectin, LecA is a widely described virulence factor in *P. aeruginosa*; it has a structural function in mature biofilms and exerts cytotoxic effects on lung tissue by reducing respiratory cilia beating frequency and respiratory cell growth during *P. aeruginosa* infections (Bajolet-Laudinat *et al.*, 1994; Diggle *et al.*, 2006b). The expression of the *P. aeruginosa lecA* and *lecB* genes is controlled by RpoS and QS, in particular by the Rhl and the PQS system (Diggle *et al.*, 2003; Winzer *et al.*, 2000). Against such background, a PAO1-L biosensor constructed with pCTX::P*lecA-lux* was used in order to test whether 488 was able to reduce *lecA* expression. An antagonism assay was performed with linearly increasing concentrations of 488 and a sigmoidal dose-response curve was generated yielding an $IC_{50\ of}$ 159.6±6.6 (Figure 3.21).

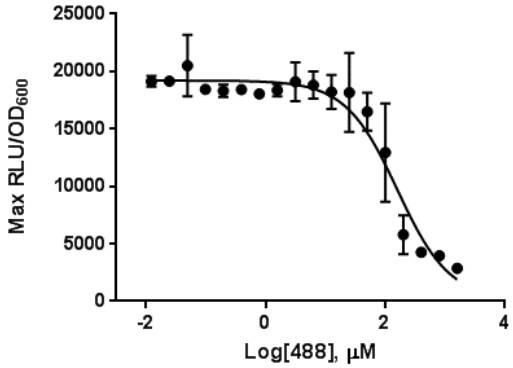

Figure 3.21 Effect of lactam 488 on expression of P*lecA::lux* in PAO1-L (IC_{50} =159.6±6.6). Error bars indicate standard deviation of technical triplicates.

3.5 THE LACTAMS AND PQSR

3.5.1 *In silico* docking of the lactams into the PqsR ligand binding site

Although the biosensor-based assays described the competition between the AQs (PQS and 7Cl-PQS) and 488 as non-competitive, an *in-silico* study to model how the lactams may interact with the PQS system receptor PqsR was carried out. The simulation was performed employing the crystal structure of the complex $PqsR^{CBD}$ (co-inducer/ligand binding domain) occupied by the PqsR inhibitor, 3-NH_2-7Cl-C9-QZN described in Ilangovan *et al.* (2013). As outlined in section 2.2.9.1, the study was performed using the structure of the complex without the QZN molecule as it represents the conformation assumed by the receptor during the interaction with an antagonist. The docking score, describing the affinity of the molecule for the PQS/HHQ ligand binding site, was generated for each lactam, using the Glide module of the Schrödinger Software Suite. In this study, the presence and absence of a molecule of water inside the CBD did not influence the final outcome. The lactam structures are shown in Figure 3.22**Error! Reference source not found.**. Figure 3.23 shows the possible lactam orientations within the ligand binding domain and Table 3.1 summarizes the docking scores generated by the analysis. According to the docking analysis, lactam 488 was predicted to be the most potent lactam inhibitor with a score of -10.5 even lower then 3-NH_2-7Cl-C9-QZN (docking score-9), the most potent PqsR antagonist discovered by Ilangovan *et al.* (2013) (Figure 3.23, Table 3.1). The high affinity of 488 is determined by the presence of several hydrogen bonds within the binding pocket "B". The -NH of the pyrrolone ring interacts through a water-mediated hydrogen bond with Gln194. The carbonyl group in position 2 with the amine group of Leu197 while the chlorine located in position 4 on the phenyl ring interacts with Thr265 forming an H-bond with its side chain (Figure 3.23 panel A). As described for 3-NH_2-7Cl-C9-QZN, this bond is thought to be responsible of the stronger binding of the molecule compared to native ligands. In fact, the halogen bond between the 7-Cl and Thr265 stabilizes

the QZN within the pocket B by clamping it with the more common, among PqsR natural ligands, H-bond with Leu207. Besides, such an interaction might play a role in conformational modifications of the receptor since it should maintain the protein in an inactive state (Ilangovan *et al.*, 2013). Only lactam 491 assumes a 488-like conformation due to the interactions with Leu197 and Gln194 and, consistent with the observations made so far in this study, it is the second highest affinity lactam with a docking score of -8.2. Lactams 131, 258 and 316 gave approximate docking scores of -6.5 (Table 3.1), revealing ~35% lower predicted binding affinities compared with 488. These lactams adopt a different conformation due to their interactions with Leu197 and Ala237 within the binding pocket.

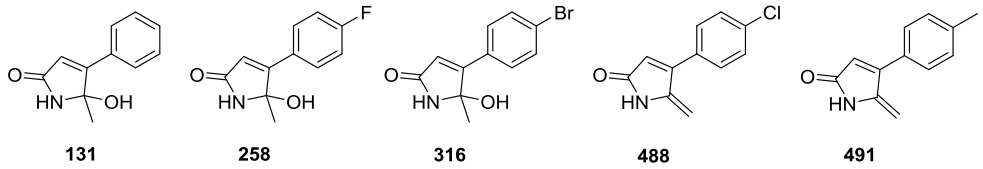

Figure 3.22 Structures of the original lactams.

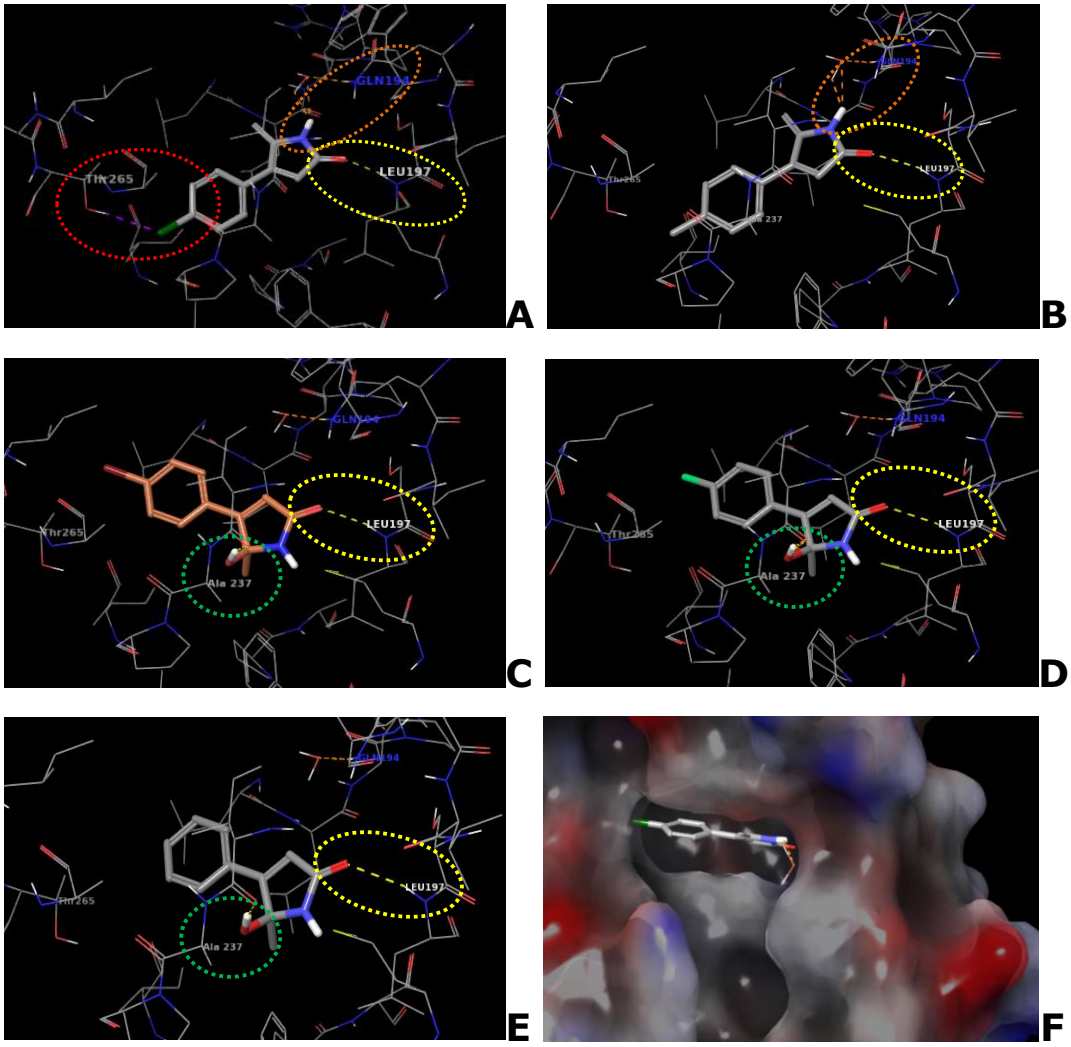

Figure 3.23 Interactions between lactams 488, 491, 316, 131 and 258 with amino acid residues within the PqsR^{CBD}. Lactams are represented as bold sticks, interactions as dotted lines highlighted by typology with coloured dotted circle; in red, halogen bond with Thr265; in yellow, hydrogen bond with Leu197; in orange, water mediated hydrogen bond with Gln194; in green, hydrogen bond with Ala237. In panel **A** 488; **B** 491; **C** 316; **D** 258; **E** 131. In panel **F**, Surface charge representation of PqsR^{CBD}. 488, represented as sticks, sits within the cavity occupied naturally by the AQ bicyclic ring.

To further probe the structure-activity relationships via *PqsR^{CDB}* docking, two lactams were designed *in silico* (Figure 3.24 and Figure 3.25). The new lactams were initially designed assuming the groups in position 5 of the pyrrolone ring and position 4 of the phenyl ring are the main structural variables. The first new lactam (476) has hydroxyl and methyl groups at the 5 position of the pyrrolone ring and chlorine at 4 position of the phenyl ring (4-(4'-chlorophenyl)-5-hydroxy-5-methyl-1,5-dihydro-2H-pyrrol-2-one). The second lactam (491-F) has a methylene group in position 5 of

the pyrrolone ring and a fluorine group in position 4 of the phenyl ring (4-(4'-fluorophenyl)-5-methylene-1,5-dihydro-2H-pyrrol-2-one).

The hydroxyl group of 476 forms a hydrogen bonding interaction with Leu207 thus the lactam assumed a different position from the other lactams within the binding site (Figure 3.25 left panel) therefore keeping the Cl group far from the Thr265. The consequent weaker interaction resulted in a docking score of -5.1 (Table 3.1). However, the new lactam 491-F assumed the same orientation as 491 and 488 (Figure 3.23 and Figure 3.25 right panel) obtaining a docking score of -9.6 (Table 3.1).

This test suggests that the interactions with Gln194 and Leu197 are likely to facilitate H-bonding with the Thr265 and offer options for further chemical synthesis.

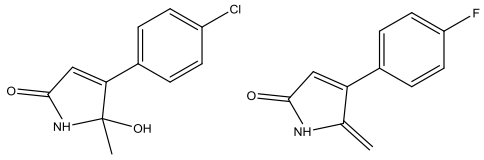

476 **491-F**

Figure 3.24 Structure of *in-silico* designed lactams: 476 and 491-F.

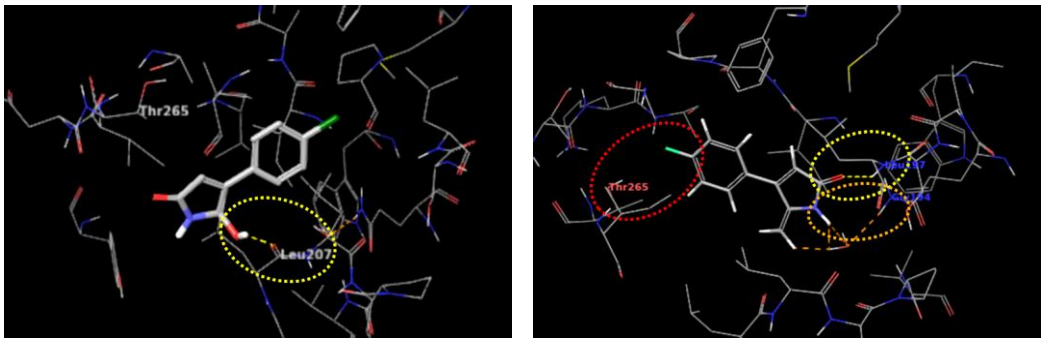

Figure 3.25 Interactions between the *in-silico* designed lactams (476, left panel and 491-F, right panel) and the amino acid residues of the PqsR^{CBD}. Lactams are represented as bold sticks, interactions as dotted lines highlighted by topology with coloured dotted circles; in red, halogen bonding with Thr265; in yellow, hydrogen bonding with Leu197; in orange, water mediated hydrogen bonding with Gln194.

Compound	*Docking score*
488	-10.501
491-F	-9,628
3-NH_2-7Cl-C9-QZN	-9.097
491	-8,242
316	-6.715
258	-6.385
131	-6.122
476	-5,090

Table 3.1 Summary of the docking scores of the lactams and the PqsR inhibitor, 3-NH2-7Cl-C9-QZN generated via the *in-silico* docking analysis. Each score corresponds to the higher probable orientation of the lactam within the PqsR ligand binding site with a molecule of water. The *in-silico* designed lactams are underlined.

3.5.2 *In silico* docking of the second set of lactams

Following the insights provided by *in-silico* investigations, several additional lactam analogues were provided by Unilever for testing as potential PqsR inhibitors. These lactams analogues are distinguished by the presence on the phenyl ring of halogens in different positions. In this series, the pyrrolone ring possesses a phenyl group in position 4 as in 488, apart from lactam 202239, which carries an N-methyl substituent at position 1 and the phenyl ring in position 3 (Figure 3.26). Because of these similarities, the new lactams assume poses and interactions within the PqsR binding pocket analogous to those of 488 and 491 (Figure 3.27) apart from 490, 476 and 2022339. Compound 490 is the only one that positions the pyrrolone ring in close proximity to Thr265 (Figure 3.27 panel C) while 476 and 2022339 do not orientate within ligand binding site similar to the native ligand and 3-NH_2-7Cl-C9-QZN antagonist. Despite the location of the Cl in position 4 as for 488, 476 and 2022339 present different substituents on the pyrrolone ring that are less likely to promote stable binding (Figure 3.27 panels G and H). From this series, 295 meets the structural requirements dictated previously by 488, the most active *pqs* system inhibitor. 295 and 488 possess similar structures with a carbonyl in position 2 and a protonated nitrogen on the pyrrolone ring, with a halogen on the 4^{th} carbon of the phenyl ring.

Consequently, the poses of the 488 and 295 match perfectly if superimposed (Figure 3.28 panel B). On the other hand, it is interesting to observe how the lactam 310 suprimposes on 488 and 295, while being unable to interact with Thr295 due to the distance of its F (Figure 3.27 panel F, Figure 3.28). As for the previous study, the binding domain grid used in this simulation contains a molecule of water assuming the interaction to occur in an aqueous environment. However, although the presence/absence of water did not impact on ligand conformation within the binding pocket (Figure 3.27 panels B and D), the docking scores were affected. In fact, the lactams 295 and 310 both superimpose within the CBD and, at the same time, show substantially different scores according

to the presence of water. Whilst 488 has the best docking score in both scenarios, in presence of water 310 and 295 have a score of -9.811 and -6.762 respectively. Conversely, without water, 310 has -7.216 while 295 -8.573 (Table 3.2). The differences might be explained by the variable subsituents on the phenyl rings of the two compounds: the bromine in 295 is sterically larger that the chlorine of 488 and the presence of water on the other side of the molecule could prevent the locking of the lactam within pocket B of PqsR. On the other hand, the water molecule may contribute to stabilize the phenyl group of 310. Interestingly, because of chlorine in position 5 of the phenyl ring, lactam 495 represents a "structural compromise" between 295, 310 and 488, and its docking scores are the third highest in both situations.

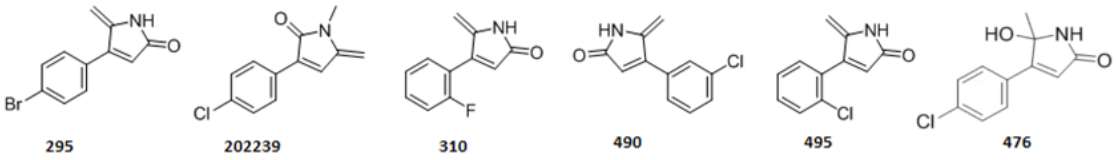

Figure 3.26 Structures of the second set of lactams

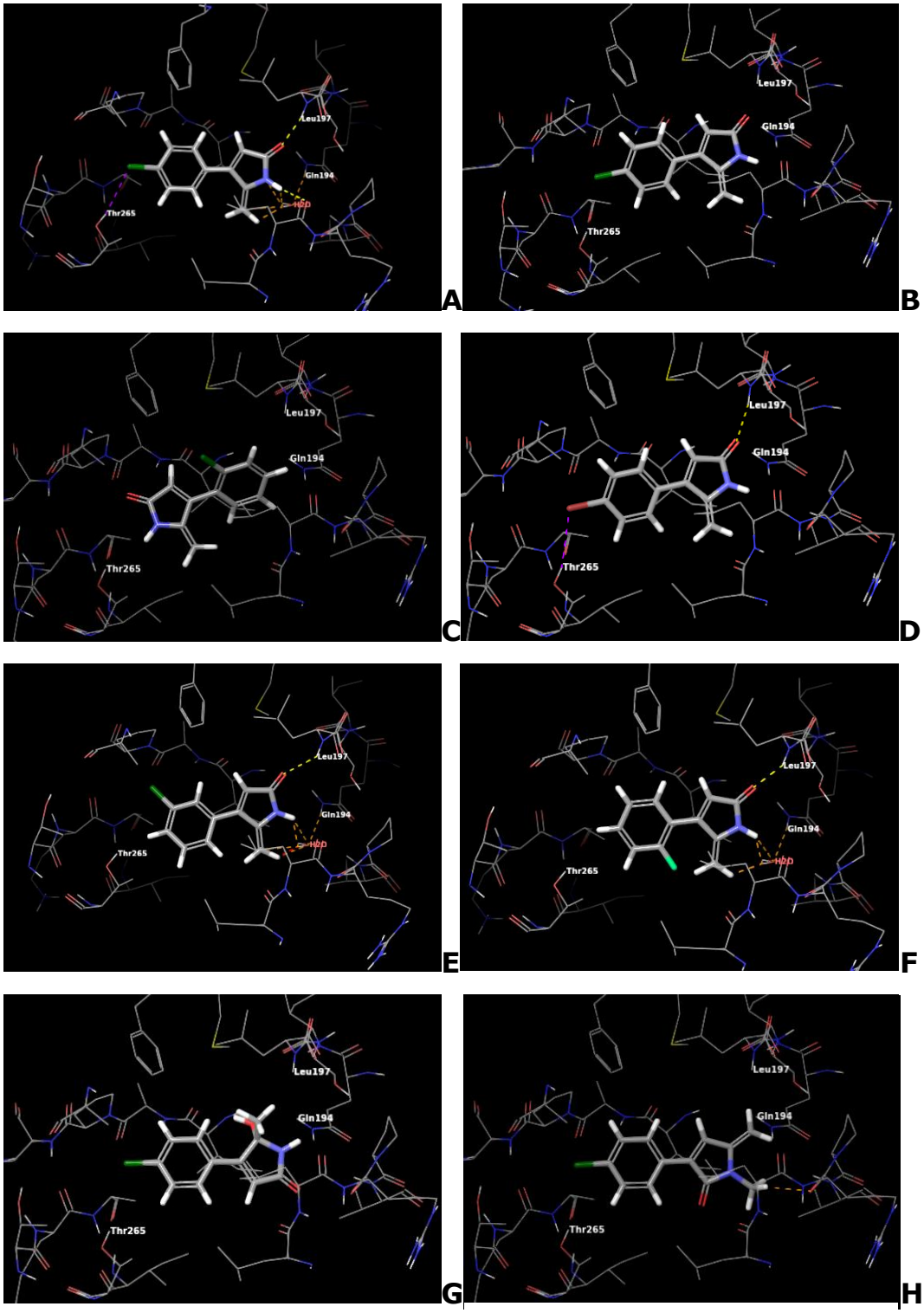

Figure 3.27 Predicted interactions between the lactams and the amino acid residues of the PqsR^{CBD}. Lactams are represented as sticks and the interactions highlighted as dotted lines. In panel **A**, 488 with H_20 in CBD; **B**, 488 without H_20; **C**, 490 without H_20; **D**, 295 without H_20; **E**, 495 with H_20; **F**, 310 with H_20 **G** 476 without H_20 **H** 2022339 without H_20. Except for 476 and 2022339, all lactams have interactions with Leu197 and Gln194. 488 and 295 interact to Thr265. The presence of the water molecule in the binding domain does not interfere with the positioning of the ligands.

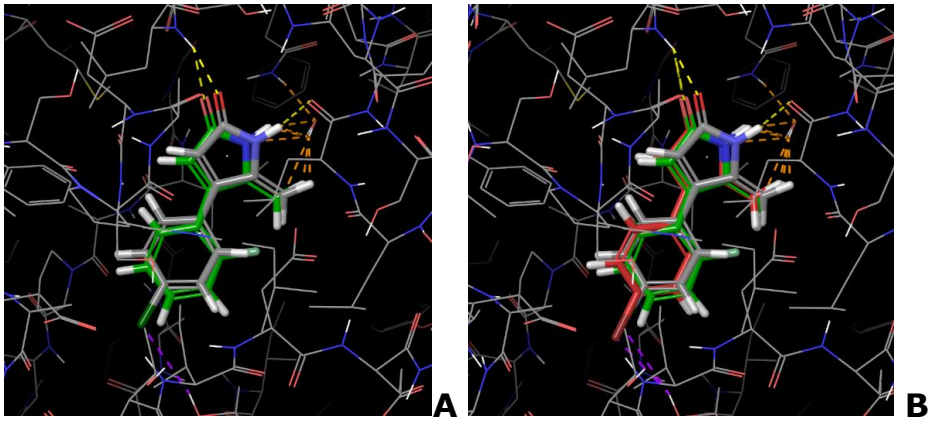

Figure 3.28 Superpose of 488 (grey), 310 (green) (panel A and B) and 295 (red) (panel B) within the PqsR^{CBD} with H_20. The halogen group in 310 is located at C4 and not C3 as in 488 and consequently does not interact with Thr265, despite the high docking score in presence of the water molecule.

Compound	***Docking score w H_20***	***Docking score w/out H_20***
488	-10.501	-8.705
310	-9.811	-7.216
495	-8.409	-7.97
491	-8,242	-7.296
476	-6.764	-7.252
295	-6.762	-8.573
490	-6.565	-7.382
2022339	-5.135	-7.353

Table 3.2 Docking scores of 488, 491 and the lactams generated by the *in-silico* binding analysis using the PqsR^{CBD} grid with and without a water molecule. Each score corresponds to the higher probable orientation of the lactam within the PqsR^{CBD}. The presence of the water molecules within the CBD influences the docking scores but not the poses.

3.5.3 Impact of the second set of lactams on PQS-dependent QS system

To establish the PQS system inhibitory properties of lactams 295, 202239,310,490,495 and 476, the inhibition of *pqsA*, the anthranilate ligase gene required for AQ-biosynthesis was evaluated using a chromosomally integrated *lux*-based *P. aeruginosa pqsA* promoter fusion. The lactams were initially tested at a concentration of 100 μM with DMSO 0.6% v/v as the solvent control (Figure 3.29). Lactam 295, which shares the same structure as 488 but with a different halogen atom (Br instead of Cl), shows inhibitory activity almost 27% higher than its Cl analogue. The other lactams were less inhibitory with 490 and 310 (which have either a Cl or F at position 5 of the phenyl ring) being 22% and 14% respectively less potent than 488. Lactam 2022339 shows moderate inhibition and is 30% less active than 488. Lactams 483, 495, 476 and the "cationic lactam", do not impact significantly on *pqsA* expression.

The antagonist assay previously performed using lactams at 100 μM was repeated using the same compounds at 250 μM in order to determine the effects of higher concentrations on the PQS system. Due to the solubility limits, the solvent-only positive control contained 0.8% v/v DMSO, therefore an LB only positive control was also used, along with the biosensor PAO1-L Δ*pqsA* P*pqsA*::*lux* as the negative control, since it is unable to produce AQs and hence light. At 250 μM (Figure 3.30), lactams 295 and 310 were slightly less potent than 488, consistent with the *in silico* predictions. Compound 490 at 100 μM does not show any appreciable inhibition of *pqsA* expression. However, 483 was more active at higher concentrations. Lactam 495 does not show inhibition, despite the relatively high affinity for the $PqsR^{CBD}$ predicted.

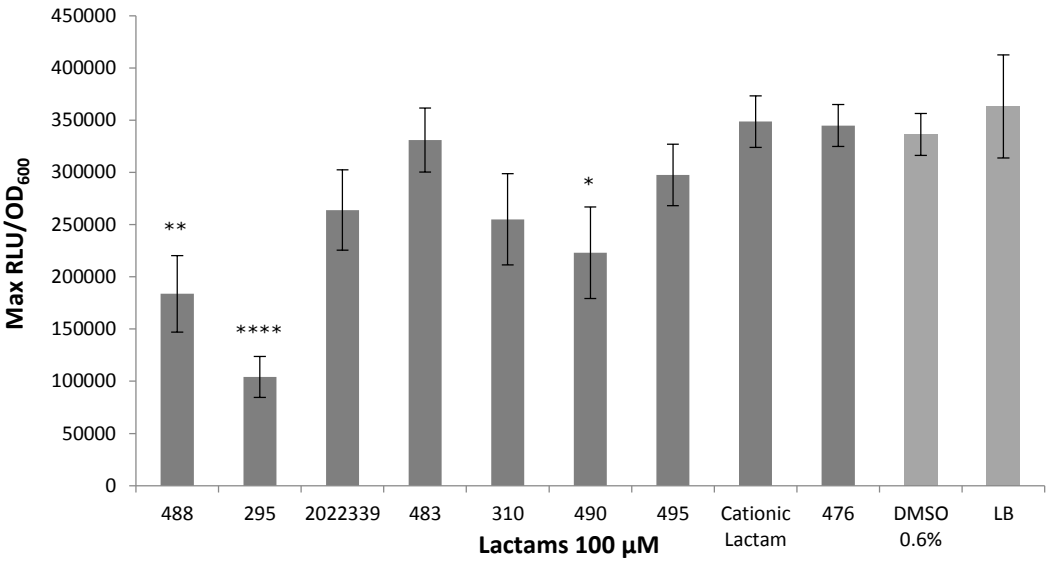

Figure 3.29 Impact of 488 and the 2nd set of lactams at 100 µM on P*pqsA::lux* expression in PAO1-L. LB only and DMSO 0.6% v/v are used as positive controls (light grey bars). Error bars represent standard deviation of biological triplicates. Multiple t-tests were performed against DMSO 0.6% control group to determine statistical significance (*) represents *p* value < 0.05, (**) *p* value < 0.01, (****) *p* value < 0.0001.

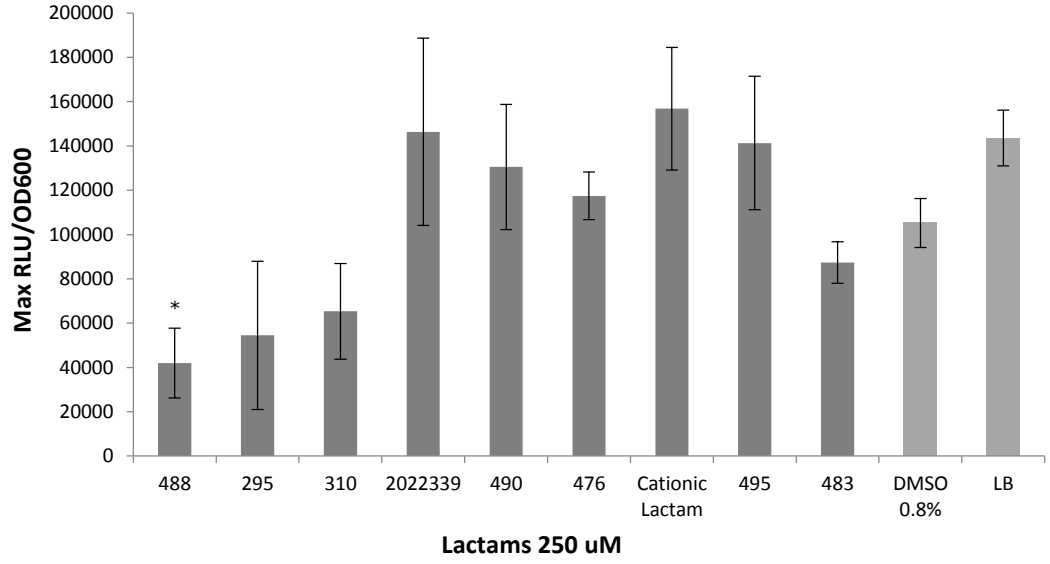

Figure 3.30 Impact of 488 and the 2nd set of lactams at 250 µM on P*pqsA::lux* expression in PAO1-L. LB only and DMSO 0.8% v/v are used as positive controls (light grey bars). Error bars represent standard deviation of biological triplicates. Multiple t-tests were performed against DMSO 0.8% control group to determine statistical significance (*) represents *p* value < 0.05.

3.5.3.1 Determination of IC_{50} values for lactams 295 and 310

The P*pqsA::lux* dose-response curves for compounds 295 and 310 against PAO1-L were constructed and IC_{50} values generated. Lactam 295 has a different shaped dose-response curve to 488 although the IC_{50} is similar (295 IC_{50}=33.08 μM, 488 IC_{50}=21.72 μM) (Figure 3.31). In fact, lactam 295 seems unable to completely inhibit *pqsA* expression even at higher concentrations in common with 488 (Figure 3.6). Lactam 310 was also analysed possessing a high IC_{50} of 293.6. (Figure 3.32). No further experiments with these lactams were carried out (Growth curves in appendix section 7.3, Figure 7.6).

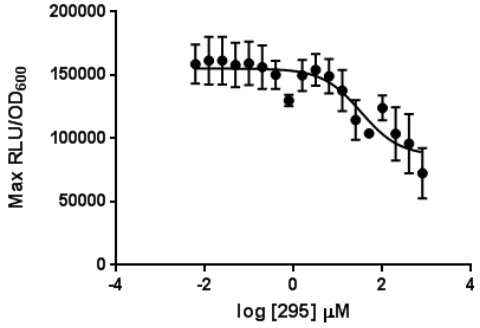

Figure 3.31 Effect of lactam 295 on expression of P*pqsA::lux* in PAO1-L (IC_{50} =33.08±4.13). Error bars represent standard deviation of technical triplicates.

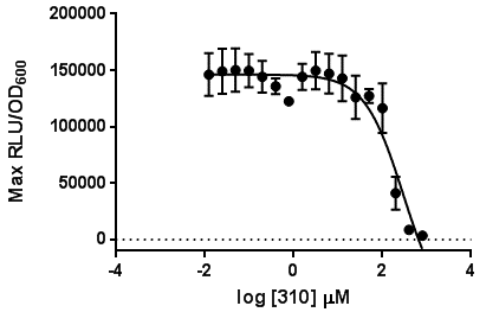

Figure 3.32 Effect of lactam 310 on expression of P*pqsA::lux* in PAO1-L (IC_{50} =293.07±15.15). Error bars represent standard deviation of technical triplicates.

3.5.4 PqsR^{CBD} expression and purification

The plasmid construct pET28a::*pqsR*$^{C94-309}$ used by Ilangovan *et al.* (2013) to study the co-inducer binding domain (CBD) of PqsR was reproduced in this work and the protein expressed following similar conditions (section Expression of the PqsR^{CBD}2.2.9.2). Once the construct had been completed and cloned, its sequence was confirmed by DNA sequencing and the plasmid was introduced into *E.coli* BL21 (DE3). Expression of *pqsR*$^{C94-309}$ was induced by the addition of IPTG (1 mM). Cells were harvested after 24h at 16 °C and lysed by sonication. After centrifuging and filtering, the supernatant containing protein was loaded onto a pre-equilibrated 5 mL Ni^{2+}affinity column and purified using an imidazole gradient 10-500 mM. The fractions and samples collected during the expression were analysed through SDS-gel (Figure 3.33). The fractions were dialyzed at 22°C O/N to avoid precipitation that might occur at 4°C. After collection, the protein was further purified using a Superdex 75 26/600 HiLoad gel filtration column which showed a neat profile (Figure 3.34). Moreover, the elution products were checked with SDS-gel electrophoresis (Figure 3.35). Protein samples destined to ITC or Circular Dichroism analysis were aliquoted and snap-frozen for storage at -80°C, unless required for crystallization: in which case, samples were concentrated and used soon after the purification.

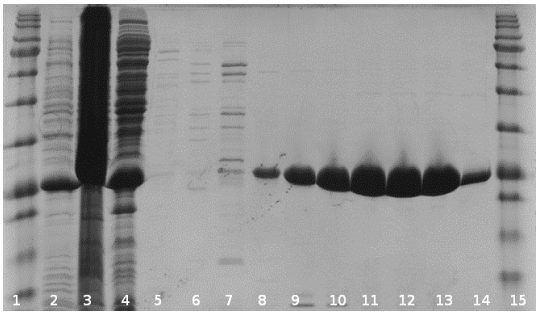

Figure 3.33 SDS-PAGE gel of the Ni^{2+} affinity column purification of PqsR C$^{94-309}$ showing purified protein fractions. 1 and **15** show molecular weight markers. **2** induced culture. **3** Soluble fraction. **4** flow through from Ni^{2+} column. **7** eluted contaminants. From **8** to 1**4** column elution from imidazole gradient using the Aktaprime™ chromatography system.

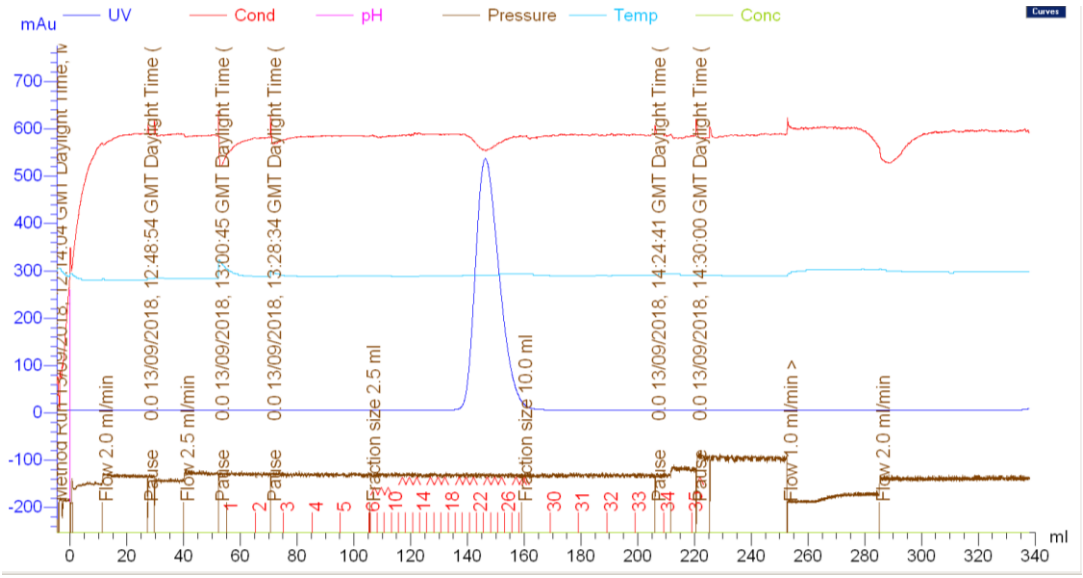

Figure 3.34 Chromatogram of PqsR C^{94-309} purification on a Superdex 75 gel filtration column. The absorbance by time profile (blue) shows the location of the PqsR peak in the elution profile. Fractions were collected and examined using SDS-PAGE.

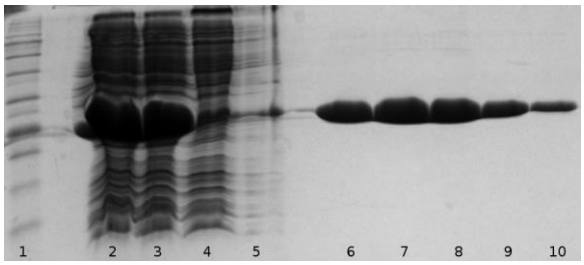

Figure 3.35 SDS-PAGE gel of the Size Exclusion column purification of PqsR C^{94-309} showing purified fractions of the protein. 1 molecular weight markers. **2** and **3** induced culture. **4** flow through from Ni^{2+} column. **5** eluted contaminants. From **6** to **10** column elution using an Aktaprime™ system.

3.5.5 Isothermal titration calorimetry (ITC) of PqsR with lactam 488

Isothermal titration calorimetry (ITC) is a highly sensitive technique used to study the thermodynamics of binding reactions in solution. It is a label-free method that relies on a "cell feedback network" and employs two thermoelectric devices. The first device measures the temperature differences between two cells, containing a reference solution (water) and the protein in an aqueous solution, respectively. The second device measures the temperature difference between the cells and the adiabatic jacket in which they are encapsulated. When the substrate/ligand is injected with a syringe inside the sample cell, the reaction takes place and heat is relased or absorbed proportionally to the rate and degree of the reaction. For each injection, the instrument detects the changes in temperature between the two devices and applies energy in order to restore the temperature difference to 0. Thus a curve is derived from the the time points at which the energy was supplied.

Aliquots of the purified $PqsR^{CBD}$ protein were thawed, centrifuged and measured with a spectrophotometer. The syringe solution, containing 400 μM 488, and the sample cell solution, containing 20 μM $PqsR^{CBD}$, were matched in order to maintain an equal amount of DMSO (4%) and salts (SEC buffer), since mismatches may perturb the reaction and compromise the outcome of the experiment. Lactam 488 bound to the PqsR binding domain with a K_D of 1.74 μM (Figure 3.36). The Wiseman C parameter, defined as [protein]/K_D, is 200 which meets the requirements for receptor saturation ($10<C<500$) according to Wiseman *et al.* (1989). The thermodynamic values, reported in Figure 3.37, describe the reaction as highly spontaneous (Gibbs free energy, $\Delta G=-7.86$) exothermic and rich of H-bonds (binding enthalpy, $\Delta H=-2.22$) and presence of extensive hydrophobic interactions and/or conformational changes that favour ligand binding (enthropy factor, $-T\Delta S=-5.63$). A blank reaction was performed by injecting 488 into a solution lacking $PqsR^{CBD}$ within the sample cell, This contained SEC buffer and DMSO 4% v/v only. No binding occurred since 488 did not interact with the buffer.

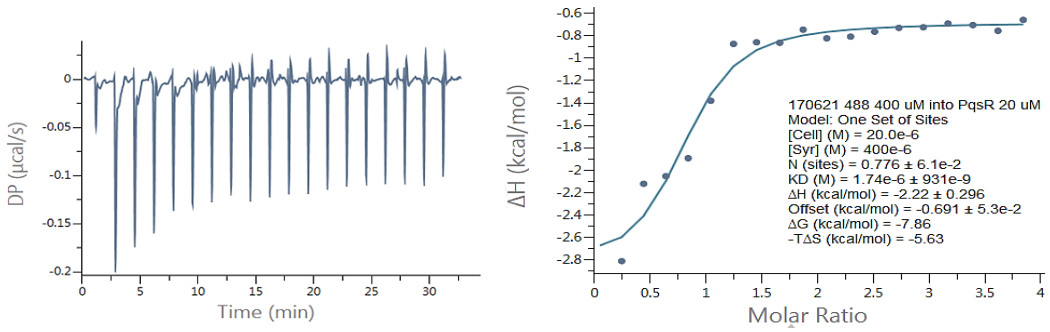

Figure 3.36 Isothermal Titration Calorimetry of 488 and PqsR^{CBD}. Thermogram (left) and binding isotherm (right).

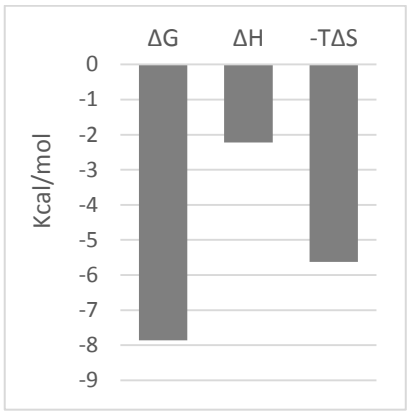

Figure 3.37 Thermodynamic measurements from Isothermal Titration Calorimetry of 488 and PqsR^{CBD}

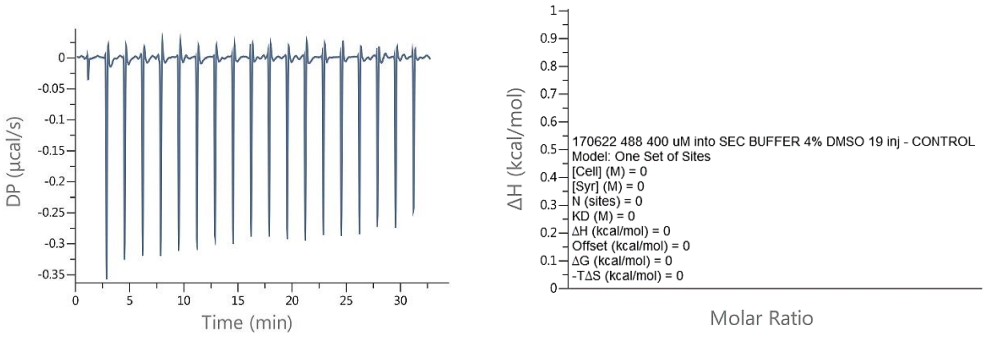

Figure 3.38 Isothermal Titration Calorimetry of 488 and SEC buffer (blank run). Thermogram (left) and binding isotherm (right) with results using a one binding model. The isotherm does not show any dot since no interaction occurred**.**

3.5.6 Protein Thermal Stability by Circular Dichroism spectroscopy

Synchrotron radiation circular dichroism (SRCD) is a consolidated spectroscopic method used in structural biology for the analysis of chiral molecules in solution, forgoing the need for the crystallization of proteins required for X-ray analysis. These SRCD experiment were designed to provide an alternative method for determining the binding kinetics of 5 PqsR ligands including the agonists C7-PQS (PQS), HHQ and NH_2-PQS and the antagonists 3-NH_2-7Cl-QZN and 488. The titration of each of the five achiral aromatic ligands into the PsqR protein carried out by far-UV CD spectroscopy revealed qualitatively that each ligand bound to the protein (Table 3.3). The apparent dissociation constants K_Ds were determined using the Hill equation indicating similar binding for 488 (Figure 3.39 A K_D=63μM), 3-NH_2-7Cl-QZN (Figure 3.39B K_D=76μM), and C7-PQS (Figure 3.39C, K_D=76μM). NH_2-PQS (Figure 3.39D K_D=110μM) and HHQ (Figure 3.39E K_D=452μM) both bound more weakly. An estimation of the protein secondary structure content from the CD spectra in the far-UV region indicated that overall, the $PsqR^{CBD}$ protein retained the α/β folding in solution when bound to one of the five achiral aromatic ligands (Figure 3.40 panel A). PsqR protein showed a weak CD signal in the near-UV region (250-330nm) that is sensitive to the local environment of the aromatic side chains of Trp, Tyr and Phe residues (Figure 3.40 panel D) which reflects the tertiary structure of the protein. Upon ligand addition to PsqR protein four out of five aromatic achiral ligands: QZN, C7-PQS, NH2-PQS and 448 induced small but discernible spectral CD differences from that of the protein alone that were consistent with ligand binding interactions observed in the far-UV region. HHQ, on the other hand, did not show any distinguishable conformational change upon addition to PsqR.

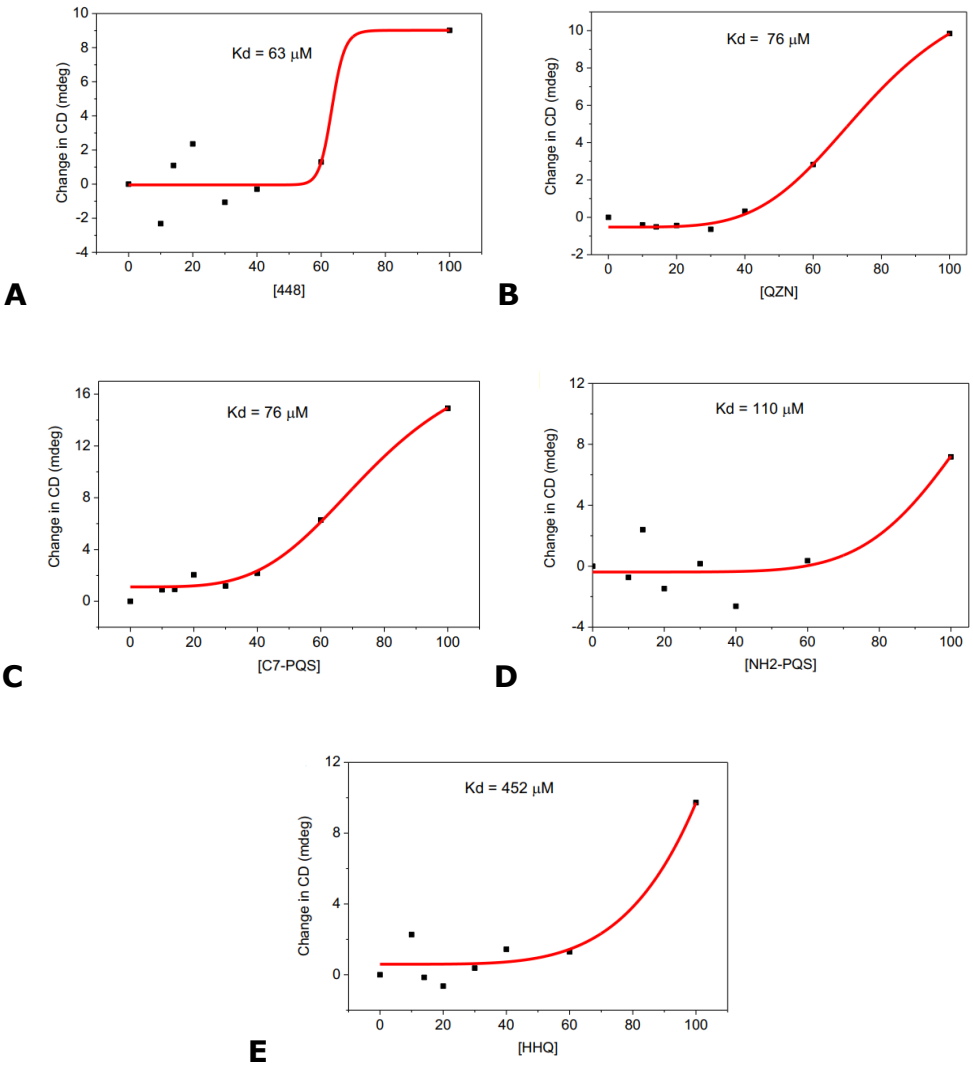

Figure 3.39 CD Titration studies investigating the binding of 488(A) QZN(B), PQS(C), NH_2-PQS(D) and HHQ(E) to the $PqsR^{CBD}$. Plot CD change at 220nm versus concentration of the ligand.The experimental data were best fitted with a Hill 1 equation.

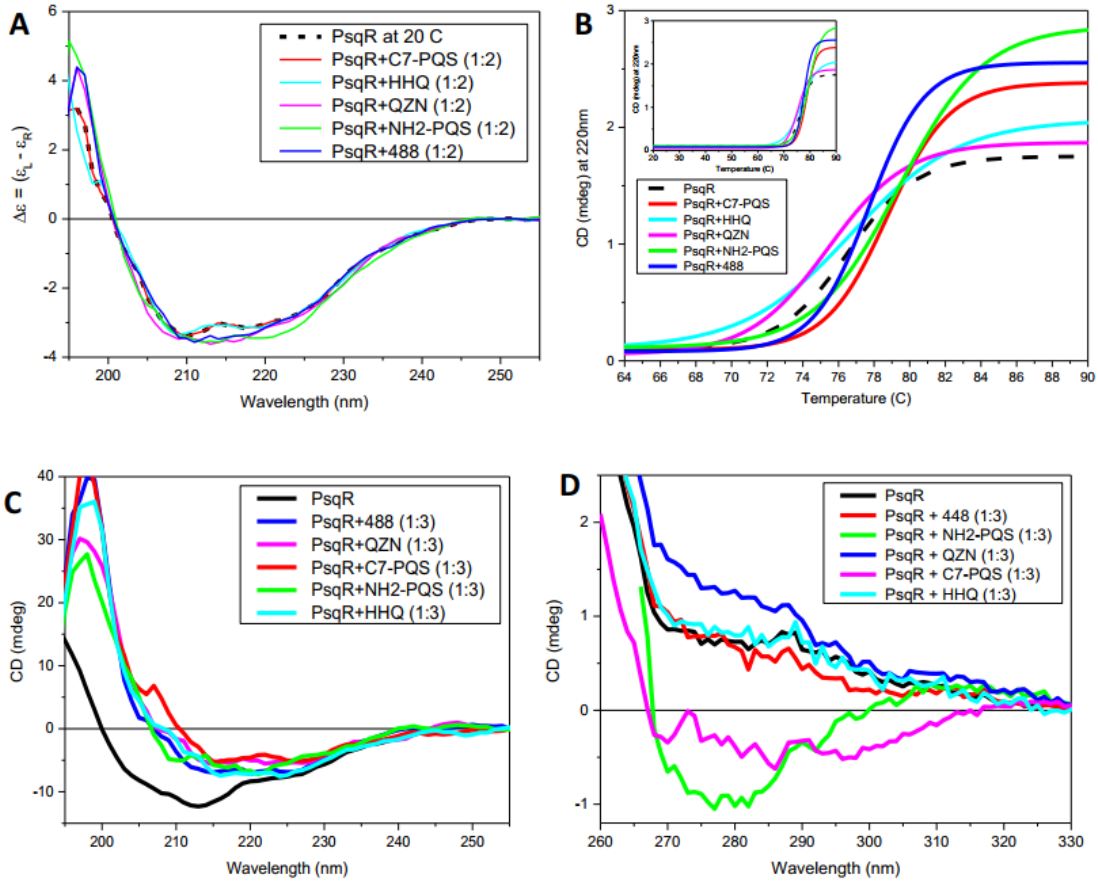

Figure 3.40 Circular Dichroism Spectra and thermal stability. In panel **A**, far-UV CD spectra of PsqR (black), PsqR+C7-PQS (1:2) (red), PsqR+HHQ (1:2) (cyan), PsqR+QZN (1:2) (magenta), PsqR+NH2-PQS (1:2) (green) and PsqR+488 (1:2) (blue) measured at 20 °C. In panel **B**, fitted thermal stability using Boltzman equation for PsqR protein with and without ligands.The inset is the thermal stability from 20 to 90 °C. In panel **C**, CD spectra of PsqR (black) with achiral aromatic ligands1:5 molar ratio: 488 (blue), QZN (magenta), C7-PQS (red), NH2-PQS (green) and HHQ (cyan). In panel **D**, near-UV CD spectraof PsqR (black), PsqR+C7-PQS (1:3) (red), PsqR+HHQ (1:3) (cyan), PsqR+QZN (1:3) (magenta), PsqR+NH2-PQS (1:3) (green) and PsqR+488 (1:3) (blue).

Achiral ligand	488	3-NH2-7Cl-QZN	PQS	NH_2-PQS	HHQ
K_D (μM)	63	76	76	110	452

Table 3.3 Dissociation constant K_Ds of 488, QZN, 3-NH2-7Cl-QZN, PQS, NH_2-PQS and HHQ obtained from the CD titration into $PqsR^{CBD}$.

3.5.7 Determination of the structure of the 488-soaked PqsR^{CBD} crystal

Crystallization of the PqsR C-terminal$^{94-309}$ construct (or CBD) was carried out using 24-well hanging drop plates containing a double gradient of pH and MPD concentration as described in section 2.2.9.10. As for ITC and Circular Dichroism, lactam 488 was chosen for its higher affinity for the PqsR^{CBD}. Diffractrometry enables the acquisition of low-resolution structural information of a wide variety of materials. Although the *in silico*, ITC and SRDC studies provided evidence of direct binding and enabled prediction of a possible structure-function relationship, the availability of crystallography data could help to define ultimately the interaction between the lactam and the PQS^{CBD}. A crystal soaking technique was chosen after attempts at co-crystallization of PqsR^{CBD} with 488 failed due to solubility limits of the lactam in the precipitant solution with low percentages of MPD, which is required for the crystallization process. After at least one week of incubation in sitting drop well plates at 19 °C, the largest crystals obtained were left soaking overnight at 19° C with lactam 488 dissolved inethylene glycol. The 488-soaked PqsR^{CBD} crystals were analysed with the I04 beamline at Diamond Light Source (Didcot, UK).A maximum resolution of 2.9 Å was obtained. The protein structure was solved using the CCP4 software suite and the complex obtained revealed the presence of 488 within thepocket B of the PqsR^{CBD} ligand-binding site consistent with the orientation predicted by the *in-silico* study (Figure 3.41), wherein the interactions with Thr265 and Leu197 are confirmed (Figure 3.42 and Figure 3.43). The chlorine of the phenyl ring is directed to the side chain of Thr265 confirming the predicted interaction, analogously to 3-NH_2-7Cl-C9-QZN as reported in Ilangovan *et al.* (2013) (Figure 3.42 panel B).

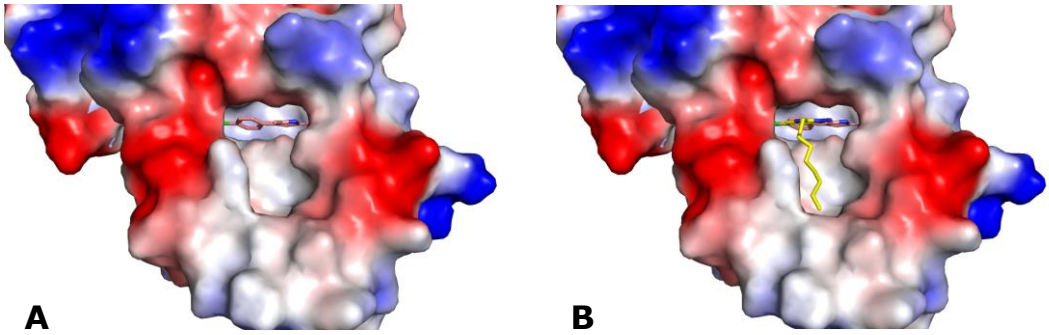

Figure 3.41 Charge surface representation of Lactam 488 and 3-NH_2-7Cl-C9-QZN within $PqsR^{CBD}$. In panel A, 488 (pink sticks) within pocket B. In panel B, superpose of 488 (pink sticks) and the QZN (yellow sticks) structures.

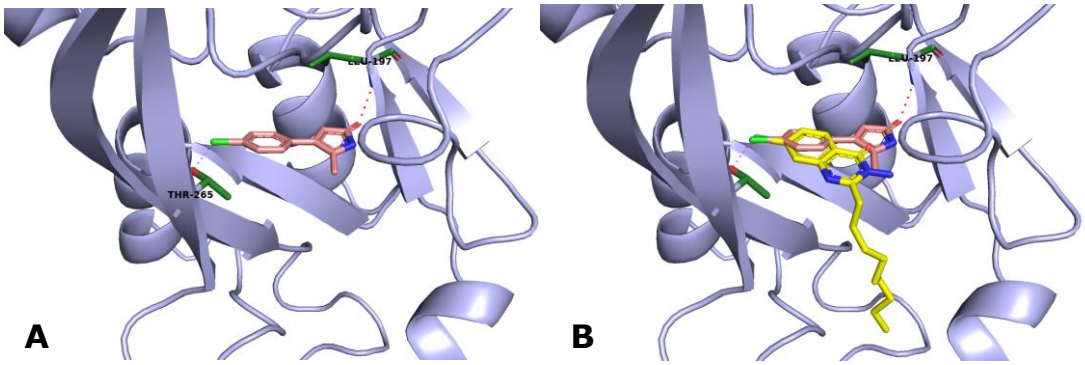

Figure 3.42 Topology diagram of the $PqsR^{CBD}$ ligand-binding site occupied by 488 and 3-NH_2-7Cl-C9-QZN. In panel A, 488 (pink sticks) and the interactions wth Leu197 and Thr265. In panel B, superpose of 488 (pink sticks) and the QZN (yellow sticks) structures.

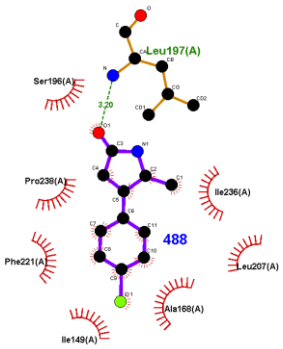

Figure 3.43 Ligplot schematic diagram of 488 within $PqsR^{CBD}$ showing hydrophobic contacts and the hydrogen bond with Leu197 (radius 3.9 Å).

3.6 CONCLUSION

The first lactam screen employing the QS transcriptional reporters was successful since demonstrated that the PQS system was effectively inhibited by the most potent lactams, 488 and 491. From antagonism assays the IC_{50}s were calculated and 488 was confirmed as the leading compound. It's action was also studied in *P. aeruginosa* strains belonging to different genomic backgrounds including PA14 and PA ATCC 15442, where 488 showed a considerable impact on the former and no activity against the latter, due to its lack of a functional PQS system, as confirmed by LC-MS/MS analysis. Using a *P. aeruginosa pqsA* mutant P*pqsA::lux* bioreporter, a series of competitive experiments with exogenous PQS and 7Cl-PQS revealed that 488 inhibits the PQS system in a non-competitive manner since increasing concentration of AQs did not overcome 488-mediated inhibition. The production of AQs in the presence of a range of concentrations of 488 was assayed qualitatively, by employing TLC with a *P. aeruginosa* biosensor overlay and quantitatively, by LC-MS/MS. While the qualitative assay suggested that the AQ biosynthesis was not affected since no changes in production of HHQ were observed, LC-MS showed that the inhibitory activity of 488 is strain-dependent with respect to AQ production.

The PQS-dependent virulence factor pyocyanin was particularly affected by 488 inhibitory activity: its expression was lower in every strain treated with the lactam. Strong pyocyanin producers such as PA14 and the Unilever-PAO1 were significantly affected.

Whilst no specific observations could be derived from the elastase production assay due perhaps to the host strain and multiple regulatory pathways involved, P*lecA::lux* biosensor activity was inhibited, though at high 488 concentrations. Also, due to the non-exclusive PQS-dependent regulation of *lecA* expression, validation of the impact of 488 on LecA production should be performed using a pCTX::P*lecA-lux* Δ*pqsA* mutant strain. Moreover, Farrow *et al.* (2008) and Rampioni *et al.* (2010) hypothesised that *lecA*, like pyocyanin, might be directly regulated by PqsE, independent of PqsR. As the gap of inhibition between AQ production

and pyocyanin suggested, 488 might have an impact on PqsE. However, further experiments are required like, for instance, by overexpressing *pqsE* in a *pqsA* mutant as shown in Rampioni *et al.* (2016).

In the *in silico* study of the binding between lactams and the PqsR ligand binding domain, 488 revealed a binding affinity even superior to 3-NH_2-7Cl-QZN the lead antagonist in the PqsR crystal structure work (Ilangovan *et al.*, 2013). Generally, all the lactams were able to fit within the PqsR binding domain, specifically within the pocket B that harbours the bicyclic ring of the AQs, though only 488 and 491 obtained high docking score values due to their stable poses and molecular interactions. This analysis revealed some interesting structural features potentially useful for future structure activity relationship-based design. Following this rationale, a new set of lactams was synthesized by Unilever. These lactams (310, 295 and 495) exhibit a structure and pose inside the CBD similar to 488. Their PQS inhibitory capability was tested with a P*pqsA::lux* transcriptional reporter and 295 exhibited greater activity than 488 at 100 μM, while at 250 μM, lactams 295 and 310 were as active as 488, consistent with the docking scores generated.

To provide evidence of direct binding to PqsR, different protein-ligand binding studies were performed using the recombinant $PqsR^{CBD}$. The ITC study confirmed the interaction of 488 and PqsR generating a K_D of 1.74 μM. The SRCD method was employed to compare qualitatively, the affinity for PqsR of a set of achiral compounds including AQs, 3-NH_2-7Cl-QZN and 488. The lactam showed the best affinity, followed by the QZN. An observation also predicted by the *in silico* studies. Finally, crystals of $PqsR^{CBD}$ protein were obtained and soaked in a solution containing 488 in order to reconstruct via X ray diffraction, a 3-D structure of the protein-inhibitor complex. These data confirmed the presence and the interactions of the 488 within the B pocket binding site.

However, the whole cell reporter gene fusions experiments gave rise to a contradiction with the competition assays which indicated that the inhibition of 488 towards the PQS system using 7Cl-PQS as the agonist was non-competitive. However, it is clear that 488 binds to the same ligand

binding pocket within the $PqsR^{CBD}$ as the AQs. The binding experiments describe a relatively strong interaction between the lactam and $PqsR^{CBD}$ protein with similar affinities as the native agonists PQS and HHQ. The nature of such an interaction, assuming that no covalent bonds are involved, is referred to as pseudo-irreversible binding. Indeed, the very low entropy obtained by the calorimetry study indicates a high number of hydrophobic interactions and/or conformational changes that are favour the binding of 488 suggesting that for PqsR, 488 behaves as an irreversible inhibitor, so explaining the non-competitive inhibitor dose response profile.

4 GLOBAL EFFECTS OF 488 ON *P. AERUGINOSA*

INTRODUCTION

Following discovery of the inhibitory effect of 488 on the PQS system of *P. aeruginosa*, further studies were performed, aimed at determining whether 488 has any other potential targets in this Gram-negative pathogen. In particular, this chapter will focus on the effect of 488 on the *P. aeruginosa* transcriptome and its consequences for biofilm development. Changes at the transcriptional level caused by exposure to 488 in liquid cultures were analysed via RNAseq. Some of the observations made were validated by biosensor or phenotypic assays which, in conjunction with the experiments described in chapter 3, helped to define a multi-faceted mode of action for 488. After studying the impact of 488 on the different types of motility, biofilm formation in the presence of 488 grown under different conditions and described via imaging and quantitative analysis was investigated. Moreover, the effect of the lactam on pre-formed biofilms exposed to an antibiotic was also evaluated. Due to the intrinsically higher resistance of biofilms to antibiotics (Costerton *et al*., 1995), new alternative strategies and technologies are being sought for the prevention or treatment of biofilms (Ciofu *et al.*, 2017). The insights provided by this set of experiments may be crucial for defining new applications and the subsequent employment of the lactam technology for identifying other targets for antibacterial drug design. In summary, the aims of this chapter are to describe the global effects of 488 on *P. aeruginosa*. Specifically, the work here presented intends to use RNAseq transcriptomics to reveal new targets and to validate the data generated with phenotypic and biosensor assays for motility and biofilm development

4.1 TRANSCRIPTOMIC STUDY OF THE EFFECTS OF 488 ON *P.AERUGINOSA*

RNA of *P. aeruginosa* PAO1-Lausanne was extracted as described in chapter 2 (section 2.2.2.10). Cultures (biological triplicates) were incubated with lactam 488 at 37°C with shaking at 200 rpm until late exponential phase (8 h and 12 h) when the PQS system genes are maximally expressed (Rampioni *et al.*, 2010). Along with a methanol solvent-only control, two different 488 concentrations were used, 50 and 100 µM that are respectively ~2 and ~4 times the IC_{50} for *pqsA* expression. As previously stated, the Unilever recommended lactam useful working concentration was ≥100 µM.

Transcriptomic analysis was undertaken to identify any differentially expressed genes within 6 sample groups, defined according to the two time extraction points and in the absence or presence of 488 at two different concentrations.

4.1.1 COG analysis overview

The data sequences generated from the analysis were arranged using the 'clusters of orthologous groups' (COGs) classification in order to identify the changes for each functional class. Figures 4.1, 4.2 and fig. 7.7 to 7.10 in the appendix section 7.4 show the distribution in percentage terms of genes affected by 488 according to their functional classification. For each comparison, the reference group is represented by the category termed "treatment dependent genes", placed at the top of each figure, which is obtained by the percentage of differentially expressed genes with COG function, either up or down, in relation to the total number of COG function genes. Consequently, the functional groups that are disproportionally represented by the columns are significantly more affected. The effect of 488 after 8 h of incubation at 50 and 100 µM are represented in Figure 4.1 and Figure 4.2, respectively. For both 488 concentrations, genes involved with RNA processing and cell motility are the most affected groups per number of downregulated genes (102 over 160 total genes, 63.75 %)

whilst the chromatin structure and dynamic group appear to be the most upregulated. The main differences emerging between *P. aeruginosa* treated with 488 at 100 μM for 8h is the greater number of down-regulated genes involved in cell cycle, motility and RNA processing alongside carbohydrate metabolism, chromatin structure and dynamics, defence mechanisms and inorganic ion transport/metabolism as the primary COG group for up-regulated genes. A similar trend was noted for the lower 488 concentration (50 μM) (Figure 4.2, Figure 7.7). Figure 7.8 shows there was little difference between the solvent control samples at 8 and 12 h apart from the slight difference in the chromatin structure/dynamics group. At 50 μM, 488 exerted a lower impact on PAO1 at 8h than after 12h (Figure 7.9) while the changes observed at 8h were sustained when the 488 concentration was increased (Figure 7.10). Interestingly, the RNA processing and chromatin structure COG groups represent only 2 (PA4951 -*orn* and PA4585 -*rtcA*) and 3 genes (PA0321, PA1409 (*aphA*) and PA3774) respectively. Thus the highest percentage of genes within a COG group down-regulated by 488 was the cell motility group consisting of 160 genes, ~65% of which were downregulated.

Table 4.1 and Table 4.2 were generated after an in-depth analysis of the differentially expressed genes obtained from the comparison between 488 (100 μM) and methanol solvent only samples after 8 h of incubation. This comparison was selected as representative of the general activity of 488 and for the high statistical reliability, since 60% of the fold-changes calculated have p values <0.05. Table 4.1 presents the differential expression in response to 488 of typical or closely related genes of the quorum sensing systems of *P. aeruginosa.* Table 4.2 summarises a selection of genes of particular interest for this study, mostly involved directly or indirectly in biofilm formation processes.

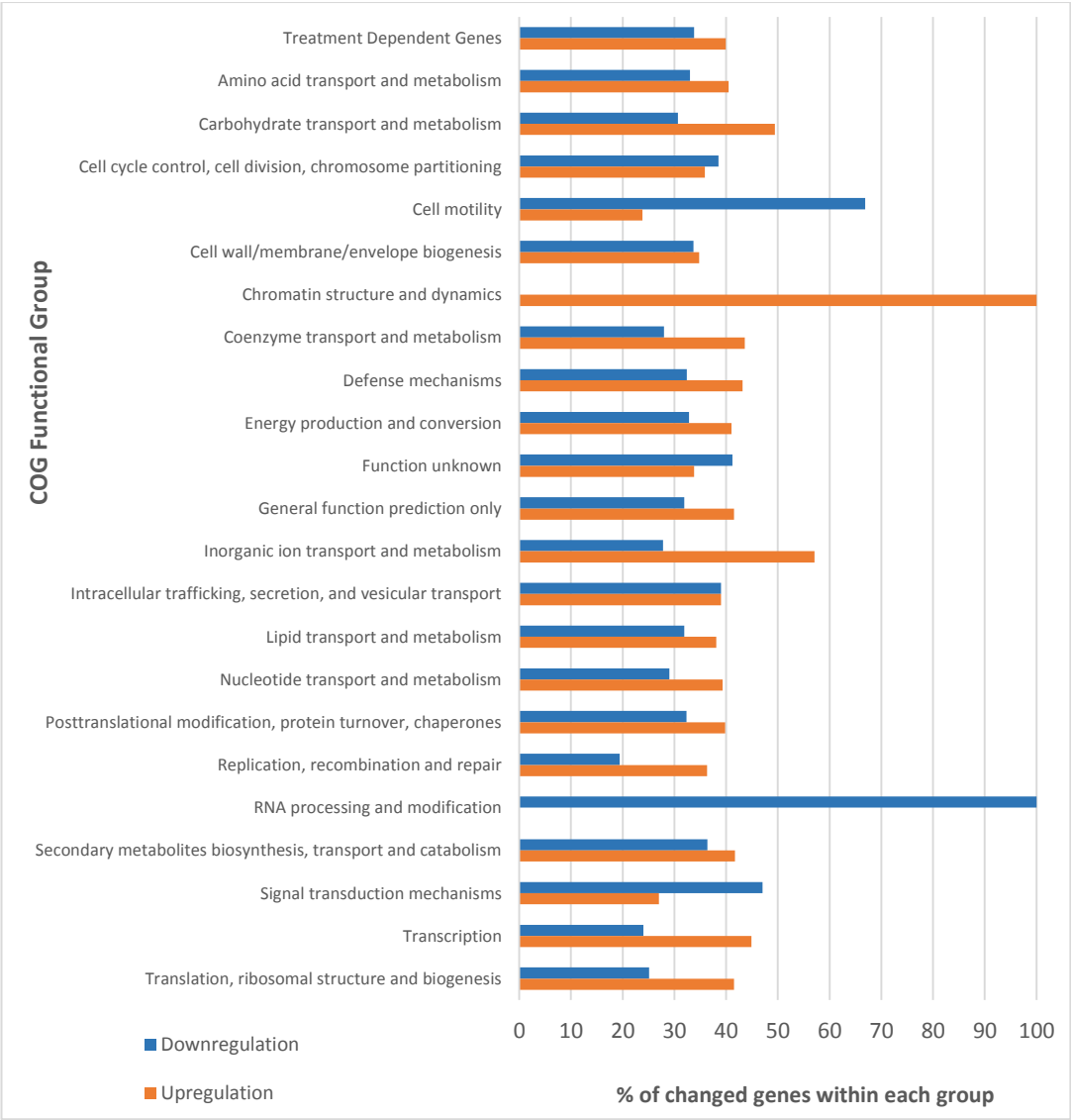

Figure 4.1 Differential expression of genes exposed to 488 (50uM) for 8 h compared with a solvent (methanol) only control using functional classification of PAO1 genes from the Pseudomonas Genome Database. Histograms representing the distribution of down-regulated (blue) and up-regulated (orange) genes according to their functional classifications. Top group represents the control.

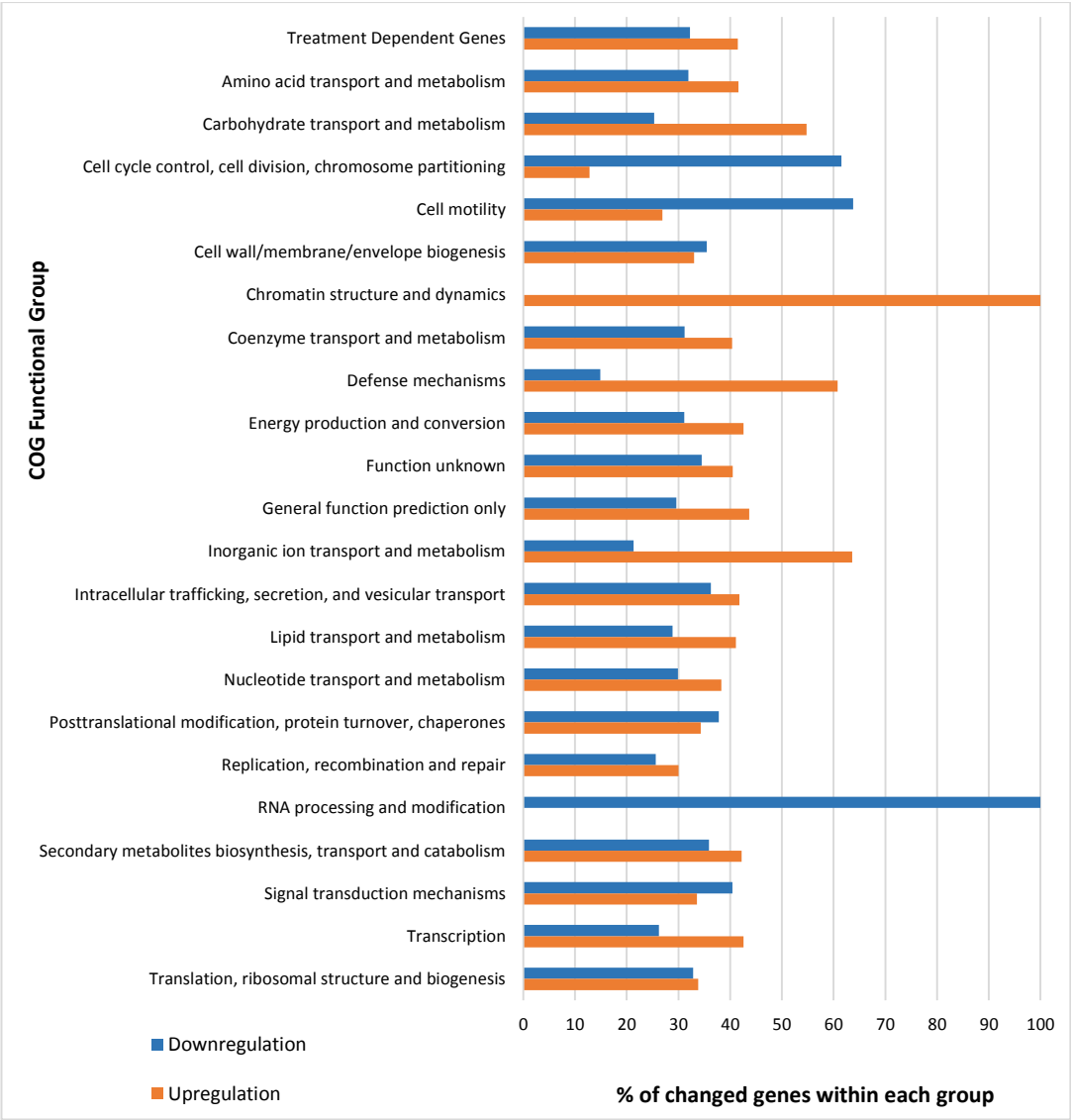

Figure 4.2 Differential expression of genes exposed to 488 (100uM) for 8 h compared with a solvent (methanol) only control using functional classification of PAO1 genes from the Pseudomonas Genome Database. Histograms representing the distribution of downregulated (blue) and upregulated (orange) genes according to their functional classifications. Top Group represents the control.

4.1.2 Differential expression of QS genes in response to 488

Exposure to 488 resulted in the downregulation of all QS genes. Along with *pqsR*, *pqsH* and the *pqsABCDE-phnAB* transcriptional unit, the AHL-dependent *las* and *rhl* QS systems appeared to be strongly affected. In particular, the *las rhl* target genes *lecB* and *phzB1* were the most downregulated in this comparison. Interestingly, while the defence mechanisms COG group, that includes several clinically relevant efflux pump mechanisms including the MexEF-OprN efflux pump (Köhler *et al.*, 1997; Lewenza *et al.*, 2005) and β-lactamases such as AmpC (Lodge *et al.*, 1993)(Table 4.2), were overall upregulated, the *mexGHI-opmD* efflux pump genes were downregulated (Table 4.1), possibly due to their association with the AQ-dependent QS system (Aendekerk *et al.*, 2005).

4.1.3 Differential gene expression in cell cycle, chromatin structure and RNA processing COG groups.

The chromatin structure and dynamics group is composed of PA0321 and *aphA* PA1409 and overexpressed PA3774 gene (LogFC=3.7); the former two encode different amidohydrolases involved in polyamine catabolism whilst the function of the latter is unknown (Chou *et al.*, 2008; Kramer *et al.*, 2016; Meyners *et al.*, 2014). From the 39 genes composing the cell cycle group, only the cell division genes *ftsA* and *ftsZ* (Yi *et al.*, 1985) showed minor but significant differential expression (-0.76 and -0.78 respectively). Due to their unknown roles in biofilm formation, cell cycle and chromatin structure, were not taken into account for further analysis. Nonetheless, the down-regulation of both the RNA processing genes, *orn* PA4951and *rtcA* PA4585 (-0.68 and -0.83 respectively), although moderate, is of interest in the context of biofilm development. The oligoribonuclease Orn is involved in the degradation of 5'-phosphoguanylyl-(3'-5')-guanosine (pGpG), an intermediate metabolite in the degradation of the intracellular second messenger, cyclic diguanylate (c-di-GMP). A Δ*orn P. aeruginosa* mutant strain showed high accumulation

of c-di-GMP levels, with consequent over-production of the biofilm extracellular matrix (Cohen *et al.*, 2015; Orr *et al.*, 2015).

Table 4.1 Log Fold Change values (logFC) and *p* values of QS related genes. From comparisons between samples obtained at 8h with or without 100uM 488. All genes have *p* value<0.02

Locus tag	Gene name	Log_2FC	*p*value	Description
PQS system				
PA0996	*pqsA*	-1.66	0.008	Anthranilate--CoA ligase
PA0997	*pqsB*	-2.07	0.001	2-heptyl-4(1H)-quinolone synthase subunit PqsB
PA0998	*pqsC*	-2.09	0.001	2-heptyl-4(1H)-quinolone synthase subunit PqsC
PA0999	*pqsD*	-2.20	0.0005	Anthraniloyl-CoA anthraniloyltransferase
PA1000	*pqsE*	-2.12	0.0003	2-aminobenzoylacetyl-CoA thioesterase
PA1003	*pqsR*	-0.87	0.001	Transcriptional regulator MvfR
PA2587	*pqsH*	-0.97	0.006	2-heptyl-3-hydroxy-4(1H)-quinolone synthase
PA1001	*phnA*	-1.92	0.002	Anthranilate synthase component 1, pyocyanine specific
PA1002	*phnB*	-1.94	0.0002	Anthranilate synthase component 2, pyocyanine specific
Rhl system				
PA3479	*rhlA*	-2.33	7.4E-09	3-(3-hydroxydecanoyloxy)decanoate synthase
PA3478	*rhlB*	-2.07	2.4E-08	ATP-dependent RNA helicase RhlB
PA1130	*rhlC*	-1.54	1.5E-08	Rhamnosyltransferase 2
PA3477	*rhlR*	-1.33	4.4E-05	Regulatory protein RhlR
PA3476	*rhlI*	-1.24	0.0006	Acyl-homoserine-lactone synthase
Las system				
PA1871	*lasA*	-2.14	0.0002	Protease LasA
PA3724	*lasB*	-2.23	0.014	Zn-dependent metalloprotease
PA1430	*lasR*	-0.91	0.006	Transcriptional activator protein LasR
Lectins				
PA2570	*lecA*	-2.56	3.6E-11	PA-I galactophilic lectin
PA3361	*lecB*	-4.04	2E-18	Fucose-binding lectin PA-IIL
Phenazine biosynthesis				
PA4210	*phzA1*	-2.68	0.0003	Phenazine biosynthesis protein PhzA1
PA4211	*phzB1*	-3.55	0.0003	-
PA4217	*phzS*	-2.92	0.0001	-
PA4212	*phzC1*	-2.88	1E-06	-
PA4216	*phzG1*	-2.83	3.6E-05	-
PA1900	*phzB2*	-2.81	7.2E-05	-
PA1902	*phzD2*	-2.75	0.0002	-
PA1901	*phzC2*	-2.74	1.8E-07	-
PA4213	*phzD1*	-2.72	0.0001	-
PA1903	*phzE2*	-2.66	5.9E-05	-
PA4214	*phzE1*	-2.65	0.0001	-
PA4209	*phzM*	-2.60	0.001	-
PA4215	*phzF1*	-2.52	0.0004	-

PA1905	*phzG2*	-2.52	8.3E-06	-
PA1904	*phzF2*	-2.48	0.0002	-
MexGHI-OpmD efflux pump				
PA4205	*mexG*	-2.13	0.0039	Uncharacterized membrane protein YphA, DoxX/SURF4 family
PA4206	*mexH*	-1.85	0.017	Multidrug efflux pump subunit AcrA
PA4207	*mexI*	-1.45	0.034	Multidrug efflux pump subunit AcrB

4.1.4 Differential gene expression in biofilm formation related pathways

Biofilm development is the result of a complex orchestration of multiple integrated regulatory and biochemical pathways. Figure 4.3 shows the Kegg pathway for biofilm formation by *P. aeruginosa* PAO1, where the genes affected by 488 have been highlighted. Firstly, mixed effects occur on the chemosensory system. The *chpB*, *chpD* and *chpE* genes are upregulated, and so possibly the *pilJK-chpABCD operon* while *pilI* and *chpE* are downregulated. It was not possible to define the levels of cAMP and the degree of expression of the virulence factor regulator protein (Vfr) since no other genes involved in the cyclic AMP signalling pathway were experimentally investigated. However, it is a reasonable to assume that cAMP levels would be decreased in the presence of 488 since the genes downstream of the Vfr and cAMP pathways show significantly low transcription levels. These include the type IV fimbrial and flagellar assembly (eg. *pile*, *pilO, fliE*, *fliQ*) as well as the the bacterial secretion systems II (*xcpP*, *xcpT xcpR*) and III (*exsA, exoS*) (Choi *et al.*, 2011; Darzins, 1994; Frithz-Lindsten *et al.*, 1997; Fulcher *et al.*, 2010; Leech & Mattick, 2006; Marsden *et al.*, 2016; Senf *et al.*, 2008; Yahr & Wolfgang, 2006). Such effects, combined with the inhibition of QS, complete what appears to be an impairment of most part of the processes facilitating a pathogenic and invasive lifestyle.

Interestingly, *hsbR* and *hsbA*, belonging to the HptB signalling system (Hsu *et al.*, 2008; Lin *et al.*, 2006), were found to be attenuated; this system specifically controls *rsmY* but not *rsmZ*. The role of these two sRNA molecules is to bind and sequester the RNA-binding protein RsmA (Brencic

et al., 2009; Valverde *et al.*, 2003), whose intracellular free state enhances the expression of secretion system VI and the exopolysaccharides (EPSs). Whilst the levels of *rsmY* and *rsmA* remained unclear, *rsmZ* showed a moderate down-regulation. Nonetheless, type VI secretion system components was found to be generally overexpressed (*clpv1, icmF1, ppkA, vgrG1*) except for of *hcp1* gene (Brencic & Lory, 2009; Mougous *et al.*, 2006).

The signal molecule c-di-GMP acts as an important biomolecular switch between motile and sessile behaviour (Liberati *et al.*, 2006; Merritt *et al.*, 2010). Its intracellular concentration is the result of specifically tuned actions of synthesis from two guanosine-5'-phosphate molecules (GTP) by diguanylate cyclases (DGCs) and degradation to pGpG and/or GMP by phosphodiesterases (PDEs) (Klebensberger *et al.*, 2007; Römling *et al.*, 2013; Ryjenkov *et al.*, 2005). The most significant differences registered on this system were the upregulation of the DGC SiaD and the, already described, downregulation of the oligoribonuclease Orn (Cohen *et al.*, 2015; Orr *et al.*, 2015), both of which should result in increased levels of c-di-GMP, thus triggering a series of processes that favour biofilm decelopment. In fact, genes involved in extracellular polymeric substance production such as polysaccharides Pel, (*pel* operon) and alginate (*alg44*, *algD*, *algE*, *algK*) and the Cup fimbriae expression (*cup*A and B clusters in particular) were also all strongly upregulated (Kulasekara *et al.*, 2005; Merighi *et al.*, 2007; Remminghorst & Rehm, 2006; Vallet *et al.*, 2001; Vasseur *et al.*, 2005).

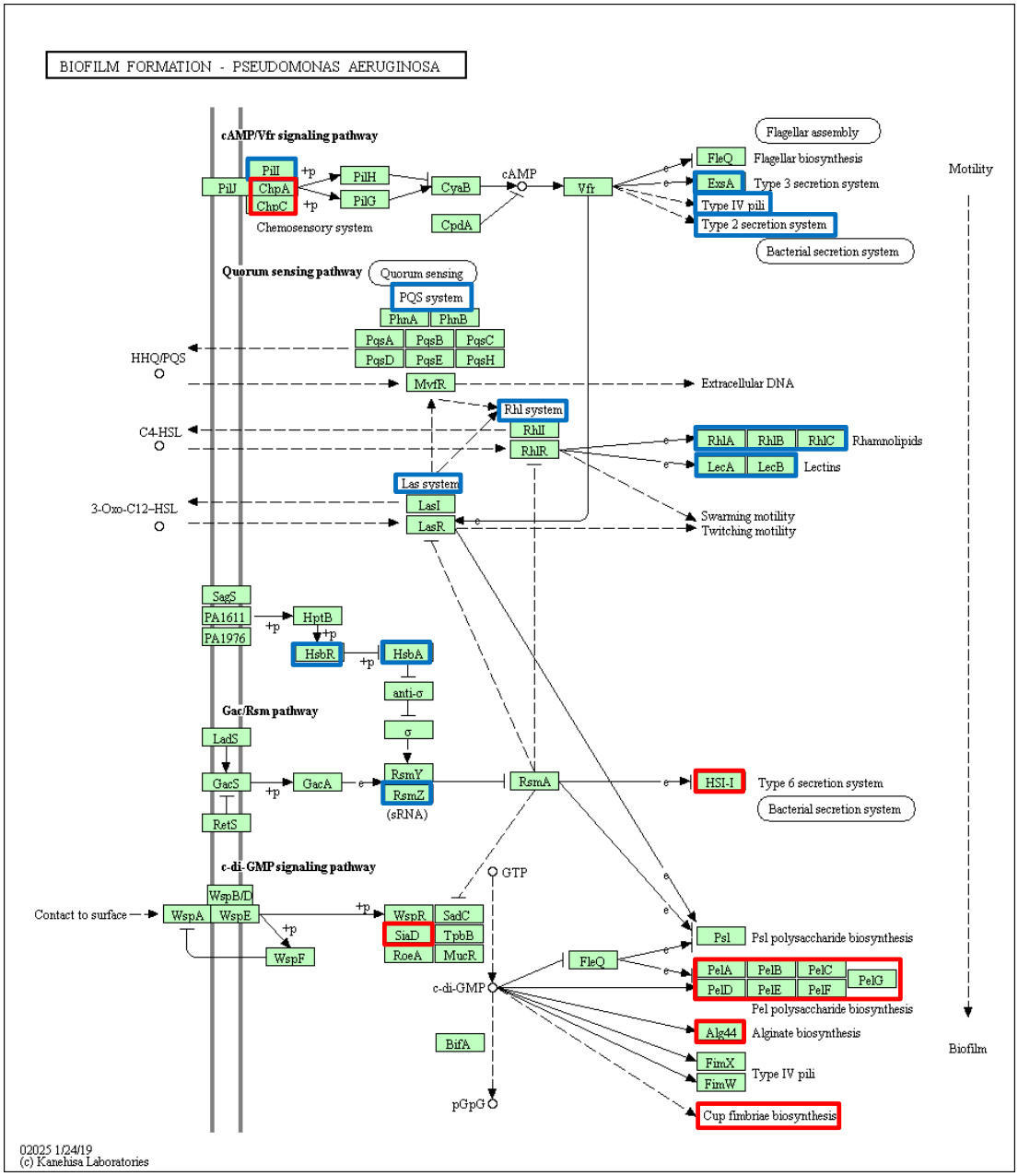

Figure 4.3 KEGG pathway of biofilm formation in *P. aeruginosa* PAO1 and the impact of 488. Upregulated genes/systems are represented with red boxes whilst downregulated in blue. From comparison between samples obtained at 8h without (solvent control) or with 488 (100 μM). All highlighted genes have $p<0.05$.

Table 4.2 Examples of differentially regulated genes from a comparison of *P. aeruginosa* cultures treated with 488 (100uM) for 8h compared with solvent control

Locus Tag	Gene name	LogFC	*p*value	Description
Type IV pili				
PA4556	*pilE*	-1.60	0.0005	Type 4 fimbrial biogenesis protein
PA4552	*pilW*	-1.40	0.002	Type 4 fimbrial biogenesis protein
PA4553	*pilX*	-1.36	0.003	Type 4 fimbrial biogenesis protein
PA4555	*pilY2*	-1.34	0.001	Tfp pilus assembly protein, tip-associated adhesin
PA5042	*pilO*	-1.05	0.0001	Type 4 fimbrial biogenesis protein
PA4550	*fimU*	-1.03	0.01	Type 4 fimbrial biogenesis protein FimU
PA4551	*pilV*	-0.99	0.049	Type 4 fimbrial biogenesis protein
PA4554	*pilY1*	-0.94	0.03	Tfp pilus assembly protein, tip-associated adhesin
PA4527	*pilC*	-0.97	0.002	Type IV fimbrial biogenesis protein
PA3385	*amrZ*	-0.92	0.014	lAginate and motility regulator Z (old name *algZ*)
PA5261	*algR*	-1.88	2.6E-09	Alginate biosynthesis regulatory protein AlgR
PA0410	*pilI*	-0.99	0.009	Twitching motility protein PilI
Flagellar assembly and motor regulation				
PA1100	*fliE*	-1.45	1.8E-06	Flagellar hook-basal body complex protein FliE
PA1447	*fliQ*	-1.30	0.0005	Flagellar biosynthesis protein FliQ
PA1101	*fliF*	-1.23	6.3E-06	Flagellar biosynthesis/type III secretory pathway M-ring protein FliF/YscJ
PA1444	*fliN*	-0.99	0.0002	Flagellar motor switch protein FliN
PA1443	*fliM*	-0.95	0.0003	Flagellar motor switch protein FliM
PA1102	*fliG*	-0.84	0.001	Flagellar motor switch protein FliG
PA1077	*flgB*	-1.19	0.007	Flagellar basal-body rod protein FlgB
PA1080	*flgE*	-1.13	0.0001	Flagellar hook protein FlgE
PA3351	*flgM*	-1.06	0.001	Negative regulator of flagellin synthesis (anti-sigma28 factor)
PA1086	*flgK*	-0.92	0.0009	Flagellar hook-associated protein 1 FlgK
PA1087	*flgL*	-1.01	0.001	Flagellar hook-associated protein type 3 FlgL
PA1453	*flhF*	-1.15	0.0001	Flagellar biosynthesis protein FlhF
PA1460	*motC*	-0.83	0.0008	Flagellar motor component MotC
PA1461	*motD*	-0.54	0.0263	Flagellar motor protein MotB
Type III secretory system				
PA1713	*exsA*	-0.99	0.001	Exoenzyme A
PA3841	*exoS*	-1.18	0.0009	Exoenzyme S
Type II secretory system				
PA3104	*xcpP*	-1.12	7.1E-05	Secretion protein XcpP
PA3101	*xcpT*	-1.12	8.07E-05	Type II secretory pathway, pseudopilin PulG
PA3103	*xcpR*	-0.60	0.018	Type II secretory pathway ATPase GspE/PulE or T4P pilus assembly pathway ATPase PilB

Bacterial chemotaxis				
PA1456	*cheY*	-1.47	2.7E-06	Regulatory component of sensory transduction system for chemotaxis
PA0416	*chpD*	1.44	0.0002	Component of chemotactic signal transduction system, part of chpA operon
PA0414	*chpB*	0.62	0.02	Component of chemotactic signal transduction system, part of chpA operon
PA0417	*chpE*	1.26	0.001	Chemotactic transduction protein ChpE, part of chpA operon
PA0179	-	-1.61	2.8E-07	DNA-binding response regulator, OmpR family, contains REC and winged-helix (wHTH) domain
PA3349	-	-1.07	0.014	CheY chemotaxis protein or a CheY-like REC (receiver) domain
Gac/Rsm Signaling Pathway				
PA3346	*hsbR*	-1.12	7.6E-05	HptB-dependent secretion and biofilm regulator HsbR
PA3347	*hsbA*	-1.53	1.2E-08	HptB-dependent secretion and biofilm anti anti-sigma factor HsbA
PA3621.1	*rsmZ*	-0.80	0.01	Regulatory RNA RsmZ
PA0090	*clpV1*	0.68	0.01	(locus HIS-I) ATP-dependent Clp protease ATP-binding subunit ClpA
PA0085	*hcp1*	-1.17	1.5E-05	(locus HIS-I) ATP-dependent Clp protease ATP-binding subunit ClpA
PA0077	*icmF1*	1.23	2.1E-05	(locus HIS-I) Type VI protein secretion system component VasK
PA0074	*ppkA*	1.93	9.6E-07	(locus HIS-I) Serine/threonine protein kinase
PA0091	*vgrG1*	1.10	0.0001	(locus HIS-I) Uncharacterized conserved protein, implicated in type VI secretion and phage assembly
c-di-GMP signaling pathway				
PA0169	*siaD*	1.18	0.0001	Two-component response regulator, PleD family, consists of two REC domains and a diguanylate cyclase (GGDEF) domain
PA3542	*alg44*	2.65	4.7E-07	Alginate biosynthesis protein Alg44
PA3546	*algD*	1.73	0.0007	GDP-mannose 6-dehydrogenase AlgD
PA3544	*algE*	2.46	5.5E-06	Alginate production outer membrane protein AlgE precursor
PA3547	*algL*	2.52	0.0001	Poly(beta-d-mannuronate) lyase precursor AlgL
PA3543	*algK*	3.08	1.1E-05	Alginate biosynthetic protein AlgK precursor
PA3064	*pelA*	1.58	7.8E-08	Polysaccharide biogenesis
PA3063	*pelB*	2.71	1.3E-08	Polysaccharide biogenesis
PA3062	*pelC*	1.62	0.001	Polysaccharide biogenesis
PA3061	*pelD*	1.93	6.6E-05	Polysaccharide biogenesis
PA3060	*pelE*	3.40	8.9E-06	Polysaccharide biogenesis
PA3059	*pelF*	2.26	7.7E-07	Polysaccharide biogenesis Glycosyltransferase involved in cell wall biosynthesis
PA3058	*pelG*	1.58	0.0003	Polysaccharide biogenesis
PA4652	*cupE5*	2.79	5.4E-06	Fimbrial usher protein CupE5, Outer membrane usher protein FimD/PapC
PA2129	*cupA2*	2.65	3E-05	Chaperone CupA2

PA2130	*cupA3*	2.96	8E-07	Outer membrane usher protein FimD/PapC
PA2131	*cupA4*	3.02	9.7E-05	Fimbrial subunit CupA4
PA2132	*cupA5*	3.80	2.5E-05	Pilus assembly protein, chaperone PapD
PA4082	*cupB2*	2.05	2.9E-05	Chaperone CupB2, probable pili asembly chaperone
PA4084	*cupB3*	2.37	7.5E-07	Usher CupB3, probable fimbrial biogenesis usher protein
PA4083	*cupB4*	2.76	0.0002	Chaperone CupB4
PA4082	*cupB5*	2.31	1.8E-08	Adhesive protein CupB5
PA4081	*cupB6*	1.49	1.9E-05	Fimbrial subunit CupB6
PA0992	*cupC1*	1.03	0.004	Fimbrial subunit CupC1
PA0993	*cupC2*	1.84	0.0006	Chaperone CupC2
RNA processing (COG)				
PA4951	*orn*	-0.68	0.007	Oligoribonuclease (3'-5' exoribonuclease)
PA4585	*rtcA*	-0.83	0.013	RNA 3'-terminal phosphate cyclase
Defense mechanisms				
PA2493	*mexE*	2.03	0.00013	Resistance-Nodulation-Cell Division (RND) multidrug efflux membrane fusion protein MexE precursor
PA2494	*mexf*	1.99	5.31E-07	Resistance-Nodulation-Cell Division (RND) multidrug efflux transporter MexF
PA2495	*oprN*	2.01	1.21E-05	Multidrug efflux outer membrane protein OprN precursor
PA4599	*mexC*	0.92	0.0005	Resistance-Nodulation-Cell Division (RND) multidrug efflux membrane fusion protein MexC precursor
PA4598	*mexD*	0.75	0.003	Resistance-Nodulation-Cell Division (RND) multidrug efflux transporter MexD
PA4597	*oprJ*	0.92	0.0006	Multidrug efflux outer membrane protein OprJ precursor
PA4110	*ampC*	0.93	0.001	Beta-lactamase precursor
PA4109	*ampR*	0.53	0.039	transcriptional regulator AmpR
Chromatin structure and dynamics (COG)				
PA0321	-	1.62	5E-05	Acetylpolyamine amidohydrolase
PA1409	*aphA*	1.45	3.12E-05	Acetylpolyamine aminohydrolase (aphA)
PA3774	-	3.77	5.4E-06	Histone deacetylase-like amidohydrolase
Cell cycle (COG)				
PA4408	*ftsA*	-0.76	0.009	Cell division protein FtsA
PA4407	*ftsZ*	-0.78	0.03	Cell division protein FtsZ
Others				
PA3223	*azoR3*	6.25	7.8E-29	FMN-dependent NADH-azoreductase
PA1962	*azoR2*	6.25	4.7E-34	FMN-dependent NADH-azoreductase
PA2113	*opdO*	4.13	2.4E-08	Pyroglutamate porin OpdO
PA2219	*opdE*	4.10	1.3E-24	Outer membrane porin OpdE
PA3206	-	1.25	1.9E-05	Probable two-component regulatory system (CpxA/CpxR)

4.2 IMPACT OF 488 ON *P. AERUGINOSA* MOTILITY

The transcriptomic data indicated that genes involved in motile behaviour are mostly down-regulated following treatment of *P. aeruginosa* with 488. (Table 4.2). To validate these data, the effects of 488 on *P. aeruginosa* swimming, swarming and twitching motility were investigated.

4.2.1 Swarming

Swarming is a type of movement that occurs on a surface. It is the result of several factors: flagellum and type IV pili exert single-cell propulsion, whilst the Rhl and Las QS, systems specifically, mediate cell-to-cell interactions and the release of rhamnolipids, the surfactants necessary to overcome the surface tension. (Heurlier *et al.*, 2004; Overhage *et al.*, 2008; Shrout *et al.*, 2006; Yeung *et al.*, 2009). For this reason, swarming motility relies on the coordination of the whole cell population, generating characteristic patterns depending on the bacterial species (Kearns, 2010). *P.aeruginosa* swarms by forming branches from an inoculum spotted in the centre of a petri dish.

PAO1-L, isogenic Δ*pqsA* and Δ*pqsAHR* mutants, PAO1-Unilever and PA ATCC 15442 were employed in this experiment. The PQS mutants were used to verify whether the lactam might be able to affect the swarming independent of its principal QS target, as suggested by the RNAseq data (section 4.1.2). PAO1-Unilever was assayed as it showed high senitivity to the action of 488, according to the experiments reported in chapter 3. On the other hand, ATCC 15442 lacks a functional AQ-dependent QS system and is characterised by a reduced swarming capability (Ng, 2018).

Figure 4.4 shows that 488 is able to reduce the swarming motility of all the strains employed in direct proportion to the quantity of lactam dissolved in the medium: whereas 50 μM were sufficient to manifest a reduction of the area covered by the cells, the effect increased at 100 μM culminating with total inhibition at 200 μM. No substantial effect was observed on PAO1-Unilever and ATCC 15442 due to their low or absent motility.

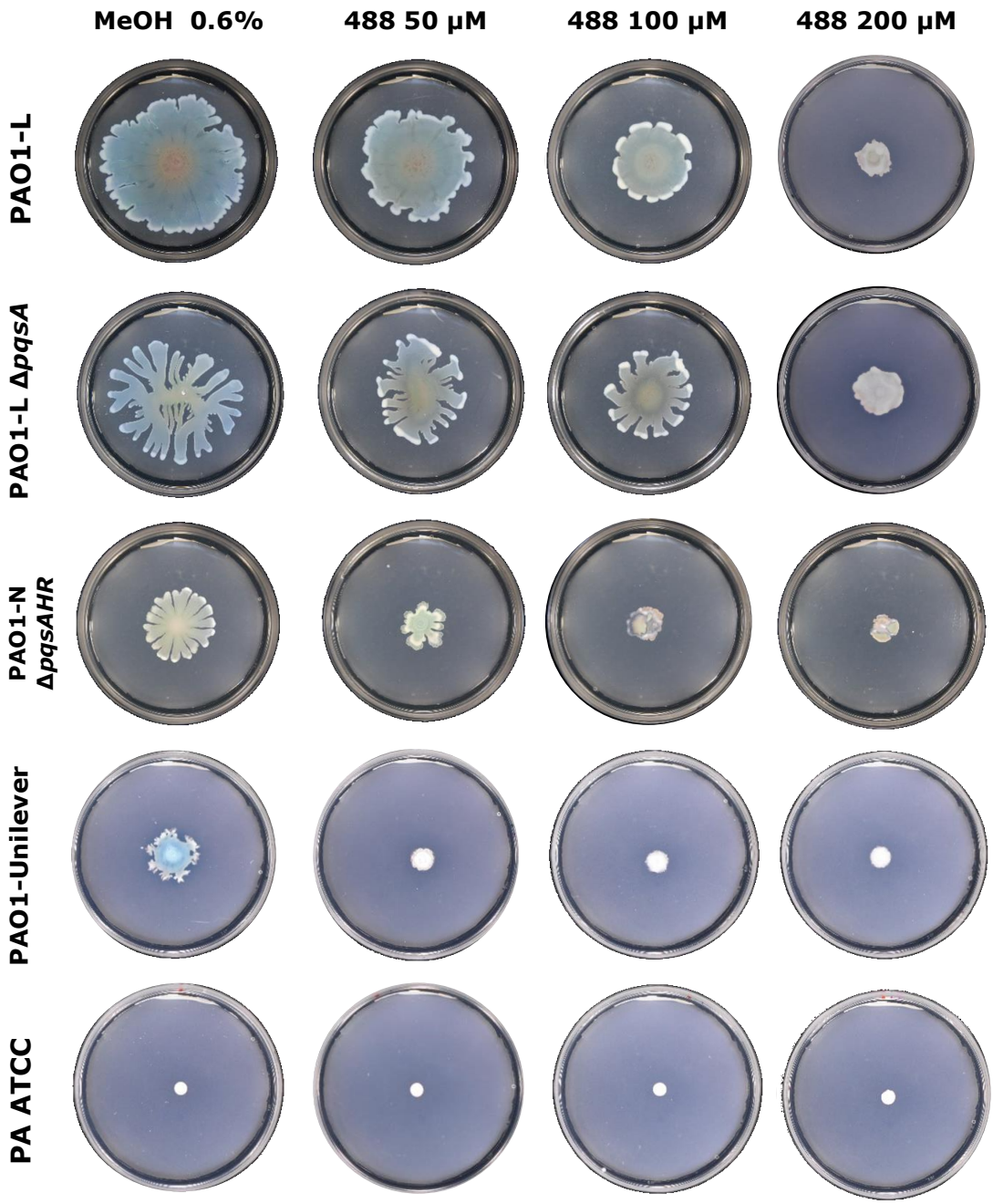

Figure 4.4 Swarming activity of *P. aeruginosa* cells in presence of 488 at 50, 100 and 200 µM. MeOH only plates were used as control. Each plate is representative of biological triplicates.

4.2.2 Swimming

Swimming motility is a single-cell movement powered uniquely by a fully functional flagellum, therefore biosurfactants like rhamnolipids, and so QS, do not affect its activity (Dasgupta *et al.*, 2003). In common with swarming, in this assay the degree of motility is quantified according to the radial migration of *P. aeruginosa* cells through the semi-solid agar from the inoculum point. Inhibition is reflected as a reduced coverage area. PAO1-L and the isogenic Δ*pqsA* and Δ*pqsR* mutants were spotted at the centre of the plate, mid-height of the 0.3 % agar medium layer containing 488 at different concentrations. Only a moderate reduction on motility can be observed in the presence of 488 at 200 μM (Figure 4.5), despite the multitude of flagellar structure/motor genes found differentially expressed from the RNAseq analysis

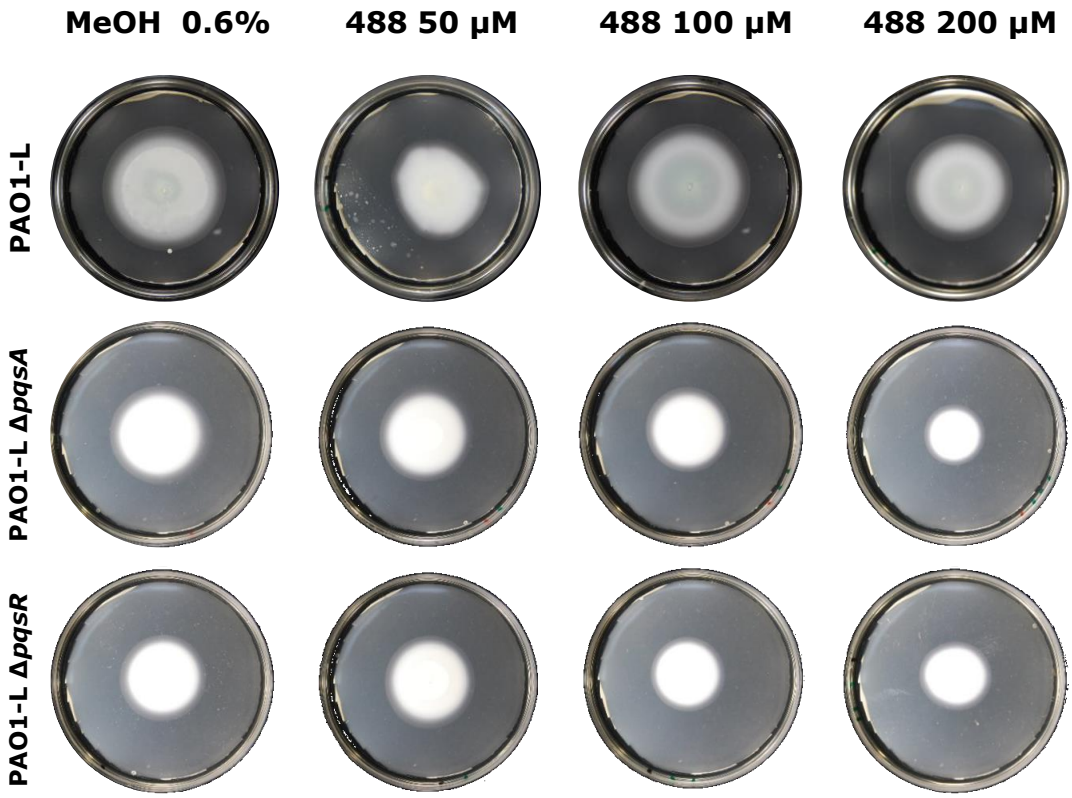

Figure 4.5 Swimming activity of *P. aeruginosa* cells with 488 at 0, 50, 100 and 200 μM. Each plate is representative of biological triplicates.

4.2.2.1 Flagellar morphology study

To visualize possible effects of 488 on *P. aeruginosa* cell morphology and flagellar assembly, PAO1-L cultures were grown in planktonic conditions, fixed and visualised with transmission electron microscopy (TEM). In Figure 4.6, representative images of treated and untreated cells are reported for comparison. The most significant difference emerged from this analysis was the flagellar localization: cells grown with 488 showed a non-polar flagellum, which is associated to a decreased swim velocity (Murray & Kazmierczak, 2006). Localization of the flagellar origin is determined by the expression of the gene *flhF* (Murray & Kazmierczak, 2006; Pandza *et al.*, 2000) which in the RNA-seq was reported with LogFC= -1.5.

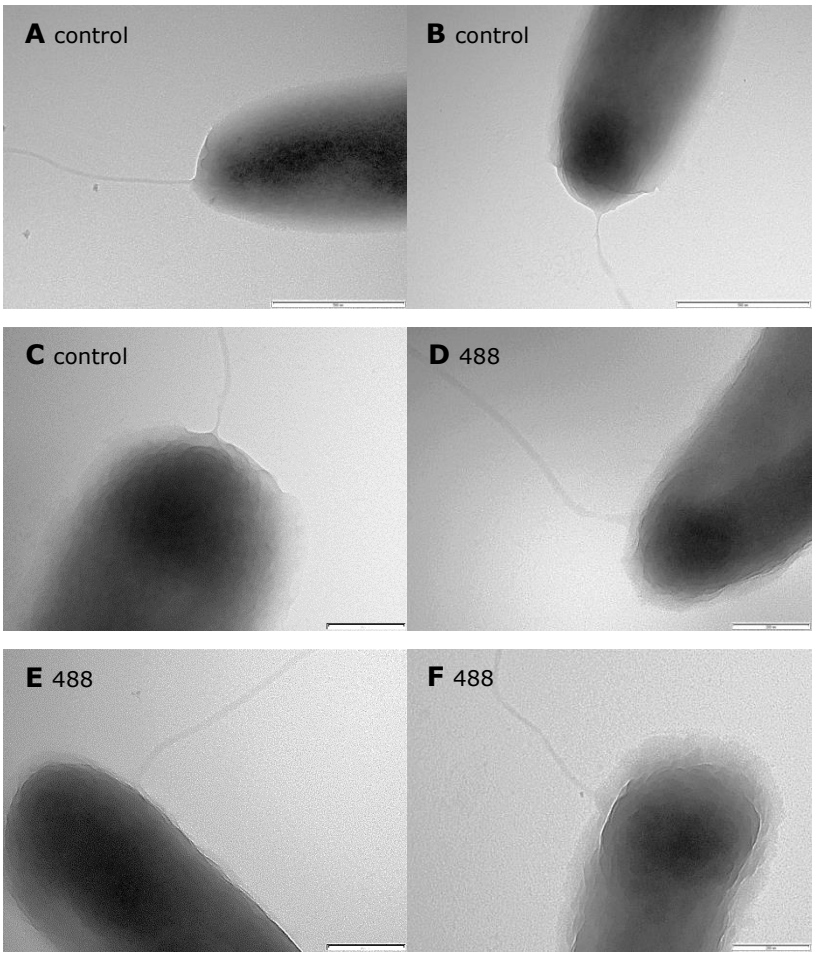

Figure 4.6 Representative TEM images of PAO1-L flagella. In panel **A**: Control DMSO 0.5%, x60k magnification, scale bar 0.5 µm. **B**: Control DMSO 0.5%, x60k , scale bar 0.5 µm. **C**: Control DMSO 0.5%, x87k magnification, scale bar 0.2 µm **D**: 488 200 µM. x20.5k scale bar 1 µm **E**: 488 200 µM. x87k scale bar 0.2 µm. **F**: 488 200 µM. x87k scale bar 1 µm

4.2.3 Twitching

Twitching motility relies on extension and retraction of type IV pili on a solid surface, independent of flagellar function (Mattick, 2002b). This phenotype is associated with colonization properties, such as adhesion and motility, of a bacterial population and it determines active expansion on new surfaces (Beatson *et al.*, 2002).

Twitching was assessed for PAO1-L and the corresponding PQS system mutants which were inoculated at the bottom of the agar layer to allow the colony expansion between the petri dish and the agar medium containing 488 at different concentrations (Figure 4.7). Although controls do not exhibit a wide area coverage, the 488 treated samples show a pronounced modification in their behaviour: interestingly, at 200 µM the total area covered is reduced in terms of radius but the twitching colony stain is darker and thicker, indicating a higher number of cells close to the centre compared to the 100 µM treatment.

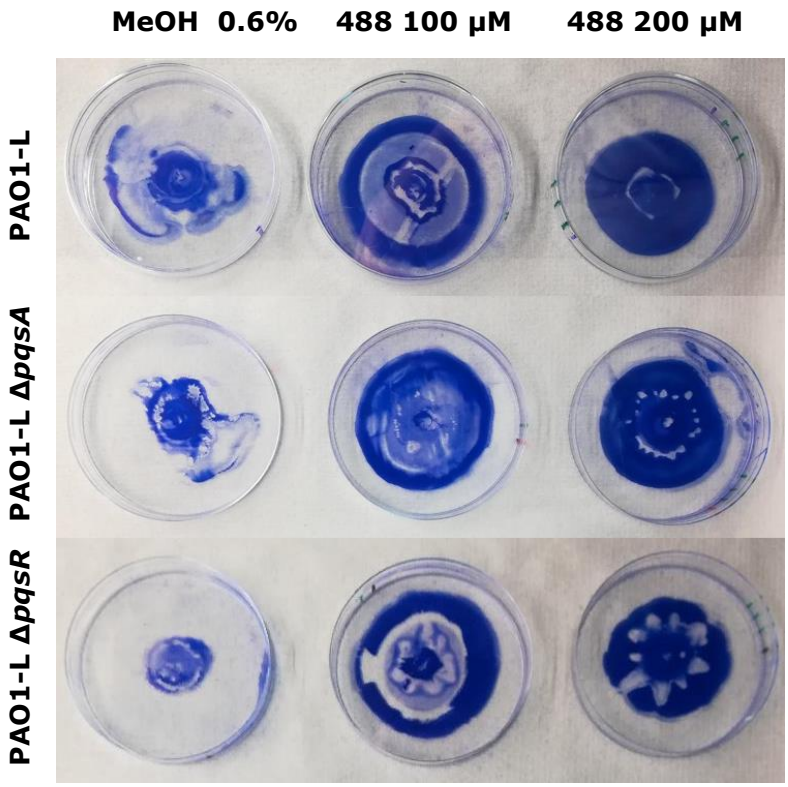

Figure 4.7 Twitching motility of *P. aeruginosa* cells *treated* with 488 at 0, 50, 100 and 200 µM. Each plate is representative of biological triplicates.

4.3 IMPACT OF 488 ON *ORN* EXPRESSION

Due to the downregulation of the RNA processing COG shown, further investigation was carried out by first constructing a *lux*-based promoter fusion for the *orn* gene, which encodes an oligoribonuclease important in c-di-GMP signalling (Cohen *et al.*, 2015). An antagonism assay was performed with increasing concentrations of 488, in order to generate a dose-response curve, An IC_{50} value of 104.9±6 was obtained (Figure 4.8).

This assay confirms the inhibition of *orn* expression gene, although a higher concentration of 488 is required compared to its impact on the PQS system (Figure 3.6).

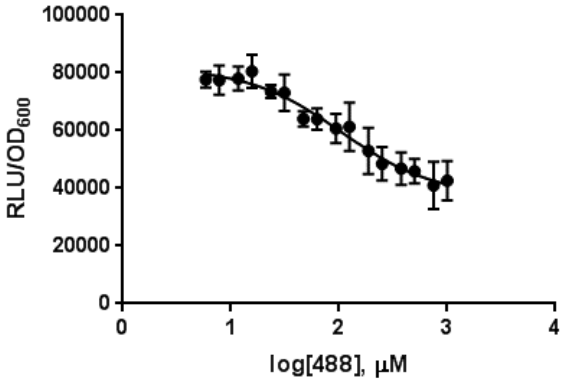

Figure 4.8 Effect of lactam 488 on expression of P*orn::lux* in PAO1-L (IC_{50} = 104.9±6 µM)

4.4 IMPACT OF 488 ON BIOFILM FORMATION

Biofilm formation in presence of 488 was investigated using different biofilm models due to the broad spectrum for potential applications, from environmental to clinical, of the lactam.

Initially, biofilms were grown statically in multi-well system plates, in order to efficiently test a wide range of conditions in a time and cost-effective manner. Subsequently, microfluidic based assays were employed. Where possible, biofilms were imaged with confocal laser-scanning microscopy, which enables the collection of 3-dimensional figures that can be used for quantification with ImageJ (Schindelin *et al.*, 2012). The live/dead assay allows for quantification of biomass and/or "estimated" viability of the biofilm, by exploiting two fluorescent dyes, Syto9 and Propidium Iodide (PI) as markers for intact or compromised viability. Biomass indices were obtained by summing the values generated with ImageJ from Syto9 and PI fluorescence intensities, while "estimated" viability was obtained from the ratio of Syto9/PI values. PI, a membrane-impermeable dye, binds to free DNA in the sample and could therefore generate background noise due to the DNA present in the extracellular matrix of the biofilm (eDNA). Therefore, the viability values reported here represent an estimate, which does not take into account the presence of eDNA. Throughout these experiments, the different *P. aeruginosa* sub-lines PAO1-L and PAO1-UW were studied in order to add strain variability to the study, in the light of the subtle differences among the sub-lines (Klockgether *et al.*, 2010; Kohler *et al.*; Luong *et al.*, 2014; Maseda *et al.*, 2000).

Finally, tests were performed on pre-formed biofilms to evaluate whether 488 might demonstrate synergistic effects with antibiotics such as ciprofloxacin, commonly used for the treatment of *P. aeruginosa* infections (Acar & Goldstein, 1997).

4.4.1 Effect of lactam 488 in static biofilm growth conditions

4.4.1.1 Crystal violet biomass quantification

Crystal violet is a one of the most common and time-effective assays used to quantify biofilm biomass and since its first description Christensen *et al.* (1982) has been through several modifications. The method followed in this study is described in Thomann *et al.* (2016) and summarized in section (2.2.6.1.1). A progressive 488 concentration-dependent increase in biomass was observed (Figure 4.9). A plateau appears to be reached at 100-150 µM where biomass quantity is stabilised.

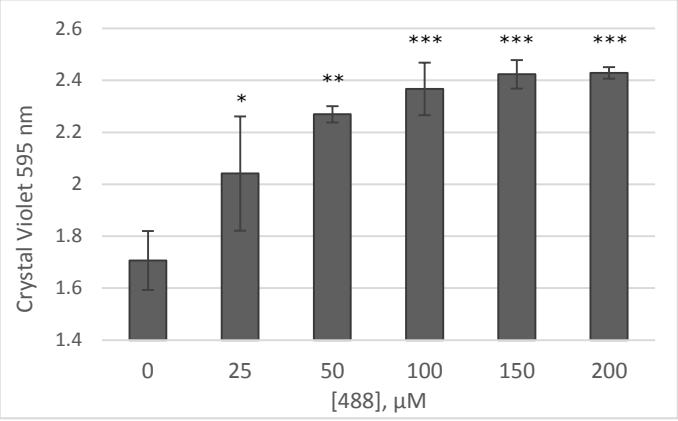

Figure 4.9 Relative quantification of PAO1-L biofilm biomass with crystal violet. Bacteria were incubated in 96 well polystyrene plates with LB 10 % at 37° C, static for 18 h. Controls contained 0.6 % v/v MeOH Error bars represent standard deviation of four biological replicates. Multiple t-tests were performed to determine statistical significance (*) represents *p* value < 0.05, (**) *p* value < 0.01 and (***) *p* value < 0.001.

4.4.1.2 Live-dead staining of PAO1-L biofilms

Although crystal violet based quantification represents an excellent screening method to rapidly determine the effects of compounds such as 488 on biofilm biomass production, the data provided are limited by the measurement of the biomass only and by the employment of 96-well plates, whose architecture interferes with proper oxygenation of the sample (Cotter *et al.*, 2009). Indeed, oxygen is a discriminative element between biofilm models since its availability influences biofilm development and the cellular metabolic pathways involved (Alvarez-Ortega & Harwood, 2007; Borriello *et al.*, 2004; Hill *et al.*, 2005). Anaerobic conditions are

found in the lungs of cystic fibrosis patients, where mucus acts as a capsule preventing oxygenation (Worlitzsch *et al.*, 2002). Thus, growth in 24-well plates was also investigated in this study as the wider wells allow for a better oxygen diffusion. Biofilms were stained after washing with Syto9/PI from the Live-Dead Backlight® stain kit. Data were collected using a TECAN Spark® plate reader. Biomass (Syto9+PI value) increased by 80% with 488 at 200 µM while no effect occurred at lower concentrations (Figure 4.10). However, cell viability ($Syto9PI^{-1}$ ratio) improved with the lactam at 25 µM and 50 µM (Figure 4.11).

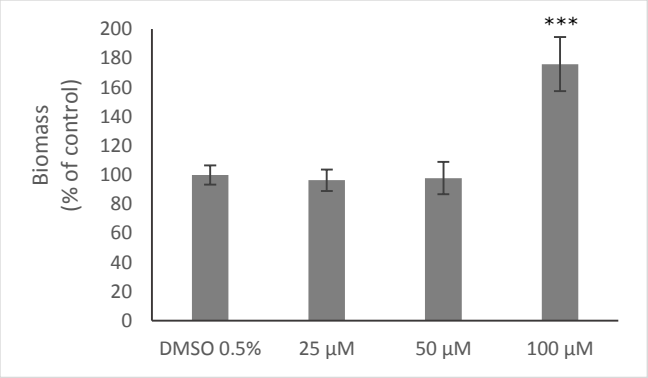

Figure 4.10 Quantification of PAO1-L biofilm biomass following treatment with 488 and staining with Syto9/PI. Bacteria were incubated in 24 well polystyrene plates with glucose-enriched M9 at 37° C static for 18 h. Control was solvent only with 0.5% v/v DMSO. Error bars represent standard deviation of biological triplicates. Statistical significance was calculated with Welch's t test, (***) represents *p* value < 0.001.

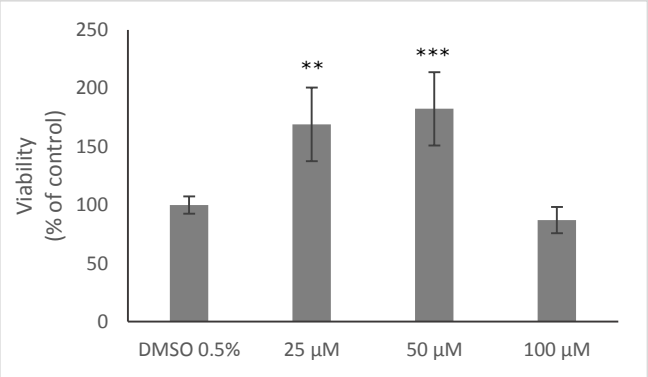

Figure 4.11 Quantification of PAO1-L biofilm viability after treatment with 488 after staining with Syto9/PI. Bacteria were incubated in 24 well polystyrene plates glucose-enriched M9 at 37° C statically for 18 h. Control was solvent only with 0.5% DMSO. Error bars represent standard deviation of biological triplicates. Statistical significance was calculated with Welch's t test, (**) represents *p* value < 0.01, (***) *p* value < 0.001.

4.4.1.3 Confocal visualization of mCherry-tagged PAO1-UW biofilms in 24-well plate assays

The assay described above was repeated using mCherry-tagged PAO1-UW. Biofilms formation was evaluated qualitatively through observation with a ZEISS LSM 700 confocal microscope and quantified by the analysis of Z-stacks collected randomly (Figure 4.12). Biomass increased significantly at 200 µM (Figure 4.13), where more structured biofilms can be observed.

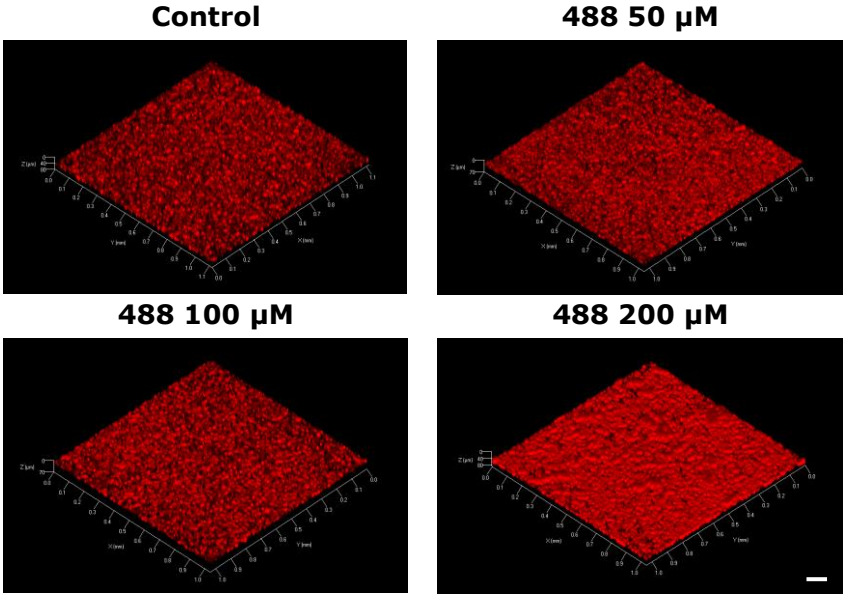

Figure 4.12 PAO1-UW mCherry-tagged biofilms grown in RPMI with 488 at 0 (control) , 50, 100 and 200 µM after 18 h of incubation at 37°C in a 24 well plate. Z-stacks collected with ZEISS LSM 700 confocal microscope, 5X magnification. Scale bar represents 100 µM.

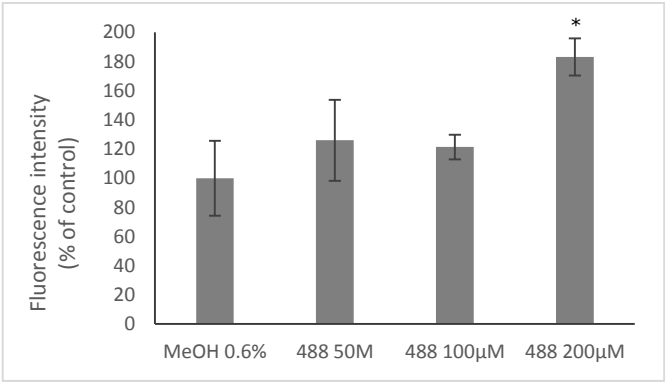

Figure 4.13 Quantification of PAO1-UW fluorescence from mCherry-tagged biofilms grown in RPMI and 488 at 50, 100 and 200 µM after 18 h of incubation at 37°C in a 24 well plate. Error bars represents standard deviation of biological triplicates. Statistical significance was calculated with Welch's t tests, (*) represents *p* value < 0.05.

4.4.2 Effect of lactam 488 in microfluidic biofilm conditions

4.4.2.1 Microfluidic system

Microfluidic systems such as the Bioflux™ (Fluxion Biosciences) is an efficient method for reproducing a constant flow in small channels, which allows simultaneous visualisation over time (Tremblay *et al.*, 2015). The relative simplicity of testing several samples simultaneously, and the highly customizable settings, compared with macro-sized fluidics (Palmer Jr, 1999), are among the main advantages of this technique. In the present study, 48-well plates were used. In this experiment, 488 did not enhance biofilm production to the same degree as in the static biofilm assays (Figure 4.14), nevertheless biomass and viability increased in the presence of the lactam (Figure 4.15) and the biofilm structure appeared as more organized compared to the untreated control.

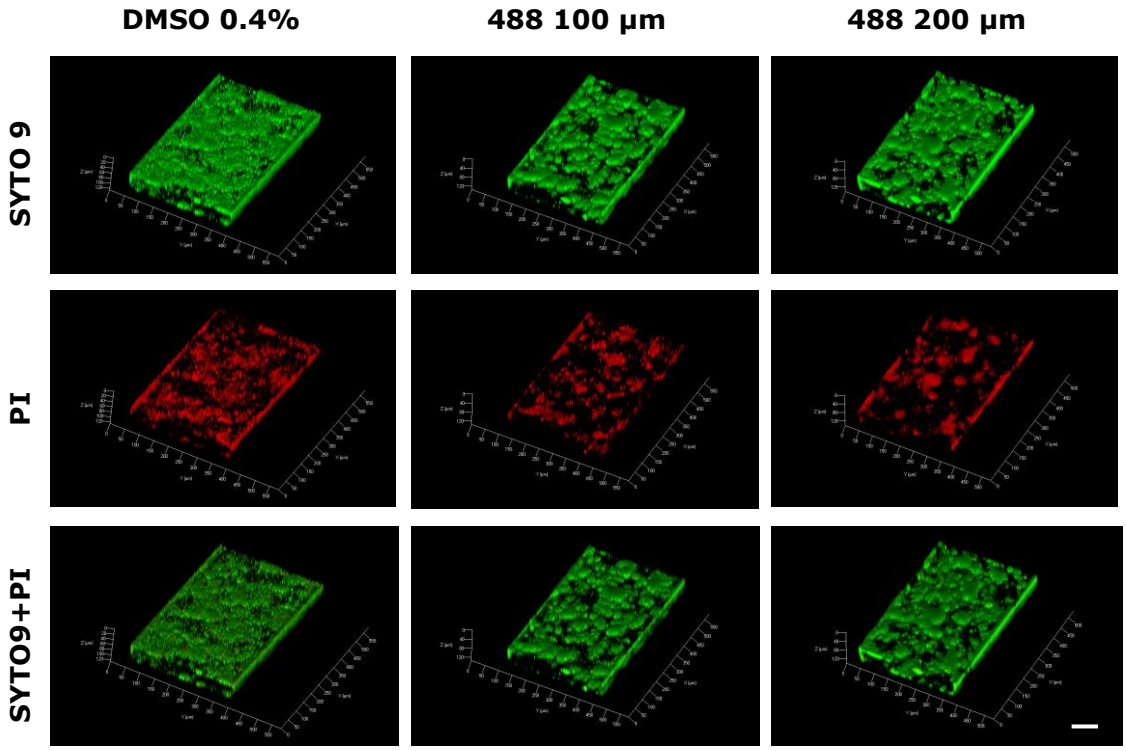

Figure 4.14 PAO1-L biofilms grown in LB 10% and treated with 488 at 0, 100 and 200 µM after 18 h of incubation at 37°C in Bioflux™ system channels. Z-stacks collected with ZEISS LSM 700 confocal microscope, 10X magnification. Green represents Syto9 fluorescence, red is PI fluorescence. Scale bar represents 100 µm.

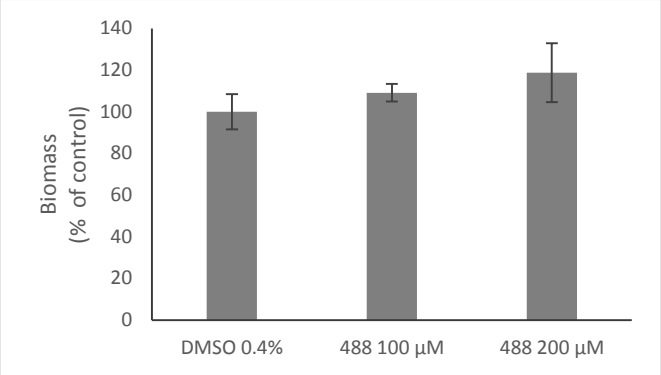

Figure 4.15 PAO1-L biofilms grown in LB 10% and 488 at 0, 100 and 200 µM after 18 h of incubation at 37°C in Bioflux™ system channels. Error bars represent standard deviation of biological replicates.

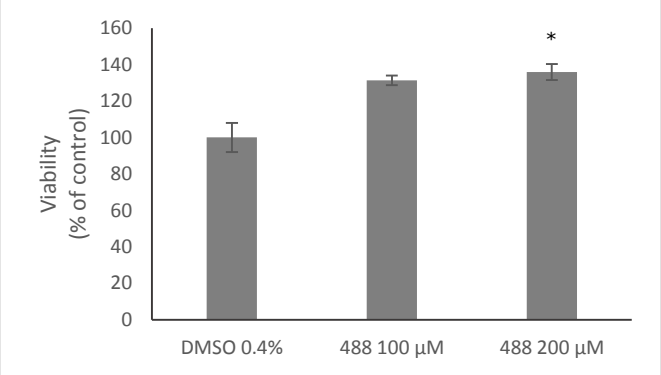

Figure 4.16 PAO1-L biofilms with LB 10% and 488 at 0, 100 and 200 µM after 18 h of incubation at 37°C in Bioflux™ system channels. Error bars represent standard deviation of biological replicates. Statistical significance was calculated with Welch's t tests, (*) represents *p* value < 0.05.

The assay was repeated as for the static evaluation, by employing a fluorescent tagged PAO1-UW (Figure 4.17). However, in this case, 488 showed an important biofilm-promoting effect at 200µM (Figure 4.18), where colonies were less diffused along the fluidic channel but bigger and highly structured.

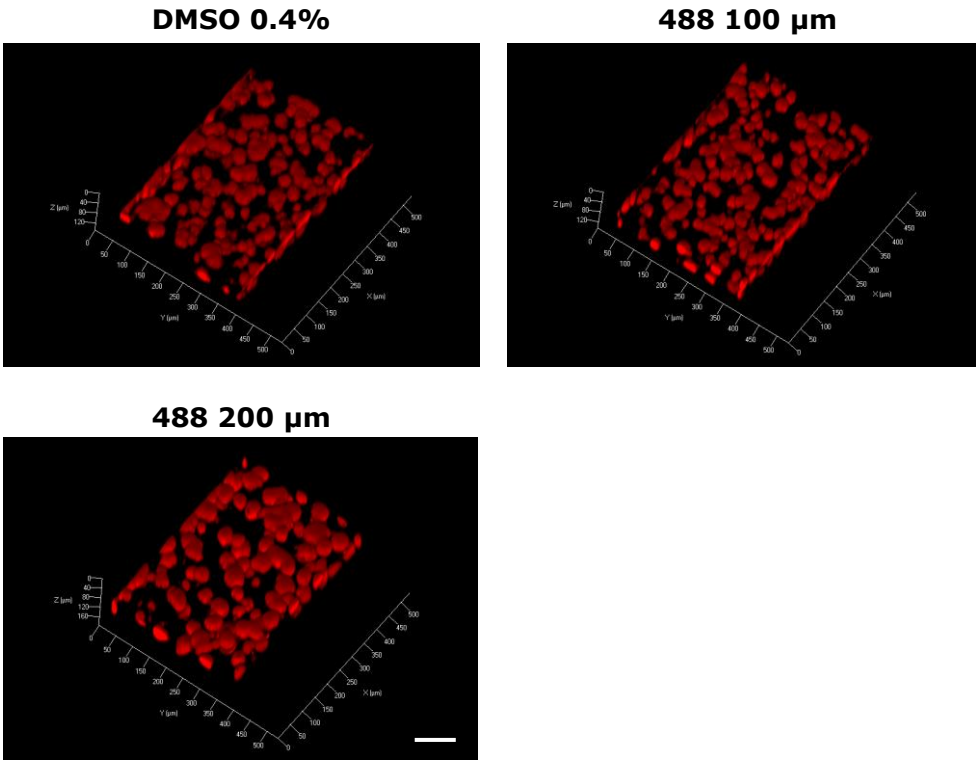

Figure 4.17 PAO1-UW mCherry-tagged biofilms grown in LB 10% and 488 at 0, 100 and 200 µM after 18 h of incubation at 37°C in Bioflux™ system channels. Z-stacks collected with ZEISS LSM 700 confocal microscope, 10X magnification. Scale bar represents 100 µM.

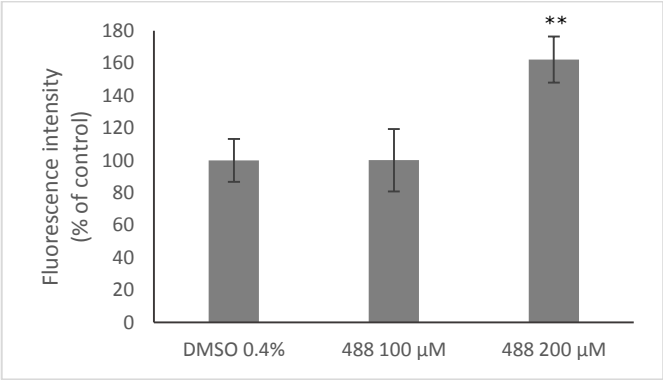

Figure 4.18 PAO1-UW mCherry-tagged biofilms grown in LB 10% and 488 at 0, 100 and 200 µM after 18 h of incubation at 37°C in Bioflux™ system channels Error bars represent standard deviation of biological replicates. Statistical significance was calculated with Welch's t tests, (**) represents *p* value < 0.01.

4.4.2.2 Rotating immersion biofilm

The rotating immersion biofilm is a new method (this laboratory, unpublished) that aims to grow biofilms under laminar flow while exposing the growing biofilm to the maximum possible aeration. The main difference between this approach and the Bioflux microfluidics method is the increased oxygenation and the consequent higher biomass production. Although the increased biofilm production of the laminar flow standardizes the assay, the method only allows one strain at a time and a limited number of glass coverslip substrata. Nevertheless, this technique allowed the testing of 488 in an oxygen-rich system, designed to simulate the biofilm formation in industrial and domestic pipes and other flow exposed environments.

Briefly, biofilms were grown on glass coverslips attached to the wheel, which periodically immersed the samples in the growth medium in presence or absence of 488 200 μM (section 2.2.6.1.3). Some coverslips recovered were stained with syto9 and PI for immediate confocal microscope visualization. The strains PAO1-UW (Figure 4.19) and PAO1-L (Figure 4.20) were assayed and quantified (Figure 4.21, Figure 4.22) with the same procedure.

For both strains, 488-treated biofilms exhibit an increase in biomass of ~20%. However, the higher PI fluorescence from PAO1-UW samples leads to a lower estimated viability.

Other samples collected from the incubation in flow conditions were further assessed for an antibiotic susceptibility test (section 4.5).

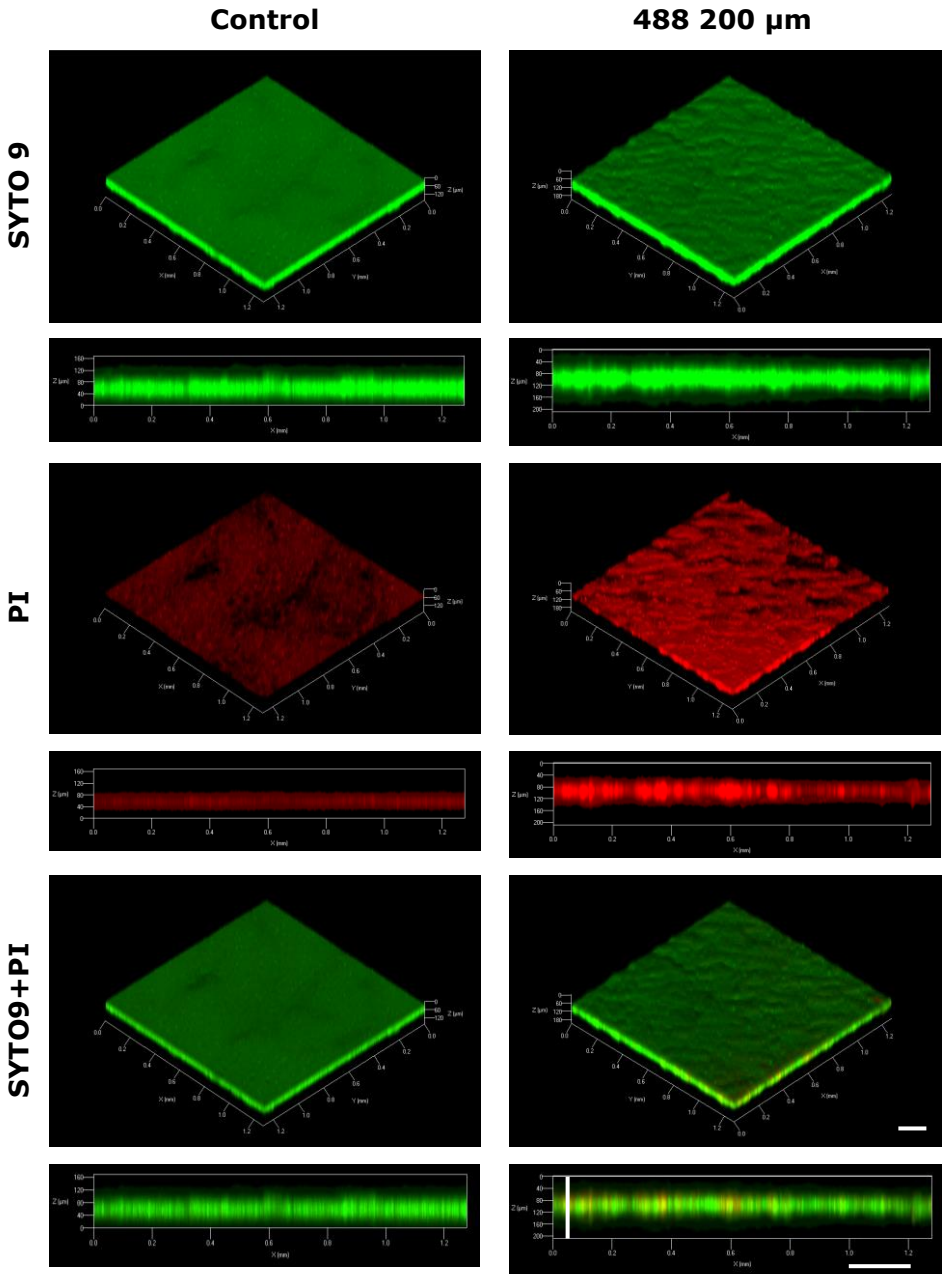

Figure 4.19 Rotating immersion biofilms of PAO1-UW stained with Syto9/PI with and without 200 µM 488. Biofilms were grown per rotating immersion at 30 ºC for 24 h in FAB enriched with 10mM glucose. Z-stacks collected with ZEISS LSM 700 confocal microscope, 5X magnification. Scale bars represent 200 µm.

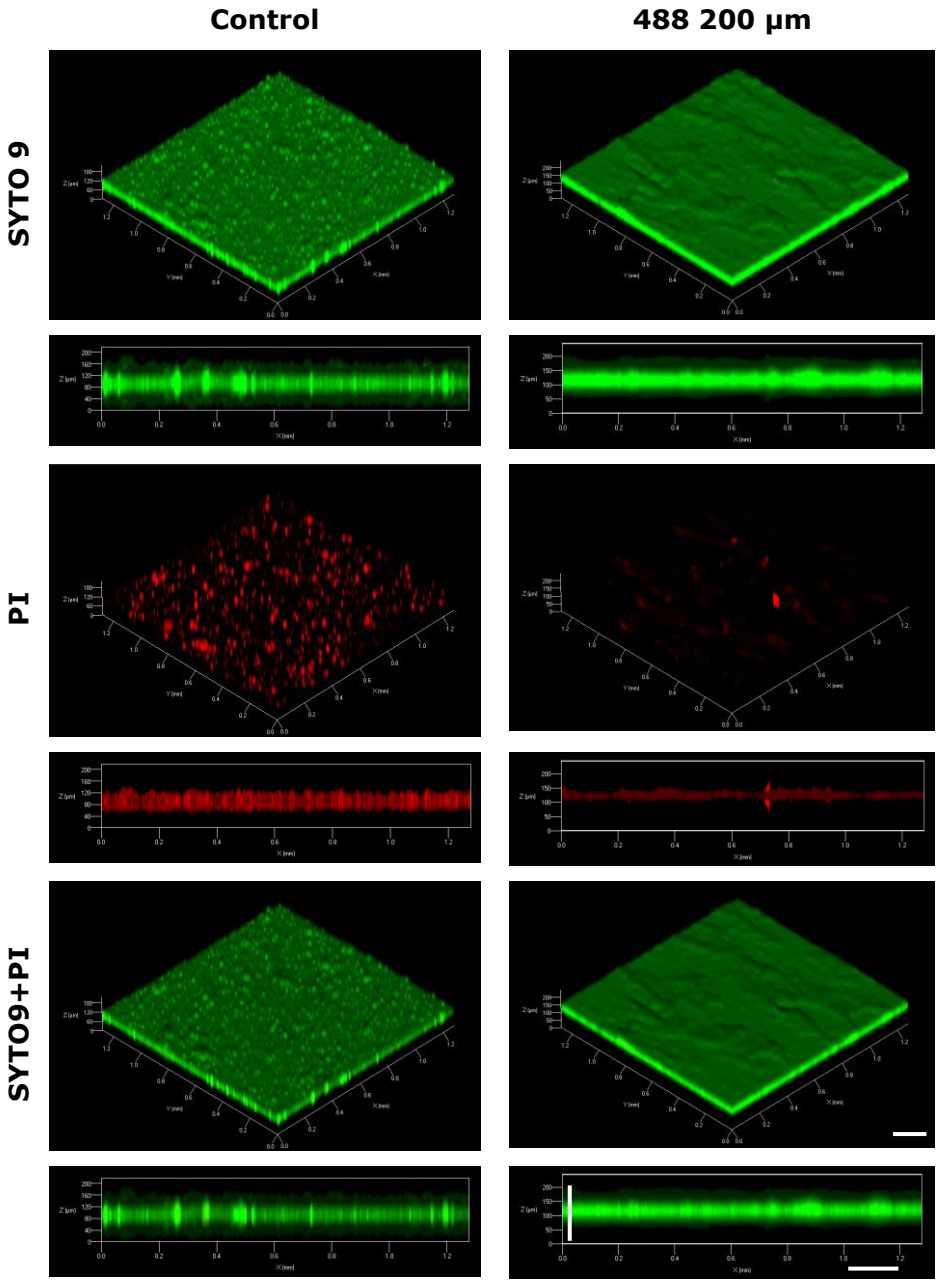

Figure 4.20 Rotating immersion biofilms of PAO1-L stained with Syto9/PI in the presence and absence of 200 µM 488. Biofilms were grown per rotating immersion at 30 ºC for 24 h in FAB enriched with 10mM glucose. Z-stacks collected with ZEISS LSM 700 confocal microscope, 5X magnification. Scale bars represent 200 µm.

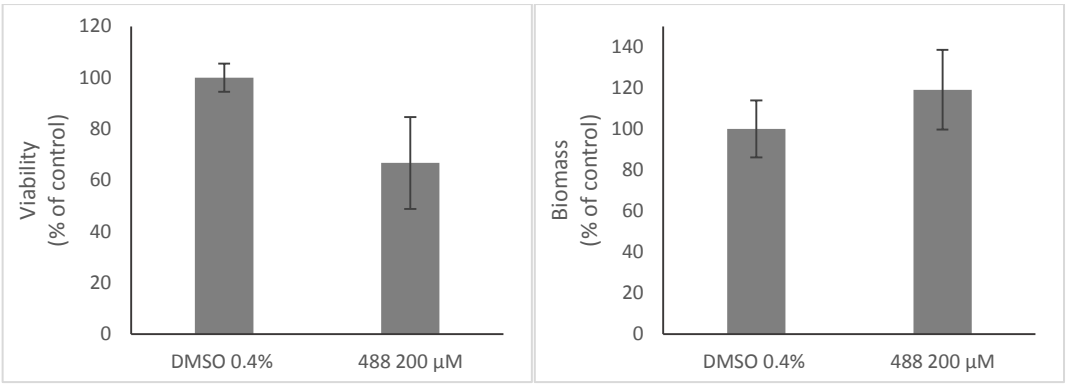

Figure 4.21 Relative quantification of PAO1-UW rotating immersion biofilms stained with Syto9/PI with and without 200 µM 488. In panel on the left, estimated viability. In panel on the right, biomass. Error bars represent standard deviation of technical triplicates.

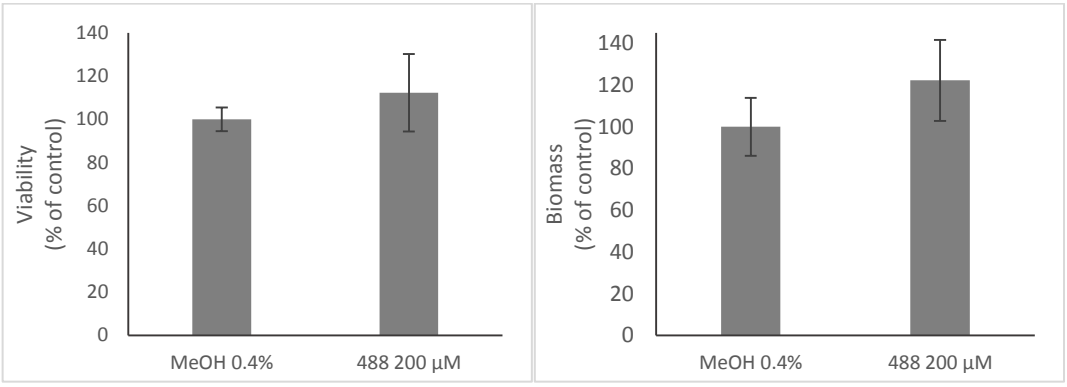

Figure 4.22 Relative quantification of PAO1-L rotating immersion biofilms stained with Syto9/PI in presence and absence of 200 µM 488. In panel on the left, estimated viability. In panel on the right, biomass. Error bars represent standard deviation of technical triplicates.

4.5 Impact of 488 on antibiotic treatment of biofilms

Ciprofloxacin is an antibiotic belonging to the fluoroquinolone class of antibiotics (Acar & Goldstein, 1997) that targets DNA topoisomerases and is effective exclusively on metabolically-active cells. In Walters *et al.* (2003), long exposures to ciprofloxacin demonstrated its ability to penetrate biofilms, although it was not able to affect viability at 3 μM (1 μgmL^{-1} MIC): the study demonstrated that low oxygen availability and the reduced metabolic activity within the biofilm were the major causes of antibiotic tolerance. In the light of its established biofilm penetration, ciprofloxacin was chosen as an antibiotic to be tested with 488 in order to determine whether the lactam could sensitize the biofilms to this antibiotic

Pre-formed PAO1-UW biofilm samples grown without the lactam were collected from the rotating immersion technique. Samples were incubated, to ensure the delivery of compounds, for a further 24 h at 30 °C in 4 petri dishes with FAB medium containing the 488-solvent only (DMSO 0.4%), 488 200 μM, ciprofloxacin 180 μM (60 μgmL^{-1}) and a combination of 488 and antibiotic at the same concentrations. (Figure 4.23).

Ciprofloxacin, employed at this concentration, was able to kill PAO1-UW bacteria and, as a consequence, to reduce the estimated viability by 80% (Figure 4.24) although the biomass quantity remained unaltered (Figure 4.25). Interestingly, 488 increased the biomass in all treated samples, along with the viability ratio, counteracting the antibiotic effect.

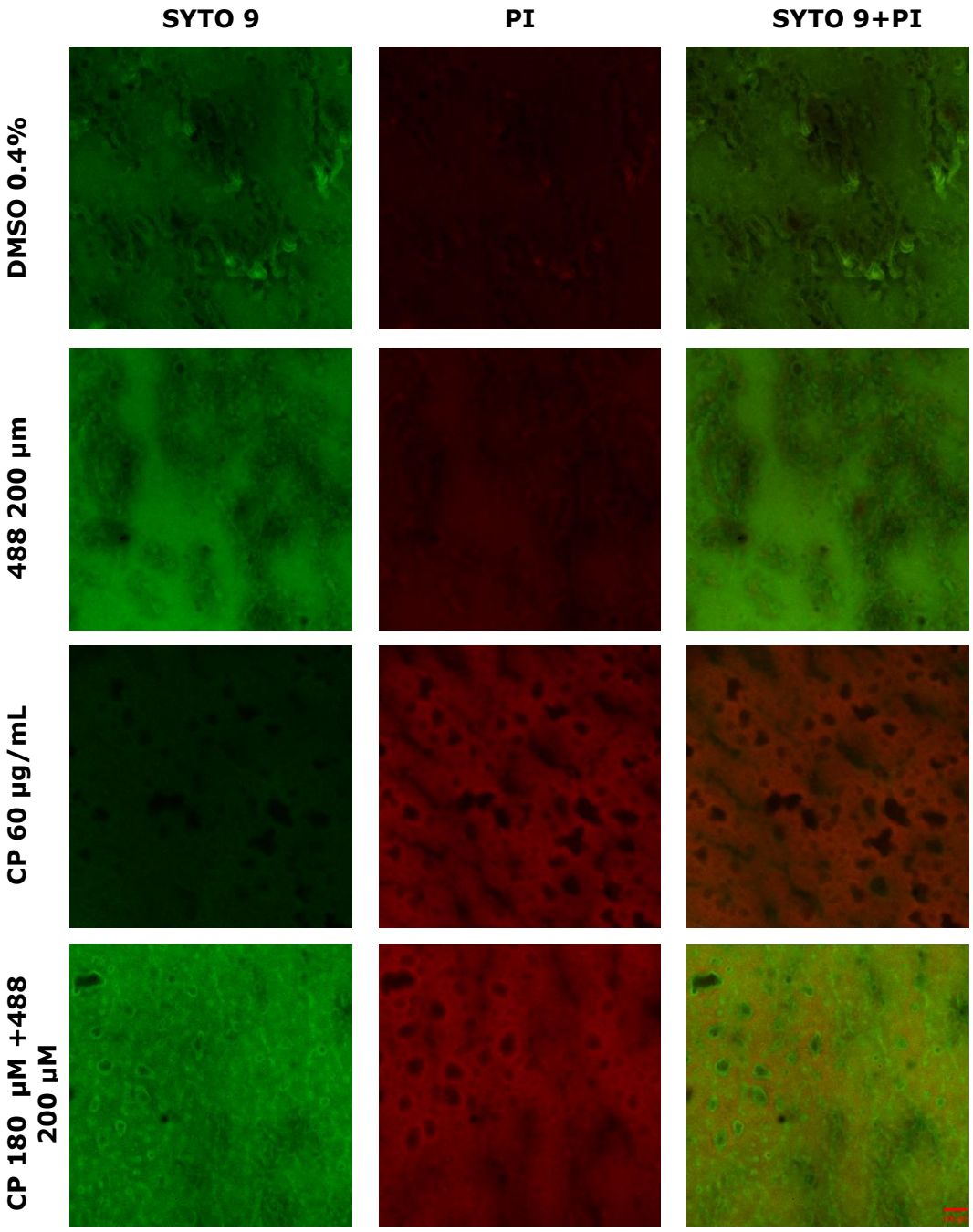

Figure 4.23 PAO1-UW biofilm incubated without or with 488 at 200 µM and without/with ciprofloxacin 180 µM, stained with Syto9-PI. Preformed-biofilms grown per rotating immersion were incubated for 24 h at 30 ºC. Z-stacks collected with ZEISS LSM 700 confocal microscope, 5X magnification. Scale bar represents 100 µm.

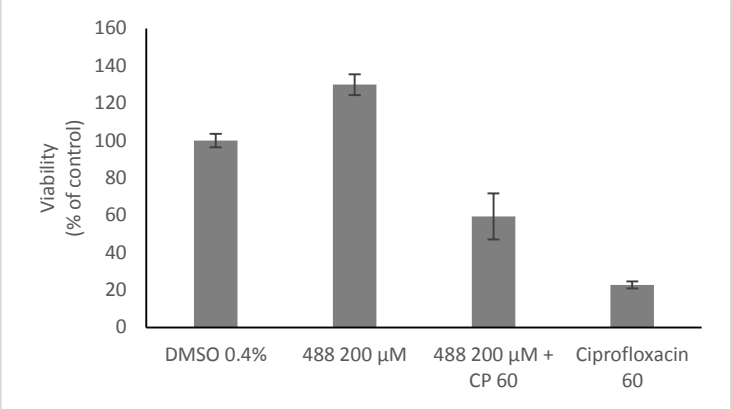

Figure 4.24 Relative quantification of estimated viability (Syto9PI^{-1}) of PAO1-W biofilms incubated without or with 488 at 200 µM and ciprofloxacin 180 µM (60 µg/mL). Error bars represent standard deviation of technical duplicates.

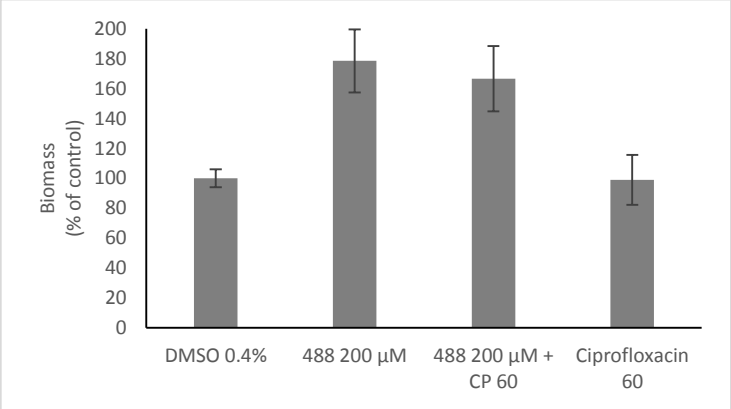

Figure 4.25 Relative quantification of biomass (Syto9+PI) of PAO1-W biofilms incubated without or with 488 at 200 µM and ciprofloxacin 180 µM (60 µg/mL). Error bars represent standard deviation of technical duplicates.

4.6 CONCLUSION

The transcriptome analysis revealed two main modes of actions that 488 could exert on *P. aeruginosa*, QS inhibitor and biofilm promoter. Firstly, the strong inhibition of the *las/rhl/pqs* QS system and related genes confirms the initial hypothesis that 488 acts as both a pqs antagonist and to a lesser extent as a *las* antagonist.

Swarming motility, highly dependent on the production of rhamnolipids as well as flagellar function (Caiazza *et al.*, 2005; Overhage *et al.*, 2008; Overhage *et al.*, 2007; Shrout *et al.*, 2006) was in fact, found affected by the lactam: a reduction in the motility radius was observed in all the samples directly proportional to the concentration of 488 used. However, for swarming motility it was not possible to discriminate between the reduction due to an impact on the rhl system or on flagellar functionality. As shown in Table 4.2, many genes involved in the flagellar biosynthesis (e.g. the *fli* operon, *flgB, flhF*) and motor stator complex (*motC*, *motD*) were found differentially expressed in the transcriptome analysis.

However, from the swimming motility assay, no effect of the lactam was observed. Although pictures acquired with TEM showed a misplaced flagellar origin in cells treated with 488, analogously to *flhF* mutants described by Murray and Kazmierczak (2006) which exhibited a decreased swim velocity in 0.5% w/v agar plates and no change at 0.3 %, the concentration herein used for the swimming assay. It is worth mentioning that other genes were not represented on the RNAseq study. FleQ, for instance, is a transcriptional regulator whose function depends on the intracellular levels of c-di-GMP. At low concentrations of this messenger molecule, FleQ activates flagellar assembly. Conversely, at high levels, c-di-GMP binds FleQ causing its inactivation, therefore leading to reduced motility and the expression of biofilm-related genes (Hickman & Harwood, 2008; Hickman *et al.*, 2005). Although it is reasonable to assume that c-di-GMP production was increased there was no direct evidence of 488 impacting on FleQ.

On the other hand, the expression of many minor type IV pili genes such as *pilI, pilE, pilC and pilY1,* was found to be compromised. Twitching assays, however, exhibited a remarkable phenotype: twitching colonies were bigger and thicker, although slightly reduced in radius when grown with 488 200 μM. At first, these results may appear discordant with the RNAseq data since this motility is commonly associated with type IV pili adhesion and motion properties (Mattick, 2002b; O'Toole & Kolter, 1998a; Wall & Kaiser, 1999); nevertheless, surface adhesion can also be mediated by fimbrial structures such as chaperone usher type pili, encoded by the *cup* gene clusters. For example, *cupA* mutants were unable to attach to abiotic surfaces while the overexpression of Cup pili was associated with increased biomass and surface coverage. For these reasons their function is fundamental for initial establishment of biofilms, regardless of type IV pili action (Pratt & Kolter, 1998; Vallet *et al.*, 2004; Vallet *et al.*, 2001). The large upregulation of the *cupA* cluster (logFC=~3) reported herein could justify the phenotypic behaviour observed in the twitching assays whereas the overexpression of Cup fimbriae might have counteracted the moderate downregulation of the type IV pili (logFC=~1).

The construction and use of a transcriptional reporter PAO1-L pCTX:: P*orn-lux* fusion confirmed the inhibition of the oligoribonuclease Orn, whose gene belongs to the RNA processing orthologous group. Its inhibition is associated with increased levels of c-di-GMP, due to the lack of a functional catabolism and therefore, enhanced biofilms (Cohen *et al.*, 2015; Orr *et al.*, 2015).

Finally, as suggested by the RNAseq data and confirmed though a variety of assays, lactam 488 does not act as a biofilm inhibitor but, conversely, as a biofilm promoter. The efficacy, however, was variable: the biomass observed increased from 20% up to 100% compared to the controls when 200 μM 488 were used, independent of the conditions employed, although more experimental replicates might provide greater statistical robustness. On the other hand, bacterial cell viability overall remained unaffected, although the presence of 488 reduced the action of ciprofloxacin on *P. aeruginosa* biofilms.

Numerous data from the RNAseq were analysed in this chapter and validated with specific assays. Nonetheless, further aspects need to be validated through further gene-specific transcriptional reporters and/or qPCR. Not last, the c-di-GMP involvement must be clarified in order to understand whether it represents a direct or indirect target of 488 action.

5 EFFECT OF 488 ON *S. AUREUS* AND *P. MIRABILIS*

INTRODUCTION

The first two chapters of this thesis focused on elucidation of the mode of action of the Unilever lactams, and specifically 488 on *P. aeruginosa*. Since the effects of the lactams used in the present work had not been determined for other bacterial species, their impact on *Proteus mirabilis* and *Staphylococcus aureus* growth was first investigated. Subsequently, for *P. mirabilis*, swarming motility, urease and biofilm development were examined. To obtain insights into potential 488 targets in *S. aureus*, a transcriptome study was undertaken. This employed the *Staphylococcus aureus* strain ATCC 6538, (NCTC 10799) a standard disinfectant susceptibility testing strain, the genome of which has been sequenced (Markarova *et al*. 2017). Finally, the effect of 488 on a novel multi-species biofilm model incorporating *P. mirabilis S. aureus* and *P. aeruginosa* was determined.

5.1 *PROTEUS MIRABILIS*

5.1.1 488 inhibits the growth of *P. mirabilis*

To determine whether 488 inhibits *P. mirabilis* growth, bacteria were inoculated in a 96 well plate containing LB and 488 serially diluted to generate a concentration range from 0 to 100 µM. The plate was incubated in a TECAN® microplate reader for 24 h and growth monitored as OD over time. Hence, the MIC of 100 µM was determined by turbidity. The results show that the samples treated with 488 do not grow at the same rate as the LB only and solvent (MeOH) 1.6% controls. Lactam 488 had a strong negative impact on growth at both 50 and 100 µM (Figure 5.1).

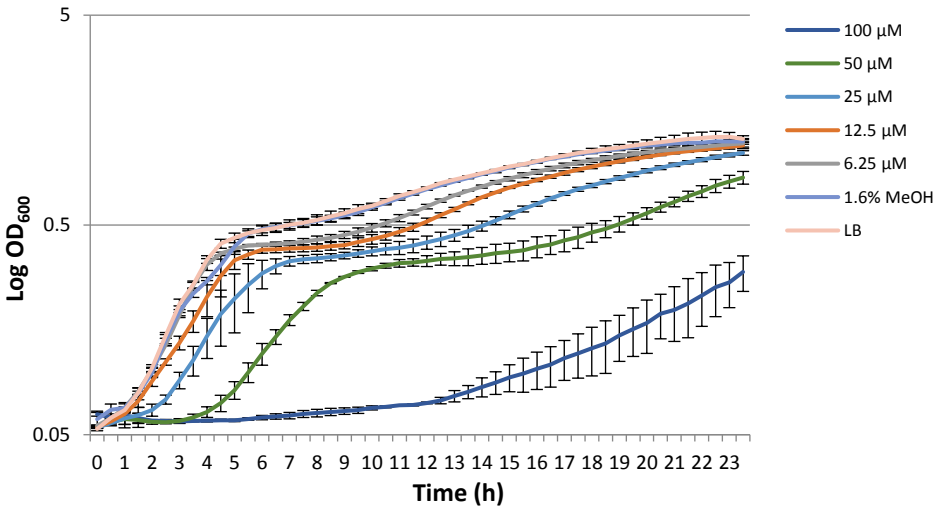

Figure 5.1 Growth curves of *P. Mirabilis* HAUSER 1885 in presence of 488 at 6.25, 12.5, 25, 50 and 100 µM. Error bar represents standard deviation of biological triplicates

5.1.2 Swarming motility

In contrast to the dendritic pattern of *P. aeruginosa, P. mirabilis* produces a swarming pattern known as a 'bull's eye'. This pattern is the result of multiple waves, each representing a population turnover between a motile phase and a consolidation phase. Every wave generates a terrace and thus the characteristic concentric rings (Rauprich et al., 1996). During the swarming phase, *P. mirabilis* cells elongate and increase the number of flagella, before de-differentiating into smaller and with fewer flagella (Copeland & Weibel, 2009; Morgenstein *et al.*, 2010). Figure 5.2 shows that swarming is reduced at 10 µM 488 but completely abolished in the presence of 100 µM. However, the latter is probably a consequence of growth inhibition.

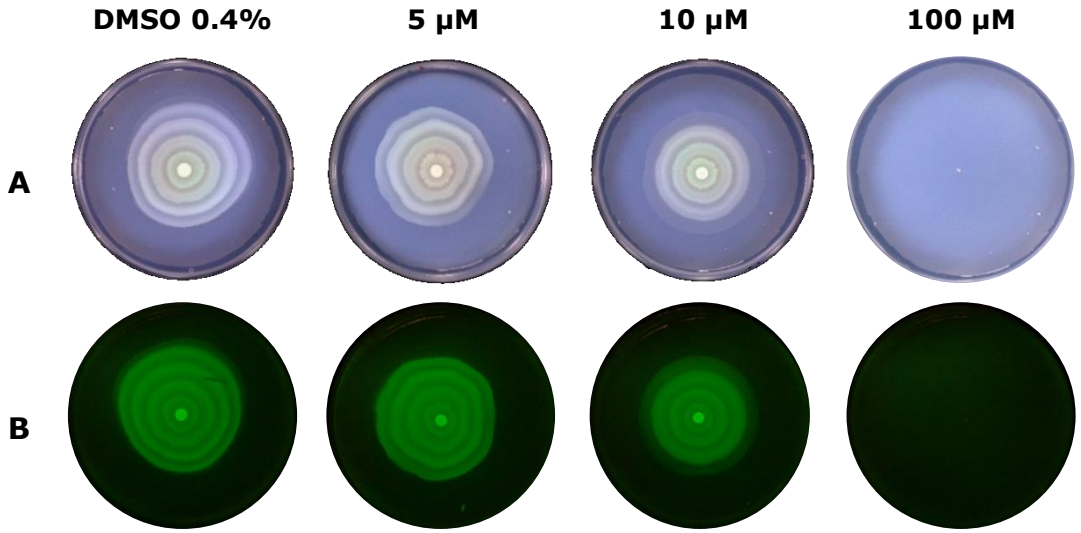

Figure 5.2 Swarming activity of *P. mirabilis HAUSER 1885* GFP-tagged in the presence of 488 at 0, 5, 10 and 100 µM. DMSO only plate was used as control. Each plate is representative of biological triplicates. Row **A**: light visualisation. Row **B**: fluorescence visualisation.

5.1.3 Urease activity

To test the effect of 488 on *P. mirabilis* urease activity, bacteria were spotted onto Christensen's Urea Agar. This medium contains the pH indicator Phenol Red, which turns red in alkaline conditions (pH 8.1). An increase in pH is a consequence of the release of ammonia formed by the action of the urease on urea (Griffith *et al.*, 1976). In Figure 5.3, two out of three biological replicates did not show any variation with 488 at 10 µM, compared with the solvent only control plate (DMSO 0.4 %). At 100 µM, no urease activity was detected probably due to complete growth inhibition.

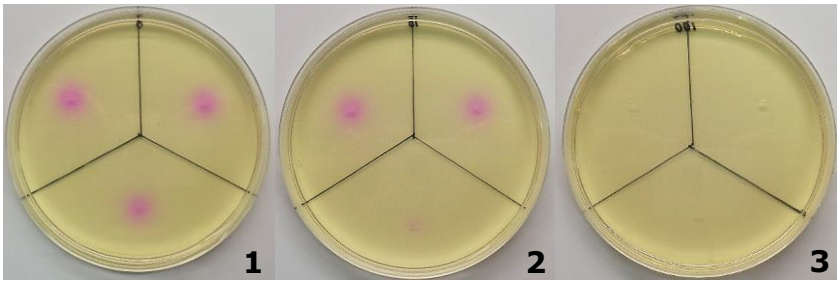

Figure 5.3 Urease activity test plates of *P. mirabilis* HAUSER 1885 without (1) and with 488 at 10 µM (2) and 100 µM (3).

5.1.4 Biofilm formation

P. mirabilis biofilms were cultured in 24 well plates in artificial urine medium (AUM) prepared according to Brooks and Keevil (1997). Although in static conditions, this medium simulates growth on urinary catheters, where *P. mirabilis* induces mineralization and the formation of struvite and apatite crystals that may provide structural support for biofilm development of other species (Griffith *et al.*, 1976; Jacobsen & Shirtliff, 2011; Li *et al.*, 2016). Moreover, biofilms formed in this medium appear as a flat layer containing swarming cells rather than mushroom-like when cultivated in LB (Jones *et al.*, 2007; Li *et al.*, 2016). Calcein 2µM was added to the medium to label mineral deposits and *P. mirabilis* Hauser 1885 DsRed-tagged was employed to avoid fluorescence spectrum overlap with

calcein. The lactam totally inhibit biofilm development at concentrations as low as 10 µM (Figure 5.4 and Figure 5.5).

The presence of biomineralisation but not biomass at 10 and 100 µM indicates the presence of living and metabolically active cells that might not be able to associate in biofilm structured colonies, despite the potential surface support provided by the crystals.

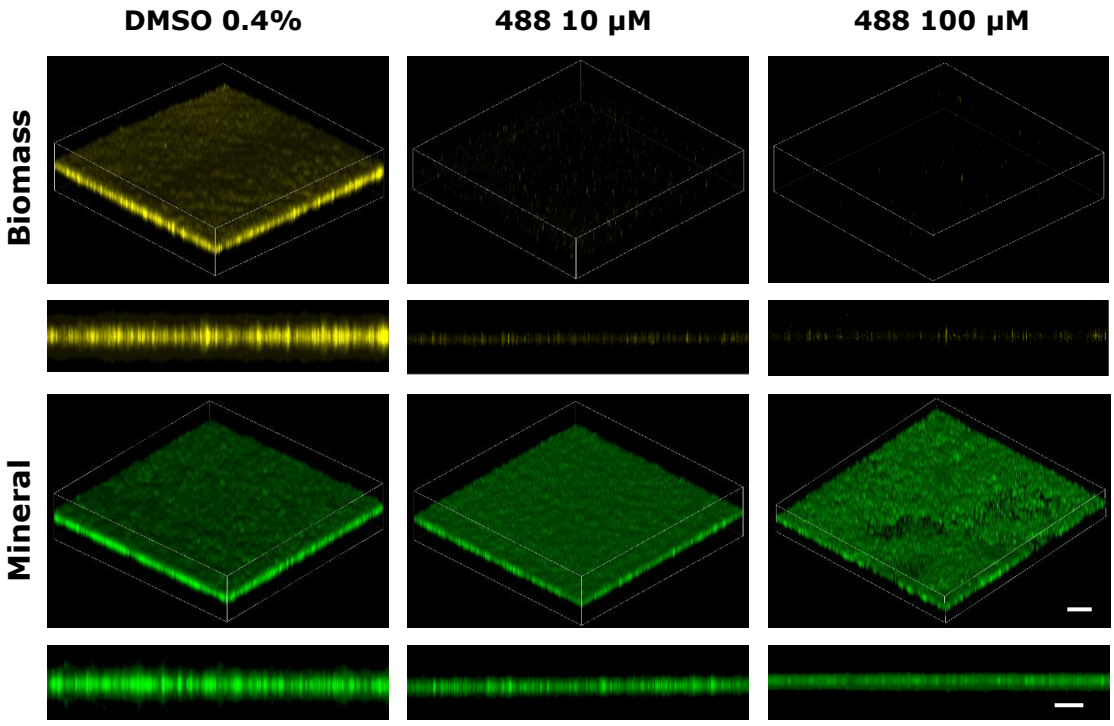

Figure 5.4 *P. mirabilis* Hauser 1885 DsRed-labelled biofilm with 488 10 and 100 µM. Cells were cultured in 24-well plate in artificial urine medium**.** Culture was incubated statically at 37 °C for 2h, and then incubated under gentle shaking for 72h. Bacterial attachment and biomineralisation were observed under a confocal fluorescence microscope. Scale bars represent 50 µm.

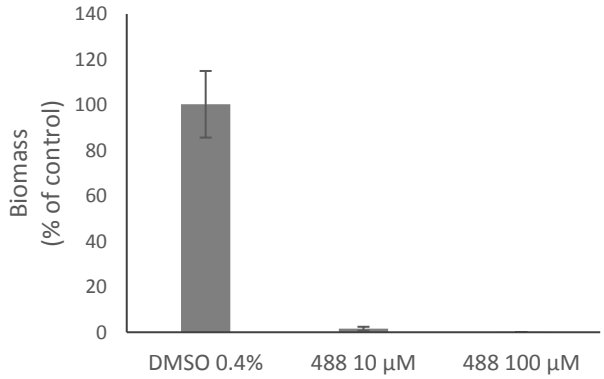

Figure 5.5 Biomass quantification *P. mirabilis* Hauser 1885 biofilm. Error bars represents standard deviation of triplicates**.**

5.2 *STAPHYLOCOCCUS AUREUS*

5.2.1 488 inhibits the growth of *S. aureus*

To study the effect of 488 on *S. aureus* USA300 and ATCC6538, growth experiments were carried out measuring OD from cultures grown in flasks with TSB. The results show that the samples with the lactam grow at a slower rate than the solvent only (DMSO 0.25%) controls (Figure 5.6). An MIC value of 30 µM was obtained after 24 h growth in 96 well plate for *S. aureus* USA300. The MIC for ATCC6538 was 50µM.

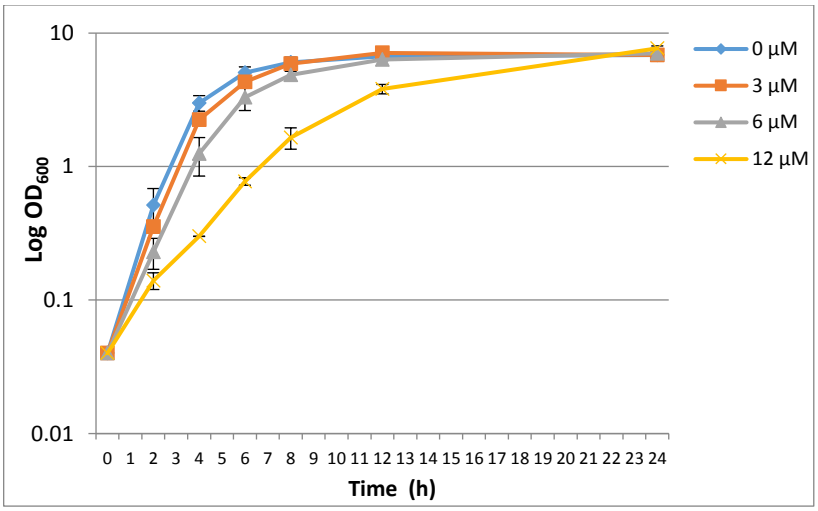

Figure 5.6 Growth of *S. aureus* USA300 in presence of 488 at 0, 3, 6, 12 µM. Error bars represent standard deviation of biological triplicates.

5.2.2 Transcriptomic study of the effects of 488 on *S. aureus* ATCC 6538

As for *P. aeruginosa*, a transcriptomic study (RNAseq) was carried out to identify potential targets for 488 in *S. aureus* USA300 and ATCC6538. To circumvent the negative impact of 488 on *S. aureus* growth, the lactam was spiked into cultures at mid-log phase (after 4.5 h) growth and RNA extraction was performed after 1 h of exposure, as reported in Petek *et al.* (2010) and Jang *et al.* (2008). Initially, RNA was extracted from USA300 LAC due to its high resistance to antibiotics and strong *agr* expression, and hence virulence (Diep *et al.*, 2006; Li *et al.*, 2009). Unfortunately no significant differences were observed, perhaps due to the low concentrations of 488 used (3 and 6 μM). RNA extraction after 488 exposure was repeated for the antimicrobial susceptibility testing strain *S. aureus* Rosenbach ATCC 6538 following exposure to 488 for 1 h at either 15 or 25 μM. This ATCC strain was chosen since it is widely employed by Unilever for antimicrobial susceptibility testing. Although it exhibited a higher tolerance for 488 (MIC 50 μM) compared to USA 300, growth was affected after 1 h of exposure (Figure 5.7). For this reason, the OD of the samples was normalized prior extraction.

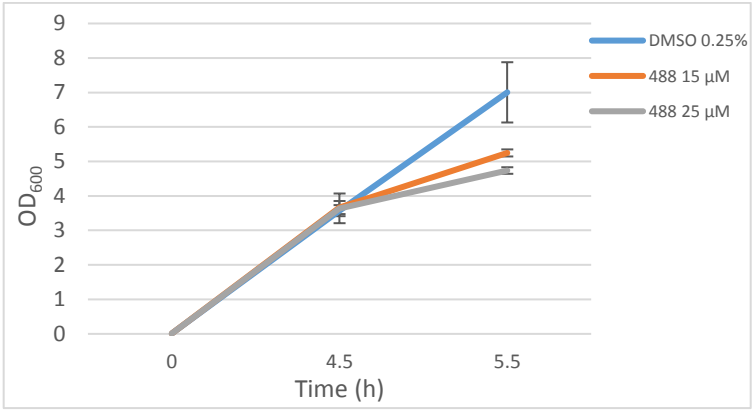

Figure 5.7 Growth of *S. aureus* ATCC 6538 for RNA-seq analysis. 488 was added 4.5 h after inoculation. Error bars represent standard deviation of biological triplicates.

The main transcriptional differences following 488 exposure, at both the concentrations used, are reported in Table 5.1. These genes were selected for their relevance to biofilm formation, or QS, or antimicrobial resistance mechanisms.

The *agr* genes that code for the *S. aureus* AIP QS system, were upregulated (logFC=~2) and conversely, the pyrimidine biosynthetic pathway genes (e.g. *pyrRPBC* operon) were strongly downregulated (logFC=~4). Interestingly, the upregulation of the *agr* system reported is related to biofilm develpment (Beenken *et al.*, 2003; Vuong *et al.*, 2000), as well as in dispersal phase (Boles & Horswill, 2008), analogously to the *pyr* operon induction (Beenken *et al.*, 2004), which, on the contrary, was reported as downregulated.

As shown in Figure 5.8, 488 exerted a strong induction of the tricarboxylic acid cycle (TCA). Following such upregulation, especially of *fumC sdhA* and *sdhB,* an increase in the levels of the fibronectin-binding proteins FnbpA/B should occur, as described for methillicin-resistant *S. aureus* USA 300 by De Backer *et al.* (2018). However, no changes were herein reported for genes *fnbA* and *fnbB*. De Backer *et al.* (2018) also describes a relationship between an *argH* deletion and a significant decrease of the ability to form biofilms; this gene, involved in the urea cycle, is 2-fold downregulated in the presence of 488 at 25 µM. De Backer *et al.* (2018) also report increased expression of the *sarA* gene in TCA and urea cycle transposon mutants. Moreover this gene is associated with reduced biofilm formation (Beenken *et al.*, 2003; Valle *et al.*, 2003). However *sarA* expression was not significantly affected by 488.

The polysaccharide intercellular adhesin PIA or poly-*N*-acetylglucosamine (PNAG), present in the extracellular matrix of *S. aureus* biofilms is dependent on the *icaADBC* operon (Heilmann *et al.*, 1996; Maira-Litrán *et al.*, 2002) which is downregulated (*icaC* logFC=-0.93) in response to 488. The MSCRAMM adhesins (microbial surface components recognizing adhesive matrix molecules), involved in the attachment phase of biofilm development, were here found to be heterogeneously regulated: for instance, with 488 at 15µM, the *clfA* gene, encoding for the important

virulence protein clumping factor A (Josefsson *et al.*, 2001; Moreillon *et al.*, 1995), was almost 3-fold upregulated whilst *clfB was* 3-fold downregulated.

In *S. aureus* biofilms, the extracellular DNA, released by cell lysis and genomic DNA release, is dependent on holin cidA/antiholin irgA regulation (Mann *et al.*, 2009; Rice *et al.*, 2007) and on the activity of autolysins such as *atl* (Houston *et al.*, 2011; Mann *et al.*, 2009). Autolysin genes were found downregulated, particularly *atl_3* (LogFC=-1.5) similarly, the holin encoding gene *cidA* levels with 488 at 25μM were 4 times lower than the control.

Several other genes that encode cell-wall proteins have mixed responses to 488. The collagen adhesin encoding gene *cna*, influenced by the *sarA* and *agr* system (Blevins *et al.*, 1999) was 2-fold upregulated. The level of *isdA*, a surface protein involved in colonization and virulence, was unaltered.

Finally, two metallo-beta-lactamase related genes were 4-fold overexpressed and the azoreductase gene azoR was found strongly upregulated, as also reported in the *P. aeruginosa* transcriptome analysis of this work (Table 4.2).This study reports a first evaluation of the RNA-seq data generated and no validation was carried out at present date.

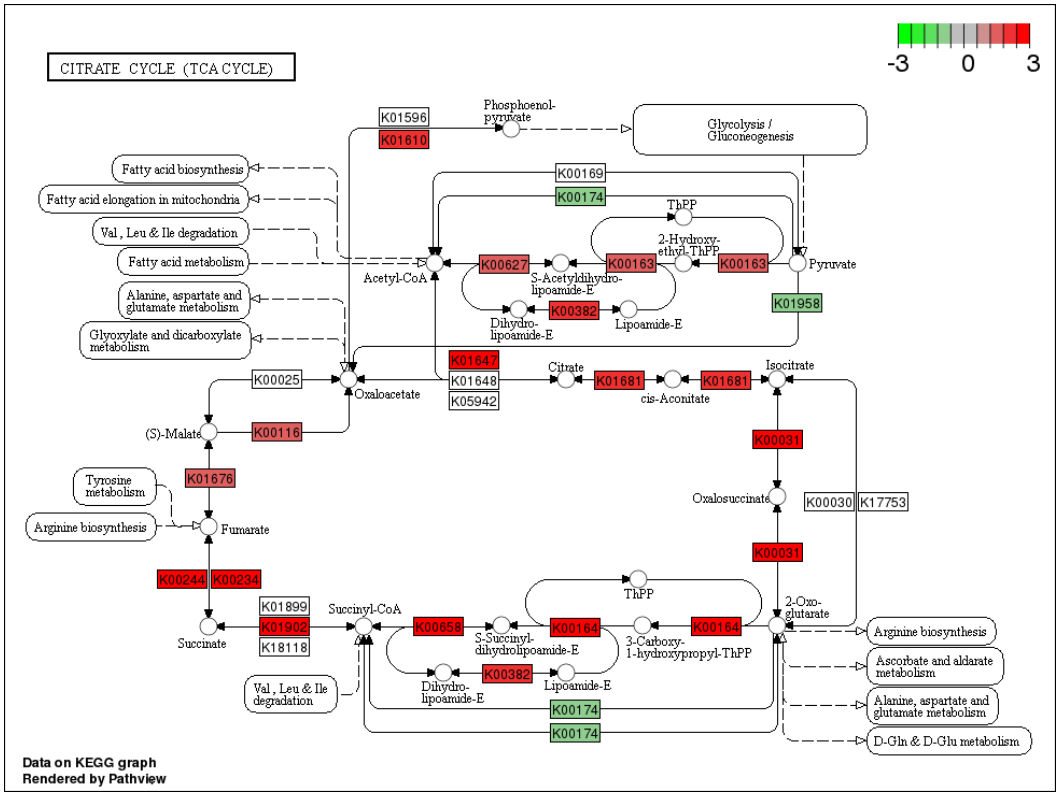

Figure 5.8 KEGG pathway showing the effect of 488 on the transcription of TCA cycle genes. The insert on the top right represents the differential expression (Ln_2FC) of *S. aureus* genes following treatment with 488 at 25 μM using a color scale from -3 (green) to +3 (red).

Table 5.1 Examples of differentially regulated genes (log_2 fold change values (logFC)) from comparisons of *S. aureus* cultures treated with 488 (15µM and 25µM) compared with a solvent control (DMSO 0.25%). *P* values for all samples <0.03.

Gene	logFC. 488 15µM vs 0	logFC. 488 25µM vs 0	Function/protein
agrA	1.09	2.39	Accessory gene regulator protein A
agrB	0.85	2.30	Accessory gene regulator protein B
agrC	1.04	2.42	Regulator protein agrC
agrD	0.80	1.87	Regulator protein agrD
pyrE	0.58	1.73	Orotate phosphoribosyltransferase
pyrH	-1.59	-1.8	Uridylate kinase
pyrC	-4.67	-4.02	Dihydroorotase
pyrD	-1.62	-4.64	Dihydroorotase
pyrR	-0.18	-5.16	Pyrimidine operon repressor chain A
pyrB	-3.92	-5.45	Aspartate transcarbamoylase chain A
pyrP	-1.69	-6.09	Uracil permease
ftsI_2	-0.13	-0.55	Penicillin-binding protein
NCTC10788_01961	1.49	2.32	Metallo-beta-lactamase
NCTC10788_01639	0.93	2.04	Metallo-beta-lactamase
NCTC10788_01181	1.1	0.84	Metallo-beta-lactamase
ytnP	0.6	0.67	Metallo-beta-lactamase
sarA	-0.64	-0.57	Staphylococcal accessory regulator A
icaC	-0.64	-0.93	intercellular adhesion protein icaC
fnbA	-0.66	-0.39	Fibronectin-binding protein A
fnbB	-0.3	-0.28	Fibronectin binding protein FnbB
argH	-1.9	-0.95	Argininosuccinate lyase
fumC	0.49	1.56	Fumarate hydratase class II
sdhA_1	1.07	2.37	Fumarate reductase flavoprotein subunit
sdhA_2	0.65	1.26	Serine dehydratase alpha chain
sdhB	0.89	1.41	L-serine dehydratase
atl_3	-0.59	-1.5	Autolysin E
atl_2	-0.38	-0.89	peptidoglycan endo-beta-N-acetylglucosaminidase
atl_1	-0.26	0.75	Autolysin
cidA	-0.43	-1.94	Holin-like protein CidA
sdrD	0.40	0.83	MSCRAMMClf-Sdr
sdrE	-0.47	-0.82	MSCRAMMClf-Sdr
sdrC	-0.97	-0.95	MSCRAMMClf-Sdr
clfA	1.41	2.39	MSCRAMMClf-Sdr
clfB	-1.40	-0.82	MSCRAMMClf-Sdr
isdA_1	-0.08	-0.58	NEAT - iron-regulated cell wall-anchored protein
isdA_2	0.003	-0.74	NEAT - iron-regulated heme-iron binding protein
isdH (Cna)	0.43	0.97	cell wall surface anchor family protein
azoR	3.36	3.04	Azoreductase

5.2.3 Effect of 488 on *S. aureus* biofilm formation

Changes in biofilm biomass of an eGFP-tagged *S. aureus* SH100 were assessed by employing a 24-well plate containing increasing concentrations of 488, from 0 to 25 μM (Figure 5.9). The z-stacks of the fluorescence output acquired by confocal laser scanning microscopy, were used to quantify changes in biomass (Figure 5.10). After visualisation, OD_{600} was measured to quantify the degree of growth inhibition (Figure 5.11). 488 exerted a small inhibitory effect on biofilm formation with a progressive reduction in biomass.

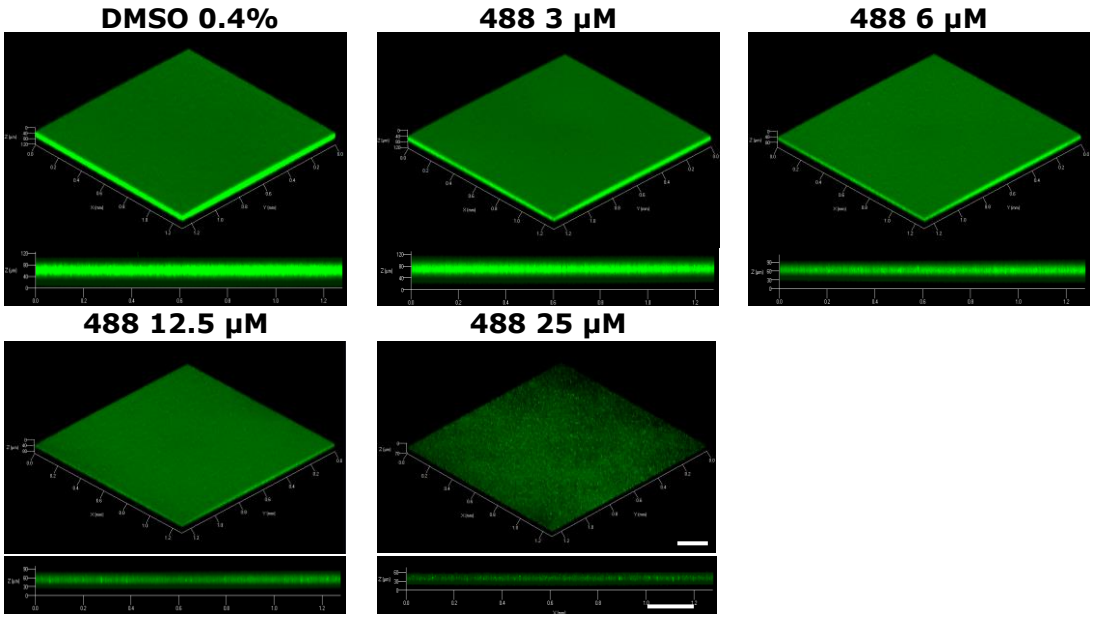

Figure 5.9 Effect of 488 on biofilm formation by *S. aureus* SH1000 tagged with eGFP in the presence and absence of 0, to 25 μM 488. Biofilms were grown statically at 37 ºC for 18 h in 10% BHI. OD_{600} was measured to assess the extent of growth inhibition (Figure 5.11). Scale bars represent 200 μm.

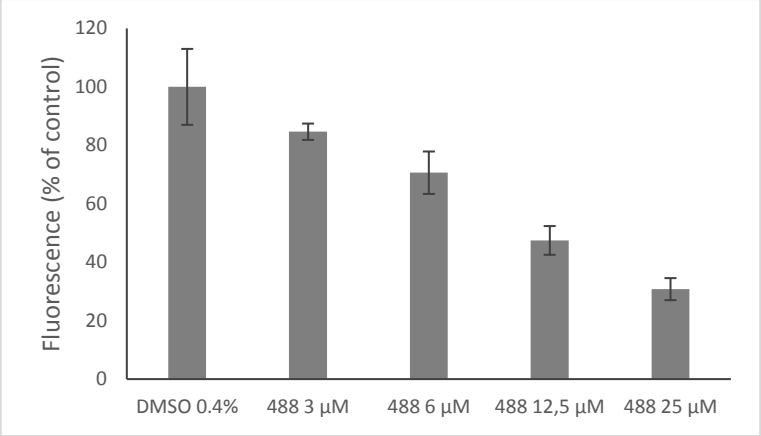

Figure 5.10 Quantification of biofilm biomass of *S. aureus* SH1000 tagged with eGFP in the presence and absence of 488 at 0-25 µM. Normalized for solvent control (DMSO 0.4%). Error bars represent standard deviation of triplicates

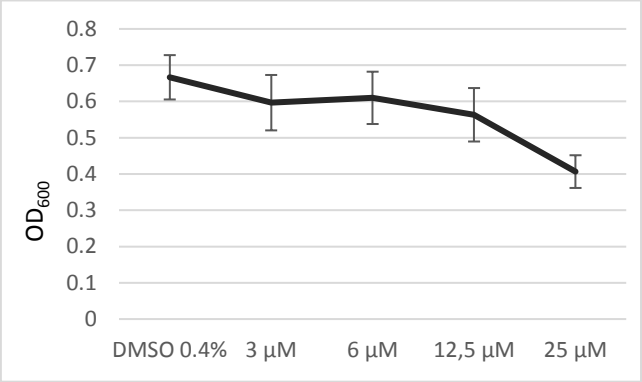

Figure 5.11 Growth of eGFP-tagged *S. aureus* SH1000 biofilms in the presence and absence of 488 at 0-25 µM. Error bars represent standard deviations of triplicates.

5.3 Effect of 488 on Multi-species biofilm formation

Due to the diverse effects of 488 on the bacterial species studied in this project, a multi-species model developed in this lab but as yet unpublished was used to study the interactions among *P. aeruginosa*, *P. mirabilis* and *S. aureus* in presence of 488. In the literature the interactions of *P. aeruginosa* with *S. aureus* and *P. mirabilis* have been widely reported in different *in vitro* models although at present no work on the three species grown in artificial urine medium (AUM) has been published. This model is an adaptation of the method of Li *et al.* (2016) where *P. mirabilis* and *P. aeruginosa* were sequentially co-cultured in AUM. Here, each species was grown for 24 h in sequential order, (1st *P. mirabilis* HAUSER 1885 DsRed-tagged, 2nd *P. aeruginosa* PAO1-UW mTurquoise-tagged, and 3rd *S. aureus* SH1000 eGFP-tagged) in presence and absence of 488 at different concentrations (12.5, 25 and 50 μM) for a total incubation time of 72 h. The medium containing the lactam was changed at the time of the new inoculum i.e. every 24 h.

Figure 5.12 shows the 3D representations of the biofilms together with the transverse sections while Figure 5.13 presents the quantification of the fluorescence output normalised against the control samples for each species. As previously observed in the single species biofilm assay (section 5.1.4) *P. mirabilis* is adversely affected by the lactam, even at the lowest concentration tested (12.5 μM), although biomineralisation still occurs as shown clearly in the bright field panel and, as dark spots, in the other fluorescence channels as shown in Figure 5.14. However, the crystals observed were larger and more sporadic with increasing concentrations of compound and were characteristically surrounded by a higher density of bacteria, particularly *P. mirabilis* and *P. aeruginosa* (Figure 5.12 and Figure 5.14), presumably due to the structural support provided (Jones *et al.*, 2007; Li *et al.*, 2016). Furthermore, increased biomineralisation increases *P. mirabilis* biomass over *P. aeruginosa* in co-cultured biofilms (Li *et al.*, 2016). The biomass of *P. aeruginosa* did not exhibit any variation in presence of 488 at 12.5 μM and 25 μM but increased by ~25 % at 50 μM,

either due to the lactam action, or the lack of competition from *P. mirabilis* in a less mineralised environment, or both. Similarly, *S. aureus* biomass showed a 15% reduction in biomass at the two lower concentrations but not at 50 μM.

Figure 5.12 shows that each species formed a flat biofilm whose stratification resulted in a multi-layered structure presenting a consistent pattern: *P. aeruginosa* was located within the lower levels of the biofilm underneath *P. mirabilis* as described in Li *et al.* (2016) for a dual species biofilm, while *S. aureus* biofilm developed on the surface, as a covering layer (Fig. 5.12).

Interestingly, 488 at 50 μM was not sufficient to inhibit either *S. aureus* growth or biofilm development. Perhaps, this behaviour could be ascribed to the presence of *P. aeruginosa*, which was reported to be able to select for resistant *S. aureus* sub-populations (SCVs) (Mitchell *et al.*, 2010) and to increase *S. aureus* attachment by enhancing production of several adhesins and extracellular matrix binding proteins (Kumar & Ting, 2015a). Alternatively, the exopolysaccharide components of the *P. aeruginosa* biofilm may have provided the foundation for *S. aureus* biofilm development (DeLeon *et al.*, 2014b; Hotterbeekx *et al.*, 2017; Tognon *et al.*, 2019).

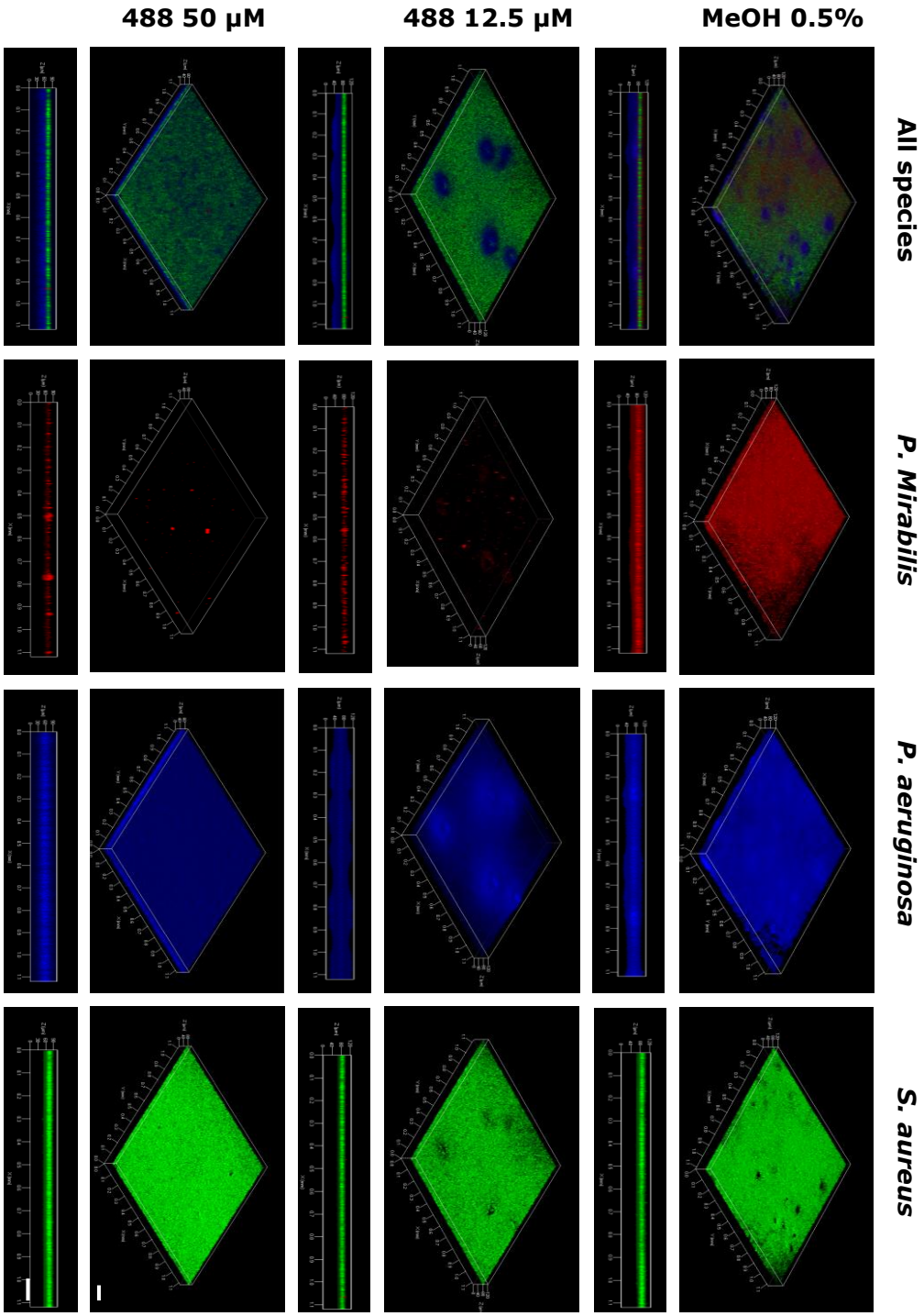

Figure 5.12 Multi-species biofilms formed with *P. mirabilis* HAUSER 1885 DsRed-tagged, *P. aeruginosa* PAO1-UW mTurquoise-tagged, and *S. aureus* SH1000 eGFP-tagged in presence and absence of 12.5 and 50 µM 488. Z-stacks collected with ZEISS LSM 700 confocal microscope, 10X magnification. Scale bars represent 100 µm.

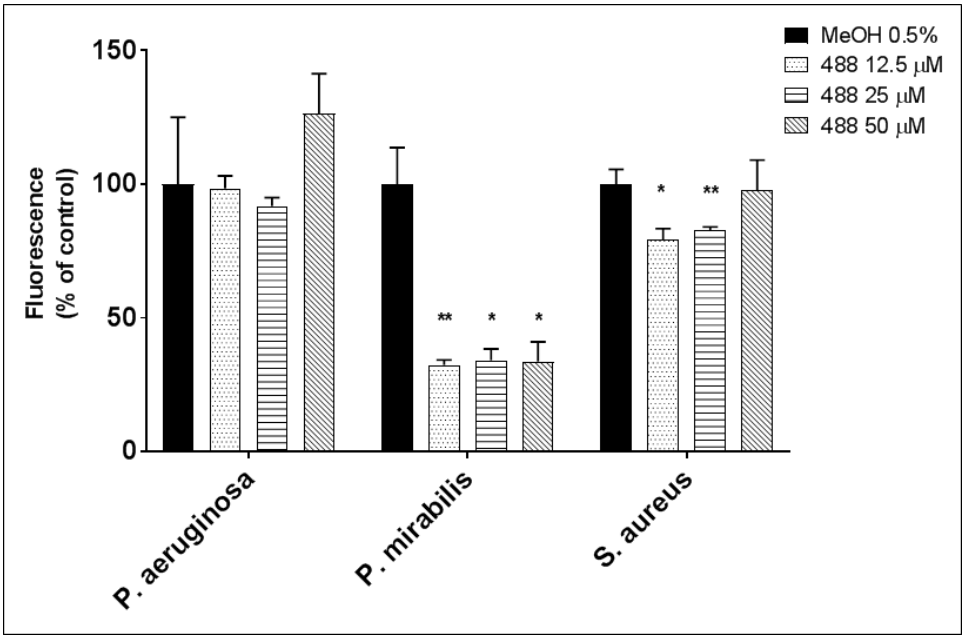

Figure 5.13 Quantification of fluorescence of multi-species biofilms with *P. mirabilis* HAUSER 1885 DsRed-tagged, *P. aeruginosa* PAO1-UW mTurquoise-tagged, and *S. aureus* SH1000 eGFP-tagged in the presence and absence of 12.5, 25 and 50 μM 488. Quantification was performed with ImageJ. Data were normalized on the solvent treated control (MeOH v/v 0.5%). Error bars represent standard deviation of biological triplicates. For each strain, statistical significance was calculated with Welch's t tests between treated samples and control samples. (*) indicates a p value < 0.05. (**) p value < 0.01

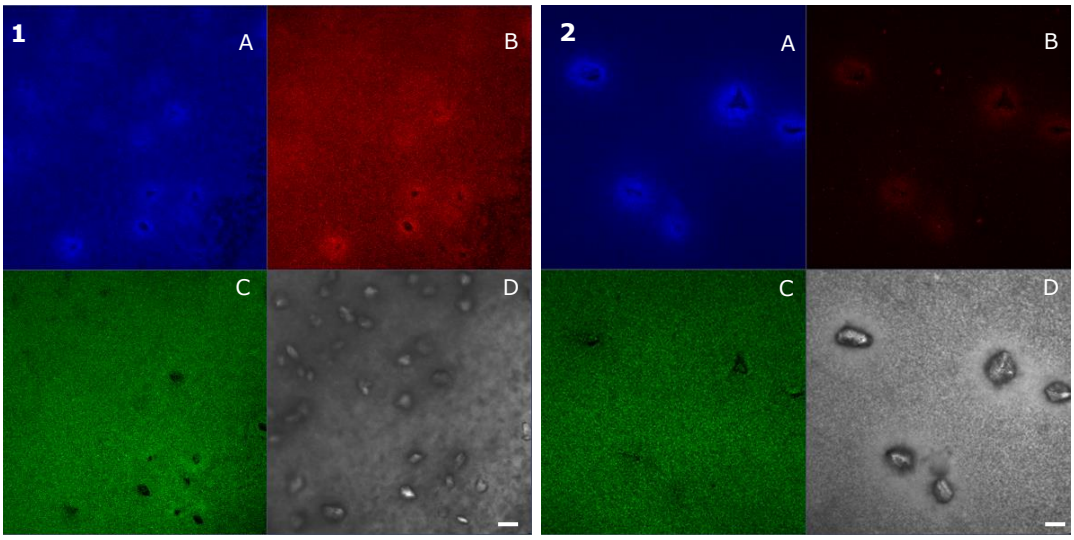

Figure 5.14 2D representations of the multispecies biofilm viewed as individual fluorescence channels and grown in the absence (1) and presence (2) of 488 at 12.5 μM. Images collected with ZEISS LSM 700 confocal microscope, 10X magnification. In panel **A** *P. aeruginosa* PAO1-UW mTurquoise-tagged. In panel **B** *P.mirabilis* HAUSER 1885 DsRed-tagged. In panel **C** *S. aureus* SH1000 eGFP-tagged. In panel **D** bright field. Scale bars represent 100 μm.

5.4 CONCLUSION

Lactam 488 showed relatively strong antimicrobial activity against planktonic *P. mirabilis* and *S. aureus*, with MICs respectively of 100 μM for the former and 30 μM and 50 μM for strains USA 300 and ATCC 6538, respectively. Because of this, the lactam was employed at lower concentrations for the experiments involving these species.

A swarming motility assay was performed for *P. mirabilis*; whereas this phenotype was negatively affected by the presence of 488 in *P. aeruginosa*, a modest impact was observed. Moreover, urease activity remained intact as shown by a pH-indicator test. This enzyme activity is clinically relevant since it is correlated to crystal formation and encrustation and blockage of urinary catheters in the case of *P. mirabilis* infection (Jacobsen & Shirtliff, 2011; Stickler *et al.*, 1993; Wilks *et al.*, 2015). The integrity of the biomineralisation process was confirmed during the visualisation with a confocal microscope where a strong biofilm inhibition activity was observed at relatively low concentrations (10 μM).

Regarding *S. aureus,* a transcriptome analysis was conducted on samples incubated for 1 h with 488. A first attempt with the strain USA 300 and lower concentrations of compound (to avoid growth inhibition) did not reveal significant changes, therefore the RNA extraction was repeated employing higher concentrations and strain ATCC 6538. Albeit preliminary, the analysis of differential changes revealed a multi-faceted mode of action that will require further clarification and validation. The QS and TCA cycle genes were found upregulated whilst pyrimidine synthetic pathway, autolysins and PIA were downregulated. Mixed responses were found for cell wall adhesin and MSCRAMM encoding genes. Biofilms were affected by 488 at relatively low micromolar concentrations, however this might be ascribed to a general growth reduction.

The antibiofilm activity of lactam 488 was also assessed in a mixed-species experiment involving three species. As in single species biofilms, *P. mirabilis* was significantly affected without undermining the mineralisation process at low concentrations. Conversely, the second strain incubated, *P.*

aeruginosa, established a thicker biofilm with 488 at 50 μM which might have acted as a support for *S. aureus* formation. Indeed, *S. aureus* biofilm biomass was reduced with 488 at 12.5 and 25 μM but it was restored to control-like levels at 50 μM. Nevertheless, in the presence of *P. aeruginosa*, *S. aureus* resisted to 488 action at, previously observed, effective concentrations.

6 DISCUSSION AND FUTURE WORK

This work began with the aim of elucidating the mode of action of a series of lactam compounds, representative of a new antibiofilm technology developed by Unilever. The first results obtained using *P. aeruginosa* as the target organism directed the investigation towards QS inhibition. Lactams such as 488 in particular, reduced the expression of the AQ-mediated QS system. Further experiments were thus carried out in this context, uncovering some of the phenotypic consequences of inhibiting AQ-dependent QS. Pyocyanin production, an important virulent factor, was significantly decreased in the presence of 488. Interestingly, the AQ levels were not reduced and the response to 488 was variable and strain dependent. This heterogeneity requires further investigation as the lactam appears to exert strain-specific effects on *P. aeruginosa* that may be related to efflux pump expression.

A competition assay between 488 and 7Cl-PQS, a potent agonist for the PQS system transcriptional regulator, PqsR generated a non-competitive binding curve. An *in silico* study provided the initial theoretical support for an interaction between 488 and PqsR. The study highlighted the importance of the H-bonding between the Leucine 197 and the carbonyl group in position 2 of the pyrrolone ring and, especially, the interaction between the chlorine at position 4 of the 488 phenyl ring and Threonine 265. Ilangovan *et al.* (2013) describes how the Threonine 265 might play a role in conformational modifications of the receptor, preventing the protein from assuming the active conformation for transcriptional regulation. In addition the H-bond between Leucine 197 and carbonyl group in position 2 of 488 enhances binding within the site. These elements are crucial for the antagonistic mechanism of the compound. These data suggested new potential ligands which were obtained from the Unilever lactam compound library. Among these, 295 showed sufficient inhibitory activity that could be usefully exploited for further testing. The antagonistic interaction between 488 and PqsR was demonstrated by expressing and purifying the ligand binding domain of PqsR which facilitated the application of different techniques to study binding. Iso-thermal calorimetry confirmed

that 488 bound strongly to PqsR. Further confirmation was obtained from synchrotron radiation circular dichroism spectroscopy experiments. Finally, diffracting crystals of $PqsR^{CBD}$ soaked in a solution saturated with 488 subjected to X-ray diffractometry revealed the lactam within the pocket B of the PqsR ligand binding site as to that obtained by *in silico* docking. The RNA-seq revealed a more faceted and complex mode of action of 488 on *P. aeruginosa.* The quorum sensing genes including the *pqs* system genes were confirmed to be among the most downregulated. Several motility genes were also downregulated but surprisingly many genes involved in biofilm development were strongly upregulated. Indeed, the swarming of *P. aeruginosa* was reduced in presence of the 488 lactam and flagellar functionality may be compromised by the possible mis-location of the flagellum.

A swimming motility assay a Δ*flhF* mutant as control with a higher concentration of agar might be sufficient to highlight the variation, as reported in Murray and Kazmierczak (2006). Besides, individual cell tracking techniques could be performed to investigate the impact of 488 on flagellar dependent motility.

As anticipated from the RNA-seq, due to overexpression of *cup*, *pel* and alginate biosynthesis genes, enhanced biofilm development was observed in several assays employing different strains, media and environmental conditions. It is clear that this aspect requires further investigation: first, a more standardized set of assays is required to determine whether this effect is enhanced or reduced in specific conditions. Secondly, the levels of cyclic-di-GMP need to be quantified, for instance by using a *pCdrA::gfp* reporter fusion (Rybtke *et al.*, 2012). However, its theoretically high levels were supported by greater biofilm formation and by the inhibition of *orn* expression as a consequence of the action 488 on the catabolism of c-di-GMP breakdown products. Finally, additional reporter gene fusion assays, qPCR and phenotypic assays are required to validate the interesting results emerging from the transcriptome analysis.

The lead lactam proved to be extremely effective in preventing *P. mirabilis* biofilm development, a crucial CAUTI pathogen, although its mechanism of

action requires deeper investigation. In *S. aureus* the targets of 488 may emerge from closer analysis and validation of the RNA-seq data. At the author's knowledge, no furanones or pyrrolones have been described with antibiotic or antibiofilm properties towards *P. mirabilis* and *S. aureus.*

The mixed-species biofilm experiments undertaken highlight the potential roles of individual species in protecting other species from antibacterial agents.

In the literature, furanones and the derived lactams have already been described as QS inhibitors, specifically LasR antagonists through *in silico* studies (Goh *et al.*, 2015; Yates *et al.*, 2002) although no direct binding has been demonstrated experimentally between any of the compounds and a *P. aeruginosa* QS receptor. The work presented here not only uncovers PqsR as a novel target for this class of compounds, but it describes its mechanism of action through a series of biochemical investigations studies.

Compared with other PqsR antagonists, like the thiocetamide based compound M64 from Starkey *et al.* (2014) ($K_{(D)}$ of 5.4 nM) (structure 4 in Figure 1.13) or the lead 4-aminoquinoline derived molecule from Soukarieh *et al.* (2018) ($K_{(D)}$ of 2.66 nM) (structure 5 in Figure 1.13), 488 does not exhibit the same binding affinity. However, its relatively high $K_{(D)}$ (1.74 μM) could be compensated by its non-competitive action, which may be considered a favourable strategy in a QS inhibition contest by preventing the triggering of the PQS pathway regardless of the agonist concentration.

Extracellular DNA levels in biofilms should be quantified after exposure to 488, considering the role of PQS in eDNA release (Spoering & Gilmore, 2006; Turnbull *et al.*, 2016; Wei & Ma, 2013) and the impact of 488 as a QS inhibitor. The previously cited antagonists, for instance, enhanced the effect of antibiotics such as tobramycin or ciprofloxacin in disrupting biofilms, although in concentrations far higher than the $K_{(D)}$s (Maura & Rahme, 2017; Soukarieh *et al.*, 2018). Moreover, M64 significantly reduced the number of persistent cells in a culture (Starkey *et al.*, 2014). Therefore, a study of the effect of 488 on persistence should be carried out, due to its significance in clinical enviroments.

Depending on the outcome of further biofilm tests over with longer treatment periods, the next step will be to test the compound *in vivo*. Derived from the same natural fimbrolides as 488, the synthetic furanone C30 promoted the infection clearance in a mouse pulmonary infection model (Hentzer *et al.*, 2003; Manefield *et al.*, 2001); however, the compound proved to be toxic at the concentrations required for QS inhibition with a *P. aeruginosa lasI-gfp* biosensor (Moore *et al.*, 2015). Among PqsR antagonists, M64 showed increased postinfection survival rates in burn and lung infection model in mice (Starkey *et al.*, 2014) and the PqsR inhibitors patented by Spero, that are active at submicromolar concentrations (50–250 nM), successfully reduced AQ production in an *in vivo* acute thigh infection murine model (Zahler, 2016). So far, only these PQS system inhibitors have proceeded to preclinical stage.

In conclusion, it will also be of importance to investigate whether repeated or prolonged exposure to the lactam selects for resistance in all the species tested, in particular *P. mirabilis* and *S. aureus*. In fact, due to the species-dependent growth inhibitory activity of 488, some species may be subjected to a high selective pressure that may trigger the emergence of resistance (Davies & Davies, 2010). Resistant bacterial cells could be genome sequenced to help identify the corresponding mutations in order to characterise the mechanism of resistance and gain further insights into the mode of action of the lactams.

7 APPENDIX

7.1 GROWTH CURVES OF *P. AERUGINOSA* PAO1-L WITH 488

Cultures of *P. aeruginosa* PAO1-L were incubated in conical flask in presence and absence of 488 and the growth was monitored by measuring the OD_{600}. An impact on growth can be observed in plateau phase on samples with 488 at 100 µM and 200 µM.

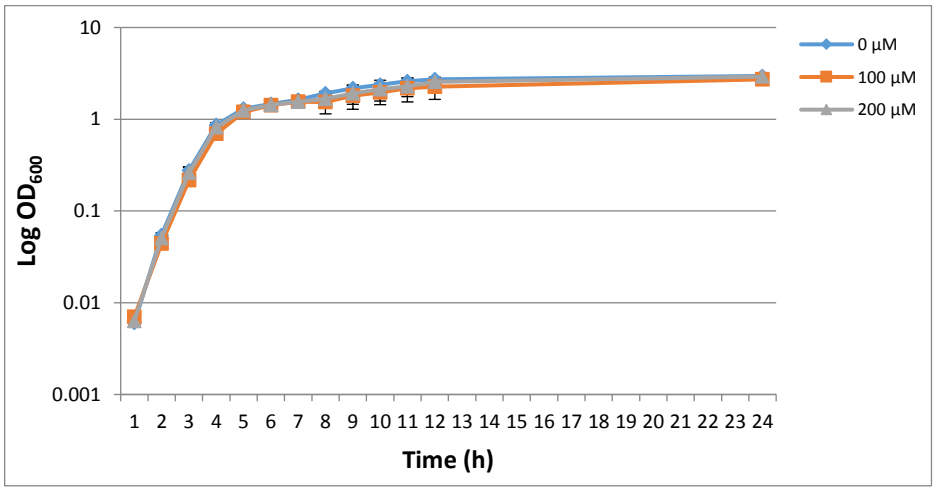

Figure 7.1 Growth curves of *P. aeruginosa* PAO1-L in presence of 488 at 100 and 200 µM. Error bar represents standard deviation of biological triplicates.

7.2 COMPETITION ASSAY VALIDATION

As control of the methodology used for competition assays, an assay using 3-NH2-7Cl-C9-Quinozolinone (7Cl-QZN) as antagonist and PQS as agonist has been performed. The strong antagonist 7Cl-QZN described in Ilangovan *et al.* (2013) has an IC_{50} value of 5 µM and it has been demonstrated to be a competitive antagonist of PqsR. The strain here used is PAO1-L Δ*pqsA* as for the other competition assays. Two kinds of curves have been generated with Prism 6 by Graphpad software using two different algorithms (Figure 7.2), both based on non-linear regression analysis and equation (7.1): the general sigmoidal dose-response function, which shows response as a function of the logarithm of concentration

(Figure 7.3), and the function named *EC_{50} shift* (Figure 7.4), that aims to build two dose-response curves determining the fold shift. Therefore in addiction to Equation 7.1, the EC_{50} shift function automatically extrapolates the EC_{50} shift values from a standardized plotting of the bottom and top plateau of dose-response curves. This function, although useful, cannot be used in case of non-competitive inhibition since the software automatically adapts the trend of the curves by a standardization of the different maximum responses occurring in non-competitive interactions in order to calculate a final EC_{50} value. The use of this function with non-competitive antagonists inevitably leads to a generation of incomplete and misleading EC_{50} shift curves (Figure 7.5) while it is effective on representing the action of competitive inhibitors such as 7Cl-QZN (Figure 7.2).

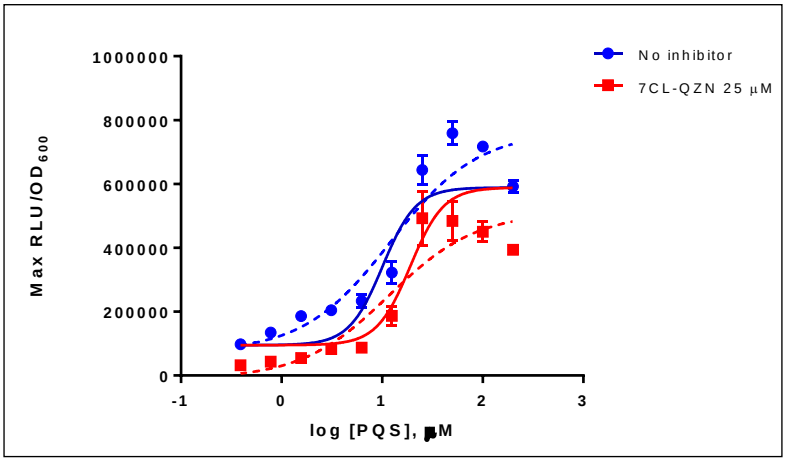

Figure 7.2 Effect of PQS on the expression of P*pqsA::lux* in PAO1-L Δ*pqsA* in presence of 7Cl-QZN. Overlap of the curves generated with different algorithms in Graphpad Prism 6. The dotted and solid curves have been generated using a general sigmoidal dose-response function and EC_{50} shift function respectively.

$$Y = Bottom + \frac{Top - Bottom}{1 + 10^{logEC50 - X}}$$

Equation 7.1 Sigmoidal dose-response equation

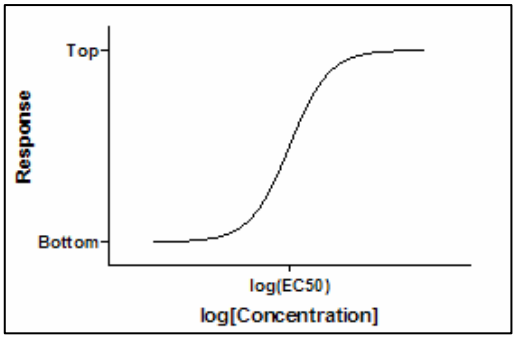

Figure 7.3 Example of Sigmoidal dose-response graph from http://www.graphpad.com/

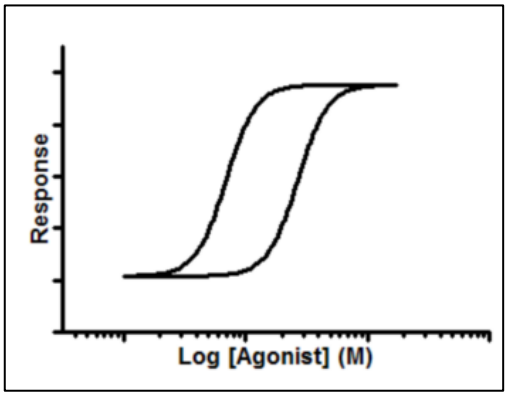

Figure 7.4 Example of curves with the EC50 shift algorithm from http://www.graphpad.com/

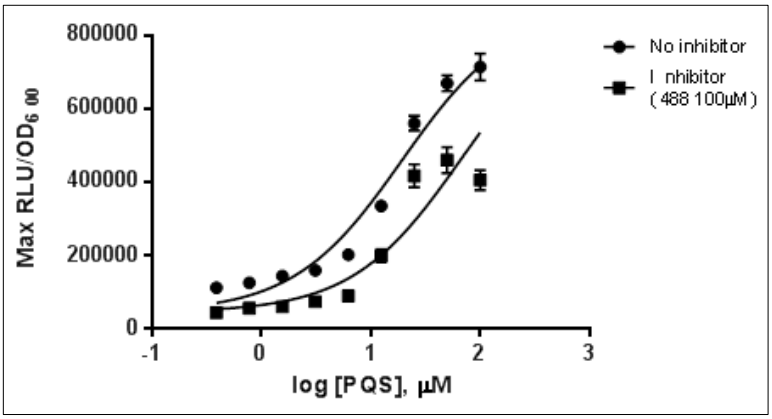

Figure 7.5 Effect of PQS on the expression of P*pqsA::lux* in PAO1-L ΔpqsA in presence of lactam 488. Curves generated with EC50 shift algorithm in Graphpad Prism 6.

7.3 Growth curves of *P. aeruginosa* PAO1-L with 295 and 310

Growth curves with biological triplicates of PAO1-L grown in 96 well plates in presence of lactams 295 and 310 were generated by using a TECAN microplate reader. The two lactams showed a moderate impact on growth, in particular 310 did not allow the reach of the plateau as the controls (DMSO 0.8 % v/v and LB).

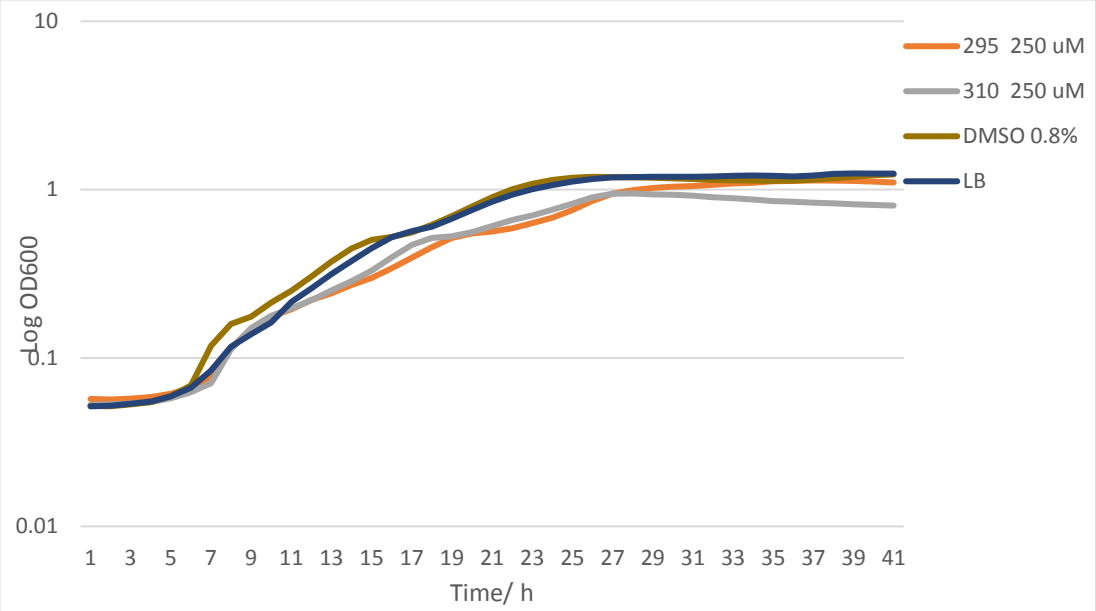

Figure 7.6 Growth curves of *P. aeruginosa* PAO1-L in presence of 295 and 310 at 250 µM. Error bar were omitted for better visualisation.

7.4 *P. AERUGINOSA* RNASEQ COG ANALYSIS – SUPPLEMENTARY TABLES

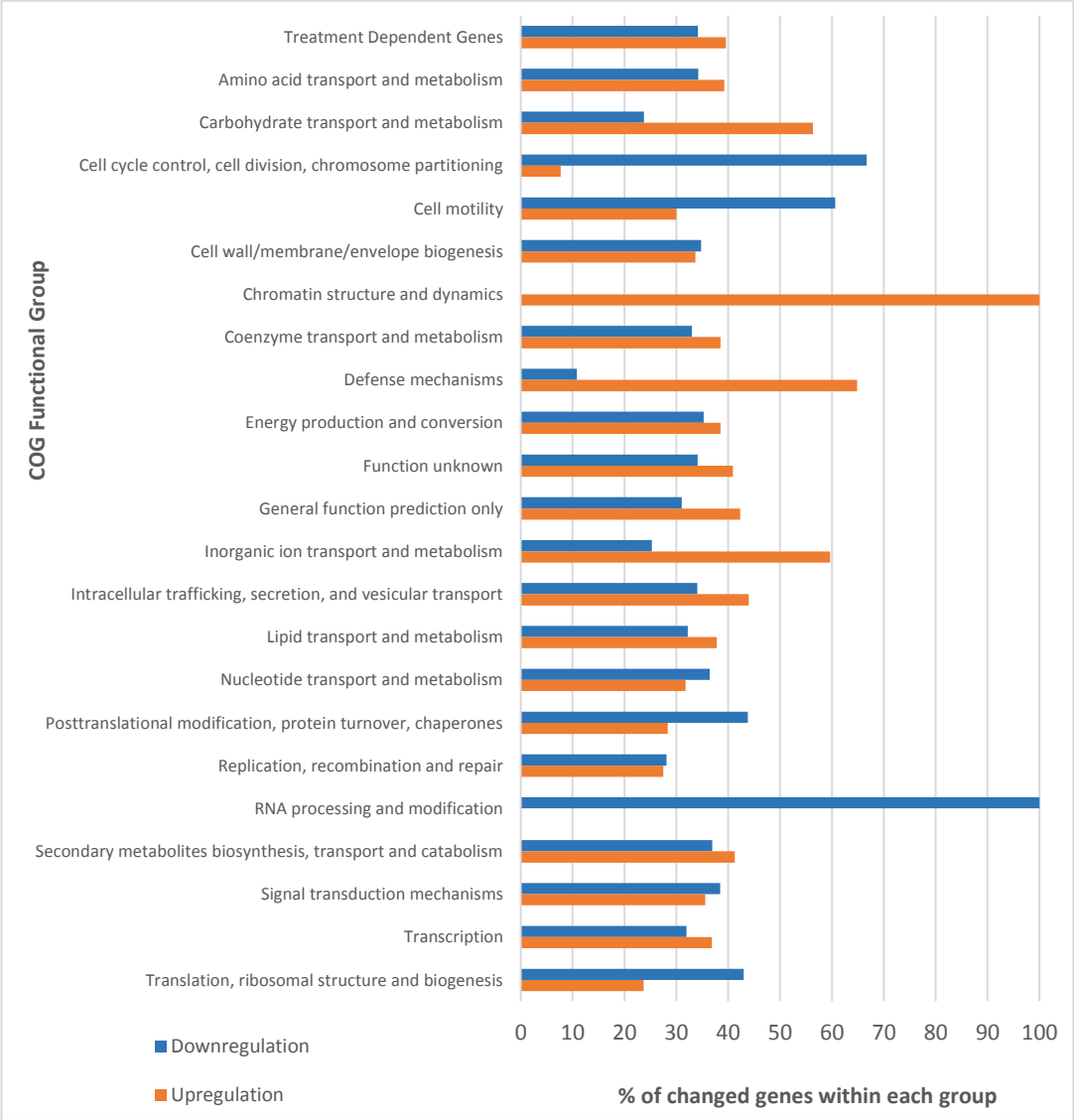

Figure 7.7 Differential expression of genes exposed to 488 (100uM) for 8 h with genes exposed to 488 (50 µM) for 8h using functional classification of PAO1 genes from the Pseudomonas Genome Database. Histograms representing the distribution of downregulated (blue) and upregulated (orange) genes according to their functional classifications. Top Group represents the control

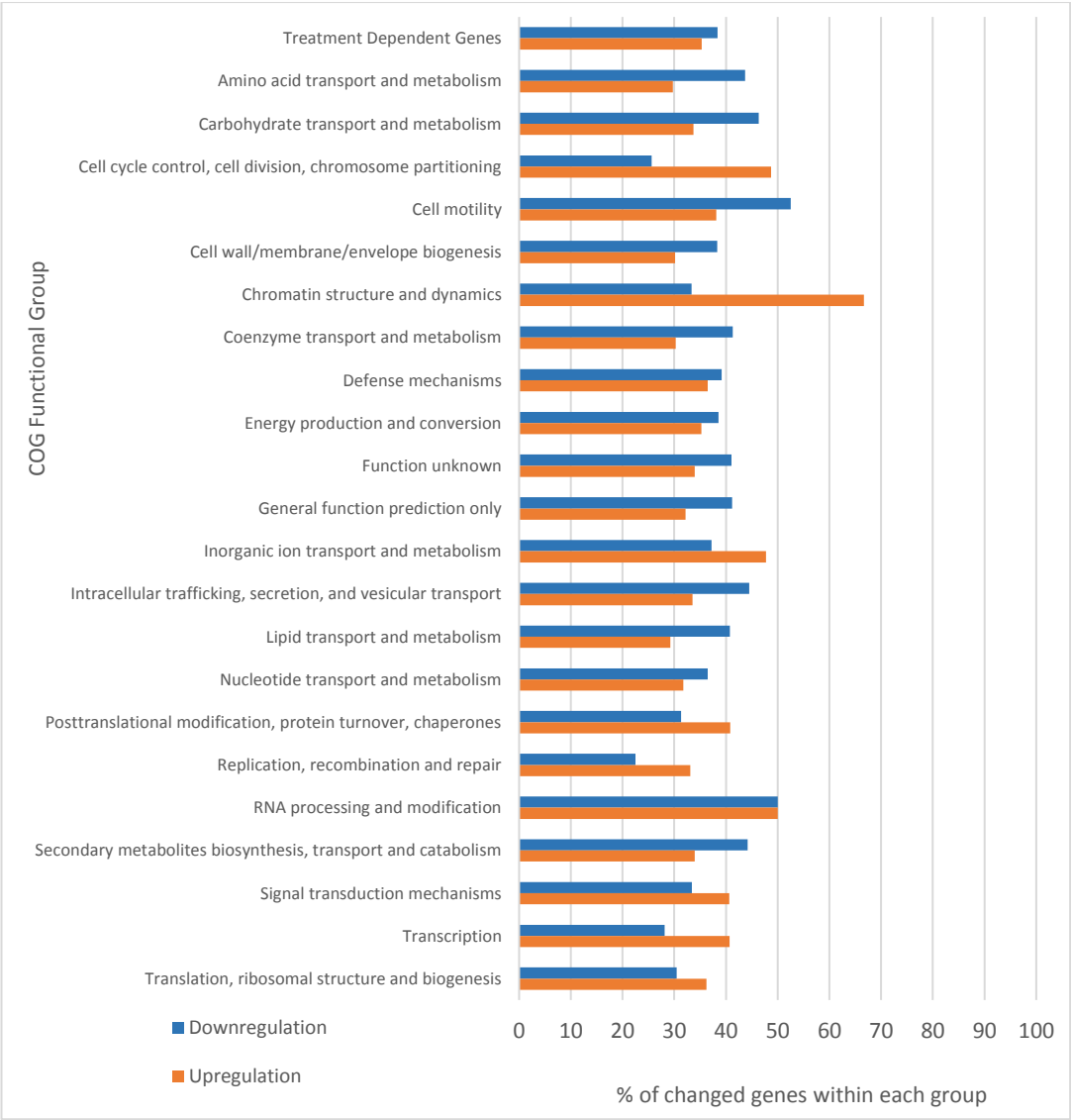

Figure 7.8 Differential gene expression comparison between samples obtained at 12h with MeOH and 8h with MeOH using functional classification of PAO1 genes from the Pseudomonas Genome Database. Histograms representing the distribution of downregulated (blue) and upregulated (orange) genes according to their functional classifications. Top Group represents the control

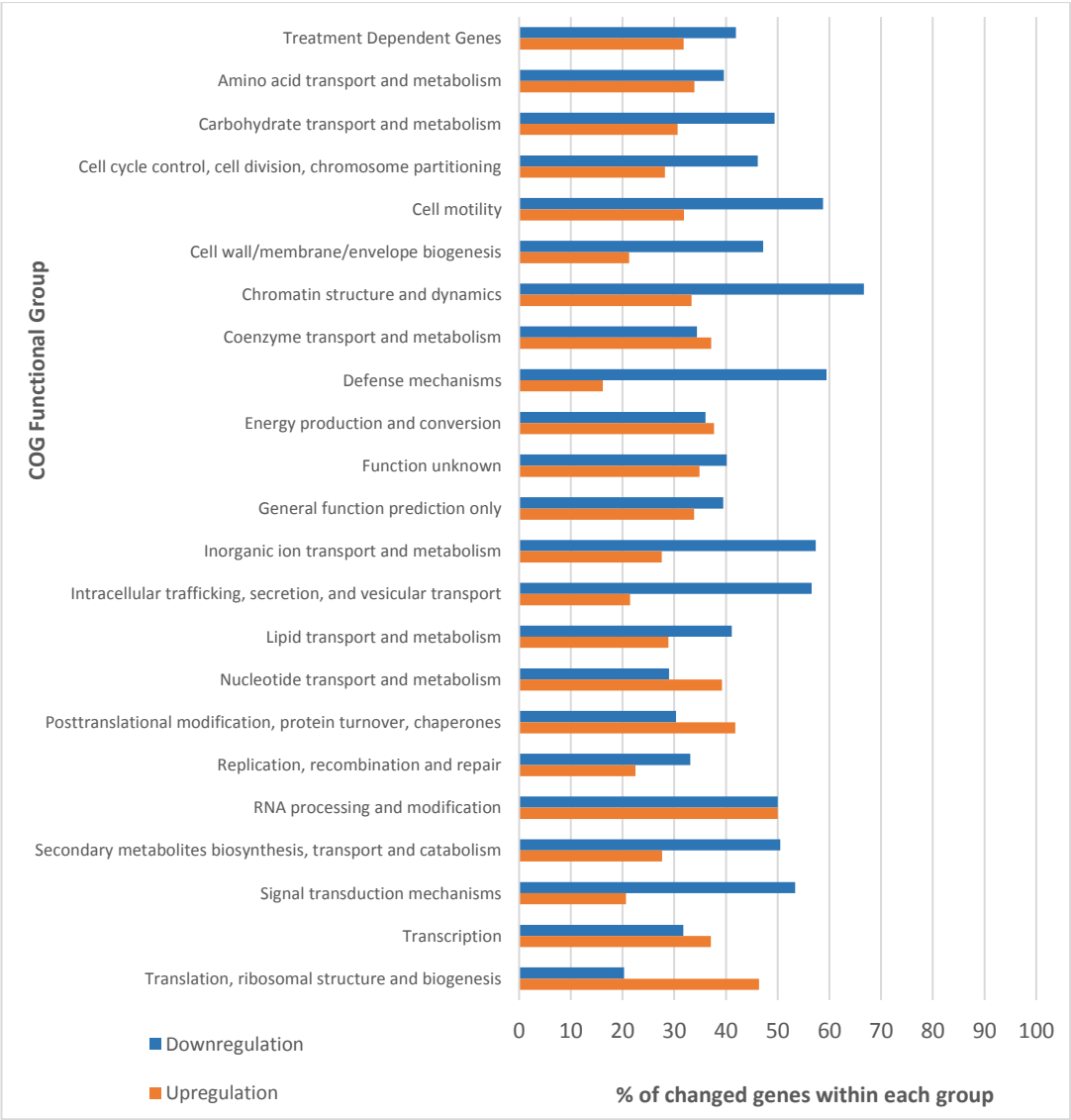

Figure 7.9 Differential expression of genes exposed to 488 (50uM) for 12 h with a solvent (methanol) only control using functional classification of PAO1 genes from the Pseudomonas Genome Database. Histograms representing the distribution of downregulated (blue) and upregulated (orange) genes according to their functional classifications. Top Group represents the control**.**

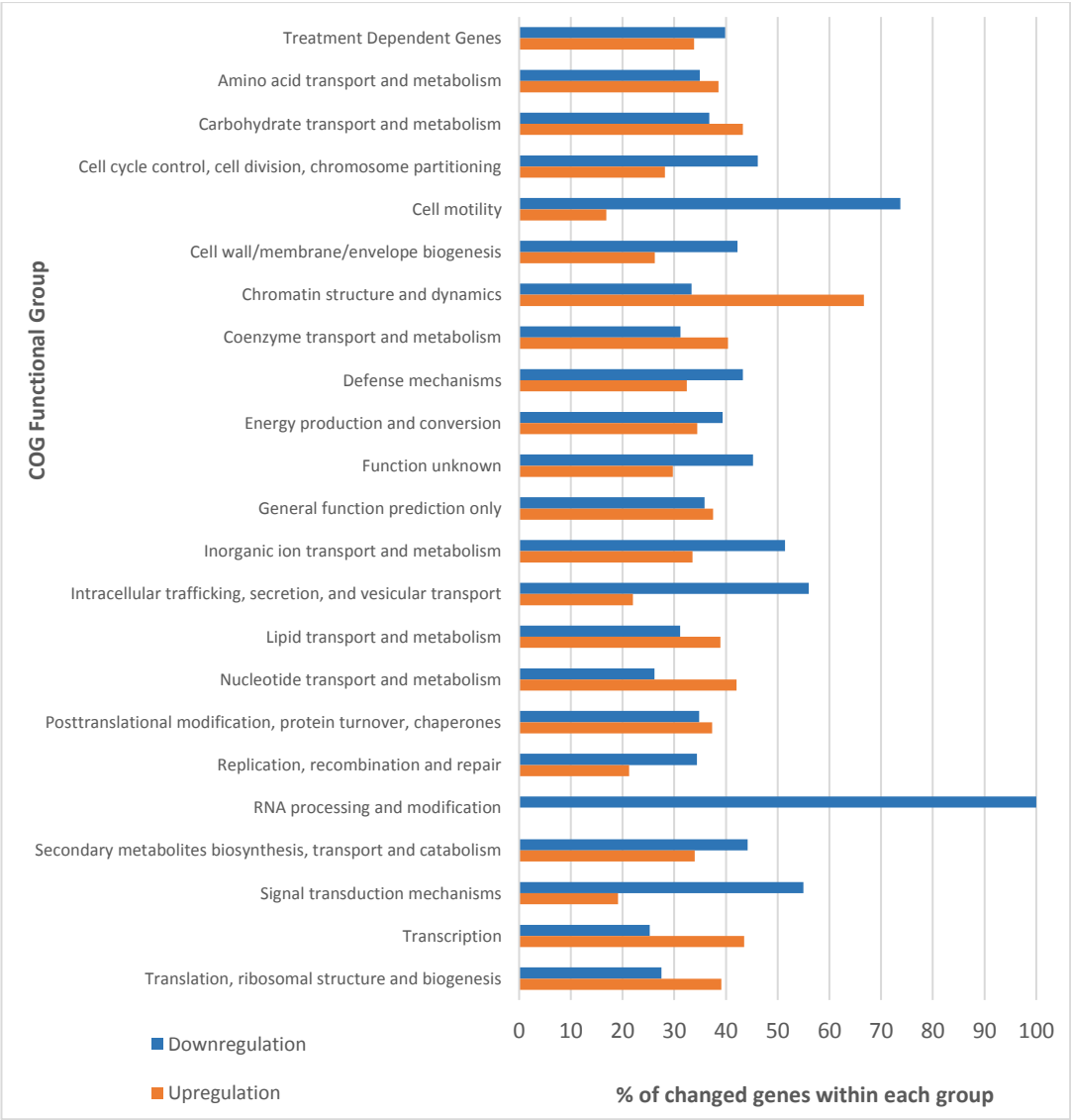

Figure 7.10 Differential expression of genes exposed to 488 (100uM) for 12 h with a solvent (MeOH) only control using functional classification of PAO1 genes from the Pseudomonas Genome Database. Histograms representing the distribution of downregulated (blue) and upregulated (orange) genes according to their functional classifications. Top Group represents the control**.**

REFERENCES

Acar, J., & Goldstein, F. (1997). Trends in bacterial resistance to fluoroquinolones. *Clinical Infectious Diseases, 24*(Supplement_1), S67-S73.

Acosta, N., Heirali, A., Somayaji, R., Surette, M. G., Workentine, M. L., Sibley, C. D., . . . Parkins, M. D. (2018). Sputum microbiota is predictive of long-term clinical outcomes in young adults with cystic fibrosis. *Thorax, 73*(11), 1016-1025.

Adonizio, A., Kong, K. F., & Mathee, K. (2008). Inhibition of quorum sensing-controlled virulence factor production in Pseudomonas aeruginosa by South Florida plant extracts. *Antimicrob Agents Chemother, 52*(1), 198-203. doi: 10.1128/AAC.00612-07

Aendekerk, S., Diggle, S. P., Song, Z., Hoiby, N., Cornelis, P., Williams, P., & Camara, M. (2005). The MexGHI-OpmD multidrug efflux pump controls growth, antibiotic susceptibility and virulence in Pseudomonas aeruginosa via 4-quinolone-dependent cell-to-cell communication. *Microbiology, 151*(Pt 4), 1113-1125. doi: 10.1099/mic.0.27631-0

Agaisse, H., Gominet, M., Økstad, O. A., Kolstø, A. B., & Lereclus, D. (1999). PlcR is a pleiotropic regulator of extracellular virulence factor gene expression in Bacillus thuringiensis. *Molecular Microbiology, 32*(5), 1043-1053.

Allegretta, G., Maurer, C. K., Eberhard, J., Maura, D., Hartmann, R. W., Rahme, L., & Empting, M. (2017). In-depth profiling of MvfR-regulated small molecules in Pseudomonas aeruginosa after quorum sensing inhibitor treatment. *Frontiers in Microbiology, 8*, 924.

Allesen-Holm, M., Barken, K. B., Yang, L., Klausen, M., Webb, J. S., Kjelleberg, S., . . . Tolker-Nielsen, T. (2006). A characterization of DNA release in Pseudomonas aeruginosa cultures and biofilms. *Molecular Microbiology, 59*(4), 1114-1128.

Alon, U. (2007). Network motifs: theory and experimental approaches. *Nat Rev Genet, 8*(6), 450-461. doi: 10.1038/nrg2102

Alvarez-Ortega, C., & Harwood, C. S. (2007). Responses of Pseudomonas aeruginosa to low oxygen indicate that growth in the cystic fibrosis lung is by aerobic respiration. *Molecular Microbiology, 65*(1), 153-165.

Amara, N., Gregor, R., Rayo, J., Dandela, R., Daniel, E., Liubin, N., . . . Meijler, M. M. (2016). Fine-Tuning Covalent Inhibition of Bacterial Quorum Sensing. *Chembiochem, 17*(9), 825-835.

Amara, N., Mashiach, R., Amar, D., Krief, P., Spieser, S. A., Bottomley, M. J., . . . Meijler, M. M. (2009). Covalent inhibition of bacterial quorum sensing. *Journal of the American Chemical Society, 131*(30), 10610-10619.

Anders, S., Pyl, P. T., & Huber, W. (2015). HTSeq--a Python framework to work with high-throughput sequencing data. *Bioinformatics, 31*(2), 166-169. doi: 10.1093/bioinformatics/btu638

Antonic, V., Stojadinovic, A., Zhang, B., Izadjoo, M. J., & Alavi, M. (2013). Pseudomonas aeruginosa induces pigment production and enhances

virulence in a white phenotypic variant of Staphylococcus aureus. *Infect Drug Resist, 6*.

Anyan, M. E., Amiri, A., Harvey, C. W., Tierra, G., Morales-Soto, N., Driscoll, C. M., . . . Shrout, J. D. (2014). Type IV pili interactions promote intercellular association and moderate swarming of Pseudomonas aeruginosa. *Proceedings of the National Academy of Sciences, 111*(50), 18013-18018.

Arias, A. A., Lambert, S., Martinet, L., Adam, D., Tenconi, E., Hayette, M.-P., . . . Rigali, S. (2015). Growth of desferrioxamine-deficient Streptomyces mutants through xenosiderophore piracy of airborne fungal contaminations. *FEMS microbiology ecology, 91*(7).

Armbruster, C. R., Wolter, D. J., Mishra, M., Hayden, H. S., Radey, M. C., Merrihew, G., . . . Parsek, M. R. (2016). Staphylococcus aureus protein A mediates interspecies interactions at the cell surface of Pseudomonas aeruginosa. *MBio, 7*(3), e00538-00516.

Aruni, A. W., Dou, Y., Mishra, A., & Fletcher, H. M. (2015). The biofilm community: rebels with a cause. *Current oral health reports, 2*(1), 48-56.

Awasthi, G., Chester, A., Chaturvedi, R., & Prakash, J. (2015). Study on Role of Pseudomonas aeruginosa on Heavy Metal Bioremediation. *Int. J. Pure App. Biosci, 3*(4), 92-100.

Azevedo, A. S., Almeida, C., Melo, L. F., & Azevedo, N. F. (2017). Impact of polymicrobial biofilms in catheter-associated urinary tract infections. *Crit Rev Microbiol, 43*(4), 423-439.

Bajolet-Laudinat, O., Girod-de Bentzmann, S., Tournier, J., Madoulet, C., Plotkowski, M., Chippaux, C., & Puchelle, E. (1994). Cytotoxicity of Pseudomonas aeruginosa internal lectin PA-I to respiratory epithelial cells in primary culture. *Infection and Immunity, 62*(10), 4481-4487.

Balasubramanian, D., Schneper, L., Kumari, H., & Mathee, K. (2012). A dynamic and intricate regulatory network determines Pseudomonas aeruginosa virulence. *Nucleic acids research, 41*(1), 1-20.

Baldan, R., Cigana, C., Testa, F., Bianconi, I., Simone, M., & Pellin, D. (2014). Adaptation of Pseudomonas aeruginosa in cystic fibrosis airways influences virulence of Staphylococcus aureus in vitro and murine models of co-infection. *Plos One, 9*. doi: 10.1371/journal.pone.0089614

Beatson, S. A., Whitchurch, C. B., Semmler, A. B., & Mattick, J. S. (2002). Quorum sensing is not required for twitching motility in Pseudomonas aeruginosa. *J Bacteriol, 184*(13), 3598-3604. doi: 10.1128/jb.184.13.3598-3604.2002

Becher, A., & Schweizer, H. P. (2000). Integration-proficient Pseudomonas aeruginosa vectors for isolation of single-copy chromosomal lacZ and lux gene fusions. *Biotechniques, 29*(5), 948-952.

Beenken, K. E., Blevins, J. S., & Smeltzer, M. S. (2003). Mutation of sarA in Staphylococcus aureus limits biofilm formation. *Infection and Immunity, 71*(7), 4206-4211.

Beenken, K. E., Dunman, P. M., McAleese, F., Macapagal, D., Murphy, E., Projan, S. J., . . . Smeltzer, M. S. (2004). Global gene expression in Staphylococcus

aureus biofilms. *J Bacteriol, 186*(14), 4665-4684. doi: 10.1128/jb.186.14.4665-4684.2004

Berghmans, T., Sculier, J.-P., & Klastersky, J. (2003). A prospective study of infections in lung cancer patients admitted to the hospital. *Chest, 124*(1), 114-120.

Billings, N., Millan, M. R., Caldara, M., Rusconi, R., Tarasova, Y., Stocker, R., & Ribbeck, K. (2013). The extracellular matrix component Psl provides fast-acting antibiotic defense in Pseudomonas aeruginosa biofilms. *PLoS Pathog, 9*(8), e1003526.

Blevins, J. S., Gillaspy, A. F., Rechtin, T. M., Hurlburt, B. K., & Smeltzer, M. S. (1999). The staphylococcal accessory regulator (sar) represses transcription of the Staphylococcus aureus collagen adhesin gene (cna) in an agr-independent manner. *Molecular Microbiology, 33*(2), 317-326.

Boles, B. R., & Horswill, A. R. (2008). Agr-mediated dispersal of Staphylococcus aureus biofilms. *PLoS Pathog, 4*(4), e1000052.

Boles, B. R., Thoendel, M., & Singh, P. K. (2005). Rhamnolipids mediate detachment of Pseudomonas aeruginosa from biofilms. *Molecular Microbiology, 57*(5), 1210-1223.

Borriello, G., Werner, E., Roe, F., Kim, A. M., Ehrlich, G. D., & Stewart, P. S. (2004). Oxygen limitation contributes to antibiotic tolerance of Pseudomonas aeruginosa in biofilms. *Antimicrob Agents Chemother, 48*(7), 2659-2664.

Boyle, B., Kukavica-Ibrulj, I., Emond-Rheault, J.-G., Jeukens, J., Freschi, L., Dupont, M.-J., . . . Charette, S. J. (2018). The Pseudomonas aeruginosa Pan-Genome Provides New Insights on Its Population Structure, Horizontal Gene Transfer, and Pathogenicity. *Genome Biology and Evolution, 11*(1), 109-120. doi: 10.1093/gbe/evy259

Brands, B., & Bockmühl, D. P. (2015). Experimental Evaluation of Hygienic Conditions in Domestic Dishwashers. *Tenside Surfactants Detergents, 52*(2), 148-154.

Brencic, A., & Lory, S. (2009). Determination of the regulon and identification of novel mRNA targets of Pseudomonas aeruginosa RsmA. *Molecular Microbiology, 72*(3), 612-632.

Brencic, A., McFarland, K. A., McManus, H. R., Castang, S., Mogno, I., Dove, S. L., & Lory, S. (2009). The GacS/GacA signal transduction system of Pseudomonas aeruginosa acts exclusively through its control over the transcription of the RsmY and RsmZ regulatory small RNAs. *Molecular Microbiology, 73*(3), 434-445. doi: doi:10.1111/j.1365-2958.2009.06782.x

Brooks, T., & Keevil, C. W. (1997). A simple artificial urine for the growth of urinary pathogens. *Lett Appl Microbiol, 24*(3), 203-206.

Burmølle, M., Webb, J. S., Rao, D., Hansen, L. H., Sørensen, S. J., & Kjelleberg, S. (2006). Enhanced biofilm formation and increased resistance to antimicrobial agents and bacterial invasion are caused by synergistic

interactions in multispecies biofilms. *Appl. Environ. Microbiol., 72*(6), 3916-3923.

Byrd, M. S., Sadovskaya, I., Vinogradov, E., Lu, H., Sprinkle, A. B., Richardson, S. H., . . . Anderson, E. M. (2009). Genetic and biochemical analyses of the Pseudomonas aeruginosa Psl exopolysaccharide reveal overlapping roles for polysaccharide synthesis enzymes in Psl and LPS production. *Molecular Microbiology, 73*(4), 622-638.

Caballero, A. R., Moreau, J. M., Engel, L. S., Marquart, M. E., Hill, J. M., & O'Callaghan, R. J. (2001). Pseudomonas aeruginosa protease IV enzyme assays and comparison to other Pseudomonas proteases. *Anal Biochem, 290*(2), 330-337. doi: 10.1006/abio.2001.4999

Caiazza, N. C., Shanks, R. M. Q., & O'Toole, G. A. (2005). Rhamnolipids Modulate Swarming Motility Patterns of Pseudomonas aeruginosa. *Journal of Bacteriology, 187*(21), 7351-7361. doi: 10.1128/jb.187.21.7351-7361.2005

Calfee, M. W., Coleman, J. P., & Pesci, E. C. (2001). Interference with Pseudomonas quinolone signal synthesis inhibits virulence factor expression by Pseudomonas aeruginosa. *Proceedings of the National Academy of Sciences, 98*(20), 11633-11637.

Cao, H., Krishnan, G., Goumnerov, B., Tsongalis, J., Tompkins, R., & Rahme, L. G. (2001). A quorum sensing-associated virulence gene of Pseudomonas aeruginosa encodes a LysR-like transcription regulator with a unique self-regulatory mechanism. *Proceedings of the National Academy of Sciences, 98*(25), 14613-14618.

Case, R. J., Labbate, M., & Kjelleberg, S. (2008). AHL-driven quorum-sensing circuits: their frequency and function among the Proteobacteria. *The ISME Journal, 2*(4), 345.

Chan, K. G., Atkinson, S., Mathee, K., Sam, C. K., Chhabra, S. R., Camara, M., . . . Williams, P. (2011). Characterization of N-acylhomoserine lactone-degrading bacteria associated with the Zingiber officinale (ginger) rhizosphere: Co-existence of quorum quenching and quorum sensing in Acinetobacter and Burkholderia. *Bmc Microbiology, 11*. doi: Artn 51

10.1186/1471-2180-11-51

Chang, C.-Y., Krishnan, T., Wang, H., Chen, Y., Yin, W.-F., Chong, Y.-M., . . . Chan, K.-G. (2014). Non-antibiotic quorum sensing inhibitors acting against N-acyl homoserine lactone synthase as druggable target. *Sci Rep, 4*, 7245.

Chew, S. C., Kundukad, B., Seviour, T., Van der Maarel, J. R., Yang, L., Rice, S. A., . . . Kjelleberg, S. (2014). Dynamic remodeling of microbial biofilms by functionally distinct exopolysaccharides. *MBio, 5*(4), e01536-01514.

Choi, D. S., Kim, D. K., Choi, S. J., Lee, J., Choi, J. P., Rho, S., . . . Gho, Y. S. (2011). Proteomic analysis of outer membrane vesicles derived from Pseudomonas aeruginosa. *Proteomics, 11*(16), 3424-3429. doi: 10.1002/pmic.201000212

Chou, H. T., Kwon, D. H., Hegazy, M., & Lu, C. D. (2008). Transcriptome analysis of agmatine and putrescine catabolism in Pseudomonas aeruginosa PAO1. *J Bacteriol, 190*(6), 1966-1975. doi: 10.1128/jb.01804-07

Christensen, G. D., Simpson, W. A., Bisno, A. L., & Beachey, E. H. (1982). Adherence of slime-producing strains of Staphylococcus epidermidis to smooth surfaces. *Infection and Immunity, 37*(1), 318-326.

Chua, S. L., Hultqvist, L. D., Yuan, M., Rybtke, M., Nielsen, T. E., Givskov, M., . . . Yang, L. (2015). In vitro and in vivo generation and characterization of Pseudomonas aeruginosa biofilm–dispersed cells via c-di-GMP manipulation. *Nat Protoc, 10*(8), 1165.

Ciofu, O., Lee, B., Johannesson, M., Hermansen, N. O., Meyer, P., & Høiby, N. (2008). Investigation of the algT operon sequence in mucoid and non-mucoid Pseudomonas aeruginosa isolates from 115 Scandinavian patients with cystic fibrosis and in 88 in vitro non-mucoid revertants. *Microbiology, 154*(1), 103-113.

Ciofu, O., Rojo-Molinero, E., Macià, M. D., & Oliver, A. (2017). Antibiotic treatment of biofilm infections. *Apmis, 125*(4), 304-319.

Cohen, D., Mechold, U., Nevenzal, H., Yarmiyhu, Y., Randall, T. E., Bay, D. C., . . . Banin, E. (2015). Oligoribonuclease is a central feature of cyclic diguanylate signaling in Pseudomonas aeruginosa. *Proceedings of the National Academy of Sciences, 112*(36), 11359-11364. doi: 10.1073/pnas.1421450112

Cole, S. J., Records, A. R., Orr, M. W., Linden, S. B., & Lee, V. T. (2014). Catheter-associated urinary tract infection by Pseudomonas aeruginosa is mediated by exopolysaccharide-independent biofilms. *Infection and Immunity, 82*(5), 2048-2058.

Coleman, J. P., Hudson, L. L., McKnight, S. L., Farrow, J. M., Calfee, M. W., Lindsey, C. A., & Pesci, E. C. (2008). Pseudomonas aeruginosa PqsA is an anthranilate-coenzyme A ligase. *Journal of Bacteriology, 190*(4), 1247-1255.

Colvin, K. M., Irie, Y., Tart, C. S., Urbano, R., Whitney, J. C., Ryder, C., . . . Parsek, M. R. (2012). The Pel and Psl polysaccharides provide Pseudomonas aeruginosa structural redundancy within the biofilm matrix. *Environmental Microbiology, 14*(8), 1913-1928.

Colwell, R. R. (1964). A study of features used in the diagnosis of Pseudomonas aeruginosa. *Microbiology, 37*(2), 181-194.

Conant, C., A Schwartz, M., & Ionescu-Zanetti, C. (2009). *Well Plate-Coupled Microfluidic Devices Designed for Facile Image-Based Cell Adhesion and Transmigration Assays* (Vol. 15).

Copeland, M. F., & Weibel, D. B. (2009). Bacterial swarming: a model system for studying dynamic self-assembly. *Soft matter, 5*(6), 1174-1187.

Cortese, Y. J., Wagner, V. E., Tierney, M., Devine, D., & Fogarty, A. (2018). Review of Catheter-Associated Urinary Tract Infections and In Vitro Urinary Tract Models. *Journal of healthcare engineering, 2018*.

Costerton, J. W., Cheng, K., Geesey, G. G., Ladd, T. I., Nickel, J. C., Dasgupta, M., & Marrie, T. J. (1987). Bacterial biofilms in nature and disease. *Annual Reviews in Microbiology, 41*(1), 435-464.

Costerton, J. W., Lewandowski, Z., Caldwell, D. E., Korber, D. R., & Lappin-Scott, H. M. (1995). Microbial biofilms. *Annual Review of Microbiology, 49*(1), 711-745.

Costerton, J. W., Stewart, P. S., & Greenberg, E. P. (1999). Bacterial biofilms: a common cause of persistent infections. *Science, 284*(5418), 1318-1322.

Cotter, J. J., O'Gara, J. P., & Casey, E. (2009). Rapid depletion of dissolved oxygen in 96-well microtiter plate Staphylococcus epidermidis biofilm assays promotes biofilm development and is influenced by inoculum cell concentration. *Biotechnology and bioengineering, 103*(5), 1042-1047.

Cowan, S. E., Gilbert, E., Liepmann, D., & Keasling, J. (2000). Commensal interactions in a dual-species biofilm exposed to mixed organic compounds. *Appl. Environ. Microbiol., 66*(10), 4481-4485.

Cystic Fibrosis Patient Registry (2015). from https://www.cff.org/Our-Research/CF-Patient-Registry/2015-Patient-Registry-Annual-Data-Report.pdf

D'Argenio, D. A., Calfee, M. W., Rainey, P. B., & Pesci, E. C. (2002). Autolysis and autoaggregation in Pseudomonas aeruginosa colony morphology mutants. *Journal of Bacteriology, 184*(23), 6481-6489.

Dalton, T., Dowd, S. E., Wolcott, R. D., Sun, Y., Watters, C., & Griswold, J. A. (2011). An in vivo polymicrobial biofilm wound infection model to study interspecies interactions. *Plos One, 6*. doi: 10.1371/journal.pone.0027317

Darveau, R. P., & Hancock, R. (1983). Procedure for isolation of bacterial lipopolysaccharides from both smooth and rough Pseudomonas aeruginosa and Salmonella typhimurium strains. *Journal of Bacteriology, 155*(2), 831-838.

Darzins, A. (1994). Characterization of a Pseudomonas aeruginosa gene cluster involved in pilus biosynthesis and twitching motility: sequence similarity to the chemotaxis proteins of enterics and the gliding bacterium Myxococcus xanthus. *Mol Microbiol, 11*(1), 137-153.

Dasgupta, N., Arora, S. K., & Ramphal, R. (2004). The flagellar system of Pseudomonas aeruginosa *Pseudomonas* (pp. 675-698): Springer.

Dasgupta, N., Wolfgang, M. C., Goodman, A. L., Arora, S. K., Jyot, J., Lory, S., & Ramphal, R. (2003). A four-tiered transcriptional regulatory circuit controls flagellar biogenesis in Pseudomonas aeruginosa. *Molecular Microbiology, 50*(3), 809-824.

Davies, J., & Davies, D. (2010). Origins and evolution of antibiotic resistance. *Microbiol. Mol. Biol. Rev., 74*(3), 417-433.

De Backer, S., Sabirova, J., De Pauw, I., De Greve, H., Hernalsteens, J.-P., Goossens, H., & Malhotra-Kumar, S. (2018). Enzymes Catalyzing the TCA- and Urea Cycle Influence the Matrix Composition of Biofilms Formed by

Methicillin-Resistant Staphylococcus aureus USA300. *Microorganisms, 6*(4), 113.

De Kievit, T. R., Gillis, R., Marx, S., Brown, C., & Iglewski, B. H. (2001). Quorum-sensing genes in Pseudomonas aeruginosa biofilms: their role and expression patterns. *Appl. Environ. Microbiol., 67*(4), 1865-1873.

Declerck, N., Bouillaut, L., Chaix, D., Rugani, N., Slamti, L., Hoh, F., . . . Arold, S. T. (2007). Structure of PlcR: Insights into virulence regulation and evolution of quorum sensing in Gram-positive bacteria. *Proceedings of the National Academy of Sciences of the United States of America, 104*(47), 18490-18495. doi: 10.1073/pnas.0704501104

DeLeon, S., Clinton, A., Fowler, H., Everett, J., Horswill, A. R., & Rumbaugh, K. P. (2014a). Synergistic interactions of Pseudomonas aeruginosa and Staphylococcus aureus in an in vitro wound model. *Infect Immun, 82*. doi: 10.1128/IAI.02198-14

DeLeon, S., Clinton, A., Fowler, H., Everett, J., Horswill, A. R., & Rumbaugh, K. P. (2014b). Synergistic interactions of Pseudomonas aeruginosa and Staphylococcus aureus in an in vitro wound model. *Infect Immun, 82*(11), 4718-4728. doi: 10.1128/iai.02198-14

Deziel, E., Gopalan, S., Tampakaki, A. P., Lepine, F., Padfield, K. E., Saucier, M., . . . Rahme, L. G. (2005). The contribution of MvfR to Pseudomonas aeruginosa pathogenesis and quorum sensing circuitry regulation: multiple quorum sensing-regulated genes are modulated without affecting lasRI, rhlRI or the production of N-acyl-L-homoserine lactones. *Molecular Microbiology, 55*(4), 998-1014. doi: 10.1111/j.1365-2958.2004.04448.x

Diep, B. A., Gill, S. R., Chang, R. F., Phan, T. H., Chen, J. H., Davidson, M. G., . . . Mongodin, E. F. (2006). Complete genome sequence of USA300, an epidemic clone of community-acquired meticillin-resistant Staphylococcus aureus. *The Lancet, 367*(9512), 731-739.

Dietrich, L. E., Teal, T. K., Price-Whelan, A., & Newman, D. K. (2008). Redox-active antibiotics control gene expression and community behavior in divergent bacteria. *Science, 321*(5893), 1203-1206.

Diggle, S. P., Lumjiaktase, P., Dipilato, F., Winzer, K., Kunakorn, M., Barrett, D. A., . . . Williams, P. (2006a). Functional genetic analysis reveals a 2-alkyl-4-quinolone signaling system in the human pathogen Burkholderia pseudomallei and related bacteria. *Chemistry & Biology, 13*(7), 701-710.

Diggle, S. P., Matthijs, S., Wright, V. J., Fletcher, M. P., Chhabra, S. R., Lamont, I. L., . . . Williams, P. (2007). The Pseudomonas aeruginosa 4-quinolone signal molecules HHQ and PQS play multifunctional roles in quorum sensing and iron entrapment. *Chemistry & Biology, 14*(1), 87-96. doi: 10.1016/j.chembiol.2006.11.014

Diggle, S. P., Stacey, R. E., Dodd, C. E. R., Cámara, M., Williams, P., & Winzer, K. (2006b). The galactophilic lectin, LecA, contributes to biofilm development in Pseudomonas aeruginosa. *Environmental Microbiology, 8*(6), 1095-1104.

Diggle, S. P., Winzer, K., Chhabra, S. R., Chhabra, S. R., Worrall, K. E., Camara, M., & Williams, P. (2003). The Pseudomonas aeruginosa quinolone signal

molecule overcomes the cell density-dependency of the quorum sensing hierarchy, regulates rhl-dependent genes at the onset of stationary phase and can be produced in the absence of LasR. *Molecular Microbiology, 50*(1), 29-43. doi: 10.1046/j.1365-2958.2003.03672.x

Donlan, R. M., & Costerton, J. W. (2002). Biofilms: Survival mechanisms of clinically relevant microorganisms. *Clinical Microbiology Reviews, 15*(2), 167-+. doi: 10.1128/Cmr.15.2.167-193.2002

Dufour, P., Jarraud, S., Vandenesch, F., Greenland, T., Novick, R. P., Bes, M., . . . Lina, G. (2002). High genetic variability of the agr locus in Staphylococcus species. *Journal of Bacteriology, 184*(4), 1180-1186.

Dulcey, C. E., Dekimpe, V., Fauvelle, D.-A., Milot, S., Groleau, M.-C., Doucet, N., . . . Déziel, E. (2013). The end of an old hypothesis: the Pseudomonas signaling molecules 4-hydroxy-2-alkylquinolines derive from fatty acids, not 3-ketofatty acids. *Chemistry & Biology, 20*(12), 1481-1491.

Dunman, P. á., Murphy, E., Haney, S., Palacios, D., Tucker-Kellogg, G., Wu, S., . . . Projan, S. (2001). Transcription Profiling-Based Identification ofStaphylococcus aureus Genes Regulated by the agrand/or sarA Loci. *Journal of Bacteriology, 183*(24), 7341-7353.

Ebadi, A., Sima, N. A. K., Olamaee, M., Hashemi, M., & Nasrabadi, R. G. (2017). Effective bioremediation of a petroleum-polluted saline soil by a surfactant-producing Pseudomonas aeruginosa consortium. *Journal of advanced research, 8*(6), 627-633.

Egorova, A. Y., Sedavkina, V., & Timofeeva, Z. Y. (2001). Heterocyclization of derivatives of 4-oxoalkanoic acids to 1, 5-disubstituted pyrrolin-2-ones. *Chemistry of Heterocyclic Compounds, 37*(6), 694-697.

Engebrecht, J., Nealson, K., & Silverman, M. (1983). Bacterial bioluminescence: isolation and genetic analysis of functions from Vibrio fischeri. *Cell, 32*(3), 773-781.

Engebrecht, J., & Silverman, M. (1984). Identification of genes and gene products necessary for bacterial bioluminescence. *Proceedings of the National Academy of Sciences, 81*(13), 4154-4158.

Engel, L. S., Hill, J. M., Moreau, J. M., Green, L. C., Hobden, J. A., & O'Callaghan, R. J. (1998). Pseudomonas aeruginosa protease IV produces corneal damage and contributes to bacterial virulence. *Investigative ophthalmology & visual science, 39*(3), 662-665.

Ertesvåg, H., & Valla, S. (1998). Biosynthesis and applications of alginates. *Polymer Degradation and Stability, 59*(1-3), 85-91.

Essar, D. W., Eberly, L., Hadero, A., & Crawford, I. P. (1990). *Identification and characterization of genes for a second anthranilate synthase in Pseudomonas aeruginosa: interchangeability of the two anthranilate synthases and evolutionary implications* (Vol. 172).

Farrow, J. M., Sund, Z. M., Ellison, M. L., Wade, D. S., Coleman, J. P., & Pesci, E. C. (2008). PqsE functions independently of PqsR-Pseudomonas quinolone signal and enhances the rhl quorum-sensing system. *Journal of Bacteriology, 190*(21), 7043-7051.

Favre-Bonte, S., Kohler, T., & Van Delden, C. (2003). Biofilm formation by Pseudomonas aeruginosa: role of the C4-HSL cell-to-cell signal and inhibition by azithromycin. *J Antimicrob Chemother, 52*(4), 598-604. doi: 10.1093/jac/dkg397

Feldman, M., Bryan, R., Rajan, S., Scheffler, L., Brunnert, S., Tang, H., & Prince, A. (1998). Role of flagella in pathogenesis ofPseudomonas aeruginosa pulmonary infection. *Infection and Immunity, 66*(1), 43-51.

Fernández, D., Rodríguez, E., Bassas, M., Viñas, M., Solanas, A., Llorens, J., . . . Manresa, A. (2005). Agro-industrial oily wastes as substrates for PHA production by the new strain Pseudomonas aeruginosa NCIB 40045: Effect of culture conditions. *Biochemical engineering journal, 26*(2-3), 159-167.

Fetzner, S. (2015). Quorum quenching enzymes. *Journal of biotechnology, 201*, 2-14.

Filkins, L. M., & O'Toole, G. A. (2015). Cystic fibrosis lung infections: polymicrobial, complex, and hard to treat. *PLoS Pathog, 11*(12), e1005258.

Finkel, S. E., & Kolter, R. (2001). DNA as a nutrient: novel role for bacterial competence gene homologs. *Journal of Bacteriology, 183*(21), 6288-6293.

Flemming, H.-C., Neu, T. R., & Wozniak, D. J. (2007). The EPS matrix: the "house of biofilm cells". *Journal of Bacteriology, 189*(22), 7945-7947.

Fletcher, M. P., Camara, M., Barrett, D. A., & Williams, P. (2014). Biosensors for qualitative and semiquantitative analysis of quorum sensing signal molecules. *Methods Mol Biol, 1149*, 245-254. doi: 10.1007/978-1-4939-0473-0_20

Fletcher, M. P., Diggle, S. P., Crusz, S. A., Chhabra, S. R., Camara, M., & Williams, P. (2007). A dual biosensor for 2-alkyl-4-quinolone quorum-sensing signal molecules. *Environ Microbiol, 9*(11), 2683-2693. doi: 10.1111/j.1462-2920.2007.01380.x

Folkesson, A., Jelsbak, L., Yang, L., Johansen, H. K., Ciofu, O., & Hoiby, N. (2012). Adaptation of Pseudomonas aeruginosa to the cystic fibrosis airway: an evolutionary perspective. *Nat Rev Microbiol, 10*. doi: 10.1038/nrmicro2907

Freschi, L., Bertelli, C., Jeukens, J., Moore, M. P., Kukavica-Ibrulj, I., Emond-Rheault, J. G., . . . Winstanley, C. (2018). Genomic characterisation of an international Pseudomonas aeruginosa reference panel indicates that the two major groups draw upon distinct mobile gene pools. *Fems Microbiology Letters, 365*(14). doi: 10.1093/femsle/fny120

Fricks-Lima, J., Hendrickson, C., Allgaier, M., Zhuo, H., Wiener-Kronish, J., Lynch, S., & Yang, K. (2011). Differences in biofilm formation and antimicrobial resistance of Pseudomonas aeruginosa isolated from airways of mechanically ventilated patients and cystic fibrosis patients. *International journal of antimicrobial agents, 37*(4), 309-315.

Frithz-Lindsten, E., Du, Y., Rosqvist, R., & Forsberg, A. (1997). Intracellular targeting of exoenzyme S of Pseudomonas aeruginosa via type III-dependent translocation induces phagocytosis resistance, cytotoxicity and disruption of actin microfilaments. *Mol Microbiol, 25*(6), 1125-1139.

Fugere, A., Lalonde Seguin, D., Mitchell, G., Deziel, E., Dekimpe, V., & Cantin, A. M. (2014). Interspecific small molecule interactions between clinical isolates of Pseudomonas aeruginosa and Staphylococcus aureus from adult cystic fibrosis patients. *Plos One, 9*. doi: 10.1371/journal.pone.0086705

Fulcher, N. B., Holliday, P. M., Klem, E., Cann, M. J., & Wolfgang, M. C. (2010). The Pseudomonas aeruginosa Chp chemosensory system regulates intracellular cAMP levels by modulating adenylate cyclase activity. *Molecular Microbiology, 76*(4), 889-904.

Fuqua, C., Parsek, M. R., & Greenberg, E. P. (2001). Regulation of gene expression by cell-to-cell communication: acyl-homoserine lactone quorum sensing. *Annu Rev Genet, 35*(1), 439-468.

Fux, C. A., Costerton, J. W., Stewart, P. S., & Stoodley, P. (2005). Survival strategies of infectious biofilms. *Trends Microbiol, 13*(1), 34-40. doi: 10.1016/j.tim.2004.11.010

Gallagher, L. A., McKnight, S. L., Kuznetsova, M. S., Pesci, E. C., & Manoil, C. (2002). Functions required for extracellular quinolone signaling by Pseudomonas aeruginosa. *J Bacteriol, 184*(23), 6472-6480.

Ganin, H., Rayo, J., Amara, N., Levy, N., Krief, P., & Meijler, M. M. (2013). Sulforaphane and erucin, natural isothiocyanates from broccoli, inhibit bacterial quorum sensing. *MedChemComm, 4*(1), 175-179.

Geisinger, E., Muir, T. W., & Novick, R. P. (2009). Agr receptor mutants reveal distinct modes of inhibition by staphylococcal autoinducing peptides. *Proceedings of the National Academy of Sciences, 106*(4), 1216-1221.

Geldreich, E. E., Nash, H. D., Reasoner, D. J., & Taylor, R. H. (1972). The necessity of controlling bacterial populations in potable waters: community water supply. *Journal-American Water Works Association, 64*(9), 596-602.

Ghelfi, F., Stevens, C. V., Laureyn, I., Van Meenen, E., Rogge, T. M., De Buyck, L., . . . Pagnoni, U. M. (2003). Synthesis of 5-methoxylated 3-pyrrolin-2-ones via the rearrangement of chlorinated pyrrolidin-2-ones. *Tetrahedron, 59*(8), 1147-1157.

Gilmore, B. (2011). Antimicrobial Ionic Liquids.

Girennavar, B., Cepeda, M. L., Soni, K. A., Vikram, A., Jesudhasan, P., Jayaprakasha, G. K., . . . Patil, B. S. (2008). Grapefruit juice and its furocoumarins inhibits autoinducer signaling and biofilm formation in bacteria. *Int J Food Microbiol, 125*(2), 204-208. doi: 10.1016/j.ijfoodmicro.2008.03.028

Givskov, M., de Nys, R., Manefield, M., Gram, L., Maximilien, R., Eberl, L., . . . Kjelleberg, S. (1996). Eukaryotic interference with homoserine lactone-mediated prokaryotic signalling. *Journal of Bacteriology, 178*(22), 6618-6622.

Gloag, E. S., Turnbull, L., Huang, A., Vallotton, P., Wang, H., Nolan, L. M., . . . Osvath, S. R. (2013). Self-organization of bacterial biofilms is facilitated by extracellular DNA. *Proceedings of the National Academy of Sciences, 110*(28), 11541-11546.

Goh, W.-K., Gardner, C. R., Chandra Sekhar, K. V. G., Biswas, N. N., Nizalapur, S., Rice, S. A., . . . Kumar, N. (2015). Synthesis, quorum sensing inhibition and docking studies of 1,5-dihydropyrrol-2-ones. *Bioorganic & Medicinal Chemistry, 23*(23), 7366-7377. doi: https://doi.org/10.1016/j.bmc.2015.10.025

Goh, W.-K., Iskander, G., Black, D. S., & Kumar, N. (2007). An efficient lactamization of fimbrolides to novel 1, 5-dihydropyrrol-2-ones. *Tetrahedron letters, 48*(13), 2287-2290.

Gohar, M., Faegri, K., Perchat, S., Ravnum, S., Økstad, O. A., Gominet, M., . . . Lereclus, D. (2008). The PlcR virulence regulon of Bacillus cereus. *Plos One, 3*(7), e2793.

Goldberg, J. B. (2010). Why is Pseudomonas aeruginosa a pathogen? *F1000 biology reports, 2*.

Gomila, M., Peña, A., Mulet, M., Lalucat, J., & García-Valdés, E. (2015). Phylogenomics and systematics in Pseudomonas. *Frontiers in Microbiology, 6*, 214.

Gominet, M., Slamti, L., Gilois, N., Rose, M., & Lereclus, D. (2001). Oligopeptide permease is required for expression of the Bacillus thuringiensis plcR regulon and for virulence. *Molecular Microbiology, 40*(4), 963-975.

Grant, S. G., Jessee, J., Bloom, F. R., & Hanahan, D. (1990). Differential plasmid rescue from transgenic mouse DNAs into Escherichia coli methylation-restriction mutants. *Proc Natl Acad Sci U S A, 87*(12), 4645-4649.

Griffith, D. P., Musher, D. á., & Itin, C. (1976). Urease. The primary cause of infection-induced urinary stones. *Investigative urology, 13*(5), 346-350.

Ha, D.-G., Kuchma, S. L., & O'Toole, G. A. (2014a). Plate-Based Assay for Swarming Motility in Pseudomonas aeruginosa. In A. Filloux & J.-L. Ramos (Eds.), *Pseudomonas Methods and Protocols* (pp. 67-72). New York, NY: Springer New York.

Ha, D. G., Kuchma, S. L., & O'Toole, G. A. (2014b). Plate-based assay for swimming motility in Pseudomonas aeruginosa. *Methods Mol Biol, 1149*, 59-65. doi: 10.1007/978-1-4939-0473-0_7

Hall-Stoodley, L., Costerton, J. W., & Stoodley, P. (2004). Bacterial biofilms: from the natural environment to infectious diseases. *Nature Reviews Microbiology, 2*(2), 95.

Hanzelka, B. L., & Greenberg, E. P. (1996). Quorum sensing in Vibrio fischeri: Evidence that S-adenosylmethionine is the amino acid substrate for autoinducer synthesis. *Journal of Bacteriology, 178*(17), 5291-5294.

Harrison, F. (2007). Microbial ecology of the cystic fibrosis lung. *Microbiology, 153*(4), 917-923.

Harrison, J. J., Turner, R. J., Marques, L. L., & Ceri, H. (2005). Biofilms: a new understanding of these microbial communities is driving a revolution that may transform the science of microbiology. *American Scientist, 93*(6), 508-515.

Hauser, A. R. (2009). The type III secretion system of Pseudomonas aeruginosa: infection by injection. *Nat Rev Microbiol, 7*(9), 654-665. doi: 10.1038/nrmicro2199

Hauser, A. R., Jain, M., Bar-Meir, M., & McColley, S. A. (2011). Clinical significance of microbial infection and adaptation in cystic fibrosis. *Clinical Microbiology Reviews, 24*(1), 29-70.

Havarstein, L. S., Coomaraswamy, G., & Morrison, D. A. (1995). An Unmodified Heptadecapeptide Pheromone Induces Competence for Genetic-Transformation in Streptococcus-Pneumoniae. *Proceedings of the National Academy of Sciences of the United States of America, 92*(24), 11140-11144. doi: DOI 10.1073/pnas.92.24.11140

Heilmann, C., Schweitzer, O., Gerke, C., Vanittanakom, N., Mack, D., & Götz, F. (1996). Molecular basis of intercellular adhesion in the biofilm-forming Staphylococcus epidermidis. *Molecular Microbiology, 20*(5), 1083-1091.

Hengge, R. (2009). Principles of c-di-GMP signalling in bacteria. *Nature Reviews Microbiology, 7*(4), 263.

Hentzer, M., Riedel, K., Rasmussen, T. B., Heydorn, A., Andersen, J. B., Parsek, M. R., . . . Høiby, N. (2002). Inhibition of quorum sensing in Pseudomonas aeruginosa biofilm bacteria by a halogenated furanone compound. *Microbiology, 148*(1), 87-102.

Hentzer, M., Wu, H., Andersen, J. B., Riedel, K., Rasmussen, T. B., Bagge, N., . . . Givskov, M. (2003). Attenuation of Pseudomonas aeruginosa virulence by quorum sensing inhibitors. *Embo Journal, 22*(15), 3803-3815. doi: Doi 10.1093/Emboj/Cdg366

Heurlier, K., Denervaud, V., Haenni, M., Guy, L., Krishnapillai, V., & Haas, D. (2005). Quorum-sensing-negative (lasR) mutants of Pseudomonas aeruginosa avoid cell lysis and death. *J Bacteriol, 187*(14), 4875-4883. doi: 10.1128/JB.187.14.4875-4883.2005

Heurlier, K., Williams, F., Heeb, S., Dormond, C., Pessi, G., Singer, D., . . . Haas, D. (2004). Positive control of swarming, rhamnolipid synthesis, and lipase production by the posttranscriptional RsmA/RsmZ system in Pseudomonas aeruginosa PAO1. *Journal of Bacteriology, 186*(10), 2936-2945.

Hibbing, M. E., Fuqua, C., Parsek, M. R., & Peterson, S. B. (2010). Bacterial competition: surviving and thriving in the microbial jungle. *Nature Reviews Microbiology, 8*(1), 15.

Hickman, J. W., & Harwood, C. S. (2008). Identification of FleQ from Pseudomonas aeruginosa as ac-di-GMP-responsive transcription factor. *Molecular Microbiology, 69*(2), 376-389.

Hickman, J. W., Tifrea, D. F., & Harwood, C. S. (2005). A chemosensory system that regulates biofilm formation through modulation of cyclic diguanylate levels. *Proceedings of the National Academy of Sciences, 102*(40), 14422-14427.

Higgins, D. A., Pomianek, M. E., Kraml, C. M., Taylor, R. K., Semmelhack, M. F., & Bassler, B. L. (2007). The major Vibrio cholerae autoinducer and its role

in virulence factor production. *Nature, 450*(7171), 883-886. doi: 10.1038/nature06284

Higgins, S., Heeb, S., Rampioni, G., P. Fletcher, M., Williams, P., & Cámara, M. (2018). *Differential Regulation of the Phenazine Biosynthetic Operons by Quorum Sensing in Pseudomonas aeruginosa PAO1-N* (Vol. 8).

Hill, D., Rose, B., Pajkos, A., Robinson, M., Bye, P., Bell, S., . . . Aaron, S. D. (2005). Antibiotic susceptibilities of Pseudomonas aeruginosa isolates derived from patients with cystic fibrosis under aerobic, anaerobic, and biofilm conditions. *Journal of clinical microbiology, 43*(10), 5085-5090.

Hoch, J. A., Silhavy, T. J., & Bourret, R. B. (1995). *Two-component signal transduction* (Vol. 2): ASM press Washington, DC:.

Hoffman, L. R., Deziel, E., D'Argenio, D. A., Lepine, F., Emerson, J., & McNamara, S. (2006). Selection for Staphylococcus aureus small-colony variants due to growth in the presence of Pseudomonas aeruginosa. *Proc Natl Acad Sci U S A, 103*. doi: 10.1073/pnas.0606756104

Hong, K. W., Koh, C. L., Sam, C. K., Yin, W. F., & Chan, K. G. (2012). Quorum quenching revisited--from signal decays to signalling confusion. *Sensors (Basel), 12*(4), 4661-4696. doi: 10.3390/s120404661

Horsburgh, M. J., Aish, J. L., White, I. J., Shaw, L., Lithgow, J. K., & Foster, S. J. (2002). Sigma B Modulates Virulence Determinant Expression and Stress Resistance: Characterization of a Functional rsbU strain Derived from Staphylococcus aureus 8325-4. *Journal of Bacteriology, 184*(19), 5457-5467. doi: 10.1128/jb.184.19.5457-5467.2002

Hotterbeekx, A., Kumar-Singh, S., Goossens, H., & Malhotra-Kumar, S. (2017). In vivo and In vitro Interactions between Pseudomonas aeruginosa and Staphylococcus spp. *Frontiers in Cellular and Infection Microbiology, 7*(106). doi: 10.3389/fcimb.2017.00106

Houston, P., Rowe, S. E., Pozzi, C., Waters, E. M., & O'Gara, J. P. (2011). Essential role for the major autolysin in the fibronectin-binding protein-mediated Staphylococcus aureus biofilm phenotype. *Infection and Immunity, 79*(3), 1153-1165.

Hsu, J.-L., Chen, H.-C., Peng, H.-L., & Chang, H.-Y. (2008). Characterization of the histidine-containing phosphotransfer protein B-mediated multistep phosphorelay system in Pseudomonas aeruginosa PAO1. *Journal of Biological Chemistry, 283*(15), 9933-9944.

Hubert, D., Réglier-Poupet, H., Sermet-Gaudelus, I., Ferroni, A., Le Bourgeois, M., Burgel, P.-R., . . . Coste, J. (2013). Association between Staphylococcus aureus alone or combined with Pseudomonas aeruginosa and the clinical condition of patients with cystic fibrosis. *Journal of Cystic Fibrosis, 12*(5), 497-503.

Hussain, R., Javorfi, T., Rudd, T. R., & Siligardi, G. (2016). High-throughput SRCD using multi-well plates and its applications. *Sci Rep, 6*, 38028. doi: 10.1038/srep38028

Hussain, R., Javorfi, T., & Siligardi, G. (2012a). Circular dichroism beamline B23 at the Diamond Light Source. *J Synchrotron Radiat, 19*(Pt 1), 132-135. doi: 10.1107/S0909049511038982

Hussain, R., Javorfi, T., & Siligardi, G. (2012b). Spectroscopic analysis: synchrotron radiation circular dichroism. *Comprehensive Chirality*(8), 438-448. doi: 10.1016/B978-0-08-095167-6.00841-7

Hussain, R., & Siligardi, G. (2016). Characterisation of Conformational and Ligand Binding Properties of Membrane Proteins Using Synchrotron Radiation Circular Dichroism (SRCD). *Adv Exp Med Biol, 922*, 43-59. doi: 10.1007/978-3-319-35072-1_4

Iglewski, B. H., Sadoff, J., Bjorn, M. J., & Maxwell, E. S. (1978). Pseudomonas aeruginosa exoenzyme S: an adenosine diphosphate ribosyltransferase distinct from toxin A. *Proceedings of the National Academy of Sciences, 75*(7), 3211-3215.

Ilangovan, A., Fletcher, M., Rampioni, G., Pustelny, C., Rumbaugh, K., Heeb, S., . . . Williams, P. (2013). Structural basis for native agonist and synthetic inhibitor recognition by the Pseudomonas aeruginosa quorum sensing regulator PqsR (MvfR). *PLoS Pathog, 9*(7), e1003508. doi: 10.1371/journal.ppat.1003508

Inouye, M., & Dutta, R. (2002). *Histidine kinases in signal transduction*: Elsevier.

Itoh, S., HONDA, H., TOMITA, F., & SUZUKI, T. (1971). Rhamnolipids produced by Pseudomonas aeruginosa grown on n-paraffin (mixture of C12, C13 and C14 fractions). *The Journal of antibiotics, 24*(12), 855-859.

Jacobsen, S. M., & Shirtliff, M. E. (2011). Proteus mirabilis biofilms and catheter-associated urinary tract infections. *Virulence, 2*(5), 460-465.

Jang, H.-J., Chang, M. W., Toghrol, F., & Bentley, W. E. (2008). Microarray analysis of toxicogenomic effects of triclosan on Staphylococcus aureus. *Applied microbiology and biotechnology, 78*(4), 695-707. doi: 10.1007/s00253-008-1349-x

Janzon, L., & Arvidson, S. (1990). The role of the delta-lysin gene (hld) in the regulation of virulence genes by the accessory gene regulator (agr) in Staphylococcus aureus. *The EMBO journal, 9*(5), 1391-1399.

Jarraud, S., Lyon, G., Figueiredo, A., Lina, G., Vandenesch, F., Etienne, J., . . . Novick, R. (2011). Exfoliatinproducing strains define a fourth agr specificity group in Staphylococcus aureus. *J Bacteriol, 193*(7027), 06355-06311.

Javorfi, T., Hussain, R., Myatt, D., & Siligardi, G. (2010). Measuring circular dichroism in a capillary cell using the b23 synchrotron radiation CD beamline at diamond light source. *Chirality, 22 Suppl 1*, E149-153. doi: 10.1002/chir.20924

Jenal, U., & Malone, J. (2006). Mechanisms of cyclic-di-GMP signaling in bacteria. *Annu. Rev. Genet., 40*, 385-407.

Jennings, L. K., Storek, K. M., Ledvina, H. E., Coulon, C., Marmont, L. S., Sadovskaya, I., . . . Filloux, A. (2015). Pel is a cationic exopolysaccharide that cross-links extracellular DNA in the Pseudomonas aeruginosa biofilm

matrix. *Proceedings of the National Academy of Sciences, 112*(36), 11353-11358.

Ji, C., Sharma, I., Pratihar, D., Hudson, L. L., Maura, D., Guney, T., . . . Tan, D. S. (2016). Designed small-molecule inhibitors of the anthranilyl-CoA synthetase PqsA block quinolone biosynthesis in Pseudomonas aeruginosa. *ACS chemical biology, 11*(11), 3061-3067.

Ji, G. Y., Beavis, R., & Novick, R. P. (1997). Bacterial interference caused by autoinducing peptide variants. *Science, 276*(5321), 2027-2030. doi: DOI 10.1126/science.276.5321.2027

Ji, G. Y., Beavis, R. C., & Novick, R. P. (1995). Cell density control of staphylococcal virulence mediated by an octapeptide pheromone. *Proceedings of the National Academy of Sciences of the United States of America, 92*(26), 12055-12059. doi: DOI 10.1073/pnas.92.26.12055

Jones, S. M., Yerly, J., Hu, Y., Ceri, H., & Martinuzzi, R. (2007). Structure of Proteus mirabilis biofilms grown in artificial urine and standard laboratory media. *Fems Microbiology Letters, 268*(1), 16-21.

Josefsson, E., Hartford, O., O'Brien, L., Patti, J. M., & Foster, T. (2001). Protection against experimental Staphylococcus aureus arthritis by vaccination with clumping factor A, a novel virulence determinant. *The Journal of infectious diseases, 184*(12), 1572-1580.

Kang, C., Wu, P., Li, Y., Ruan, B., Li, L., Tran, L., . . . Dang, Z. (2015). Understanding the role of clay minerals in the chromium (VI) bioremoval by Pseudomonas aeruginosa CCTCC AB93066 under growth condition: microscopic, spectroscopic and kinetic analysis. *World Journal of Microbiology and Biotechnology, 31*(11), 1765-1779.

Kaufmann, G. F., Sartorio, R., Lee, S. H., Mee, J. M., Altobell, L. J., Kujawa, D. P., . . . Janda, K. D. (2006). Antibody interference with N-acyl homoserine lactone-mediated bacterial quorum sensing. *Journal of the American Chemical Society, 128*(9), 2802-2803. doi: Doi 10.1021/Ja0578698

Kearns, D. B. (2010). A field guide to bacterial swarming motility. *Nature Reviews Microbiology, 8*(9), 634.

Kempner, E. S., & Hanson, F. E. (1968). Aspects of Light Production by Photobacterium Fischeri. *Journal of Bacteriology, 95*(3), 975-&.

Khalifa, A. B., Moissenet, D., Thien, H. V., & Khedher, M. (2011). Virulence factors in Pseudomonas aeruginosa: mechanisms and modes of regulation. *Annales De Biologie Clinique, 69*(4), 393-403. doi: 10.1684/abc.2011.0589

Khoury, A. E., Lam, K., Ellis, B., & Costerton, J. W. (1992). Prevention and control of bacterial infections associated with medical devices. *ASAIO journal (American Society for Artificial Internal Organs: 1992), 38*(3), M174-178.

Kim, S.-K., & Lee, J.-H. (2016). Biofilm dispersion in Pseudomonas aeruginosa. *Journal of microbiology, 54*(2), 71-85.

Kim, S.-K., Park, H.-Y., & Lee, J.-H. (2015). Anthranilate deteriorates the structure of Pseudomonas aeruginosa biofilms and antagonizes the biofilm-enhancing indole effect. *Appl. Environ. Microbiol., 81*(7), 2328-2338.

Kirketerp-Møller, K., Zulkowski, K., & James, G. (2011). Chronic wound colonization, infection, and biofilms *Biofilm infections* (pp. 11-24): Springer.

Klausen, M., Aaes-Jørgensen, A., Molin, S., & Tolker-Nielsen, T. (2003). Involvement of bacterial migration in the development of complex multicellular structures in Pseudomonas aeruginosa biofilms. *Molecular Microbiology, 50*(1), 61-68.

Klebensberger, J., Lautenschlager, K., Bressler, D., Wingender, J., & Philipp, B. (2007). Detergent-induced cell aggregation in subpopulations of Pseudomonas aeruginosa as a preadaptive survival strategy. *Environ Microbiol, 9*(9), 2247-2259. doi: 10.1111/j.1462-2920.2007.01339.x

Klein, T., Henn, C., de Jong, J. C., Zimmer, C., Kirsch, B., Maurer, C. K., . . . Hartmann, R. W. (2012). Identification of small-molecule antagonists of the Pseudomonas aeruginosa transcriptional regulator PqsR: biophysically guided hit discovery and optimization. *ACS chemical biology, 7*(9), 1496-1501.

Klockgether, J., Munder, A., Neugebauer, J., Davenport, C. F., Stanke, F., Larbig, K. D., . . . Wiehlmann, L. (2010). Genome diversity of Pseudomonas aeruginosa PAO1 laboratory strains. *Journal of Bacteriology, 192*(4), 1113-1121.

Köhler, T., Michéa-Hamzehpour, M., Henze, U., Gotoh, N., Kocjancic Curty, L., & Pechère, J. C. (1997). Characterization of MexE–MexF–OprN, a positively regulated multidrug efflux system of Pseudomonas aeruginosa. *Molecular Microbiology, 23*(2), 345-354.

Kohler, T., Van Delden, C., Curty, L., & Hamzehpour, M. JC 925 Pechere. 2001. Overexpression of the MexEF-OprN multidrug efflux system 926 affects cell-to-cell signaling in Pseudomonas aeruginosa. *J Bacteriol, 183*, 5213-5927.

König, G. M., Wright, A. D., & Bernardinelli, G. (1995). Determination of the absolute configuration of a series of halogenated furanones from the marine alga Delisea pulchra. *Helvetica chimica acta, 78*(3), 758-764.

Kotresha, D., & Vidyasagar, G. (2008). Isolation and characterisation of phenol-degrading Pseudomonas aeruginosa MTCC 4996. *World Journal of Microbiology and Biotechnology, 24*(4), 541-547.

Kramer, A., Herzer, J., Overhage, J., & Meyer-Almes, F. J. (2016). Substrate specificity and function of acetylpolyamine amidohydrolases from Pseudomonas aeruginosa. *BMC Biochem, 17*, 4. doi: 10.1186/s12858-016-0063-z

Kulasekara, H. D., Ventre, I., Kulasekara, B. R., Lazdunski, A., Filloux, A., & Lory, S. (2005). A novel two-component system controls the expression of Pseudomonas aeruginosa fimbrial cup genes. *Molecular Microbiology, 55*(2), 368-380.

Kulkarni, A. G., & Kaliwal, B. (2014). Bioremediation of methomyl by soil isolate—Pseudomonas aeruginosa. *J Environ Sci, Toxicol Food Technol, 8*(12), 1-10.

Kumar, A., & Ting, Y. P. (2015a). Presence of P seudomonas aeruginosa influences biofilm formation and surface protein expression of S taphylococcus aureus. *Environmental Microbiology, 17*(11), 4459-4468.

Kumar, A., & Ting, Y. P. (2015b). Presence of Pseudomonas aeruginosa influences biofilm formation and surface protein expression of Staphylococcus aureus. *Environ Microbiol, 17*. doi: 10.1111/1462-2920.12890

Kung, V. L., Ozer, E. A., & Hauser, A. R. (2010). The accessory genome of Pseudomonas aeruginosa. *Microbiol. Mol. Biol. Rev., 74*(4), 621-641.

Kunin, C. (1994). Infections of the urinary tract due to Pseudomonas aeruginosa. *INFECTIOUS DISEASE AND THERAPY SERIES, 12*, 237-237.

Laarman, A. J., Bardoel, B. W., Ruyken, M., Fernie, J., Milder, F. J., van Strijp, J. A., & Rooijakkers, S. H. (2012). Pseudomonas aeruginosa alkaline protease blocks complement activation via the classical and lectin pathways. *J Immunol, 188*(1), 386-393. doi: 10.4049/jimmunol.1102162

Lamont, I. L., Konings, A. F., & Reid, D. W. (2009). Iron acquisition by Pseudomonas aeruginosa in the lungs of patients with cystic fibrosis. *Biometals, 22*(1), 53-60. doi: 10.1007/s10534-008-9197-9

Latifi, A., Foglino, M., Tanaka, K., Williams, P., & Lazdunski, A. (1996). A hierarchical quorum-sensing cascade in Pseudomonas aeruginosa links the transcriptional activators LasR and RhIR (VsmR) to expression of the stationary-phase sigma factor RpoS. *Molecular Microbiology, 21*(6), 1137-1146. doi: DOI 10.1046/j.1365-2958.1996.00063.x

Lau, G. W., Ran, H. M., Kong, F. S., Hassett, D. J., & Mavrodi, D. (2004). Pseudomonas aeruginosa pyocyanin is critical for lung infection in mice. *Infection and Immunity, 72*(7), 4275-4278. doi: 10.1128/Iai.72.7.4275-4278.2004

Leech, A. J., & Mattick, J. S. (2006). Effect of site-specific mutations in different phosphotransfer domains of the chemosensory protein ChpA on Pseudomonas aeruginosa motility. *J Bacteriol, 188*(24), 8479-8486. doi: 10.1128/jb.00157-06

Lépine, F., Déziel, E., Milot, S., & Rahme, L. G. (2003). A stable isotope dilution assay for the quantification of the Pseudomonas quinolone signal in Pseudomonas aeruginosa cultures. *Biochimica et Biophysica Acta (BBA)-General Subjects, 1622*(1), 36-41.

Lépine, F., Milot, S., Déziel, E., He, J., & Rahme, L. G. (2004). Electrospray/mass spectrometric identification and analysis of 4-hydroxy-2-alkylquinolines (HAQs) produced by Pseudomonas aeruginosa. *Journal of the American Society for Mass Spectrometry, 15*(6), 862-869. doi: 10.1016/j.jasms.2004.02.012

Lereclus, D., Agaisse, H., Gominet, M., Salamitou, S., & Sanchis, V. (1996). Identification of a Bacillus thuringiensis gene that positively regulates transcription of the phosphatidylinositol-specific phospholipase C gene at the onset of the stationary phase. *Journal of Bacteriology, 178*(10), 2749-2756.

Lesic, B., Lépine, F., Déziel, E., Zhang, J., Zhang, Q., Padfield, K., . . . Tzika, A. A. (2007). Inhibitors of pathogen intercellular signals as selective anti-infective compounds. *PLoS Pathog, 3*(9), e126.

Lewenza, S., Gardy, J. L., Brinkman, F. S., & Hancock, R. E. (2005). Genome-wide identification of Pseudomonas aeruginosa exported proteins using a consensus computational strategy combined with a laboratory-based PhoA fusion screen. *Genome Res, 15*(2), 321-329. doi: 10.1101/gr.3257305

Li, M., Diep, B. A., Villaruz, A. E., Braughton, K. R., Jiang, X., DeLeo, F. R., . . . Otto, M. (2009). Evolution of virulence in epidemic community-associated methicillin-resistant Staphylococcus aureus. *Proceedings of the National Academy of Sciences, 106*(14), 5883-5888.

Li, X., Lu, N., Brady, H. R., & Packman, A. I. (2016). Biomineralization strongly modulates the formation of Proteus mirabilis and Pseudomonas aeruginosa dual-species biofilms. *FEMS microbiology ecology, 92*(12), fiw189.

Liberati, N. T., Urbach, J. M., Miyata, S., Lee, D. G., Drenkard, E., Wu, G., . . . Ausubel, F. M. (2006). An ordered, nonredundant library of Pseudomonas aeruginosa strain PA14 transposon insertion mutants. *Proceedings of the National Academy of Sciences, 103*(8), 2833-2838.

Lightbown, J., & Jackson, F. (1954). Inhibition of cytochrome system of heart muscle and of Staphylococcus aureus by 2-heptyl-4-hydroxyquinoline-N-oxide, an antagonist of dihydrostreptomycin. *The Biochemical journal, 58*(4), xlix.

Lin, C.-T., Huang, Y.-J., Chu, P.-H., Hsu, J.-L., Huang, C.-H., & Peng, H.-L. (2006). Identification of an HptB-mediated multi-step phosphorelay in Pseudomonas aeruginosa PAO1. *Research in microbiology, 157*(2), 169-175.

Lina, G., Jarraud, S., Ji, G., Greenland, T., Pedraza, A., Etienne, J., . . . Vandenesch, F. (1998). Transmembrane topology and histidine protein kinase activity of AgrC, the agr signal receptor in Staphylococcus aureus. *Molecular Microbiology, 28*(3), 655-662.

Lindsay, D., & von Holy, A. (2006). Bacterial biofilms within the clinical setting: what healthcare professionals should know. *Journal of Hospital Infection, 64*(4), 313-325. doi: 10.1016/j.jhin.2006.06.028

Lodge, J., Busby, S., & Piddock, L. (1993). Investigation of the Pseudomonas aeruginosa ampR gene and its role at the chromosomal ampC beta-lactamase promoter. *Fems Microbiology Letters, 111*(2-3), 315-320. doi: 10.1111/j.1574-6968.1993.tb06404.x

Lu, C., Kirsch, B., Zimmer, C., De Jong, J. C., Henn, C., Maurer, C. K., . . . Hartmann, R. W. (2012). Discovery of antagonists of PqsR, a key player in 2-alkyl-4-quinolone-dependent quorum sensing in Pseudomonas aeruginosa. *Chemistry & Biology, 19*(3), 381-390.

Lu, C., Maurer, C. K., Kirsch, B., Steinbach, A., Hartmann, R. W., Müsken, M., & Häussler, S. (2017). Pqsr modulators: Google Patents.

Luo, Y., Zhao, K., Baker, A. E., Kuchma, S. L., Coggan, K. A., Wolfgang, M. C., . . . O'Toole, G. A. (2015). A hierarchical cascade of second messengers

regulates Pseudomonas aeruginosa surface behaviors. *MBio, 6*(1). doi: 10.1128/mBio.02456-14

Luong, P. M., Shogan, B. D., Zaborin, A., Belogortseva, N., Shrout, J. D., Zaborina, O., & Alverdy, J. C. (2014). Emergence of the P2 phenotype in Pseudomonas aeruginosa PAO1 strains involves various mutations in mexT or mexF. *Journal of Bacteriology, 196*(2), 504-513.

Magnuson, R., Solomon, J., & Grossman, A. D. (1994). Biochemical and genetic characterization of a competence pheromone from B. subtilis. *Cell, 77*(2), 207-216.

Mahanta, N., Gupta, A., & Khare, S. (2008). Production of protease and lipase by solvent tolerant Pseudomonas aeruginosa PseA in solid-state fermentation using Jatropha curcas seed cake as substrate. *Bioresource Technology, 99*(6), 1729-1735.

Maier, R. M., & Soberon-Chavez, G. (2000). Pseudomonas aeruginosa rhamnolipids: biosynthesis and potential applications. *Applied microbiology and biotechnology, 54*(5), 625-633.

Maira-Litrán, T., Kropec, A., Abeygunawardana, C., Joyce, J., Mark, G., Goldmann, D. A., & Pier, G. B. (2002). Immunochemical properties of the staphylococcal poly-N-acetylglucosamine surface polysaccharide. *Infection and Immunity, 70*(8), 4433-4440.

Maliniak, M. L., Stecenko, A. A., & McCarty, N. A. (2016). A longitudinal analysis of chronic MRSA and Pseudomonas aeruginosa co-infection in cystic fibrosis: a single-center study. *J Cyst Fibros, 15*. doi: 10.1016/j.jcf.2015.10.014

Manefield, M., de Nys, R., Kumar, N., Read, R., Givskov, M., Steinberg, P., & Kjelleberg, S. A. (1999). Evidence that halogenated furanones from Delisea pulchra inhibit acylated homoserine lactone (AHL)-mediated gene expression by displacing the AHL signal from its receptor protein. *Microbiology-Sgm, 145*, 283-291.

Manefield, M., Harris, L., Rice, S. A., de Nys, R., & Kjelleberg, S. (2000). Inhibition of luminescence and virulence in the black tiger prawn (Penaeus monodon) pathogen Vibrio harveyi by intercellular signal antagonists. *Appl. Environ. Microbiol., 66*(5), 2079-2084.

Manefield, M., Welch, M., Givskov, M., Salmond, G. P., & Kjelleberg, S. (2001). Halogenated furanones from the red alga, Delisea pulchra, inhibit carbapenem antibiotic synthesis and exoenzyme virulence factor production in the phytopathogen Erwinia carotovora. *Fems Microbiology Letters, 205*(1), 131-138.

Mann, E. E., Rice, K. C., Boles, B. R., Endres, J. L., Ranjit, D., Chandramohan, L., . . . Bayles, K. W. (2009). Modulation of eDNA release and degradation affects Staphylococcus aureus biofilm maturation. *Plos One, 4*(6), e5822.

Mann, E. E., & Wozniak, D. J. (2012). Pseudomonas biofilm matrix composition and niche biology. *Fems Microbiology Reviews, 36*(4), 893-916.

Marquart, M. E., Caballero, A. R., Chomnawang, M., Thibodeaux, B. A., Twining, S. S., & O'Callaghan, R. J. (2005). Identification of a novel secreted

protease from Pseudomonas aeruginosa that causes corneal erosions. *Investigative ophthalmology & visual science, 46*(10), 3761-3768.

Marsden, A. E., Intile, P. J., Schulmeyer, K. H., Simmons-Patterson, E. R., Urbanowski, M. L., Wolfgang, M. C., & Yahr, T. L. (2016). Vfr Directly Activates exsA Transcription To Regulate Expression of the Pseudomonas aeruginosa Type III Secretion System. *J Bacteriol, 198*(9), 1442-1450. doi: 10.1128/jb.00049-16

Martinelli, D., Grossmann, G., Séquin, U., Brandl, H., & Bachofen, R. (2004). Effects of natural and chemically synthesized furanones on quorum sensing in Chromobacterium violaceum. *Bmc Microbiology, 4*(1), 25.

Mase, N., Nishi, T., Takamori, Y., Yoda, H., & Takabe, K. (1999). First synthesis of (R)-(−)-5-hydroxy-3-methyl-3-pyrrolin-2-one (jatropham) by lipase-catalyzed kinetic resolution. *Tetrahedron: Asymmetry, 10*(23), 4469-4471.

Maseda, H., Saito, K., Nakajima, A., & Nakae, T. (2000). Variation of the mexT gene, a regulator of the MexEF-oprN efflux pump expression in wild-type strains of Pseudomonas aeruginosa. *Fems Microbiology Letters, 192*(1), 107-112.

Mashburn-Warren, L., Howe, J., Garidel, P., Richter, W., Steiniger, F., Roessle, M., . . . Whiteley, M. (2008). Interaction of quorum signals with outer membrane lipids: insights into prokaryotic membrane vesicle formation. *Molecular Microbiology, 69*(2), 491-502. doi: 10.1111/j.1365-2958.2008.06302.x

Mashburn, L. M., Jett, A. M., Akins, D. R., & Whiteley, M. (2005). Staphylococcus aureus serves as an iron source for Pseudomonas aeruginosa during in vivo coculture. *J Bacteriol, 187*. doi: 10.1128/JB.187.2.554-566.2005

Mathee, K. (2018). *Forensic investigation into the origin of Pseudomonas aeruginosa PA14 — old but not lost* (Vol. 67).

Mattick, J. S. (2002a). Type IV pili and twitching motility. *Annual Review of Microbiology, 56*, 289-314. doi: 10.1146/annurev.micro.56.012302.160938

Mattick, J. S. (2002b). Type IV pili and twitching motility. *Annual Reviews in Microbiology, 56*(1), 289-314.

Maura, D., & Rahme, L. G. (2017). Pharmacological inhibition of the Pseudomonas aeruginosa MvfR quorum-sensing system interferes with biofilm formation and potentiates antibiotic-mediated biofilm disruption. *Antimicrob Agents Chemother, 61*(12), e01362-01317.

Mavrodi, D. V., Bonsall, R. F., Delaney, S. M., Soule, M. J., Phillips, G., & Thomashow, L. S. (2001). Functional analysis of genes for biosynthesis of pyocyanin and phenazine-1-carboxamide from Pseudomonas aeruginosa PAO1. *Journal of Bacteriology, 183*(21), 6454-6465.

Mayville, P., Ji, G., Beavis, R., Yang, H., Goger, M., Novick, R. P., & Muir, T. W. (1999). Structure-activity analysis of synthetic autoinducing thiolactone peptides from Staphylococcus aureus responsible for virulence. *Proceedings of the National Academy of Sciences, 96*(4), 1218-1223.

McCoy, A. J., Grosse-Kunstleve, R. W., Adams, P. D., Winn, M. D., Storoni, L. C., & Read, R. J. (2007). Phaser crystallographic software. *Journal of Applied Crystallography, 40*(4), 658-674. doi: doi:10.1107/S0021889807021206

McDougal, L. K., Steward, C. D., Killgore, G. E., Chaitram, J. M., McAllister, S. K., & Tenover, F. C. (2003). Pulsed-field gel electrophoresis typing of oxacillin-resistant Staphylococcus aureus isolates from the United States: establishing a national database. *Journal of clinical microbiology, 41*(11), 5113-5120.

McGrath, S., Wade, D. S., & Pesci, E. C. (2004). Dueling quorum sensing systems in Pseudomonas aeruginosa control the production of the Pseudomonas quinolone signal (PQS). *Fems Microbiology Letters, 230*(1), 27-34. doi: 10.1016/S0378-1097(03)00849-8

MDowell, P., Affas, Z., Reynolds, C., Holden, M. T., Wood, S. J., Saint, S., . . . Bycroft, B. W. (2001). Structure, activity and evolution of the group I thiolactone peptide quorum-sensing system of Staphylococcus aureus. *Molecular Microbiology, 41*(2), 503-512.

Meliani, A., & Bensoltane, A. (2015). Review of Pseudomonas attachment and biofilm formation in food industry. *Poultry, Fisheries & Wildlife Sciences*, 1-7.

Merighi, M., Lee, V. T., Hyodo, M., Hayakawa, Y., & Lory, S. (2007). The second messenger bis-(3′-5′)-cyclic-GMP and its PilZ domain-containing receptor Alg44 are required for alginate biosynthesis in Pseudomonas aeruginosa. *Molecular Microbiology, 65*(4), 876-895.

Merritt, J. H., Ha, D.-G., Cowles, K. N., Lu, W., Morales, D. K., Rabinowitz, J., . . . O'Toole, G. A. (2010). Specific control of Pseudomonas aeruginosa surface-associated behaviors by two c-di-GMP diguanylate cyclases. *MBio, 1*(4), e00183-00110.

Meyers, D. J., Palmer, K. C., Bale, L. A., Kernacki, K., Preston, M., Brown, T., & Berk, R. S. (1992). In vivo and in vitro toxicity of phospholipase C from Pseudomonas aeruginosa. *Toxicon. 1992, 30*(2), 161-169.

Meyners, C., Wawrzinek, R., Kramer, A., Hinz, S., Wessig, P., & Meyer-Almes, F. J. (2014). A fluorescence lifetime-based binding assay for acetylpolyamine amidohydrolases from Pseudomonas aeruginosa using a [1,3]dioxolo[4,5-f][1,3]benzodioxole (DBD) ligand probe. *Anal Bioanal Chem, 406*(20), 4889-4897. doi: 10.1007/s00216-014-7886-5

Michalska, M., & Wolf, P. (2015). Pseudomonas Exotoxin A: optimized by evolution for effective killing. *Frontiers in Microbiology, 6*, 963. doi: 10.3389/fmicb.2015.00963

Michelsen, C. F., Christensen, A. M., Bojer, M. S., Hoiby, N., Ingmer, H., & Jelsbak, L. (2014). Staphylococcus aureus alters growth activity, autolysis, and antibiotic tolerance in a human host-adapted Pseudomonas aeruginosa lineage. *J Bacteriol, 196*. doi: 10.1128/JB.02006-14

Miller, M. B., & Bassler, B. L. (2001). Quorum sensing in bacteria. *Annual Reviews in Microbiology, 55*(1), 165-199.

Mitchell, G., Séguin, D. L., Asselin, A.-E., Déziel, E., Cantin, A. M., Frost, E. H., . . . Malouin, F. (2010). Staphylococcus aureus sigma B-dependent emergence of small-colony variants and biofilm production following exposure to Pseudomonas aeruginosa 4-hydroxy-2-heptylquinoline-N-oxide. *Bmc Microbiology, 10*(1), 33.

Monsó, E., Ruiz, J., Rosell, A., Manterola, J., Fiz, J., Morera, J., & Ausina, V. (1995). Bacterial infection in chronic obstructive pulmonary disease. A study of stable and exacerbated outpatients using the protected specimen brush. *Am J Respir Crit Care Med, 152*, pp1316-1320.

Moore, J. D., Rossi, F. M., Welsh, M. A., Nyffeler, K. E., & Blackwell, H. E. (2015). A Comparative Analysis of Synthetic Quorum Sensing Modulators in Pseudomonas aeruginosa: New Insights into Mechanism, Active Efflux Susceptibility, Phenotypic Response, and Next-Generation Ligand Design. *Journal of the American Chemical Society, 137*(46), 14626-14639. doi: 10.1021/jacs.5b06728

Moradali, M. F., Ghods, S., & Rehm, B. H. (2017). Pseudomonas aeruginosa lifestyle: a paradigm for adaptation, survival, and persistence. *Frontiers in Cellular and Infection Microbiology, 7*, 39.

Moreillon, P., Entenza, J. M., Francioli, P., McDevitt, D., Foster, T. J., Francois, P., & Vaudaux, P. (1995). Role of Staphylococcus aureus coagulase and clumping factor in pathogenesis of experimental endocarditis. *Infection and Immunity, 63*(12), 4738-4743.

Morfeldt, E., Taylor, D. v., Von Gabain, A., & Arvidson, S. (1995). Activation of alpha-toxin translation in Staphylococcus aureus by the trans-encoded antisense RNA, RNAIII. *The EMBO journal, 14*(18), 4569-4577.

Morgenstein, R. M., Szostek, B., & Rather, P. N. (2010). Regulation of gene expression during swarmer cell differentiation in Proteus mirabilis. *Fems Microbiology Reviews, 34*(5), 753-763.

Moritz, M. M., Flemming, H.-C., & Wingender, J. (2010). Integration of Pseudomonas aeruginosa and Legionella pneumophila in drinking water biofilms grown on domestic plumbing materials. *International journal of hygiene and environmental health, 213*(3), 190-197.

Mougous, J. D., Cuff, M. E., Raunser, S., Shen, A., Zhou, M., Gifford, C. A., . . . Mekalanos, J. J. (2006). A Virulence Locus of Pseudomonas aeruginosa Encodes a Protein Secretion Apparatus. *Science, 312*(5779), 1526-1530. doi: 10.1126/science.1128393

Mukherjee, A. K., & Bordoloi, N. K. (2012). Biodegradation of benzene, toluene, and xylene (BTX) in liquid culture and in soil by Bacillus subtilis and Pseudomonas aeruginosa strains and a formulated bacterial consortium. *Environmental Science and Pollution Research, 19*(8), 3380-3388.

Murray, T. S., & Kazmierczak, B. I. (2006). FlhF is required for swimming and swarming in Pseudomonas aeruginosa. *Journal of Bacteriology, 188*(19), 6995-7004.

NCBI's COG database. (2014). from ftp://ftp.ncbi.nih.gov/pub/COG/COG2014/static/lists/listPseaer.html

Nelder, J. A., & Wedderburn, R. W. M. (1972). Generalized Linear Models. *Journal of the Royal Statistical Society. Series A (General), 135*(3), 370-384. doi: 10.2307/2344614

Ng, W. (2018). *Retarded swarming motility in Bacillus subtilis NRS-762 and Pseudomonas aeruginosa PRD-10*.

Nicotra, M. B., Rivera, M., Dale, A. M., Shepherd, R., & Carter, R. (1995). Clinical, pathophysiologic, and microbiologic characterization of bronchiectasis in an aging cohort. *Chest, 108*(4), 955-961.

Niewerth, H., Bergander, K., Chhabra, S. R., Williams, P., & Fetzner, S. (2011). Synthesis and biotransformation of 2-alkyl-4 (1H)-quinolones by recombinant Pseudomonas putida KT2440. *Applied microbiology and biotechnology, 91*(5), 1399.

Nitschke, M., & Costa, S. (2007). Biosurfactants in food industry. *Trends in Food Science & Technology, 18*(5), 252-259.

Novick, R. P., & Geisinger, E. (2008). Quorum sensing in staphylococci. *Annu Rev Genet, 42*, 541-564. doi: 10.1146/annurev.genet.42.110807.091640

Novick, R. P., Projan, S., Kornblum, J., Ross, H., Ji, G., Kreiswirth, B., . . . Moghazeh, S. (1995). Theagr P2 operon: An autocatalytic sensory transduction system inStaphylococcus aureus. *Molecular and General Genetics MGG, 248*(4), 446-458.

Novick, R. P., Ross, H., Projan, S., Kornblum, J., Kreiswirth, B., & Moghazeh, S. (1993). Synthesis of staphylococcal virulence factors is controlled by a regulatory RNA molecule. *The EMBO journal, 12*(10), 3967-3975.

O'Toole, G. A. (2018). Cystic Fibrosis Airway Microbiome: Overturning the Old, Opening the Way for the New. *J Bacteriol, 200*(4). doi: 10.1128/JB.00561-17

O'Toole, G. A., Kaplan, H. B., & Kolter, R. (2000). Biofilm formation as microbial development. *Annual Reviews in Microbiology, 54*(1), 49-79.

O'Toole, G. A., & Kolter, R. (1998a). Flagellar and twitching motility are necessary for Pseudomonas aeruginosa biofilm development. *Mol Microbiol, 30*(2), 295-304.

O'Toole, G. A., & Kolter, R. (1998b). Initiation of biofilm formation in Pseudomonas fluorescens WCS365 proceeds via multiple, convergent signalling pathways: a genetic analysis. *Molecular Microbiology, 28*(3), 449-461.

Okstad, O. A., Gominet, M., Purnelle, B., Rose, M., Lereclus, D., & Kolsto, A. B. (1999). Sequence analysis of three Bacillus cereus loci carrying PIcR-regulated genes encoding degradative enzymes and enterotoxin. *Microbiology, 145 (Pt 11)*, 3129-3138. doi: 10.1099/00221287-145-11-3129

Oliver, A., Cantón, R., Campo, P., Baquero, F., & Blázquez, J. (2000). High Frequency of Hypermutable Pseudomonas aeruginosa in Cystic Fibrosis Lung Infection. *Science, 288*(5469), pp. 1251-1253.

Orr, M. W., Donaldson, G. P., Severin, G. B., Wang, J., Sintim, H. O., Waters, C. M., & Lee, V. T. (2015). Oligoribonuclease is the primary degradative enzyme for pGpG in Pseudomonas aeruginosa that is required for cyclic-di-GMP turnover. *Proceedings of the National Academy of Sciences, 112*(36), E5048-E5057. doi: 10.1073/pnas.1507245112

Ortori, C. A., Halliday, N., Camara, M., Williams, P., & Barrett, D. A. (2014). LC-MS/MS quantitative analysis of quorum sensing signal molecules. *Methods Mol Biol, 1149*, 255-270. doi: 10.1007/978-1-4939-0473-0_21

Oton, E. V. (2018). *Pseudomonas aeruginosa PQS mediated virulence regulation and interference.* (PhD thesis), University of Nottingham.

Otto, M. (2004). Quorum-sensing control in Staphylococci–a target for antimicrobial drug therapy? *Fems Microbiology Letters, 241*(2), 135-141.

Overhage, J., Bains, M., Brazas, M. D., & Hancock, R. E. (2008). Swarming of Pseudomonas aeruginosa is a complex adaptation leading to increased production of virulence factors and antibiotic resistance. *Journal of Bacteriology, 190*(8), 2671-2679.

Overhage, J., Lewenza, S., Marr, A. K., & Hancock, R. E. (2007). Identification of genes involved in swarming motility using a Pseudomonas aeruginosa PAO1 mini-Tn5-lux mutant library. *Journal of Bacteriology, 189*(5), 2164-2169.

Overhage, J., Schemionek, M., Webb, J. S., & Rehm, B. H. (2005). Expression of the psl operon in Pseudomonas aeruginosa PAO1 biofilms: PslA performs an essential function in biofilm formation. *Appl. Environ. Microbiol., 71*(8), 4407-4413.

Palmer Jr, R. J. (1999). [12] Microscopy flowcells: Perfusion chambers for real-time study of biofilms *Methods Enzymol* (Vol. 310, pp. 160-166): Elsevier.

Pamp, S. J., & Tolker-Nielsen, T. (2007). Multiple roles of biosurfactants in structural biofilm development by Pseudomonas aeruginosa. *J Bacteriol, 189*(6), 2531-2539. doi: 10.1128/JB.01515-06

Pandza, S., Baetens, M., Park, C., Au, T., Keyhan, M., & Matin, A. (2000). The G-protein FlhF has a role in polar flagellar placement and general stress response induction in Pseudomonas putida. *Molecular Microbiology, 36*(2), 414-423.

Papi, A., Bellettato, C. M., Braccioni, F., Romagnoli, M., Casolari, P., Caramori, G., . . . Johnston, S. L. (2006). Infections and Airway Inflammation in Chronic

Obstructive Pulmonary Disease Severe Exacerbations. *Am J Respir Crit Care Med, 176*, pp 1114–1121.

Park, J., Jagasia, R., Kaufmann, G. F., Mathison, J. C., Ruiz, D. I., Moss, J. A., . . . Janda, K. D. (2007). Infection control by antibody disruption of bacterial quorum sensing signaling. *Chemistry & Biology, 14*(10), 1119-1127. doi: 10.1016/j.chembiol.2007.08.013

Park, P. W., Pier, G. B., Preston, M. J., Goldberger, O., Fitzgerald, M. L., & Bernfield, M. (2000). Syndecan-1 shedding is enhanced by LasA, a secreted

virulence factor of Pseudomonas aeruginosa. *J Biol Chem, 275*(5), 3057-3064.

Parsek, M. R., & Tolker-Nielsen, T. (2008). Pattern formation in Pseudomonas aeruginosa biofilms. *Current opinion in microbiology, 11*(6), 560-566.

Pastar, I., Nusbaum, A. G., Gil, J., Patel, S. B., Chen, J., Valdes, J., . . . Davis, S. C. (2013). Interactions of methicillin resistant Staphylococcus aureus USA300 and Pseudomonas aeruginosa in polymicrobial wound infection. *Plos One, 8*(2), e56846.

Pearson, J. P., Feldman, M., Iglewski, B. H., & Prince, A. (2000). Pseudomonas aeruginosa cell-to-cell signaling is required for virulence in a model of acute pulmonary infection. *Infection and Immunity, 68*(7), 4331-4334.

Pearson, J. P., Pesci, E. C., & Iglewski, B. H. (1997). Roles of Pseudomonas aeruginosa las and rhl quorum-sensing systems in control of elastase and rhamnolipid biosynthesis genes. *Journal of Bacteriology, 179*(18), 5756-5767.

Petek, M., Baebler, Š., Kuzman, D., Rotter, A., Podlesek, Z., Gruden, K., . . . Urleb, U. (2010). Revealing fosfomycin primary effect on Staphylococcus aureus transcriptome: modulation of cell envelope biosynthesis and phosphoenolpyruvate induced starvation. *Bmc Microbiology, 10*(1), 159.

Pettus Jr, J. A., Wing, R. M., & Sims, J. J. (1977). Marine natural products XII isolation of a family of multihalogenated gamma-methylene lactones from the red seaweed Delisea fimbriata. *Tetrahedron letters, 18*(1), 41-44.

Piletska, E. V., Stavroulakis, G., Larcombe, L. D., Whitcombe, M. J., Sharma, A., Primrose, S., . . . Piletsky, S. A. (2011). Passive control of quorum sensing: prevention of Pseudomonas aeruginosa biofilm formation by imprinted polymers. *Biomacromolecules, 12*(4), 1067-1071. doi: 10.1021/bm101410q

Pomerantsev, A. P., Pomerantseva, O. M., Camp, A. S., Mukkamala, R., Goldman, S., & Leppla, S. H. (2009). PapR peptide maturation: role of the NprB protease in Bacillus cereus 569 PlcR/PapR global gene regulation. *FEMS Immunology & Medical Microbiology, 55*(3), 361-377.

Pratt, L. A., & Kolter, R. (1998). Genetic analysis of Escherichia coli biofilm formation: roles of flagella, motility, chemotaxis and type I pili. *Molecular Microbiology, 30*(2), 285-293.

Primer-BLAST website. (2019). from https://www.ncbi.nlm.nih.gov/tools/primer-blast/

Provencher, S. W., & Glockner, J. (1981). Estimation of globular protein secondary structure from circular dichroism. *Biochemistry, 20*(1), 33-37.

Raghupathi, P. K., Zupančič, J., Brejnrod, A. D., Jacquiod, S., Houf, K., Burmølle, M., . . . Sørensen, S. J. (2018). Microbial diversity and putative opportunistic pathogens in dishwasher biofilm communities. *Appl. Environ. Microbiol., 84*(5), e02755-02717.

Ramirez-Estrada, S., Borgatta, B., & Rello, J. (2016). Pseudomonas aeruginosa ventilator-associated pneumonia management. *Infect Drug Resist, 9*, 7-18. doi: 10.2147/IDR.S50669

Rampioni, G., Bertani, I., Zennaro, E., Polticelli, F., Venturi, V., & Leoni, L. (2006). The quorum-sensing negative regulator RsaL of Pseudomonas aeruginosa binds to the lasI promoter. *Journal of Bacteriology, 188*(2), 815-819.

Rampioni, G., Falcone, M., Heeb, S., Frangipani, E., Fletcher, M. P., Dubern, J.-F., . . . Williams, P. (2016). Unravelling the genome-wide contributions of specific 2-alkyl-4-quinolones and PqsE to quorum sensing in Pseudomonas aeruginosa. *PLoS Pathog, 12*(11), e1006029.

Rampioni, G., Leoni, L., & Williams, P. (2014). The art of antibacterial warfare: deception through interference with quorum sensing–mediated communication. *Bioorganic chemistry, 55*, 60-68.

Rampioni, G., Pustelny, C., Fletcher, M. P., Wright, V. J., Bruce, M., Rumbaugh, K. P., . . . Williams, P. (2010). Transcriptomic analysis reveals a global alkyl-quinolone-independent regulatory role for PqsE in facilitating the environmental adaptation of Pseudomonas aeruginosa to plant and animal hosts. *Environmental Microbiology, 12*(6), 1659-1673.

Raposo, A., Pérez, E., de Faria, C. T., Ferrús, M. A., & Carrascosa, C. (2017). Food Spoilage by Pseudomonas spp.—An Overview. *Food Borne Pathogens and Antibiotic Resistance*.

Rasamiravaka, T., Labtani, Q., Duez, P., & El Jaziri, M. (2015). The formation of biofilms by Pseudomonas aeruginosa: a review of the natural and synthetic compounds interfering with control mechanisms. *Biomed Research International, 2015*, 759348. doi: 10.1155/2015/759348

Rasmussen, T. B., Bjarnsholt, T., Skindersoe, M. E., Hentzer, M., Kristoffersen, P., Kote, M., . . . Givskov, M. (2005). Screening for quorum-sensing inhibitors (QSI) by use of a novel genetic system, the QSI selector. *Journal of Bacteriology, 187*(5), 1799-1814. doi: 10.1128/Jb.187.5.1799-1814.2005

Rauprich, O., Matsushita, M., Weijer, C. J., Siegert, F., Esipov, S. E., & Shapiro, J. A. (1996). Periodic phenomena in Proteus mirabilis swarm colony development. *Journal of Bacteriology, 178*(22), 6525-6538.

Remminghorst, U., & Rehm, B. H. (2006). Alg44, a unique protein required for alginate biosynthesis in Pseudomonas aeruginosa. *FEBS Lett, 580*(16), 3883-3888. doi: 10.1016/j.febslet.2006.05.077

Rice, K. C., Mann, E. E., Endres, J. L., Weiss, E. C., Cassat, J. E., Smeltzer, M. S., & Bayles, K. W. (2007). The cidA murein hydrolase regulator contributes to DNA release and biofilm development in Staphylococcus aureus. *Proceedings of the National Academy of Sciences, 104*(19), 8113-8118.

Rittschof, D. (2001). Natural Product Antifoulants and Coatings Development (pp. 543-566).

Robinson, M. D., McCarthy, D. J., & Smyth, G. K. (2010). edgeR: a Bioconductor package for differential expression analysis of digital gene expression data. *Bioinformatics, 26*(1), 139-140. doi: 10.1093/bioinformatics/btp616

Rocchetta, H., Burrows, L., & Lam, J. (1999). Genetics of O-antigen biosynthesis inPseudomonas aeruginosa. *Microbiol. Mol. Biol. Rev., 63*(3), 523-553.

Römling, U., Galperin, M. Y., & Gomelsky, M. (2013). Cyclic di-GMP: the first 25 years of a universal bacterial second messenger. *Microbiology and Molecular Biology Reviews, 77*(1), 1-52.

Römling, U., Gomelsky, M., & Galperin, M. Y. (2005). C-di-GMP: the dawning of a novel bacterial signalling system. *Molecular Microbiology, 57*(3), 629-639.

Ruby, E. G. (1996). Lessons from a cooperative, bacterial-animal association: The Vibrio fischeri Euprymna scolopes light organ symbiosis. *Annual Review of Microbiology, 50*, 591-624. doi: DOI 10.1146/annurev.micro.50.1.591

Rueden, C. T., Schindelin, J., Hiner, M. C., DeZonia, B. E., Walter, A. E., Arena, E. T., & Eliceiri, K. W. (2017). ImageJ2: ImageJ for the next generation of scientific image data. *BMC Bioinformatics, 18*(1), 529. doi: 10.1186/s12859-017-1934-z

Rutherford, S. T., & Bassler, B. L. (2012). Bacterial Quorum Sensing: Its Role in Virulence and Possibilities for Its Control. *Cold Spring Harbor Perspectives in Medicine, 2*(11). doi: ARTN a012427

10.1101/cshperspect.a012427

Ryan, R. P., Fouhy, Y., Lucey, J. F., & Dow, J. M. (2006). Cyclic di-GMP signaling in bacteria: recent advances and new puzzles. *Journal of Bacteriology, 188*(24), 8327-8334.

Rybtke, M. T., Borlee, B. R., Murakami, K., Irie, Y., Hentzer, M., Nielsen, T. E., . . . Tolker-Nielsen, T. (2012). Fluorescence-based reporter for gauging cyclic di-GMP levels in *Pseudomonas aeruginosa*. *Applied and Environmental Microbiology, 78*(15), 5060-5069. doi: 10.1128/AEM.00414-12

Ryder, C., Byrd, M., & Wozniak, D. J. (2007). Role of polysaccharides in Pseudomonas aeruginosa biofilm development. *Current opinion in microbiology, 10*(6), 644-648.

Ryjenkov, D. A., Tarutina, M., Moskvin, O. V., & Gomelsky, M. (2005). Cyclic diguanylate is a ubiquitous signaling molecule in bacteria: insights into biochemistry of the GGDEF protein domain. *Journal of Bacteriology, 187*(5), 1792-1798.

Saenz, H. L., Augsburger, V., Vuong, C., Jack, R. W., Götz, F., & Otto, M. (2000). Inducible expression and cellular location of AgrB, a protein involved in the maturation of the staphylococcal quorum-sensing pheromone. *Archives of microbiology, 174*(6), 452-455.

Safdari, M.-S., Kariminia, H.-R., Nejad, Z. G., & Fletcher, T. H. (2017). Study potential of indigenous Pseudomonas aeruginosa and Bacillus subtilis in bioremediation of diesel-contaminated water. *Water, Air, & Soil Pollution, 228*(1), 37.

Sagel, S. D., Gibson, R. L., Emerson, J., McNamara, S., Burns, J. L., Wagener, J. S., . . . Network, C. F. F. T. D. (2009). Impact of Pseudomonas and Staphylococcus infection on inflammation and clinical status in young

children with cystic fibrosis. *The Journal of pediatrics, 154*(2), 183-188. e183.

Said-Salim, B., Dunman, P. M., McAleese, F. M., Macapagal, D., Murphy, E., McNamara, P. J., . . . Kreiswirth, B. N. (2003). Global regulation of Staphylococcus aureus genes by rot. *Journal of Bacteriology, 185*(2), 610-619. doi: 10.1128/Jb.185.2.610-619.2003

Sakthipriya, N., Doble, M., & Sangwai, J. S. (2016). Systematic investigations on the biodegradation and viscosity reduction of long chain hydrocarbons using Pseudomonas aeruginosa and Pseudomonas fluorescens. *Environmental Science: Processes & Impacts, 18*(3), 386-397.

Sánchez-Carrillo, C., Padilla, B., Marín, M., Rivera, M., Cercenado, E., Vigil, D., . . . Bouza, E. (2009). Contaminated feeding bottles: the source of an outbreak of Pseudomonas aeruginosa infections in a neonatal intensive care unit. *American journal of infection control, 37*(2), 150-154.

Sato, H., Frank, D. W., Hillard, C. J., Feix, J. B., Pankhaniya, R. R., Moriyama, K., . . . Long, R. M. (2003). The mechanism of action of the Pseudomonas aeruginosa-encoded type III cytotoxin, ExoU. *The EMBO journal, 22*(12), 2959-2969.

Schindelin, J., Arganda-Carreras, I., Frise, E., Kaynig, V., Longair, M., Pietzsch, T., . . . Cardona, A. (2012). Fiji: an open-source platform for biological-image analysis. *Nature Methods, 9*, 676. doi: 10.1038/nmeth.2019

https://www.nature.com/articles/nmeth.2019#supplementary-information

Schooling, S. R., & Beveridge, T. J. (2006). Membrane vesicles: an overlooked component of the matrices of biofilms. *Journal of Bacteriology, 188*(16), 5945-5957.

Senf, F., Tommassen, J., & Koster, M. (2008). Polar secretion of proteins via the Xcp type II secretion system in Pseudomonas aeruginosa. *Microbiology, 154*(Pt 10), 3025-3032. doi: 10.1099/mic.0.2008/018069-0

Serra, R., Grande, R., Butrico, L., Rossi, A., Settimio, U. F., & Caroleo, B. (2015). Chronic wound infections: the role of Pseudomonas aeruginosa and Staphylococcus aureus. *Expert Rev Anti-Infect Ther, 13*. doi: 10.1586/14787210.2015.1023291

Seth, A. K., Geringer, M. R., Galiano, R. D., Leung, K. P., Mustoe, T. A., & Hong, S. J. (2012). Quantitative comparison and analysis of species-specific wound biofilm virulence using an in vivo, rabbit-ear model. *Journal of the American College of Surgeons, 215*(3), 388-399.

Sharon, C., Furugoh, S., Yamakido, T., Ogawa, H., & Kato, Y. (1998). Purification and characterization of a lipase from Pseudomonas aeruginosa KKA-5 and its role in castor oil hydrolysis. *Journal of Industrial Microbiology and Biotechnology, 20*(5), 304-307.

Shetye, G. S., Singh, N., Gao, X., Bandyopadhyay, D., Yan, A., & Luk, Y.-Y. (2013). Structures and biofilm inhibition activities of brominated furanones for Escherichia coli and Pseudomonas aeruginosa. *MedChemComm, 4*(7), 1079-1084.

Shih, P.-C., & Huang, C.-T. (2002). Effects of quorum-sensing deficiency on Pseudomonas aeruginosa biofilm formation and antibiotic resistance. *Journal of Antimicrobial Chemotherapy, 49*(2), 309-314.

Shrout, J. D., Chopp, D. L., Just, C. L., Hentzer, M., Givskov, M., & Parsek, M. R. (2006). The impact of quorum sensing and swarming motility on Pseudomonas aeruginosa biofilm formation is nutritionally conditional. *Molecular Microbiology, 62*(5), 1264-1277.

Sibley, C. D., Duan, K., Fischer, C., Parkins, M. D., Storey, D. G., & Rabin, H. R. (2008). Discerning the complexity of community interactions using a Drosophila model of polymicrobial infections. *PLoS Pathog, 4*. doi: 10.1371/journal.ppat.1000184

Siligardi, G., & Hussain, R. (2015). CD Spectroscopy: An Essential Tool for Quality Control of Protein Folding. In R. J. Owens (Ed.), *Structural Proteomics: High-Throughput Methods* (pp. 255-276). New York, NY: Springer New York.

Silva, R. M. P., Rodríguez, A. Á., De Oca, J. M. G. M., & Moreno, D. C. (2009). Biosorption of chromium, copper, manganese and zinc by Pseudomonas aeruginosa AT18 isolated from a site contaminated with petroleum. *Bioresource Technology, 100*(4), 1533-1538.

Simon, M. I., Crane, B., & Crane, A. (2007). *Two-component signaling systems* (Vol. 423): Academic Press.

Simon, R., Priefer, U. B., & hler, A. (1983). *A Broad Host Range Mobilization System for In Vivo Genetic Engineering: Transposon Mutagenesis in Gram Negative Bacteria* (Vol. 1).

Singh, A. K., & Mallick, N. (2009). Exploitation of inexpensive substrates for production of a novel SCL–LCL-PHA co-polymer by Pseudomonas aeruginosa MTCC 7925. *Journal of industrial microbiology & biotechnology, 36*(3), 347-354.

Slamti, L., & Lereclus, D. (2005). Specificity and polymorphism of the PlcR-PapR quorum-sensing system in the Bacillus cereus group. *J Bacteriol, 187*(3), 1182-1187. doi: 10.1128/JB.187.3.1182-1187.2005

Smith, J. J., Travis, S. M., Greenberg, E. P., & Welsh, M. J. (1996). Cystic Fibrosis Airway Epithelia Fail to Kill Bacteria Because of Abnormal Airway Surface Fluid. *Cell*

85(2), 229–236.

Soberón-Chávez, G., Lépine, F., & Déziel, E. (2005). Production of rhamnolipids by Pseudomonas aeruginosa. *Applied microbiology and biotechnology, 68*(6), 718-725.

Soukarieh, F., Vico Oton, E., Dubern, J.-F., Gomes, J., Halliday, N., de Pilar Crespo, M., . . . Quiroga, J. (2018). In silico and in vitro-guided identification of inhibitors of alkylquinolone-dependent quorum sensing in Pseudomonas aeruginosa. *Molecules, 23*(2), 257.

Spoering, A. L., & Gilmore, M. S. (2006). Quorum sensing and DNA release in bacterial biofilms. *Current opinion in microbiology, 9*(2), 133-137.

Stamm, W. E. (1991). Catheter-associated urinary tract infections: epidemiology, pathogenesis, and prevention. *The American journal of medicine, 91*(3), S65-S71.

Starkey, M., Lepine, F., Maura, D., Bandyopadhaya, A., Lesic, B., He, J., . . . Tzika, A. (2014). Identification of anti-virulence compounds that disrupt quorum-sensing regulated acute and persistent pathogenicity. *PLoS Pathog, 10*(8), e1004321.

Stewart, P. S. (2003). Diffusion in Biofilms. *Journal of Bacteriology, 185*(5), 1485-1491. doi: 10.1128/jb.185.5.1485-1491.2003

Stewart, P. S., & Costerton, J. W. (2001). Antibiotic resistance of bacteria in biofilms. *The Lancet, 358*(9276), 135-138.

Stickler, D., Ganderton, L., King, J., Nettleton, J., & Winters, C. (1993). Proteus mirabilis biofilms and the encrustation of urethral catheters. *Urological research, 21*(6), 407-411.

Stoodley, P., Sauer, K., Davies, D. G., & Costerton, J. W. (2002). Biofilms as complex differentiated communities. *Annu Rev Microbiol., 56*, 187-209.

Stover, C. K., Pham, X. Q., Erwin, A. L., Mizoguchi, S. D., Warrener, P., Hickey, M. J., . . . Olson, M. V. (2000). Complete genome sequence of Pseudomonas aeruginosa PAO1, an opportunistic pathogen. *Nature, 406*(6799), 959-964. doi: 10.1038/35023079

Suter, S. (1994). The role of Baderial proteases in the pathogenesis of cystic fibrosis. *American journal of respiratory and critical care medicine, 150*(6_Pt_2), S118-S122.

Tanabe, T., Funahashi, T., Shiuchi, K., Okajima, N., Nakao, H., & Miyamoto, K. (2012). Characterization of Vibrio parahaemolyticus genes encoding the systems for utilization of enterobactin as a xenosiderophore. *Microbiology, 158*. doi: 10.1099/mic.0.059568-0

Tateda, K., Comte, R., Pechere, J.-C., Köhler, T., Yamaguchi, K., & Van Delden, C. (2001). Azithromycin inhibits quorum sensing in Pseudomonas aeruginosa. *Antimicrob Agents Chemother, 45*(6), 1930-1933.

Thoendel, M., & Horswill, A. R. (2009). Identification of Staphylococcus aureus AgrD residues required for autoinducing peptide biosynthesis. *Journal of Biological Chemistry, 284*(33), 21828-21838.

Thoendel, M., & Horswill, A. R. (2010). Biosynthesis of peptide signals in gram-positive bacteria *Advances in applied microbiology* (Vol. 71, pp. 91-112): Elsevier.

Thomann, A., de Mello Martins, A. G., Brengel, C., Empting, M., & Hartmann, R. W. (2016). Application of dual inhibition concept within looped autoregulatory systems toward antivirulence agents against Pseudomonas aeruginosa infections. *ACS chemical biology, 11*(5), 1279-1286.

Tielker, D., Hacker, S., Loris, R., Strathmann, M., Wingender, J., Wilhelm, S., . . . Jaeger, K.-E. (2005). Pseudomonas aeruginosa lectin LecB is located in the outer membrane and is involved in biofilm formation. *Microbiology, 151*(5), 1313-1323.

Tognon, M., Köhler, T., Luscher, A., & van Delden, C. (2019). Transcriptional profiling of Pseudomonas aeruginosa and Staphylococcus aureus during in vitro co-culture. *Bmc Genomics, 20*(1), 30.

Toyofuku, M., Roschitzki, B., Riedel, K., & Eberl, L. (2012). Identification of proteins associated with the Pseudomonas aeruginosa biofilm extracellular matrix. *J Proteome Res, 11*(10), 4906-4915. doi: 10.1021/pr300395j

Tremblay, J., & Deziel, E. (2010). Gene expression in Pseudomonas aeruginosa swarming motility. *Bmc Genomics, 11*, 587. doi: 10.1186/1471-2164-11-587

Tremblay, Y. D., Vogeleer, P., Jacques, M., & Harel, J. (2015). Development of a high throughput microfluidic method to study biofilm formation and host-pathogen interactions in pathogenic Escherichia coli. *Applied and Environmental Microbiology*, AEM. 04208-04214.

Trunk, K., Benkert, B., Quack, N., Munch, R., Scheer, M., Garbe, J., . . . Jahn, D. (2010). Anaerobic adaptation in Pseudomonas aeruginosa: definition of the Anr and Dnr regulons. *Environ Microbiol, 12*(6), 1719-1733. doi: 10.1111/j.1462-2920.2010.02252.x

Turnbull, L., Toyofuku, M., Hynen, A. L., Kurosawa, M., Pessi, G., Petty, N. K., . . . Shimoni, R. (2016). Explosive cell lysis as a mechanism for the biogenesis of bacterial membrane vesicles and biofilms. *Nature communications, 7*, 11220.

Turnbull, L., & Whitchurch, C. B. (2014). Motility Assay: Twitching Motility. In A. Filloux & J.-L. Ramos (Eds.), *Pseudomonas Methods and Protocols* (pp. 73-86). New York, NY: Springer New York.

Turner, K. H., Everett, J., Trivedi, U., Rumbaugh, K. P., & Whiteley, M. (2014). Requirements for Pseudomonas aeruginosa acute burn and chronic surgical wound infection. *PLoS Genet, 10*(7), e1004518. doi: 10.1371/journal.pgen.1004518

Tyson, G. W., Chapman, J., Hugenholtz, P., Allen, E. E., Ram, R. J., Richardson, P. M., . . . Banfield, J. F. (2004). Community structure and metabolism through reconstruction of microbial genomes from the environment. *Nature, 428*(6978), 37.

Vagin, A. A., Steiner, R. A., Lebedev, A. A., Potterton, L., McNicholas, S., Long, F., & Murshudov, G. N. (2004). REFMAC5 dictionary: organization of prior chemical knowledge and guidelines for its use. *Acta Crystallographica Section D, 60*(12 Part 1), 2184-2195. doi: doi:10.1107/S0907444904023510

Valle, J., Toledo-Arana, A., Berasain, C., Ghigo, J. M., Amorena, B., Penadés, J. R., & Lasa, I. (2003). SarA and not σB is essential for biofilm development by Staphylococcus aureus. *Molecular Microbiology, 48*(4), 1075-1087.

Vallet, I., Diggle, S. P., Stacey, R. E., Cámara, M., Ventre, I., Lory, S., . . . Filloux, A. (2004). Biofilm formation in Pseudomonas aeruginosa: fimbrial cup gene clusters are controlled by the transcriptional regulator MvaT. *Journal of Bacteriology, 186*(9), 2880-2890.

Vallet, I., Olson, J. W., Lory, S., Lazdunski, A., & Filloux, A. (2001). The chaperone/usher pathways of Pseudomonas aeruginosa: identification of fimbrial gene clusters (cup) and their involvement in biofilm formation. *Proceedings of the National Academy of Sciences, 98*(12), 6911-6916.

Valverde, C., Heeb, S., Keel, C., & Haas, D. (2003). RsmY, a small regulatory RNA, is required in concert with RsmZ for GacA-dependent expression of biocontrol traits in Pseudomonas fluorescens CHA0. *Mol Microbiol, 50*(4), 1361-1379.

Vannini, A., Volpari, C., Gargioli, C., Muraglia, E., Cortese, R., De Francesco, R., . . . Di Marco, S. (2002). The crystal structure of the quorum sensing protein TraR bound to its autoinducer and target DNA. *The EMBO journal, 21*(17), 4393-4401.

Vasseur, P., Vallet-Gely, I., Soscia, C., Genin, S., & Filloux, A. (2005). The pel genes of the Pseudomonas aeruginosa PAK strain are involved at early and late stages of biofilm formation. *Microbiology, 151*(Pt 3), 985-997. doi: 10.1099/mic.0.27410-0

Vuong, C., Saenz, H. L., Götz, F., & Otto, M. (2000). Impact of the agr quorum-sensing system on adherence to polystyrene in Staphylococcus aureus. *The Journal of infectious diseases, 182*(6), 1688-1693.

Wade, D. S., Calfee, M. W., Rocha, E. R., Ling, E. A., Engstrom, E., Coleman, J. P., & Pesci, E. C. (2005). Regulation of Pseudomonas quinolone signal synthesis in Pseudomonas aeruginosa. *J Bacteriol, 187*(13), 4372-4380. doi: 10.1128/JB.187.13.4372-4380.2005

Wall, D., & Kaiser, D. (1999). Type IV pili and cell motility. *Molecular Microbiology, 32*(1), 01-10.

Walters, M. C., Roe, F., Bugnicourt, A., Franklin, M. J., & Stewart, P. S. (2003). Contributions of antibiotic penetration, oxygen limitation, and low metabolic activity to tolerance of Pseudomonas aeruginosa biofilms to ciprofloxacin and tobramycin. *Antimicrob Agents Chemother, 47*(1), 317-323.

Warren, J. W. (2001). Catheter-associated urinary tract infections. *International journal of antimicrobial agents, 17*(4), 299-303.

Warren, J. W., Steinberg, L., Hebel, J., & Tenney, J. H. (1989). The prevalence of urethral catheterization in Maryland nursing homes. *Archives of Internal Medicine, 149*(7), 1535-1537.

Watson, W. T., Minogue, T. D., Val, D. L., von Bodman, S. B., & Churchill, M. E. (2002). Structural basis and specificity of acyl-homoserine lactone signal production in bacterial quorum sensing. *Molecular cell, 9*(3), 685-694.

Watters, C., DeLeon, K., Trivedi, U., Griswold, J. A., Lyte, M., Hampel, K. J., . . . Rumbaugh, K. P. (2013). Pseudomonas aeruginosa biofilms perturb wound resolution and antibiotic tolerance in diabetic mice. *Med Microbiol Immunol, 202*(2), 131-141.

Wei, Q., & Ma, L. Z. (2013). Biofilm matrix and its regulation in Pseudomonas aeruginosa. *International Journal of Molecular Sciences, 14*(10), 20983-21005. doi: 10.3390/ijms141020983

Wei, Y., Perez, L. J., Ng, W.-L., Semmelhack, M. F., & Bassler, B. L. (2011). Mechanism of Vibrio cholerae autoinducer-1 biosynthesis. *ACS chemical biology, 6*(4), 356-365.

Welsh, M. A., Eibergen, N. R., Moore, J. D., & Blackwell, H. E. (2015). Small molecule disruption of quorum sensing cross-regulation in Pseudomonas aeruginosa causes major and unexpected alterations to virulence phenotypes. *Journal of the American Chemical Society, 137*(4), 1510-1519.

Wenner, J. J., & Rettger, L. F. (1919). A Systematic Study of the Proteus Group of Bacteria. *J Bacteriol, 4*(4), 331-353.

West, S. A., & Buckling, A. (2003). Cooperation, virulence and siderophore production in bacterial parasites. *Proc Biol Sci, 270*. doi: 10.1098/rspb.2002.2209

Whitchurch, C. B., Tolker-Nielsen, T., Ragas, P. C., & Mattick, J. S. (2002). Extracellular DNA Required for Bacterial Biofilm Formation. *Science, 295*, 1487.

Wilks, S. A., Fader, M. J., & Keevil, C. W. (2015). Novel insights into the Proteus mirabilis crystalline biofilm using real-time imaging. *Plos One, 10*(10), e0141711.

Williams, H. D., Zlosnik, J. E., & Ryall, B. (2006). Oxygen, cyanide and energy generation in the cystic fibrosis pathogen Pseudomonas aeruginosa. *Advances in microbial physiology, 52*, 1-71.

Williams, P. (2017). Strategies for inhibiting quorum sensing. *Emerging Topics in Life Sciences, 1*(1), 23-30.

Williams, P., & Cámara, M. (2009). Quorum sensing and environmental adaptation in Pseudomonas aeruginosa: a tale of regulatory networks and multifunctional signal molecules. *Current opinion in microbiology, 12*(2), 182-191.

Williams, P., Winzer, K., Chan, W. C., & Camara, M. (2007). Look who's talking: communication and quorum sensing in the bacterial world. *Philosophical Transactions of the Royal Society B: Biological Sciences, 362*(1483), 1119-1134.

Wilton, M., Charron-Mazenod, L., Moore, R., & Lewenza, S. (2016). Extracellular DNA acidifies biofilms and induces aminoglycoside resistance in Pseudomonas aeruginosa. *Antimicrob Agents Chemother, 60*(1), 544-553.

Winzer, K., Falconer, C., Garber, N. C., Diggle, S. P., Camara, M., & Williams, P. (2000). The Pseudomonas aeruginosa lectins PA-IL and PA-IIL are controlled by quorum sensing and by RpoS. *Journal of Bacteriology, 182*(22), 6401-6411.

Wiseman, T., Williston, S., Brandts, J. F., & Lin, L.-N. (1989). Rapid measurement of binding constants and heats of binding using a new titration calorimeter. *Analytical Biochemistry, 179*(1), 131-137. doi: https://doi.org/10.1016/0003-2697(89)90213-3

Witzgall, F., Ewert, W., & Blankenfeldt, W. (2017). Structures of the N-Terminal Domain of PqsA in Complex with Anthraniloyl-and 6-Fluoroanthraniloyl-AMP: Substrate Activation in Pseudomonas Quinolone Signal (PQS) Biosynthesis. *Chembiochem, 18*(20), 2045-2055.

Wolz, C., Hohloch, K., Ocaktan, A., Poole, K., Evans, R. W., Rochel, N., . . . Doring, G. (1994). Iron release from transferrin by pyoverdin and elastase from Pseudomonas aeruginosa. *Infect Immun, 62*(9), 4021-4027.

Wood, T. K., Knabel, S. J., & Kwan, B. W. (2013). Bacterial persister cell formation and dormancy. *Appl. Environ. Microbiol., 79*(23), 7116-7121.

Worlitzsch, D., Tarran, R., Ulrich, M., Schwab, U., Cekici, A., Meyer, K. C., . . . Weiss, T. (2002). Effects of reduced mucus oxygen concentration in airway Pseudomonas infections of cystic fibrosis patients. *The Journal of clinical investigation, 109*(3), 317-325.

Wretlind, B., & Pavlovskis, O. R. (1983). Pseudomonas aeruginosa elastase and its role in pseudomonas infections. *Rev Infect Dis., 5*(5), 998-1004.

Xiao, G. P., Deziel, E., He, J. X., Lepine, F., Lesic, B., Castonguay, M. H., . . . Rahme, L. G. (2006a). MvfR, a key Pseudomonas aeruginosa pathogenicity LTTR-class regulatory protein, has dual ligands. *Molecular Microbiology, 62*(6), 1689-1699. doi: 10.1111/j.1365-2958.2006.05462.x

Xiao, G. P., He, J. X., & Rahme, L. G. (2006b). Mutation analysis of the Pseudomonas aeruginosa mvfR and pqsABCDE gene promoters demonstrates complex quorum-sensing circuitry. *Microbiology-Sgm, 152*, 1679-1686. doi: 10.1099/mic.0.28605-0

Yahr, T. L., & Wolfgang, M. C. (2006). Transcriptional regulation of the Pseudomonas aeruginosa type III secretion system. *Mol Microbiol, 62*(3), 631-640. doi: 10.1111/j.1365-2958.2006.05412.x

Yang, L., Barken, K. B., Skindersoe, M. E., Christensen, A. B., Givskov, M., & Tolker-Nielsen, T. (2007). Effects of iron on DNA release and biofilm development by Pseudomonas aeruginosa. *Microbiology, 153*(5), 1318-1328.

Yang, L., Liu, Y., Wu, H., Høiby, N., Molin, S., & Song, Z. j. (2011). Current understanding of multi-species biofilms. *International journal of oral science, 3*(2), 74.

Yarwood, J. M., Bartels, D. J., Volper, E. M., & Greenberg, E. P. (2004). Quorum sensing in Staphylococcus aureus biofilms. *Journal of Bacteriology, 186*(6), 1838-1850.

Yates, E. A., Philipp, B., Buckley, C., Atkinson, S., Chhabra, S. R., Sockett, R. E., . . . Williams, P. (2002). N-acylhomoserine Lactones undergo lactonolysis in a pH-, temperature-, and acyl chain length-dependent manner during growth of Yersinia pseudotuberculosis and Pseudomonas aeruginosa. *Infection and Immunity, 70*(10), 5635-5646. doi: 10.1128/Iai.70.10.5635-5646.2002

Ye, Y., Fang, F., & Li, Y. (2015). Synthesis and anti-biofilm activities of dihydro-pyrrol-2-one derivatives on Pseudomonas aeruginosa. *Bioorganic & medicinal chemistry letters, 25*(3), 597-601.

Yeung, A. T., Torfs, E. C., Jamshidi, F., Bains, M., Wiegand, I., Hancock, R. E., & Overhage, J. (2009). Swarming of Pseudomonas aeruginosa is controlled by a broad spectrum of transcriptional regulators, including MetR. *Journal of Bacteriology, 191*(18), 5592-5602.

Yi, Q. M., Rockenbach, S., Ward, J. E., Jr., & Lutkenhaus, J. (1985). Structure and expression of the cell division genes ftsQ, ftsA and ftsZ. *J Mol Biol, 184*(3), 399-412.

Yoon, M. Y., Lee, K.-M., Park, Y., & Yoon, S. S. (2011). Contribution of cell elongation to the biofilm formation of Pseudomonas aeruginosa during anaerobic respiration. *Plos One, 6*(1), e16105.

Yu, S., Jensen, V., Seeliger, J., Feldmann, I., Weber, S., Schleicher, E., . . . Blankenfeldt, W. (2009). Structure elucidation and preliminary assessment of hydrolase activity of PqsE, the Pseudomonas quinolone signal (PQS) response protein. *Biochemistry, 48*(43), 10298-10307.

Zahler, R. (2016). Aryloxyacetylindoles and analogs as antibiotic tolerance inhibitors. *WO Patent WO2016112088A1*.

Zhang, Z., Adappa, N. D., Doghramji, L. J., Chiu, A. G., Cohen, N. A., & Palmer, J. N. (2015). Different clinical factors associated with Staphylococcus aureus and Pseudomonas aeruginosa in chronic rhinosinusitis. *Int Forum Allergy Rhinol, 5*. doi: 10.1002/alr.21532

Zinna, F., Resta, C., Górecki, M., Pescitelli, G., Di Bari, L., Jávorfi, T., . . . Siligardi, G. (2017). Circular Dichroism Imaging: Mapping the Local Supramolecular Order in Thin Films of Chiral Functional Polymers. *Macromolecules, 50*(5), 2054-2060. doi: 10.1021/acs.macromol.6b02590

Zulianello, L., Canard, C., Kohler, T., Caille, D., Lacroix, J. S., & Meda, P. (2006). Rhamnolipids are virulence factors that promote early infiltration of primary human airway epithelia by Pseudomonas aeruginosa. *Infection and Immunity, 74*(6), 3134-3147. doi: 10.1128/Iai.01772-05